PART VII:

FOS

- FOS

Chapter 29
FOS Instrument Overview

In This Chapter...

The Faint Object Spectrograph (FOS) was designed by the FOS Investigation Definition Team (IDT) consisting of Richard J. Harms (Principal Investigator), Roger Angel, Frank Barko, Edward Beaver, Ralph Bohlin, Margaret Burbidge, Arthur Davidsen, Holland Ford, and Bruce Margon. The instrument was built by the University of California, San Diego and prime subcontractor Martin Marietta Corporation Aerospace Division. A general overview of the instrument is given in Harms et al., 1982, in *The Space Telescope Observatory,* ed. by D.N.B. Hall (Washington:NASA), p.55.

There have been significant improvements in our understanding of the FOS. *All FOS data should be recalibrated fully* to assure that the latest and most accurate calibration files and the best algorithms are used.

This part of the *HST Data Handbook* describes the basics of the FOS and is the main source of modern information for understanding, recalibrating, and analyzing FOS spectra. References to more detailed information from other sources—appropriate only for the most expert users and unusual situations—are also provided.

We expect that, as more time passes since the removal of the FOS from HST in February 1997, the predominate users of these chapters will be archival researchers. These investigators may not be as familiar with FOS data and its

assessment, calibration, and analysis as the original General Observers (GOs). Accordingly, we have included more detail about instrument operation, data assessment, and calibration than in previous versions of this handbook.

Five chapters are included in the FOS section:

- Chapter 29 gives a summary of the important sources of FOS information, apart from this handbook, a description of the instrument, an overview of the operational history and features of the FOS, and a brief introduction to FOS data-taking modes.
- Chapter 30 describes the basic structure of each important type of FOS data file. We present an overview of how to assess the quality of an FOS observation with detailed reference to the FOS paper products that have been re-designed to facilitate this activity. There are also examples of how to compare a planned observation with the dataset returned from the executed observation for the purpose of understanding anomalies.
- Chapter 31 includes a description of how data are calibrated in the Routine Science Data Processing (RSDP) pipeline and recalibrated with STSDAS, problems that can arise in this procedure, and how you should recalibrate your data with updated calibration files.
- Chapter 32 describes error sources and gives a statement of calibration accuracies.
- Chapter 33 considers several individual data analysis topics including description of some FOS-specific STSDAS tasks.

Although FOS was retired as an active instrument, STScI continues to provide analysis support for FOS data. Questions should be sent to `help@stsci.edu`. Any future updates to FOS documentation and calibration will be announced in the HST Spectrographs Space Telescope Analysis Newsletter (STAN).

29.1 FOS Documentation

In this section we list important sources of documentation for the FOS and its various types of output data.

29.1.1 Instrument Handbooks

Six versions of the *FOS Instrument Handbook* were written. Two of these—the updated pre-launch edition, version 1.1, and the last, version 6.0—exist as electronic documents (currently available only in PostScript format on the FOS WWW Documentation page).

Version 6.0 is the most complete and accurate description of the capabilities of the instrument and practical information for its use. For example detailed discussions of target acquisition procedures, their specificity, and their limitations were included. Version 1.1 gives an excellent and thorough technical-level

description of the instrument. The other versions contain little additional useful information.

29.1.2 Instrument Science Reports

Instrument Science Reports (ISRs) are technical reports that describe calibrations, anomalies, and operational capabilities of the instrument. ISRs are generally written for a technical audience, so we have tried to incorporate the relevant results into this handbook. When an ISR may be particularly helpful, as in treatment of a topic beyond the scope of this volume, we provide the appropriate reference. Most ISRs are available on the FOS WWW Documentation page. Paper copies of all ISRs are available from the STScI Help Desk and can be obtained through `help@stsci.edu`.

29.1.3 WWW Resources

The FOS WWW pages are accessible from the main STScI WWW page and are the primary repository of all FOS information and documentation. A wide variety of documentation, including this handbook, FOS news updates, reference file guides, frequently asked question (FAQ) lists, Calibration Workshop papers, and ISRs can be found here. The FOS WWW page is directly available at:

`http://www.stsci.edu/ftp/instrument_news/FOS/topfos.html`

29.2 General Outline for Handling FOS Data

A brief outline of the steps suggested for an FOS project follows:

1. Select data for retrieval from HST Archive.
2. Examine the data in StarView. (FOS paper products could also be used for an initial quick look).
3. Recalibrate *all* data to benefit from the latest calibration updates and **calfos** enhancements, as described in Chapter 31 (which includes a calibration checklist).
4. Run FOS paper products to evaluate data quality and anomalies. (Refer to the exposure logsheet or RPS2 (RPSS) Phase II specifications if desired).
5. Analyze your data.

You must have some basic knowledge of the FOS and its capabilities in order to refine your archive data search. The remaining sections of this chapter provide an overview of the FOS and, for certain very detailed information, direct you to other sources of information such as the *FOS Instrument Handbook*.

On the basis of your understanding of FOS modes and capabilities you will search the Archive and retrieve observations that may meet your objectives. Using StarView to browse and retrieve data from the Archive is described in Chapter 29.

StarView provides an easy way to quickly assess prospective data, reflecting the original post-observation calibration. Large sets or bulk retrievals can be assessed efficiently at your site with the FOS paper products.

Next, you must recalibrate the observations to obtain the benefit of the FOS closeout calibration and algorithm updates. The accuracies of any FOS data stored in the HST Archive will be improved by recalibration. Chapter 31 describes the recalibration process.

After recalibrating the data, you will want to assess the results and understand the limitations of the calibration as they apply to your data. The FOS paper products, described in Chapter 30, are useful for this purpose. After you evaluate your overall data quality with the paper products you should refer to the description of error sources and accuracy limitations found in Chapter 32. Occasionally, the details of the original observation strategy can be useful in understanding calibration limits for particular types of data. Referring to the exposure logsheet and the data quality assessment material in Chapter 30 may help.

Analyze your data. Although the major focus of this handbook is on understanding FOS calibrations and their accuracies as applied to your data, a few routines that may be useful for specific types of analysis of FOS data are discussed in Chapter 33.

29.3 FOS Instrument Basics

This section provides the basic information needed to understand the geometry and operation of the FOS instrument and the optical components affecting the light path. *FOS Instrument Handbook* versions 1.1 and 6.0 give more details about the instrument performance and capabilities. The final sections of this chapter are summary discussions of each FOS target acquisition and science observing mode.

29.3.1 FOS History and the Introduction of COSTAR

The FOS operated successfully throughout its six-year mission on HST. There were however a number of major milestones during that period, most notably the installation of COSTAR, which corrected the effects of primary mirror aberration for the FOS. Table 29.1 summarizes the most important HST milestones that affected FOS.

During the summer of 1991 (part of the Science Verification (SV) period) substantial changes in certain FOS photocathode granularity patterns (flatfields) were observed, particularly for FOS/RD. Detailed monitoring during the remainder of the period prior to the First Servicing Mission (January 1, 1992,

through December 15, 1993) revealed moderate variations in flatfield combined with overall time- and OTA focus-dependent changes in instrument sensitivity.

The aberration of the primary mirror affected FOS acquisitions and science observations. Modifications to ACQ/BINARY procedures to compensate for the extended PSF wings reduced the likelihood of target acquisition failure by early 1992, but throughout the pre-servicing period aberration-related *crowded field* acquisition failures occurred. The FOS geomagnetically-induced image motion (GIM) was discovered early in SV. In addition to photometric effects, this motion degraded the accuracy of ACQ/BINARY target acquisitions until the implementation of an onboard compensation algorithm in April, 1993.

Y-bases were monitored and regularly updated throughout the FOS operational lifetime. Temporal trending of some FOS y-bases was established by the summer of 1993 and subsequent updates included predicted values based upon the observed trending.

Installation of the Corrective Optics Space Telescope Axial Replacement (COSTAR) on the spacecraft in December of 1993 corrected the effects of spherical aberration of the HST primary mirror on the FOS. COSTAR deployed two correcting mirrors, M1 and M2, into the optical path of FOS. The COSTAR mirrors introduced a modest anamorphic magnification which differed by approximately two percent between the COSTAR *x* and *y*. Aperture and pixel sizes decreased to approximately 0.86 of their pre-COSTAR values. COSTAR restored the design PSF at a modest cost in efficiency attributable to the two corrector reflections. Additional information concerning the impact of COSTAR on FOS is in “Influence of COSTAR on FOS Data” on page 29-19.

Other updates were made to either improve or extend various aspects of instrumental operation and calibration. These included commanding updates to improve the efficiency of ACQ/PEAK, to enhance the brightness dynamic range and reduce the failure rate of ACQ/BINARY, and to enable the use of ACQ/PEAK for moving target acquisitions. Software updates to implement scattered light correction, correctly calibrate OBJ-OBJ observations, and substantially improve flux calibration were also implemented.

29.3.2 Optical Layout

Figure 29.1 shows an optical layout of the FOS. Light entered the FOS through a pair of entrance ports roughly 490" off the optical axis of HST. The light from the object of interest then passed through one of the two independent optical channels, each of which focused nearly stigmatic spectral images on the photocathode of a photon-counting Digicon detector. These two channels differed only in the wavelength sensitivity of their respective detectors, and were referred to as FOS/RD (or Red Side) and FOS/BL (Blue Side). The FOS aperture wheel, located at the HST focal surface, contained separate sets of single or paired apertures (including one blank for background measurements) for each detector which ranged in size from 0.1" to 4.3" (pre-COSTAR) projected onto the sky. From the aperture wheel the optical beam then passed through the polarization analyzer (which included a clear aperture for non-polarimetric observations) and

Table 29.1: Important Dates in FOS History

Date	Event
April 1990	HST launched with FOS onboard
January 1, 1992	SV ends (updated reference files, aperture locations and sizes, and y-bases)
After July 1, 1992	FOS calibration observations commence use of high-precision ACQ/PEAK (0.025" accuracy each coord)
April 5, 1993	Onboard GIM correction implemented
June 1993	ACQ/BINARY 8-steps to success implemented (11 groups became success, not failure)
December 1993	Servicing Mission (SM) 1
About January 1, 1994	COSTAR FOS M1, M2 mirrors deployed
January 1-26, 1994	Calibration of COSTAR-assisted FOS; no FOS observations in this period are formally calibrated due to many different COSTAR mirror positions
February 1, 1994	FOS COSTAR mirrors properly positioned - photometry now possible
March 21, 1994	Scattered light correction algorithm implemented in pipeline
May 30, 1994	FOS post-COSTAR aperture locations updated; SMOV ends
July 1994	More efficient ACQ/PEAK including moving targets implemented
July-November 1994	No header ACQ/PEAK scan parameter information (FOS paper products will not work for ACQ/PEAK taken in this time period)
November 1994	GHRS/FOS acquisition assists initiated
December 1994	Reuse_target_offset implemented
February 5, 1995	Jitter files routinely provided on GO tapes and placed in archive
January 15, 1996	Improved scattered light correction algorithm implemented
March 17, 1996	AIS flux calibration implemented in pipeline
February 13, 1997	FOS removed from HST

on to the grazing incidence mirror, a *roof* prism, which deflected the beam 22 degrees upward. This deflection was required in order to allow the apertures to be placed near the HST optical axis to minimize astigmatism, while meeting the packaging constraints within the FOS. The deflected beam then passed through an order-sorting filter, when required, in the fore part of the filter-grating wheel, and on to an off-axis paraboloidal mirror which collimated the beam and directed it back to the filter-grating wheel. The beam was then dispersed or imaged (for the one imaging position). and focused onto the detector by the selected element on the filter-grating wheel.

29.3.3 Detectors

As described above, the FOS had two Digicon detectors with independent optical paths (Figure 29.1). The Digicons operated by accelerating photoelectrons emitted from a two-dimensional transmissive photocathode onto a linear array of 512 silicon diodes. All 512 FOS diodes were exposed by dispersed light, i.e., none of the diodes were dedicated to background measurement or other purposes. The photoelectron pulses were counted (if a pulse had an amplitude above a programmable threshold) in each of the individual diode channels. A separate microprocessor for each detector controlled the electronics, mechanisms, and Digicons. The counts were summed in microprocessor memory for a mode-dependent preset time and then read from the FOS to the HST computer.

The bi-alkali (Na_2 KSb) blue detector (FOS/BL) photocathode on a magnesium fluoride faceplate was sensitive from 1150 Å to 5400 Å, while the tri-alkali (Na_2 KSb Cs) red Digicon (FOS/RD) photocathode on a fused silica faceplate covered the wavelength range from 1620 Å to 8500 Å. Figure 29.2 shows the quantum efficiencies of both detectors. Note that the graphs in Figure 29.2 are illustrative only; the plotted values are not accurate enough for quantitative use in data analysis. The general characteristics of FOS/BL and FOS/RD are compiled in Table 29.2.

Both photocathodes had spatial irregularities in response (granularity) and localized blemishes that could limit the S/N achieved. These spatially variable features could be removed with appropriate flatfielding provided adequate care was taken in target centering. The diodes themselves also had small response irregularities that were of little consequence and were also removed by routine flatfielding.

Figure 29.1: FOS Optical Path

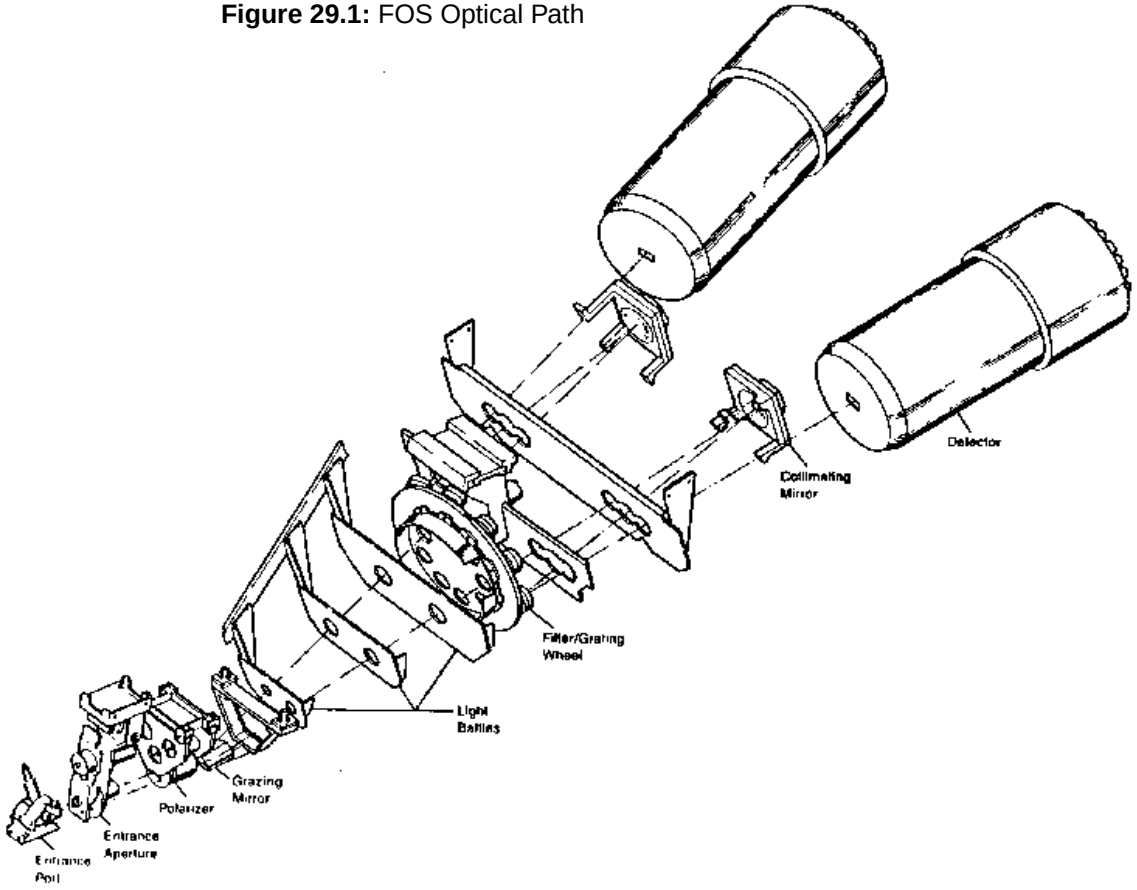

Figure 29.2: Detector Quantum Efficiencies

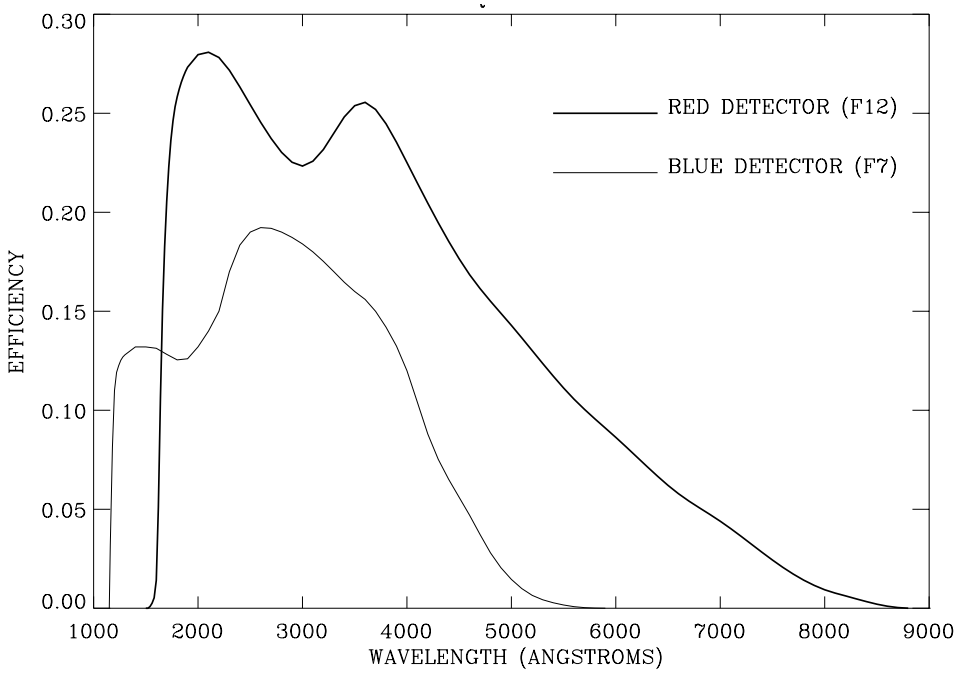

Table 29.2: Detector Characteristics

Attribute	Value
Wavelength coverage	FOS/BL: 1150Å to 5400Å in several grating settings. FOS/RD: 1620Å to 8500Å in several grating settings.
Spectral resolution	High: $\lambda/\Delta\lambda \approx 1300$. Low: $\lambda/\Delta\lambda \approx 250$.
Time resolution	$\Delta t \geq 0.033$ seconds.
Acquisition aperture	4.3″ x 4.3″ (4.3): pre-COSTAR 3.71″ x 3.66″ (4.3) : post-COSTAR
Science apertures	Largest: 4.3″ x 1.43″ (pre); 3.71″ x 1.29″ (post) (4.3). Smallest: 0.09″ square paired (0.1-PAIR).
Diode size	pre-COSTAR: width=0.356″; height=1.43″ post-COSTAR: width=0.305+/-.004″; height=1.291+/-.007″
Plate-scale	pre-COSTAR: FOS/BL and FOS/RD x=y=0.0896″ pixel^{-1} post-COSTAR[a]: FOS/BL x=.0774+/-.001″ pixel^{-1}; y=.0786+/-.001″ pixel^{-1} FOS/RD x=.0752+/-.001″ pixel^{-1}; y=.0812+/-.002″ pixel^{-1}
Mean dark count rate	FOS/BL: 0.0064 counts s^{-1} diode^{-1} FOS/RD: 0.0109 counts s^{-1} diode^{-1}
Example post-COSTAR exposure times 0.9″ (1.0) aperture	F_{1300}=2.5 x 10^{-13}, SNR=20/(1.0Å), t=260s. F_{2800}=1.3 x 10^{-13}, SNR=20/(2.0Å), t=10s (FOS/BL). F_{2800}=1.3 x 10^{-13}, SNR=20/(2.0Å), t=6.6s (FOS/RD).

a. Post-COSTAR telescope movement commanding assumed mean of *x* and *y* values as the mean plate-scale for each detector.

29.3.4 Apertures

The entrance aperture mechanism allowed selection of any one of twelve apertures for each detector. Table 29.3 lists the apertures.

The FOS aperture naming convention was to use the pre-COSTAR aperture size as aperture designation for all observing epochs despite the 16% scale magnification introduced by the COSTAR optics. There was a large aperture for acquiring targets using on-board software (pre-COSTAR: 4.3" x 4.3"; post-COSTAR: 3.7" x 3.7"; designation 4.3[1]). Since the diode array extended only 1.29" (1.43" pre-COSTAR) in the direction perpendicular to the dispersion, this largest aperture had an effective collecting area of 3.7" x 1.29" (pre-COSTAR: 4.3" x 1.43"). Other apertures included several circular apertures with sizes 0.86" (1.0), 0.43" (0.5), and 0.26" (0.3), as well as paired (UPPER and LOWER) square apertures with sizes 0.86" (1.0-PAIR), 0.43"

1. Henceforth, if pre- or post-COSTAR time periods are not specifically stated, we will routinely use post-COSTAR aperture sizes with the pre-COSTAR size aperture designation in parentheses.

Table 29.3: FOS Apertures

Designation (Header Desig.)	Number	Shape	Pre-COSTAR Size (″)	Post-COSTAR Size (″)
0.3 (B-2)	Single	Round	0.30 dia	0.26 dia
0.5 (B-1)	Single	Round	0.50 dia	0.43 dia
1.0 (B-3)	Single	Round	1.00 dia	0.86 dia
0.1-PAIR[a] A-4)	Pair	Square	0.10[a]	0.09[b]
0.25-PAIR[a] (A-3)	Pair	Square	0.25	0.21
0.5-PAIR[a] (A-2)	Pair	Square	0.50	0.43
1.0-PAIR[a] (C-1)	Pair	Square	1.00	0.86
0.25X2.0 (C-2)	Single	Rectangular	0.25 x 2.00	0.21 x 1.71
0.7X2.0-BAR (C-4)	Single	Rectangular	0.70 x 2.00	0.60 x 1.71
2.0-BAR (C-3)	Single	Square	2.00	1.71
BLANK (B-4)	NA	NA	NA	NA
4.3 (A-1)	Single	Square	4.3 x 4.3	3.66 x 3.71[c]
FAILSAFE	Pair	Square	0.50 and 4.3	0.43 and 3.7

a. Pre-COSTAR separation of PAIR apertures was 2.82", whereas post-COSTAR separation was 2.57"; pre-COSTAR aperture positions were assumed symmetric about center of SINGLE apertures. post-COSTAR PAIR “A” apertures were assumed symmetric about center of A-1 and PAIR “C” apertures symmetric about center of C-2.
b. Three of the four A-4 apertures have been consistently measured as one size and the fourth, the FOS/BL LOWER aperture, approximately 25% smaller in each dimension. Due to measurement uncertainties, the FOS/BL LOWER aperture size was determined as ranging from 0.1" (pre-COSTAR) to a size 25% smaller (see *FOS ISRs* 019 and 138).
c. Post-COSTAR size was not the same in both coordinates due to the COSTAR anamorphism (magnification factor in *x* different from that in *y*).

(0.5-PAIR), 0.21" (0.25-PAIR), and 0.09" (0.1-PAIR), for isolating spatially resolved features and for measuring the sky. In addition, a slit and two barred apertures were available (Figure 29.3 and Table 29.3). *Separate aperture sets* existed for FOS/BL and FOS/RD. Aperture size measurements were performed both pre-launch and on-orbit. Precise aperture sizes were reported in

FOS ISRs 019 and 138, for the pre- and post-COSTAR cases, respectively. Aperture positioning repeatability was extremely accurate.

Aperture Center Locations

Before COSTAR was installed, all SINGLE FOS apertures were assumed to be concentric and all spacecraft-centering operations used this assumption. Post-COSTAR SMOV calibrations indicated that the `1.0` and smaller SINGLE apertures were concentric, but that the `4.3` aperture was slightly offset, particularly for FOS/RD, from this center. This offset affected the positional accuracy determined by ACQ/BINARY and required that different flatfields be employed for the `4.3` than for the other SINGLE apertures. The degree of uncertainty in this small offset also affected precise positional determination based upon `4.3` aperture imaging or ACQ/BINARY alone. Pre-COSTAR telescope commanding assumed that the mid-point between each set of paired apertures was concentric with the SINGLE apertures. Post-COSTAR measurements led to the adoption of aperture locations that placed all of the "A" apertures at a common center, all of the "B" apertures (all SINGLE) at a slightly displaced common center, and the "C" apertures at another common center. The `1.0-PAIR` apertures were slightly displaced from all of the other paired apertures and required separate flatfields. The individual components of paired apertures were separated by approximately 2.57". All post-COSTAR telescope commanding after May 30, 1994 included these aperture location offsets.

29.3.5 Dispersers

FOS dispersers provided both "high" spectral resolution (1-6 Å-diode^{-1}, $\lambda/\Delta\lambda \approx$ 1300) and "low" spectral resolution (6-25 Å-diode^{-1}, $\lambda/\Delta\lambda \approx 250$). Their designations and basic properties are presented in Table 29.4. Full optical specification of the FOS dispersers is found in Harms et al., SPIE, 183, 74, 1989 and *FOS ISR* 127. The actual spectral resolution depended on the point spread function of HST, the dispersion, the aperture, and whether the target was physically extended. Representative line widths are given in Table 29.5.

Unlike the apertures, the same dispersers were used with both FOS/BL and FOS/RD. The dispersers and appropriate blocking filters were mounted on the Filter Grating Wheel (FGW) which always rotated in the same direction to specified locations in the beam. Due to the physical nature of the mechanism involved, the repeatability of FGW positioning in the beam was not as precise as for aperture positioning. For certain types of FOS observations, FGW positional uncertainty is an important "error source" (see Chapter 33 and *FOS ISRs* 131, 142, and 145.

29.3.6 Detector Geometry

From the photocathode, electrons were deflected magnetically *without magnification* onto the diode array of the Digicon. In this way the electronic image of the light transmitted by the aperture was projected onto the diode array. The relative size of the different apertures as they were projected onto a section of

the diode array is shown in panel (a) of Figure 29.3, which is displayed from the perspective of an observer positioned directly "behind" the detector looking out toward the sky. The individual diodes were 50 x 200 microns in physical dimension which corresponded to spacings of 0".31 (post-COSTAR) or 0".35 (pre-COSTAR) along the dispersion direction and height of 1".29 (1".43) perpendicular to it. In the FOS detector coordinate system (and throughout this handbook) dispersion lies along the *x-direction*. The *x*-coordinate is always defined positive to the left in the sense of Figure 29.3. Wavelength *always* increased with increasing x for FOS/BL gratings, but always decreased with increasing *x* for FOS/RD gratings and vice versa for the prisms. The *y*-axis of the FOS coordinate frame was perpendicular to the dispersion and was defined positive toward the "top" of the detector as shown. (As one "looks through the detector toward the sky," if east were aligned toward the +*x*-axis, then north was aligned with the +*y*-axis.) The lower paired apertures were closest to the optical axis of HST.

Panel (b) of Figure 29.3 shows three other apertures—two occulting bars and one slit—which were nearly concentric with the 4.3 aperture. Panel (c) shows the orientation of the +*y*-axis in the (V2,V3) plane for the post-COSTAR era.

COSTAR introduced a 180 degree rotation of the telescope (V2,V3) coordinate frame, not the instrument (*x*,*y*) frame. Therefore, before COSTAR, the (V2,V3) coordinate frame was rotated 180 degrees with respect to the orientations shown in Figure 29.3. The angle between FOS/BL and FOS/RD slit orientations (+*y*-directions) was always 73.6 degrees.

The deflection of the photoelectrons was controlled by an internal magnetic field, which in turn depended on a high-voltage setting. The unit of distance in the *y*-direction was the so-called *Y-base unit*. The high voltage was adjusted so that a deflection of 256 Y-base units corresponded to the 200 micron physical height of the diodes (both pre and post-COSTAR). The photocathode coordinate system extended from –2048 to +2048 Y-base units. Each disperser directed incoming light onto a different location on the photocathode as shown in Figure 29.4.

29.3.7 Waveplates and Polarizers

The FOS polarization analyzer positioned one of three elements into the optical path; a clear aperture, a thin magnesium fluroide waveplate (plate "B") plus Wollaston prism assembly, or a thick MgFl waveplate (plate "A") plus Wollaston prism assembly. One waveplate was permanently located in front of each Wollaston, however the waveplate could be rotated so as to alter the position angle of the waveplate fast axis relative to the Wollaston, in increments of 22.5 degrees. The polarimetry appendix of *FOS Instrument Handbook* version 1.1 presents a technical description of the FOS polarimeter.

The technique used for spectropolarimetry in the FOS was very similar to that developed for ground-based instruments. When introduced into the beam, the Wollaston prism assembly produced twin dispersed images of the aperture with opposite senses of polarization at the detector. In order to determine the linear and circular polarization properties of the incoming beam, usually 8 or 16

observations were taken with the waveplate turned in 45 or 22.5 degree intervals relative to the Wollaston prism. This allowed the polarization effects in the dispersing optics following the analyzing prism to be fully removed from the science observations. Waveplate "A" was recommended for use with the disperser G400H and "B" waveplate was recommended for use with the G130H, G190H, and G270H dispersers. Polarizer position "C" (clear) was the default for all non-spectropolarimetric observations.

Table 29.4: FOS Dispersers

Grating	Diode No. at Low λ	Low λ (Å)	Diode No. at High λ	High λ (Å)	Δλ (Å-Diode^{-1})	Blocking Filter
			Blue Digicon			
G130H (H13)	53	1140[a]	516[b]	1606	1.00	–
G190H (H19)	1	1573	516	2330[c]	1.47	–
G270H (H27)	1	2221	516	3301	2.09	SiO_2
G400H (H40)	1	3240	516	4822	3.07	WG 305
G570H (H57)	1	4574	516	6872[d]	4.45	WG 375
G160L (L15)	319	1140[a]	516	2508[c]	6.87	–
G650L (L65)	295	3540	373	9022[d]	25.11	WG 375
PRISM[e] (PRI)	333	1500[f]	29	6000[d]	–	–
			Red Digicon[i]			
G190H (H19)	503	1590[g]	1	2312	-1.45	–
G270H (H27)	516	2222	1	3277	-2.05	SiO_2
G400H (H40)	516	3235	1	4781	-3.00	WG 305
G570H (H57)	516	4569	1	6818	-4.37	WG 375
G780H (H78)	516	6270	126	8500[h]	-5.72	OG 530
G160L (L15)	124	1571[g]	1	2424	-6.64	–
G650L (L65)	211	3540	67	7075	-25.44	WG 375
PRISM[e] (PRI)	237	1850	497	8950[h]	–	–

a. The blue Digicon MgF_2 faceplate absorbed light shortward of 1140 Å.
b. The photocathode electron image typically was deflected across 5 diodes, effectively adding 4 diodes to the length of the diode array.
c. The second order overlapped the first order longward of 2300 Å, but its contribution was at a few percent.
d. Quantum efficiency of the blue tube was very low longward of 5500 Å.
e. PRISM wavelength direction was reversed with respect to gratings of the same detector.
f. The sapphire prism absorbed some light shortward of 1650 Å.
g. The red Digicon fused silica faceplate strongly absorbed light shortward of 1650Å.
h. Quantum efficiency of the red detector was very low longward of 8500 Å.
i. Dispersion direction was reversed for `FOS/RD` relative to `FOS/BL`.

Table 29.5: FOS Line Widths (FWHM) as a Function of Aperture Size

Designation	Size (″)	Aperture Filled with Uniform Source		Pre-COSTAR Point Source at 3400Å FWHM	Post-COSTAR Point Source at 3400Å FWHM
		G130H (Blue) FWHM[a]	G570H (Red) FWHM		
0.3	0.26(circular)	1.00 ± .01	0.95 ± .02	1.06	0.92
0.5	0.43(circular)	1.27 ± .04	1.20 ± .01	1.14	0.93
1.0	0.86(circular)	2.29 ± .02	2.23 ± .01	1.34	0.96
0.1-PAIR	0.09(square)	0.97 ± .03	0.92 ± .02	1.00	0.91
0.25-PAIR	0.21(square)	0.98 ± .01	0.96 ± .01	1.00	0.92
0.5-PAIR	0.43(square)	1.30 ± .04	1.34 ± .02	1.18	0.94
1.0-PAIR	0.86(square)	2.65 ± .02	2.71 ± .02	1.40	0.96
0.25X2.0	0.21 X 1.71(slit)	0.99 ± .01	0.96 ± .01	1.00	0.92
0.7X2.0-BAR	0.60 X 1.71	1.83 ± .02	1.90 ± .01	1.30	1.26
2.0-BAR	1.71	5.28 ± .07	5.43 ± .04	1.40	1.34
4.3	3.66 X 3.71	12.2 ± 0.1	12.2 ± 0.1	1.50	0.96

a. The FWHM are given in units of diodes. A pre-COSTAR diode was 0.356″ wide and 1.43″ high. A post-COSTAR diode was 0.305″ wide and 1.29″ high.

29.3.8 Internal Wavelength Calibration

Two Pt-Ne hollow-cathode lamps provided emission line spectra for calibrating the FOS wavelength scales. The lamp beams passed through the same optics as an external source, but they did not fill the collimator. As a result, it was possible to have an offset in the photocathode position of any particular wavelength in the dispersed internal beam and the dispersed external beam. This internal to external wavelength offset is discussed in more detail in “Wavelength Calibration” on page 32-49. Due to the effect of the FGW positional uncertainty mentioned in “Dispersers” on page 29-11, highly accurate FOS external wavelengths could be determined only with the aid of an internal WAVECAL exposure taken immediately before or after the science exposure with no intervening movement of the FGW.

Figure 29.3: Post-COSTAR Aperture Sizes Projected On Diode Array Viewed from Behind Detector Looking toward Sky

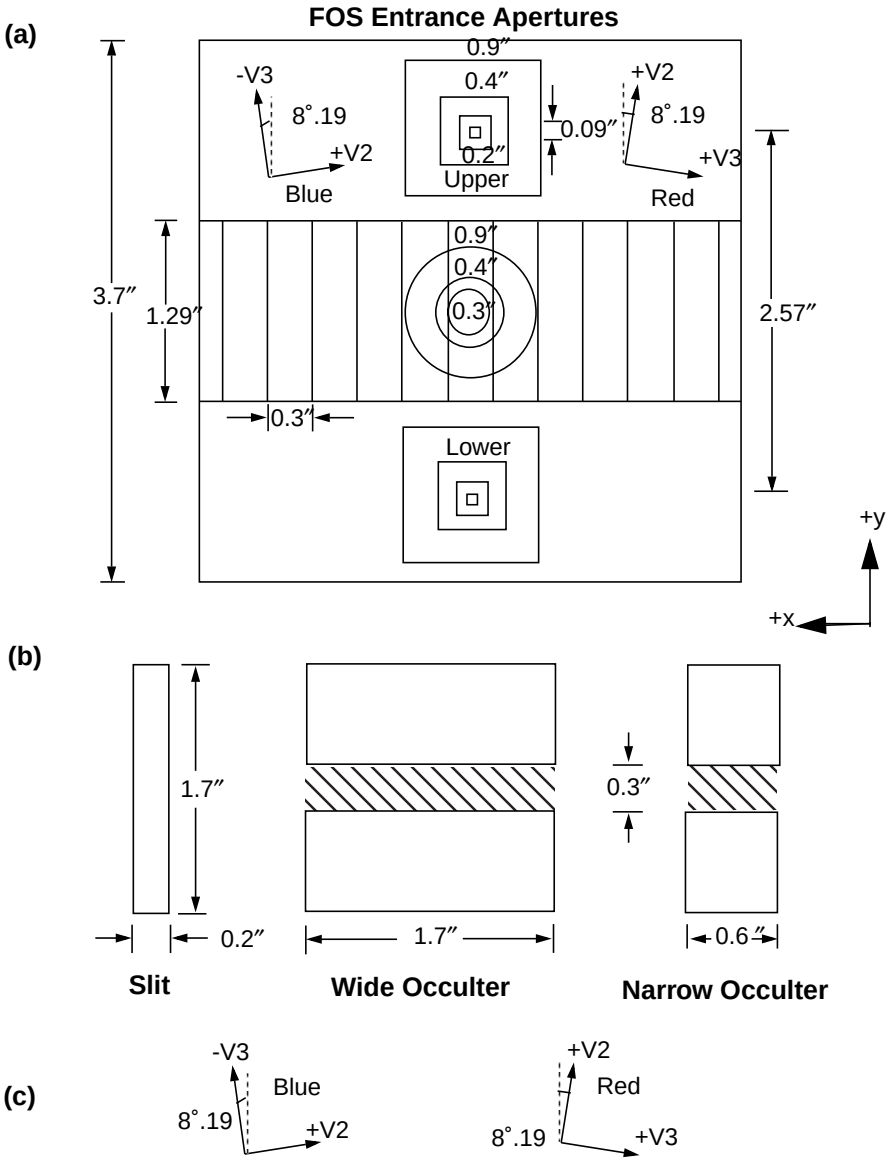

29.3.9 Data Acquisition Fundamentals

The FOS had several parameters that could be altered to change the way data was accumulated and read out. These parameters are summarized in Table 29.6.

To maximize the science data output from the FOS, routine data-taking commanding oversampled spectra and shifted the object spectrum with respect to the diode array during several subintegrations. These two procedures were called *substepping* and *overscanning*.

Table 29.6: Data Acquisition and Readout Parameters

Parameter	Description
INTS	Number of repetitions of the livetime/deadtime cycle, whereby electrons were counted in the selected diode accumulators with no changes in the magnetic deflection. Changing INTS provided a means for altering the amount of time data were collected at a given deflection value while keeing the livetime short so that as little good data as possible was rejected. The header keyword is INTS.
SUBSTEPS	Number of magnetic field deflections of the photoelectrons in the dispersion direction. The default value was 4 (quarter-stepping). The data went into new memory locations with each substep. The corresponding header keyword is NXSTEPS.
OVERSCAN	Number of times to repeat the addition of counts into the memory array. The accumulation in the memory array was such that data acquired from an offset of one diode was added at each overscan. Each offset was accompanied by a corresponding magnetic deflection in the dispersion direction so that the data from the photocathode location falls into the same memory location independent of the diode which sampled it. The default value of this parameter is 5. The purpose of overscanning was to average the response of the different diodes, including the dead diodes. The header keyword is OVERSCAN.
YSTEPS	Number of magnetic deflections of the electrons in the direction perpendicular to the dispersion. This parameter was used to map the photocathode (IMAGE mode), to switch between the two spectra produced by the polarizer, or to acquire either of the paired apertures. In the standard ACCUM mode this parameter had the default value of 1. The header keyword is YSTEPS.
SLICES/BIN	A slice consists of an entire deflection sequence. Data from each slice went to a new memory location. This was used for time resolved spectrophotometry. The header keyword is SLICE.
PATTERN	A pattern was a complete series of slices. Counts in subsequent patterns were added to the corresponding previous values in the data array. The header keyword NPAT determined the number of times a pattern should be executed to achieve the exposure time.
READOUT	A readout sent the science data to the CU/SDF computer for either storage on the tape recorder or for telemetry to the ground. FOS readouts were non-destructive and were performed at regular intervals (~4 min for the FOS/BL and ~2 min for the FOS/RD) without memory clears in order to protect against loss of data. The last readout contained all the data accumulated since the previous memory clear. In the standard ACCUM mode each readout is stored as a separate group in the data files.
Memory clears	A memory clear set to zero all locations in the science data array to allow input of new data. The number of times that a memory clear was repeated in a given observation is given in the NMCLEARS keyword.

Substepping was used to better sample the spectrum in the wavelength direction. This was necessary because a spectral resolution element mapped to a single diode, so critical sampling of the line spread function required substepping. *Overscanning* was used to assure that each pixel in the final spectrum contained data received from multiple diodes (to smooth out diode-to-diode variations and insure against data loss when a single diode was disabled). Both substepping and overscanning relied on the magnetic focus assembly in the Digicon detector to magnetically deflect the photoelectrons in the dispersion direction so that they fell on slightly different locations on the diode array.

For substepping, the spectrum was deflected by a fraction of a diode in the dispersion direction (where the fraction was given by 1/NXSTEPS and NXSTEPS is a header keyword; see Chapter 30). The diodes were read out into unique memory locations for each substep and the substepping was performed NXSTEPS times.

Figure 29.4: Approximate Location of Spectra on the Photocathode.
Dashed Lines Represent Red Detector, Solid Lines Represent Blue Detector

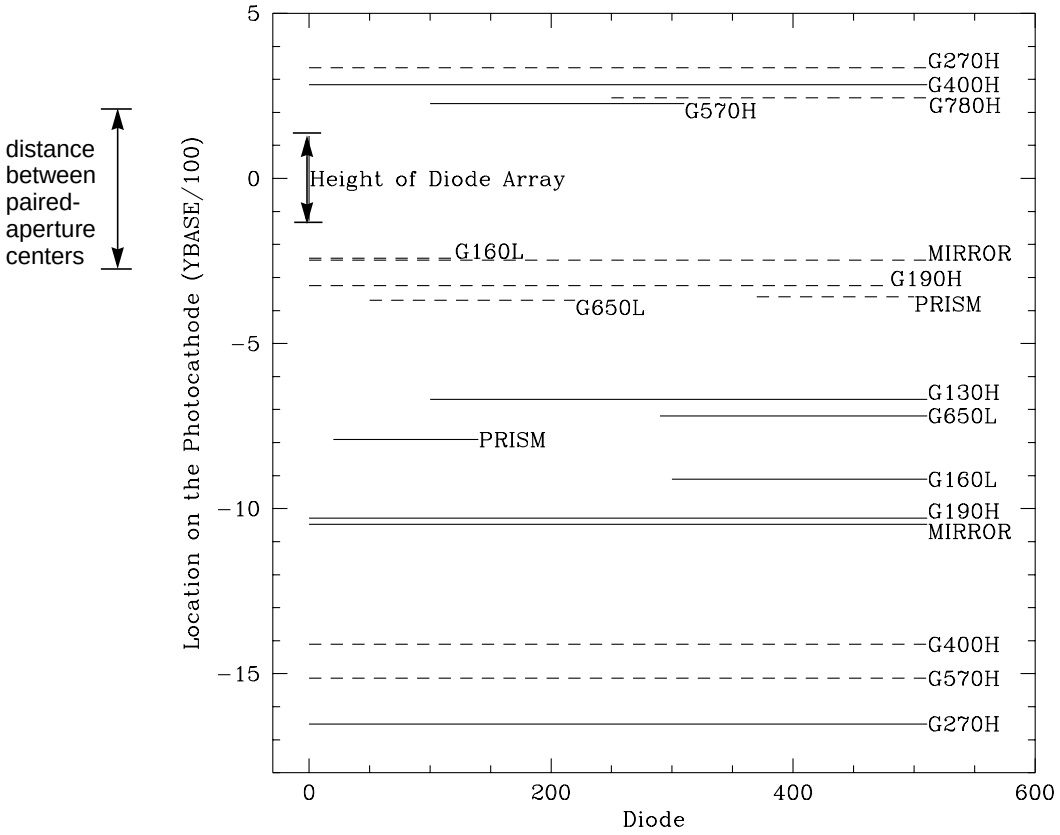

For *overscanning*, the process of substepping was continued over more than one diode in the dispersion direction. A complete round of substepping was performed for each overscan step. The number of overscan steps performed was determined by the overscan parameter (header keyword OVERSCAN). Each time a given wavelength position was deflected onto and measured by a new overscan diode, its counts were co-added into the same memory location in the FOS microprocessor. When using the full 512-element diode array, the result was a spectrum with 512 * NXSTEPS plus a small number (NXSTEPS x (OVERSCAN – 1)) of *edge* pixels. Each pixel (excluding the edge pixels) had data contributed from the number of diodes specified by OVERSCAN. Thus, substepping changed the number of pixels in the final spectrum; and overscanning principally changed the number of diodes that contributed to a single pixel. Although the number of diodes in the diode array was 512, the actual number of diodes read out could be restricted via a wavelength range specification in certain modes. The number of pixels in any observation is given by the equation:

$$\#\ of\ pixels = (\#\ of\ diodes + (\text{OVERSCAN} - 1)) \times \text{NXSTEPS}$$

Although other values could be specified, all FOS data acquisition modes, except ACQ/PEAK, used by default, NXSTEPS=4 and OVERSCAN=5. ACQ/PEAK observations used NXSTEPS=1 and OVERSCAN=1.

The default values of NXSTEPS=4 and OVERSCAN=5 yielded a typical spectrum of 2064 pixels in which a given diode contributed to the data in NXSTEPS x OVERSCAN, normally 20, consecutive pixels and a given pixel normally contained contributions from 5 adjacent diodes. The exposure time devoted to the first 2048 pixels (that is, all but edge pixels—described below) was 1/NXSTEPS (1/4) of the total exposure time specified for the observation.

Due to the nature of FOS overscanning, (OVERSCAN – 1) groups of NXSTEPS pixels at the +*x* edge of the diode array (long wavelength end for FOS/BL gratings and vice versa for FOS/RD) had contributions from fewer than OVERSCAN diodes. There were 16 such pixels in the default case, with the first four of these receiving 4/5 of the exposure of the first "normal" 2048 pixels, the next group of four receiving 3/5 of the typical exposure, the next four 2/5, and the last 4 1/5 of the normal pixel exposure. All standard pipeline routines within STSDAS and **calfos** handle these calculations automatically.

STScI FOS calibrations, which are described in chapter 31, support only OVERSCAN=5 observations. FOS calibrations are also designed for NXSTEPS=4, but may be easily adapted to all allowed values of NXSTEPS by a straightforward automatic resampling of standard NXSTEPS=4 reference files.

Note: Due to this FOS-specific substepping, the typical effective exposure *per pixel* in any FOS observation was the total observation exposure time divided by NXSTEPS. A few (i.e., NXSTEP*(OVERSCAN-1), typically 16, "edge" pixels had even less effective exposure.

29.3.10 Photon Counting Characteristics

The FOS Digicons were photon counting detectors. The output of the diodes was stored in 16-bit accumulators within the FOS microprocessor. These accumulators were readout at intervals defined by the detector and the data-taking mode, e.g., roughly every two minutes for FOS/RD ACCUM. Sufficiently bright sources could produce more than 65535 counts (2^{16}–1) in an interval and thereby suffer one, *or more*, occurrences of accumulator "wrap around." (see "unwrap" on page 33-11).

29.3.11 Other Characteristics

To minimize external influences on the magnetic deflection of electrons from the photocathode onto the diode array, both Digicons were magnetically shielded. However—especially for FOS/RD—the shielding was inadequate. Thus, telescope orientation relative to the Earth's magnetic field influenced the magnetic

deflection characteristics of the FOS. This produced a *geomagnetically induced image motion* (GIM, occasionally referred to as GIMP). A post-observation pipeline correction algorithm corrected for this effect *in the x-direction only* prior to April 5, 1993. In order to minimize this effect, on-board software was implemented on April 5, 1993, to compensate for this error in both detector coordinates. Residual uncertainties remained, however, which affected the calibration accuracy of the instrument, as described further in “Geomagnetically Induced Image Motion (GIM)” on page 32-14.

The FOS Y-bases—the amount of magnetic deflection necessary to direct the photoelectrons from the photocathode onto the diode array—did not remain constant over the FOS lifetime due to hysteresis in the repeated magnetization and de-magnetization cycling of the Digicons. The detectors accumulated residual magnetization over time that required progressively larger deflections to steer the photoelectrons onto the diode array. Uncertainties in the Y-base values remain an important limitation on photometric accuracy (see “Y-bases” on page 32-7 and “Image Centering (Image Location) Factors” on page 32-22).

29.3.12 Influence of COSTAR on FOS Data

COSTAR was installed in HST during the First Servicing Mission in December 1993 to correct the spherical aberration of the HST primary mirror. COSTAR restored the point spread function (PSF) to nearly the HST design specifications. Aperture throughputs were also dramatically improved. For example, the throughputs of the `4.3`, `1.0`, and `0.3` apertures increased by factors of 1.3, 2.0, and 2.5, respectively. The throughput increase for the `4.3` aperture was compensated to a large extent by losses due to the two additional reflections, but small aperture relative throughput improvements allowed much of the original FOS science program goals to be pursued post-COSTAR, particularly in those programs that required excellent small aperture PSFs and LSFs.

The two COSTAR correcting mirrors, M1 and M2, introduced a modest anamorphic magnification which differed by approximately two percent between COSTAR *x* and *y*. All aperture and pixel scales decreased to approximately 0.86 of their pre-COSTAR values. For example, the height of the diodes projected on the sky changed from 1.43" pre-COSTAR to 1.29" post-COSTAR.

Between December 28, 1993, and February 1, 1994, numerous adjustments were made to the COSTAR mirrors. No effective instrumental calibration is available for any FOS data taken in that time period. By February 1, 1994, the COSTAR FOS-correction mirrors had been optimally aligned. The post-COSTAR FOS instrumental configuration that is calibrated by STScI began on February 1, 1994.

Throughout most spectral regions COSTAR introduced only moderate modifications to the wavelength dependence of instrumental sensitivity, however, an unanticipated broad decrease in instrumental sensitivity was recorded for FOS/BL in the wavelength range 1600–2400 Å. This feature was roughly Gaussian in shape and at 2000 Å. the post-COSTAR sensitivity was approximately 70% of its expected post-COSTAR value.

Additionally, the narrower post-COSTAR PSF more selectively illuminated fine-scale photocathode granularity rather than smoothing it out as was the case with the aberrated PSF. As a result, very precise target acquisitions became an important requirement for both science and calibration programs that needed to achieve high flatfielding accuracy.

The narrower PSF also led to a narrower line spread function (LSF) for post-COSTAR data compared to the pre-COSTAR era. Polarimetric data were affected, because additional optical elements (mirrors) were introduced into the light path, and this changed the characteristics of the incoming wavefronts. On the other hand, the internal wavelength calibration was not measurably affected, although some indication of grating-dependent internal-to-external wavelength offset changes was seen.

29.4 Science Observing Modes

The FOS employed one of six basic data taking modes to acquire science data:

- Spectrophotometry (ACCUM).
- Rapid Readout (RAPID).
- Time-Resolved Photometry (PERIOD).
- Spectropolarimetry.
- Image.
- Paired Aperture Observing.

ACCUM was by far the most commonly used observing mode. In this section we provide basic descriptions of each of these science data taking modes and their scientific uses. More detailed discussions of each instrument mode including operational characteristics, the diagnostic paper products, the structure of the electronic data products and methods of data quality analysis are provided in Chapter 30.

29.4.1 Spectrophotometry Mode (ACCUM)

ACCUM was the standard FOS spectrophotometric data taking mode. Data were acquired with NXSTEPS=4 and OVERSCAN=5 only. Spectra were read out at approximate 2 minute (FOS/RD) or 4 minute (FOS/BL) intervals and the accumulated sum after each read was stored and recorded in consecutive groups in the standard output data files (see next chapter for description of these files). Therefore, each consecutive spectrum was made up of the sum of all previous intervals of data in an ACCUM observation.

29.4.2 Rapid Readout Mode (RAPID)

Observations requiring higher time resolution than that provided by ACCUM mode used RAPID mode in which the diode array was read out at a rate set by the observer. Readout rates as fast as 0.033 sec were possible (0.035 sec was the fastest ever implemented). NXSTEPS=1, 2, or 4 and OVERSCAN=5 (or, rarely, 1) were normally used, though the full set of commandable values was available. The actual percentage of specified dwell time that was spent exposing could vary substantially depending upon how instrumental parameters were chosen. Timing precision more accurate than 0.125 seconds requires special analysis of engineering data stream information (see timing discussion in Chapter 33). Unlike ACCUM, the actual spectrum obtained in each individual time interval was recorded in the output data products.

29.4.3 Time-Resolved Spectrophotometry (PERIOD)

As a result of implementation errors there were no fully successful PERIOD mode observations made in the FOS science program. Successful tests were performed during Science Verification.

This mode was designed for objects with known periodicity in the 50 msec to 100 sec range. To maintain the phase information of these observations, the known period (CYCLE-TIME) of the object was divided into *bins* or *slices*, where each bin had a duration time = period / bins. The spectra acquired in this mode were stored in the different bins which corresponded to a given phase of the period. The spectral information obtained in each period cycle was added to the appropriate phase bin (so long as the period was known accurately). Onboard memory limitations placed substantial restrictions on the number of diodes that could be read out and the number of phase bins that could be sampled.

29.4.4 Spectropolarimetry Mode

Polarimetry data consist of a number of consecutive ACCUM-like exposures (POLSCAN=16, 8, or 4) with the waveplate set at POLSCAN different angles (all within one target visibility period). The Wollaston prism split the light beam into two spectra corresponding to the orthogonal directions of polarization. Although SINGLE apertures were always used, both spectra illuminated different portions of the photocathode—one above, one below the standard SINGLE aperture Y-base location for the disperser employed. Hence, each exposure consisted of the two orthogonal spectra obtained with a single waveplate angle. The first spectrum corresponded to the first pass direction (ordinary ray), the second to the second pass direction (extraordinary ray). These spectra were deflected alternately (*not simultaneously*) onto the diode array, recorded as the two pass directions, and stored as a single group in the raw data file. The total exposure time specified in the exposure logsheet was divided equally among each of the POLSCAN steps with one-half of the resultant exposure times spent observing each pass direction. These requirements, combined with large instrument overheads, placed tight limits on the length of any individual polarizer position exposure.

Chapter 32 discusses how Y-base positional uncertainties and GIM effects, coupled with the large pre-COSTAR PSF and the influence of the additional reflections in COSTAR, limited the accuracies of FOS polarimetric observations.

29.4.5 Image Mode

IMAGE mode observations could be made with either the camera MIRROR (as in ACQ images discussed above) or with a disperser in the beam. Normally IMAGE mode observations used NXSTEPS=4 and OVERSCAN=5, but the full set of commandable values were available. In IMAGE mode observations both the number and length of rasters and the *y*-position of each raster could be specified, so that: 1) a white-light image of all or a portion of the aperture was possible with the MIRROR, and 2) spectra from different portions of the aperture were sampled with a disperser.

ACQ mode images, discussed above, simply used a pre-defined, optimized set of IMAGE mode parameters. Most dispersed light IMAGE mode observations were made for specialized calibration purposes, but this mode was occasionally used for interactive target acquisitions of moving targets (the so-called dispersed light interactive target acquisition technique).

29.4.6 Science Data-Taking with Paired Apertures

Depending upon the value of the STEP-PATT RPS2 (RPSS) parameter, paired aperture observations could invoke a different detector readout pattern from that employed for single apertures for ACCUM and RAPID exposures. In certain circumstances (see next chapter) readout deflections were alternated equally between upper and lower paired apertures at approximate 10 second intervals for the duration of the exposure. An additional, but never used, pattern allowed such upper and lower aperture samplings and an additional background sample halfway between the apertures.

29.5 Target Acquisition

In order for FOS to have observed a target, that target must, naturally, have been located in the instrument aperture. Several techniques for positioning the target in the aperture were available to FOS observers, including:

- ***An FOS Onboard target acquisition:*** Used either a Binary Acquisition (ACQ/BINARY), a Peakup or Peakdown (ACQ/PEAK), an interactive acquisition (INT ACQ), an early FOS Image (ACQ) or a firmware acquisitions (ACQ/FIRMWARE).

- ***Blind pointing*** (i.e., observe at the telescope pointing immediately following the guide star acquisition without further refinement of telescope position). This was rarely used because the one sigma accuracy was on the order of 1".
- ***GHRS-assisted acquisition***: GHRS could be used to acquire an object followed by slew and additional centering with FOS. This option was rarely used as the equivalent FOS overheads were more efficient. Conversely, FOS-assisted acquisitions for GHRS were common in Cycles 5 and 6 (see *GHRS ISR* 068 and *FOS Instrument Handbook* version 6 for details).
- ***WF/PC1-assisted acquisition***: Similar in principle to GHRS-assisted acquisition except centering slew calculated on ground after WF/PC-1 exposure. Rarely used, this option was only available pre-COSTAR (prior to December 15, 1993).
- ***Reuse target offset***: In order to avoid unnecessary overhead times, a new technique was developed for proposals that required more than one visit to a target within a few days (up to two months). This *reuse target offset* method, first employed in December 1994, allowed the instrument to use a target offset that was derived in the acquisition for an initial visit during subsequent visits so that these later visits need use only a single-stage peak-up/peak-down acquisition to reconfirm the correct centering of the target in the aperture. Limiting accuracies of 0.03" were commonly achieved.

The overwhelming majority of FOS target acquisitions used the onboard acquisition modes ACQ/BINARY and ACQ/PEAK. A brief description of each of the FOS acquisition modes is provided below, and a more complete description of the acquisition modes, the data they produced and how to determine the target centering accuracy for a particular observation is provided in “Assessing FOS Acquisitions” on page 30-26.

Researchers will want to remember that FOS instrument performance (flatfields and sensitivity, especially) is best understood for the very center of the apertures. The accuracy inherent to the target acquisition strategy employed will therefore determine the calibration accuracy that can later be reached with a particular dataset. For each set of FOS observations of a given source, the first dataset taken was the FOS target acquisition image.[2]

The target acquisition employed for a given observation will determine the accuracy of the target centering in the science aperture, which in turn affects the calibration accuracy of the science data itself. Analysis of FOS observation data quality is incomplete without retrieval and assessment of the target acquisition exposures.

2. If a blind pointing was done, there will not have been a target acquisition image, unless one was specifically requested.

29.5.1 FOS Onboard Acquisitions

BINARY acquisition (ACQ/BINARY)

In a BINARY acquisition, single raster images of the target were made with the MIRROR in each of the upper, middle, and lower thirds of the 4.3 aperture. The aperture segment containing the brightest image was determined and the brightest pixel provided the *x*-position of the target. Next a scheme involving a series of up to eight successively smaller electronic deflections was employed to find the Y-base that placed the target on the edge of the diode array. During this procedure all image offsets were performed electronically—the target was not moved until the actual aperture centering slew was calculated by the algorithm. Due to its efficiency (but with limited centering accuracy), ACQ/BINARY was the acquisition method of choice for point sources fainter than V~15 in programs for which S/N < 30 was sufficient. The method had a restricted dynamic range of brightness and, in the pre-COSTAR period, was severely limited by the aberrated PSF. Acquisition of faint sources that required high pointing accuracy often began with ACQ/BINARY and concluded with one or more ACQ/PEAK sequences.

Peakup or Peakdown Acquisition (ACQ/PEAK)

In an ACQ/PEAK sequence, NXSTEP=1 integrations were performed at a series of defined positions on the sky with a science aperture and either MIRROR or a disperser in place. At the end of the slew sequence, the telescope was returned to the position with either the most (peakup) or fewest (peakdown) counts (return to brightest or return to faintest). Overheads for ACQ/PEAK slew patterns were large (30-45 seconds per dwell). ACQ/PEAK was generally required for the following types of observations:

- All exposures requiring S/N>30.
- High wavelength accuracy.
- Pointing more accurate than 0.2".
- Objects too bright to acquire with the MIRROR.
- Objects too variable to acquire with ACQ/BINARY.
- Centering targets in apertures smaller than `1.0`.
- Positioning bright sources behind the occulting bars.

Interactive Acquisition Image (INT ACQ)

In an interactive acquisition, the camera MIRROR was used to obtain an image of the `4.3` aperture field. The image was downlinked and analyzed in real time to determine the required slew to center the target. The slew was uplinked and FOS science observations proceeded, generally at the start of the next target visibility. This method was employed for a number of moving target acquisitions.

Early FOS Acquisition Image (ACQ)

When taking an early FOS acquisition image, a camera MIRROR image of the `4.3` aperture was acquired in similar fashion to that described for INT ACQ above, but, in this case, the science observations were performed at a later date. Often the early FOS image was used to determine geometry of crowded fields or

precise offsets from a nearby bright target likely to be acquired by ACQ/PEAK or ACQ/BINARY.

Firmware Acquisition (ACQ/FIRMWARE)

Firmware acquisition was an engineering mode that mapped the camera MIRROR image of the `4.3` aperture in *x* and *y* with small, selectable *y* raster increments. The microprocessor filtered this aperture map in real time and found *y*-positions of the peaks by fitting triangles through the data. ACQ/FIRMWARE was less efficient than ACQ/BINARY and failed if more than one object were found. This mode was used for a small number of pre-COSTAR planetary satellite acquisitions and was not used in the post-COSTAR science program.

Chapter 30

FOS Data Structures and Data Assessment

In This Chapter...

This chapter assumes that you have selected and retrieved some FOS data from the HST Data Archive or that you have your own data. We describe the contents of the delivered data, the structure of the various data files, and how to assess them with particular emphasis on the utility of the FOS paper products. We also provide a few examples of how Phase II proposals were turned into observations and data products.

30.1 Contents of Delivered Data

Unless you have read your FOS data from very old data tapes, the data you have on your machine will be in FITS format. These files need to be converted to GEIS format with the STSDAS routine **strfits**, as is described in Chapter 2 (Volume 1). The resulting GEIS format files will have default suffixes, as described in Table 30.1.

You will be most interested in the contents of the `.c1*`, `.c0*`, and `.c2*` files as these contain the flux-calibrated data, wavelengths and errors for an exposure. The easiest way to get a quick glance at your spectra is by using the routine **splot** or **fwplot** if you want to plot wavelength vs. flux (see “FOS and GHRS Spectra” on page 3-17). We recommend that you generate the FOS paper products for your data with the STSDAS routine **pp_dads** and obtain a variety of displays and

tables which, as we shall see in “FOS Paper Products” on page 30-15, can facilitate the assessment of your data quality.

Table 30.1: FOS File Name Suffixes

Suffix	File Contents	Suffix	File Contents
Raw Data Files (input for calfos)		***Calibrated Data Files (output from calfos)***	
.d0h/.d0d	Science data image	.c0h/.c0d	Calibrated wavelengths
.q0h/.q0d	Science data quality	.c1h/.c1d	Calibrated fluxes
.shh/.shd	Standard header packet	.c2h/.c2d	Propagated statistical error
.d1h/.d1d	Science trailer line	.c3h/.c3d	Special statistics
.ulh/.uld	Unique data log	.c4h/.c4d	Count rate
.x0h/.x0d	Science header line	.c5h/.c5d	Flat-fielded object spectra
.xqh/.xqd	Science header line data quality	.c6h/.c6d	Flat-fielded sky spectra
.q1h / .q1d	Science trailer line data quality	.c7h/.c7d	Background spectra
		.c8h/.c8d	Flat-fielded object minus smoothed sky spectra
		.cqh/.cqd	Calibrated science data quality
Additional Files			
.jih/.jit	Jitter files (.cmh, .cmj, .cmi)	.trl	Trailer file
.pdq/.ocx	PODPS/OPUS data quality files		

30.1.1 Uncalibrated (Raw) Data Files

Table 30.1 lists the science files that are used as required input to **calfos**. These files are described briefly below.

Science Data Files (.d0h/.d0d)

Science data files contain single-precision floating point values that represent the number of detected counts accumulated in each pixel. The number of data elements in the one-dimensional science data array depends on the observation mode; specifically, the number of diodes, the number of substeps, the number of Y steps, and the number of repeats (sometimes called *slices* or *bins*) used in the observation. The maximum number of data elements is 12288. The associated header file also provides information on the different steps to be performed during pipeline calibration processing, and the reference files and tables to be used in the calibration.

Science Header Line (.x0h/.x0d)

The science header line (SHL) file is a one dimensional array with a length equal to a line of the science data. It contains a partial copy of the unique data log.

Science Trailer Line (.d1h/.d1d)

The science trailer line (STL) file is also a one dimensional array containing the number of measurements rejected from the various combinations of *x* substeps, *y* steps, repeats, etc. The information in these files is used to compute the total effective exposure time per pixel which is later used to convert the counts into count rates.

Data Quality Files (.q1h/.q1d)

The science data files, science header line files, and the science trailer files have corresponding data quality files that contain the flags for bad or suspect data. These raw data quality files have quality flags as follows:

- *Good* data has the data quality flag =1.
- *Raw data dropouts* and *filled raw data* have the data quality flag =16.
- Data *failing a Reed-Solomon error check* has the data quality flag =100.
- *Fill data* have the data quality flag =800.

The data quality files are identified by the suffixes .`q0h`, .`q0d`, .`xqh`, .`xqd`, .`q1h`, and .`q1d` corresponding to the science data, science header, and science trailer files. Table 30.2 lists FOS data quality flags.

Standard Header Packet (.shh/.shd)

The standard header packet (SHP) contains the telemetry values for engineering data and some FOS-unique data. The engineering data include temperatures, currents, and voltages at various points in the instrument. The FOS-unique data varies depending on the onboard processing used for a given observation. The header packet also contains information used in the operation of the spacecraft, such as target name, position and velocity of the telescope, the right ascension and declination of the target, the sun, and the moon, and other proposal information used in the observation which was provided in Phase II of the proposal process.

Unique Data Log (.ulh/.uld)

The unique data log (UDL) contains the mechanism control blocks used to control the entrance aperture, entrance port, polarizer, and filter grating wheel assembly. This file also contains the discriminator level, disabled diode table, serial engineering data, instrument configuration, and exposure parameters.

Trailer File (.trl)

The trailer file contains many messages generated by the so-called “generic conversion” of the data from what was onboard the spacecraft into STSDAS images. These messages may contain information on missing or filled data packets. Informational messages produced by **calfos** during calibration are also stored in the trailer file. The trailer file is identified by the suffix .`trl`.

30.1.2 Calibrated Data Files

Several types of calibrated output files are produced by **calfos**. These are listed in Table 30.1. More extensive descriptions of each type of file are provided below.

Calibrated Wavelength Files (.c0h/.c0d)

These files contain single-precision floating point calibrated vacuum wavelengths corresponding to the center of each pixel of the science data. All FOS wavelength solutions assume the first pixel is pixel 0.

Calibrated Flux Files (.c1h/.c1d)

These files contain single-precision floating point calibrated fluxes (in ergs sec^{-1} cm^{-2} $Å^{-1}$) corresponding to each pixel of the science data.

Calibrated Statistical Error Files (.c2h/.c2d)

These files contain the statistical errors of the original data. These files are calibrated in lock-step with the science data files. *Errors caused by sky and background subtraction, flatfields, and sensitivity are not included in the error estimates.*

Calibrated Special Mode Data Files (.c3h/.c3d)

Data acquired in the rapid-readout, time-resolved, or spectropolarimetry modes require processing steps in addition to (or complementing) those used for standard ACCUM data. The calibrated data are then stored in special mode data files. For RAPID mode, the files contain the total flux, integrated over all pixels, and the associated statistical error for each readout. For TIME RESOLVED mode, the files contain the pixel-by-pixel average of all slices or bins, the difference between each slice or bin and the average, and the average propagated statistical errors. For POLARIMETRY mode, the file contains the Stokes I, Q, U, and V parameters, the linear and circular polarization, and the polarization position angle. The polarimetric quantities and the propagated errors are calculated for each of the separate pass directions, the combined pass direction data, and the combined pass direction corrected for interference and instrumental orientation.

Calibrated Data Quality Files (.cqh/.cqd)

The quality flags in these files flag the bad pixel values in the calibrated files. The quality flags from the raw data are updated and additional flags are added for problems detected in the calibration process. The data quality flags are defined in Table 30.2.

Intermediate Calibrated Output Data Files (.c4* - c8*)

At most, six sets of intermediate calibrated output files are produced depending on the observation mode.

- ***Count Rate Object (and Sky) Spectra:*** The files containing the count rate spectra are corrected for overscanning, noise rejection, and lost signal caused by disabled diodes. These files are identified by the suffixes .c4h and .c4d.

Table 30.2: FOS Data Quality Flag Values

Flag Value	Description
Category 1: Data not useful. Data values set to zero.	
800	Data filled
700	Data filled due to GIM correction
400	Disabled channel
300	Severe saturation (uncertainty greater than 50%)
200	Inverse sensitivity invalid ($\lambda < 1100$ Å or $\lambda > 7000$ Å)
Category 2: Data Uncertain. Uncertainty not Indicated in Error Calc.	
190	Large saturation correction (uncertainty greater than 20%)
170	Intermittent noisy channel
160	Intermittent dead channel
130	Moderate saturation correction (uncertainty greater than 5%)
120	Sky or background fixed or extrapolated
100	Reed-Solomon decoding error
Category 3: Data uncertain. Uncertainty in propagated error file	
50	Sampling less than 50% of nominal

- ***Flatfielded Object Count Rate Spectrum:*** These files contain .c4 object-only data further corrected for paired pulses, detector background, flatfield structure and, if applicable, pipeline corrected for GIM effects. The flatfielded object spectrum files are identified by the suffixes .c5h and .c5d.
- ***Flatfielded Sky Count Rate Spectrum:*** These files contain .c4 sky-only data further corrected for flatfield structure and, if applicable, also pipeline corrected for GIM effects. The flatfielded sky spectrum files are produced only if a sky observation was obtained. These files are identified by the suffixes .c6h and .c6d.
- ***Background Count Rate Spectrum:*** The scaled background spectrum that has been subtracted from the .c4 product is identified by the suffixes .c7h and .c7d.
- ***Flatfielded and sky-subtracted Object Count Rate Spectrum:*** If the sky is observed, then a smoothed sky-subtracted object spectrum prior to flux calibration is produced. The files containing the smoothed sky-subtracted object spectrum are identified by the suffixes .c8h and .c8d.

Trailer File (.trl)

We list the trailer file again as any log comments written by the pipeline **calfos** procedures are appended to spacecraft and generic conversion information already in the file. The trailer file is identified by the suffix `.trl`.

30.1.3 Paired-Aperture File Structures

The FOS paired apertures were sampled in two different ways which lead to very different internal file structures and data products:

- ***Case 1***: RPS2 (RPSS) specification of STEP-PATT=SINGLE which leads to group parameter APER_POS=SINGLE and header keyword YSTEP1=OBJ.
- ***Case 2***: RPS2 (RPSS) specification of STEP-PATT=OBJ-OBJ or OBJ-SKY (in early cycles referred to as STAR-SKY) which leads to group parameter APER_POS=UPPER or LOWER and header keywords YSTEP1 and YSTEP2 being populated with either OBJ (STAR) or SKY as appropriate. Anomalies exist in some archived datasets that will result in incorrect **calfos** processing of paired aperture data (see “Paired Aperture Calibration Anomaly” on page 31-25).

For case 1, the files are identical to those for single aperture data and as described in the foregoing data product sections.

For case 2, measures were taken from the upper and lower sections of the aperture (always starting in the lower aperture section which has the more negative Y-base value) in approximate 10-second alternating segments, readout to memory at the interval appropriate to the data-taking mode (either ACCUM or RAPID). In the `.d0*` files the data are stored in groups that are twice as long as single aperture groups, e.g., the default paired aperture ACCUM group size is 4128 pixels. The first 2064 pixels correspond to data readout at the Y-base for data taken in YSTEP1 and the second 2064 pixels are from YSTEP2. YSTEP1, which can be either OBJ (STAR) or SKY, always corresponds to the lower aperture. (The mapping of OBJ (STAR) and SKY to upper and lower halves of the aperture was dependent upon user-specification.) Case 2 `.c4*` files contain twice as many groups as in case 1 with the odd-numbered group containing to the count rate spectrum groups for YSTEP1 and the even-numbered groups containing the count rate spectrum groups for YSTEP2.

30.1.4 Other Important Observation-related Files

Observation Log Files (.jih/.jit)

As of February 1995, the observation log (or jitter) files (`.jih`, `.jit` ,etc), which are provided by the Observatory Monitoring System (OMS), became routinely available (some files from the October 1994 through February 1995 time period are also available). These can give useful information, such as telescope performance during the observation and the position of the target within the aperture. A so-called *jitter ball* is a routine part of all FOS paper products for

which jitter files exist (see Figure 30.8). This plot shows (V2,V3) motions of the FGSs needed to keep the guide stars centered, recorded every six seconds throughout the exposure. See Appendix C for a description of the observation logs and jitter files.

PODPS Data Quality File (.pdq)

STScI staff performed a quick Data Quality Assessment (DQA) of the target acquisitions and the science observations. This assessment identified any target acquisition failures, guide star acquisition failures, other spacecraft anomalies, or instrumental problems; the assessment was recorded in the data quality keywords of the PDQ (Procedural Data Quality) file. PDQ files are archived to data class PDQ and can be retrieved from the HST Archive using StarView. The FOS paper products list each relevant PDQ file comment for every exposure.

OCX files (Observatory Support System (OSS) Observer Comment files) contain information about the success or failure of target acquisitions and science observations. Before April 17, 1992, OCX files were not always archived separately, and, in some cases, were prepended to the RSDP pipeline history file, the `.trl` trailer file. After February 1995, OCX files were produced only to document real-time activity (e.g., interactive target acquisition) in support of an observation. After October 1996, OCX files may contain information about observation execution problems.

The PDQ files and the comments they contain should not be over-interpreted. The remarks were based upon a visual examination of the data and the experience of the OPUS staff. Technical remarks are usually sound, but some comments about the “quality” of the observations can arise from an incomplete knowledge of the science goals of the original proposer. Unless the object was significantly miscentered, for example, the achieved signal-to-noise is probably close to what was expected, even if it may appear low in a single exposure. To assess whether or not a low or varying flux is meaningful, you should examine the jitter file or other records of spacecraft performance. The lack of a comment is also not a guarantee that there were not some problems with the data.

30.1.5 Reference Files and Tables

The calibration pipeline used reference files and tables to flux calibrate FOS data. Data in the archive and the data that were sent to GOs were calibrated with the reference files that were available at the time of the observation. These are generally not the “best” files to use to calibrate these data today. StarView allows you to retrieve either the “used” or the “best” reference files. The “best” reference files reflect our accumulated experience of FOS calibrations and derive from the late 1997 FOS closeout calibration analyses.

Naming and Structure of FOS Reference Files and Tables

The reference files and tables are typically referred to by the name of the Calibration Data Base System (CDBS) reference relation that holds their names. The suffixes of the reference tables and files are of the form .cy*n*, .r*n*h and .r*n*d where *n* represents a value from 0 to 9 and A to D (see Table 30.3). These files are

maintained in the CDBS. The STScI web site also includes a catalog of these tables and files.

A thorough description of the internal header and data formats of FOS reference files and tables is beyond the scope of this document, but all this information can be found in rigorous detail in STScI document ICD-47 which is available from the FOS WWW page and in paper format from `help@stsci.edu`. A description of what each FOS reference file and table is used for is found in “Details of the FOS Pipeline Process” on page 31-13.

Except for some spectropolarimetric reference files, which are twice this length (for two pass directions), all reference files contain a vector of length:

$$(N_{chan} + N_{over} - 1) \times N_x$$

Where

- *Nchan* – is the number of channels observed (keyword NCHNLS).
- *Nover* – is the number of channels multiplexed (keyword OVERSCAN).
- *Nx* – is the number of substeps (keyword NXSTEPS).

Although the reference files can be generated for any combination of NXSTEPS, FCHNL (first channel), NCHNLS, and OVERSCAN, the routine calibration reference files have a length of 2064 pixels, corresponding to the standard keyword values:

- NXSTEPS = 4
- FCHNL = 0
- NCHNLS = 512
- OVERSCAN = 5

For other values of FCHNL, NCHNLS, and NXSTEPS **calfos** interpolates from or resamples the standard reference files. *Only* OVERSCAN = 5 i*s supported by FOS calibration*.

Table 30.3: FOS Reference Files and Tables

Header Keyword	Filename Suffix	File Contents
CCS0	.cy0	Aperture areas
CCS1	.cy1	Aperture positions
CCS2	.cy2	Sky emission line positions
CCS3	.cy3	Sky and background filter widths
CCS4	.cy4	Polarimetry parameters
CCS5	.cy5	Sky shift parameters
CCS6	.cy6	Wavelength dispersion coefficients
CCS7	.cy7	GIM correction scale factors
CCS8	.cy8	Predicted background (count rate)
CCS9	.cy9	Un-illuminated diodes for scattered light correction
CCSA	.cya	OTA focus positions for aperture throughputs
CCSB	.cyb	Aperture throughput coefficients
CCSC	.cyc	Throughput corrections versus focus
CCSD	.cyd	Instrument sensitivity throughput correction factors
CCG2	.cmg	Paired-pulse coefficients
BACHFILE	.r0h & .r0d	Default background file (count rate)
FL*n*HFILE	.r1h & .r1d	Flatfield file
IV*n*HFILE	.r2h & .r2d	Inverse sensitivity file (ergs cm^{-2} $Å^{-1}$ $count^{-1}$ $diode^{-1}$)
RETHFILE	.r3h & .r3d	Retardation file for polarimetry data
DDTHFILE	.r4h & .r4d	Disabled diode file
DQ*n*HFILE	.r5h & .r5d	Data quality initialization file
AISHFILE	.r8h & .r8d	Average inverse sensitivity file

30.2 Headers, Keywords, and Group Parameters

Header files provide much of the information needed to reduce FOS data. A description of each keyword is generally provided in the header itself. Some important header parameters, such as exposure timing information, background correction, or scattered light correction, have different values for each group of data within the file. Such parameters are termed *group parameters*. Table 30.4 is a description of the different topics covered in the various header files. The header files used most often are the standard header packet (.shh), the science data

header file (.d0h), and the calibrated science data header file (.c1h). Most of the information needed to understand the data is found among the header keyword types that describe general information (Table 30.4a) and among the processing and calibration information (Table 30.4c) sections of the headers. Table 30.5 lists many important header keywords used to interpret FOS data.

IRAF tasks such as **imhead** or **hselect** can be used to list the various header keywords. Values of group parameters, on the other hand, can be obtained only with **imhead**. Table 30.6 provides a listing of all FOS group parameters, with typical values and explanatory comments for each.

Table 30.4: Information in FOS Header Keywords

Keyword Type	Information in Keywords	Source
a.) General Information		
General data	General structure information for data file in standard FITS style	All headers
Group Parameters: OSS	Acquisition data description, including time of acquisition (modified Julian date), maximum and minimum data values, and axes information	All headers
Group Parameters: PODPS	Observation type and ground-based GIM correction values from GIMP_CORR	Calibrated header files
Generic Conversion Keywords	Existence of science trailer line and reject array	.d0h
FOS Descriptor Keywords	Description of FOS file and GIM correction	All headers
COSTAR Keywords	Positions of the COSTAR FOS M1 mirror	.shh
b.) Engineering Information		
Time Conversion Keywords	Spacecraft and Universal time at start of observation	.shh
CDBS Keywords in SHP	Engineering data regarding temperatures, currents, and voltages at various points in the instrument	.shh
CDBS Keywords in UDL	Data acquisition details, such as number of channels used, value of magnetic field deflections used	.ulh

Table 30.4: Information in FOS Header Keywords (Continued)

Keyword Type	Information in Keywords	Source
c.) Processing and Calibration Information		
Statistical Keywords	Processing information	.shh, .d0h, and calibrated data headers
Calibration Flags and Indicators	Type of observation and configuration of aperture, grating, and detector	.d0h and calibrated data headers
Calibration Reference Files & Tables	Reference files and tables for calfos processing (either used or to be used)	.d0h and calibrated data headers
Calibration Switches	Calibration steps for calfos processing (either used or to be used)	.d0h and calibrated data headers
Pattern Keywords	Magnetic field deflection pattern used in acquiring the data	.d0h and all calibrated data header files
Calibration Keywords	Observing time, user-supplied GIM offset table name, LIVETIME, DEADTIME, position angle of aperture, burst noise rejection limit	.d0h and calibrated data headers
Aperture Position	Aperture position in RA and Dec	.d0h and calibrated data headers
Exposure Information	Exposure information and commanded FGS lock	.d0h and calibrated data headers
d.) Observer-Supplied Observing Information from Phase II Proposal		
Support Schedule: Program Info	Information on cover page of proposal and type of output data requested by GO	.shh
Support Schedule: Flags and Indicators	Type of observation requested by GO, for example, the aperture, the detector, the number of channels, etc.	.shh
Proposal Info	Observing strategy, e.g., instrument configuration, target description, and information on flux, exposure, moving target, spatial scan etc.	.shh
Target and Proposal ID	Target and PEP information	.shh
e.) Observing Information Produced in TRANS Stage		
Support Schedule: Data Group II	Telescope pointing and instrument configuration on the sky, i.e., target RA and Dec and offset objects, position angle of diode array, OFFSET information, spacecraft velocity, guide stars, etc.	.shh
Onboard Ephemeris Model	Spacecraft ephemeris	.shh

Table 30.5: FOS Header Keywords

Keyword	Description and Comments
General Information from Header File—usually in .d0h or .c1h	
GCOUNT	Number of groups in data file
YTYPE	Nature of observation, important for paired aperture observations. (Not real values in d0h file). Values are OBJ, BKG, or SKY
YPOS*n*	Location of diode center in Y-base units, of the *n*th group, useful for interpreting ACQ/BIN data. If there is only one group then YPOS is the Y-base of that one group. Not populated with real values in the .d0h file
YBASE	YPOS of group #1
XBASE	XDAC units needed to center aperture on the diode array for group #1
DEFDDTBL	UDL disabled diode table to be used (value: T) or DDTHFILE table to be used (value: F)
BUNIT	Flux units of the data. Values: COUNTS, COUNTS/SEC, ERGS/SEC/ CM^2/A, or ANGSTROM
FILLCNT	Number of sequences of filled data
ERRCNT	Number of sequences with bad data
INSTRUME	Instrument used for the observation. This will be FOS.
ROOTNAME	Rootname of the observation set. Will start with letter “y”
FILETYPE	Type of data in the file: SHP is science header packet, UDL is unique data log, SDQ is raw science data quality, WAV is wavelength, FLX is calibrated flux, ERR is calibrated flux error, MOD is CALFOS special mode processed data, SCI is object, sky, or background science data, OBJ is object data, BKG is background data, CDQ is calibration data quality, SKY is sky data, NET is sky-subtracted object data
GRNDMODE	Ground software mode of FOS. Can be SPECTROSCOPY, TARGET ACQUISITION, IMAGE, RAPID-READOUT, SPECTRO-POLARIMETRY, or TIME-RESOLVED
DETECTOR	Detector in use for the observation. AMBER or BLUE
APER_ID	Aperture used for the observation; A-1 corresponds to the 4.3″, A-2 to the 0.5″ pair (square), A-3 to the 0.25 pair (square), A-4 to the 0.1 pair (square), B-1 to the 0.5″ (round), B-2 to the 0.3″ (round), B-3 to the 1.0″ (round), B-4 is blank, C-1 to the 1.0″ pair (square), C-2 to the 0.25″x2.0″ slit, C-3 to the 0.7″x2.0″ bar, and C-4 to the 2.0″ bar apertures respectively
POLAR_ID	Polarization waveplate used for the observation. A is the waveplate A, B is the waveplate B and C is no polarizer used (clear)
FGWA_ID	Filter and grating used for the observation. H*xx* means G*xx*0H filter, L15 means G160L, L65 means G650L, PRI means PRISM, and CAM means camera (mirror).
POLANG	Initial angular position of the polarizer in degrees
FCHNL	First diode used in observation (first diode in array is designated as zero)
NCHNLS	Number of diodes used in the observation, useful for interpreting ACQ/BIN data and exposure time. Usually 512 (except target acquisition and other specific modes, see below)
OVERSCAN	Number of overscans used in the observation, useful for interpreting ACQ/BIN data and exposure time. Usually 5. FOS reference files and calibration support *only* OVERSCAN=5.
NXSTEPS	Number of X substeps used in the observation, useful for interpreting ACQ/BIN data and exposure time. Usually 4

Table 30.5: FOS Header Keywords (Continued)

Keyword	Description and Comments
MINWAVE	Minimum wavelength in Å. (Not populated in .c0h file)
MAXWAVE	Maximum wavelength in angstroms. (Not populated in .c0h file)
YFGIMPEN	Onboard GIM correction enabled. T or F
KYDEPLOY	COSTAR mirror deployment for the FOS. T or F
Exposure Time Information—usually in .d0h or .c1h	
FPKTTIME	Time of first data packet sent to the SDF, i.e., approximate time of the *end* of the group exposure. The units are modified Julian date. Each group has its own unique FPKTIME, accurate to about 1/8 second.
LPKTTIME	Approximate time of the last data packet sent to the SDF. The units are modified Julian date.
DATE-OBS	FPKTTIME of group 1 converted to standard notation for date
TIME-OBS	FPKTTIME of group 1 converted to standard notation for time, truncated to integer value; thus these are only accurate to 1/8 of a second
EXPSTART	Exposure start time in modified Julian date
EXPOSURE	Exact exposure time per pixel in seconds for each group. Note that this keyword is not populated with real values in the d0h file
Pattern Keywords for Exposure Times—usually in .c0h or .c1h	
LIVETIME	Time, in units of 7.8125 microseconds, during which accumulator is open
DEADTIME	Time, in units of 7.8125 microseconds, in which accumulator is closed
INTS	Number of repetitions of the live time/dead time cycle
YSTEPS	Number of Y substeps used in the observation. Usually 1
NPAT	Number of patterns used per readout
SLICES	Number of repeats of the magnetic field deflection sequence. Usually 1
NREAD	Number of readouts per memory clear. For the ACCUM mode this is usually the number of groups. For RAPID mode this is 1
NMCLEARS	Number of memory clears per obs. 1 for ACCUM, number of groups for RAPID mode when NMCLEARS > 1
Aperture Orientation Information—usually .shh and .d0h of acquisition image	
OPMODE	Operation mode of the FOS for the observation. Can be: ACQ, ACQ/BIN, ACQ/PEAK, ACQ/FIRMWARE, IMAGE, ACCUM, RAPID or PERIOD
PA_APER	Position angle of the aperture in degrees
RA_APER1	RA of aperture center in degrees
DECAPER1	Dec of aperture center in degrees

Table 30.6: FOS Group Parameter Keywords

Keyword	Typical Value	Alternate Name in Header	Description
CRVAL1	1.	PTYPE1	Reference pixel value
CRPIX1	1.	PTYPE2	Pixel number of reference pixel
CD1_1	1.	PTYPE3	Pixel increment
DATAMIN	1.946443E-14	PTYPE4	Minimum value in the data
DATAMAX	1.118037E-13	PTYPE5	Maximum value in the data
RA_APER	297.4443291667	PTYPE6	Right ascension of aperture (deg)
DEC_APER	48.961	PTYPE7	Declination of aperture (deg)
FILLCNT	0	PTYPE8	Number of segments containing fill
ERRCNT	0	PTYPE9	Error count of the data
FPKTTIME	50441.0428552372	PTYPE10	Time of the first packet (Modified Julian Date)
LPKTTIME	50441.0428653645	PTYPE11	Time of the last packet (Modified Julian Date)
CTYPE1	PIXEL	PTYPE12	First coordinate type
APER_POS	SINGLE	PTYPE13	Aperture used
PASS_DIR	0	PTYPE14	Polarization pass direction
YPOS	-1597.	PTYPE15	*y*-position on photocathode (Y-bases)
YTYPE	OBJ	PTYPE16	Observation type: OBJ, SKY, BCK
EXPOSURE	62.5	PTYPE17	Exposure time per pixel (seconds)
X_OFFSET	0.	PTYPE18	x_offset for GIMP correction (diodes)
Y_OFFSET	0.	PTYPE19	y_offset for GIMP correction (defl.units)
SCT_VAL	0.1351963	PTYPE20	Scattered light correction value (cts/sec/pixel)
SCT_ERR	0.01424327	PTYPE21	Scattered light correction error (cts/sec/pixel)

30.3 FOS Paper Products

The FOS *paper products* are a package of summary text and diagnostic graphics that can be generated for any set of FOS observations. The FOS products were redesigned in 1996 to enhance their clarity and usefulness. Paper products can be generated for any FOS data by using **pp_dads** which is in the STSDAS **hst_calib.paper_prod** package. In order to generate a full set of FOS paper products you will need the following six types of files: .d0h/.d0d, .c0h/.c0d, .c1h/.c1d, .shh/.shd, .jih/.jit, and .pdq (the first four sets are required to obtain a minimal set of products). Please refer to the task help file for information on how to run this package.

The FOS paper products produce title pages for an observation series and several pages of summary and diagnostics for each rootname in the series. At the exposure level three generic types of output are produced:

- Plots for each exposure, designed to provide diagnostic information for rapid data quality assessment.
- A spacecraft and exposure summary page which provides any Routine Science Data Pipeline (RSDP) post-observation assessments concerning data quality, guiding and jitter information including, if possible, a jitter ball plot, and extracts of important quantitative information from the data headers.
- A calibration status listing giving the status of all pipeline calibration flags as well as listing the reference files and tables used in the **calfos** calibration of the data.

Table 30.7 lists the types of FOS exposure-related paper products produced for each observing mode. Additionally, the order of the pages in the output products for a particular mode is given by reading from top to bottom along a column in this table.

Examples of FOS paper products are shown below for reference in this chapter. We have not included the title or closing pages in order to save space, but these examples do show representative cases of each type of mode-specific plot.

30.3.1 Title Pages

The first (cover) page produced by **pp_dads** lists the proposal number and the name of the Principal Investigator. A closing page is produced that is virtually identical to the cover page.

Following the first page is a list of targets for the observations and a list of the individual exposures (see Figure 30.1). On this listing each exposure has a data quality flag that will be set if any .pdq file comment of sufficient severity exists. These comments are printed on the HST Performance Summary section of the Observation Summary paper product page for the relevant exposure. Many .pdq file comments are benign, so a raised data quality flag should simply serve as an indication that you need to check further. The presence of a telemetry gap in the

Table 30.7: FOS Paper Products by Observing Mode

Paper Product	ACCUM	RAPID	IMAGE grating	Polar-imetry	PER-IOD	IMAGE MIRROR	ACQ/ BIN	ACQ/ PEAK	ACQ/ FIRM
Flux vs Wavelength	***Last group***	***First group***	–	–	–	–	–	–	–
Counts vs Wavelength	***Last group***	***First group***	***All steps***	–	–	–	–	–	–
Group Counts	***If > 1 group***	***If > 1 group***	–	–	–	–	–	–	–
ACQ/BINARY diagram	–	–	–	–	–	–	✓	–	–
ACQ/PEAK scan plot	–	–	–	–	–	–	–	✓	–
Grayscale	–	–	–	–	–	✓	–	–	–
Observation Summary	✓	✓	✓	✓	✓	✓	✓	✓	✓
Calibration Summary	✓	✓	✓	✓	✓	✓	✓	✓	✓

data is not sufficient to cause the data quality flag to be set, but all telemetry gap messages from the `.pdq` file will also be printed on the HST Performance Summary section of the Observation Summary paper product page.

30.3.2 Observation Summary Page

This one-page summary sheet (see Figure 30.8) is divided into sections that describe basic exposure characteristics, telescope performance characteristics (OMS summary), calibration pipeline performance, and OPUS data quality evaluation comments.

Exposure Summary

The right-hand section of the page presents information from keywords that characterize the exposure, including target name, proposal-specified coordinates (not actual telescope pointing), disperser, aperture, observing mode, total exposure time, observation date, aperture position angle on sky, substepping and overscanning values, mean total dark per pixel for the exposure, mean scattered light correction per pixel (if applicable), and average readout time (for RAPID mode only).

OMS Summary

The OMS (Observatory Monitoring System) Summary presents, if the jitter file information is available, the jitter plot (*jitter ball*) which shows samplings made every six seconds of the spacecraft motion about nominal pointing in the (V2,V3) plane. The plot is always scaled based upon the extrema of the data being

plotted. Also included is a summary of the rms jitter in V2 and V3 in units of milliarcseconds, as well as the number of recenterings and losses-of-lock during the exposure. More information about OMS engineering data is available in Appendix C.

Comments

Any comments found in the .pdq file are printed following the OMS statistics in the HST Telescope Performance Summary section. These comments include those made by OPUS personnel in their routine post-observation review of the observational data quality and automatic comments included by OPUS observation-evaluation software. Although such comments are often benign, the presence of most is sufficient to cause the Observation List observational quality flag to be set to "not OK."

Pipeline Performance

A listing of pipeline calibration anomalies, if any, is presented in the lower-left corner of the page.

30.3.3 Exposure Diagnostic Plots

For the purpose of data quality assessment, this is the most important section of the FOS paper products. Depending upon the observing mode, 0–3 pages of diagnostic plots and diagrams are produced for each individual exposure. Table 30.7 lists the types of plots that are generated for each observing mode. Following is a description of each type of plot:

Flux vs. Wavelength

Two plots are provided (see Figure 30.5). The upper plot is a standard calibrated flux (.c1 file) vs. wavelength (.c0 file) with the display auto-scaled to the data extrema. The lower plot presents log(flux) vs. wavelength. Points with zero or negative values prior to the log operation are not plotted. This plot is made only for ACCUM and RAPID mode. For ACCUM mode, the last data group is plotted; for RAPID the first group is plotted.

Corrected Counts vs. Wavelength

Corrected counts are the count-rates in each pixel of the .c5 file (raw observational data that have been corrected for all instrumental effects except the instrumental sensitivity correction to calibrated fluxes) *multiplied by* the effective exposure of each pixel. In this manner we plot a quantity that is easily manipulated (take the square root) to give a good approximation of the formal statistical S/N as a function of wavelength (see Figure 30.6).

The wavelength scale (from the .c0 file) is magnified by plotting the first half of the observed wavelength range in the upper half of the diagram and the balance of the spectrum in the lower half of the display.

This plot is made only for ACCUM, RAPID, and dispersed-light IMAGE mode. For ACCUM mode, the last data group is plotted and for RAPID the first group is plotted. For IMAGE mode all *y*-steps are plotted vs *pixel number* as IMAGE mode spectra are not wavelength calibrated.

Group Counts

Again the ordinate is “corrected counts.” Here we plot the sum of the corrected counts over all pixels for each readout of the diode array vs. readout (group) number for all readouts in the exposure (see Figure 30.7). Note that the left-hand vertical axis is labeled in counts, but the right-hand vertical axis is labeled in percent of the maximum ordinate value. This provides an easy way of assessing the consistency of the counts between groups.

This plot provides a light curve of the target during the observations. This is an interesting display for variable objects, and it is also an easy way to assess the photometric repeatability of the measures and the stability of the telescope and the instrument during an entire observation.

We strongly recommend that the group counts plot be inspected for every ACCUM and RAPID mode observation in your data since it is a quick way to identify many of the more common problems that can affect FOS data.

This plot is made only for ACCUM and RAPID modes. For ACCUM mode, the individual groups are decomposed to produce the counts actually accumulated during each readout.

ACQ/BINARY Deflection Diagram

There are several portions of this diagram (see Figure 30.3). Up to a maximum of eleven individual accumulated counts vs. pixel number (detector *x*-axis) plots are given. The first three correspond to mappings of the middle, lower, and upper thirds of the 4.3 aperture respectively. The remainder are for each of the magnetic deflections used to place the target on a *y*-edge of the diode array (and thereby produce a signal roughly half of the maximum detected in the first three images). The group number and Y-base for the deflection is printed on each plot.

To the left of these count-level plots is a diagram showing the relative *y*-position of diode center (in Y-base units) of each individual step in the binary search sequence. The final derived target Y-base position is also marked. Recall that one diode height is 256 Y-base units.

The calculated (*x*,*y*) and equivalent (V2,V3) offsets are given in arcseconds. The *x*-offset is also given in pixels and the *y*-offset in Y-bases.

A compass rose showing the orientation of the detector +x and +y axes with respect to north and east on the sky is also given. The sense of the *x*-axis in the count-level plots and the *y*-direction in the deflection graphic are identical to the sense of the same directions illustrated in the compass rose.

ACQ/PEAK Scan Diagram

This diagram shows the relative position of each dwell point in an ACQ/PEAK scan pattern plotted in the FOS detector (*x*,*y*) plane (see Figure 30.4). Note that *x* and *y* are displayed as if we are viewing the sky by looking through the detector from its back side. A compass rose shows the correct orientation of north and east

on the sky. Ordinal numbers are printed next to each scan position as are the total counts detected during each dwell.

ACQ/PEAK is a “return-to-brightest” (for peakup) algorithm. No attempt to centroid the contours or interpolate a position intermediate between dwell points is made. The dwell point with the highest number of counts is marked as the location to which the telescope moved after the peakup sequence. Check the OMS jitter ball, if available, to insure that no significant positioning errors occurred in the slew to the brightest location.

The calculated (*x*,*y*) and equivalent (V2,V3) offsets are given in arcseconds. The *x*- and *y*-step sizes for the scan pattern are also given.

The distribution of counts in each ACQ/PEAK pattern can be used to estimate the degree of centering error after movement to the brightest dwell point.

Grayscale Image

A grayscale plot is made of the two-dimensional image in the FOS instrument coordinate (*x*,*y*) plane (see Figure 30.2). The units on both axes are FOS pixels. For a standard post-COSTAR ACQ image 1 pixel corresponds to approximately 0.075". A rule depicting the scale of 1" is also given.

A grayscale vs. counts key is provided. The orientation of the detector coordinates relative to north and east is provided via a compass rose.

This plot is provided only for IMAGE mode observations that use the MIRROR and for standard ACQ images.

30.3.4 Calibration Summary Page

This page (see Figure 30.9) presents in successive columns all **calfos** switch settings for each step in the calibration process, their status, the reference file or table used, the pedigree (if available) of the reference file, and a description of the action of each calibration switch or step. The shaded banner again gives logsheet line number, observation rootname, and proposal ID.

Figure 30.1: Visit Summary Listing

Visit: 04 **Proposal: 06750** *FOS*

Target List

Target Name	R.A. (J2000)	Dec. (J2000)	Description
TT-HYA	11:13:12.51	-26:27:54.4	STAR;B6-B9.5 V-IV;K III-I;INTERACTI

Observation List

Logsheet Line#	Rootname	Target Name	Operating Mode	Detector	Aperture	Spectral Element	Obs Date	Exposure (sec)	Quality Flags Obs	Proc
4.004	Y38J0404T	TT-HYA	ACQ/PEAK	BLUE	0.26 SINGLE CIRC	H19	7/05/96	27.0	○	
4.030	Y38JA402T	TT-HYA	ACCUM	BLUE	0.86 SINGLE CIRC	H19	7/05/96	1960.0	○	

Quality flags: ○ = OK ● = Not OK Blank = Unknown or file missing

Figure 30.2: ACQ Image Plot

Logsheet Line# 509.500 **Observation: Y2DE020GT** **Proposal: 05536** *FOS*

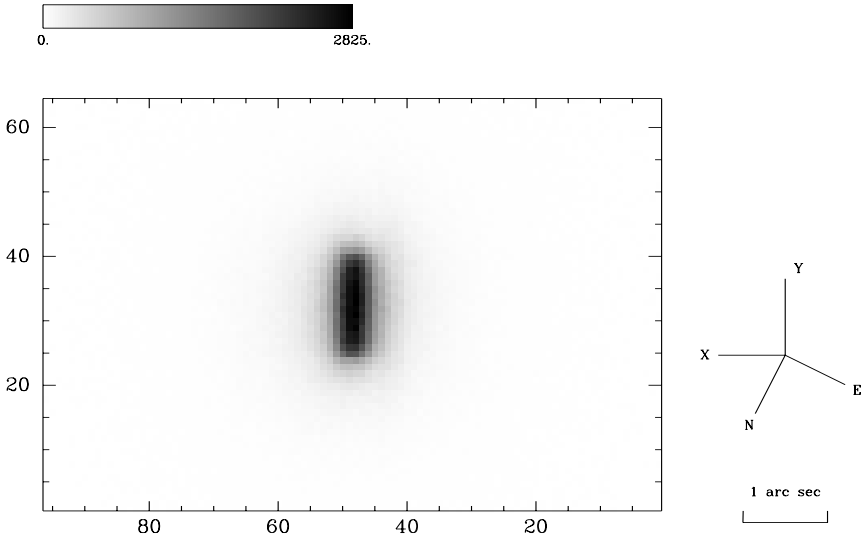

Figure 30.3: ACQ/BINARY Plot

Logsheet Line# 12.121 **Observation: Y38E1201T** **Proposal: 6577** *FOS*

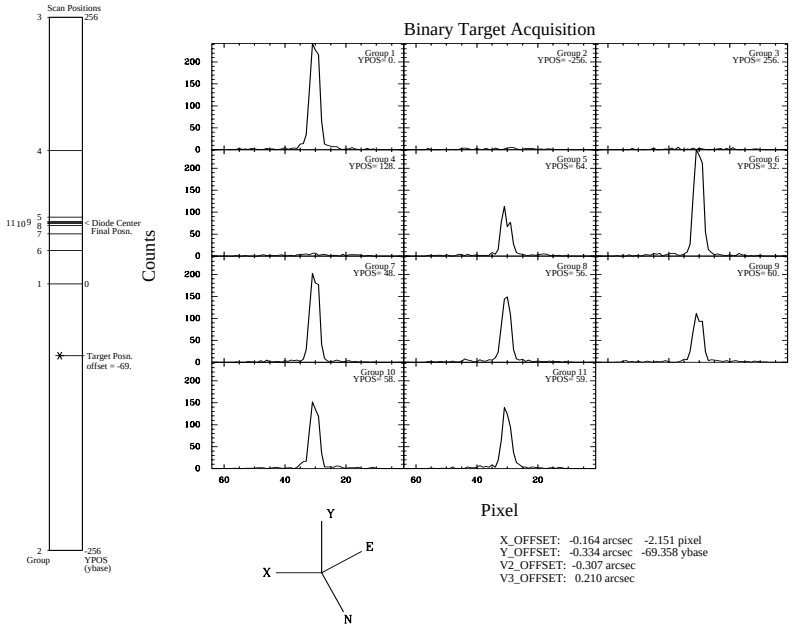

Figure 30.4: ACQ/PEAK Plot

Logsheet Line# 508.500 **Observation: Y2DE0204T** **Proposal: 5536** *FOS*

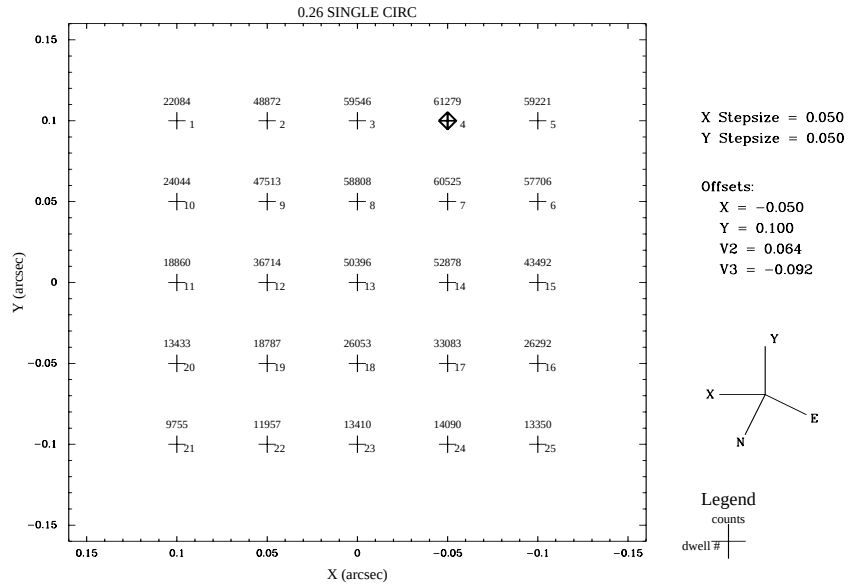

Figure 30.5: F_λ vs λ and log F_λ vs λ Plot

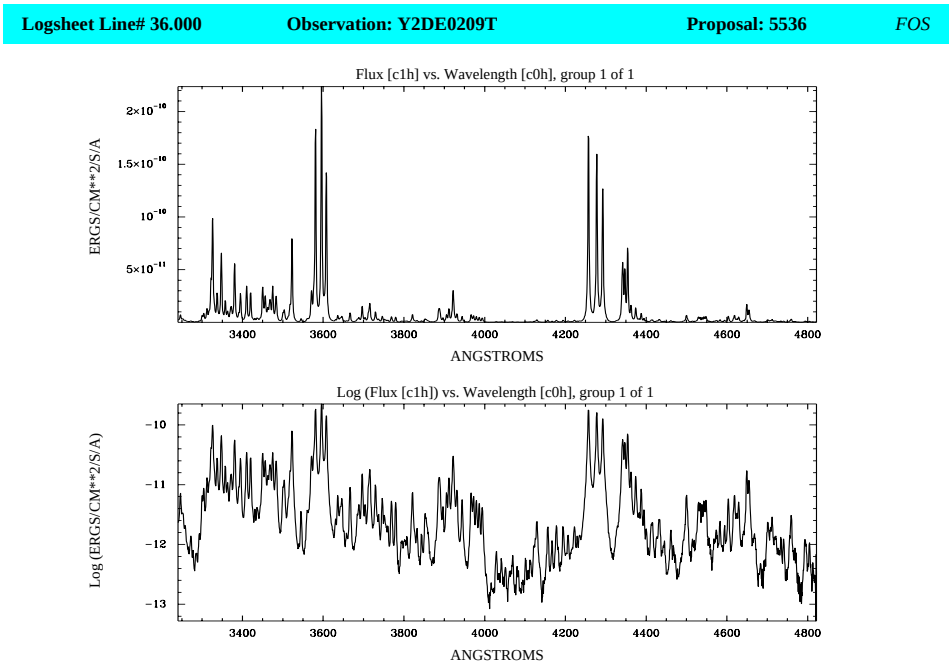

Figure 30.6: Corrected Counts vs λ Plot

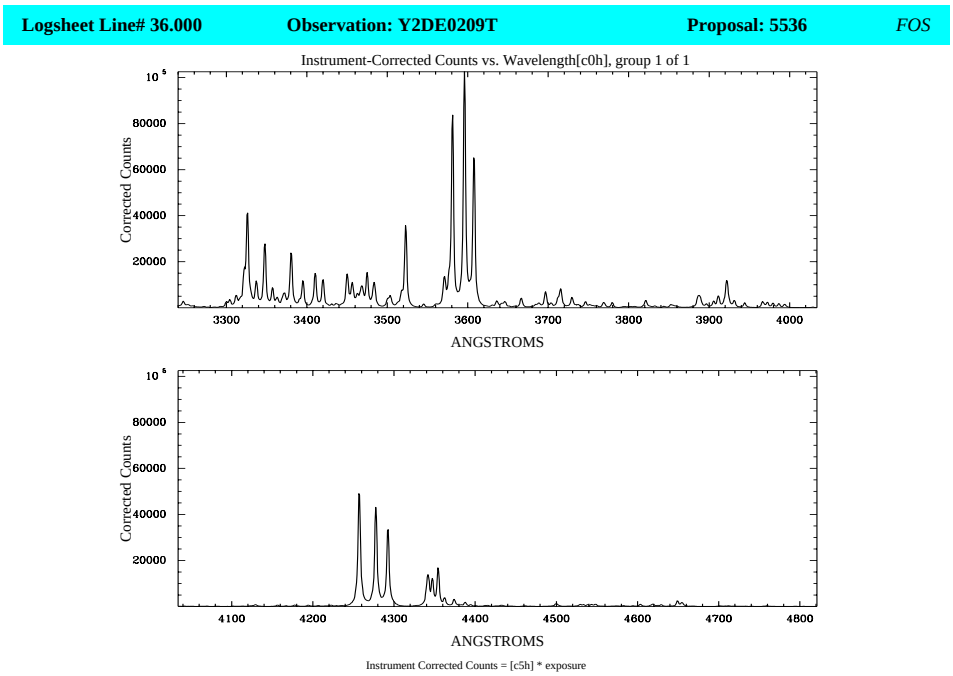

Figure 30.7: Group Count Plot

Logsheet Line# 2.500 **Observation: Y2GN0205T** **Proposal: 5498** *FOS*

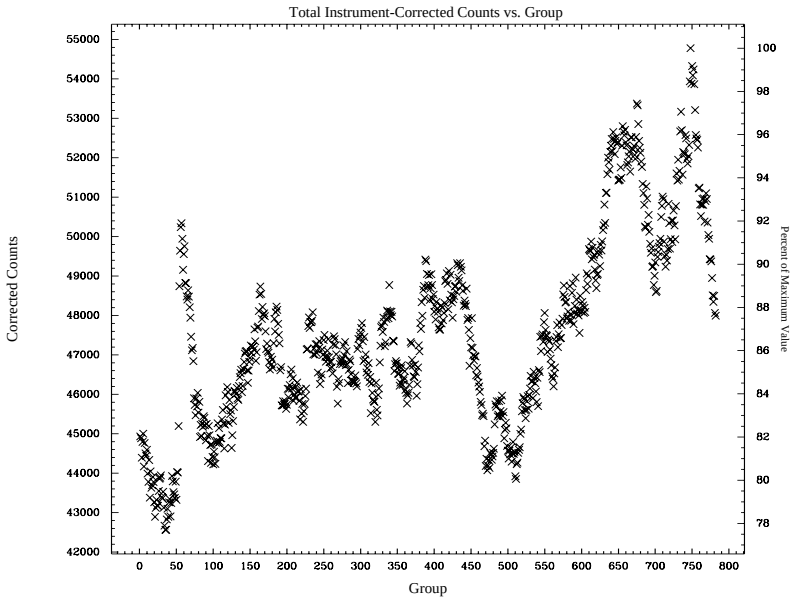

Figure 30.8: Observation Summary Page with Jitter Ball

Logsheet Line# 1.008 **Observation: Y2XS0108T** **Proposal: 06042** *FOS*

HST Spacecraft Performance Summary

Recenterings:
V2 Jitter (RMS):
V3 Jitter (RMS):

Losses of Locks:
V2 Jitter (PP):
V3 Jitter (PP):

No apparent problems

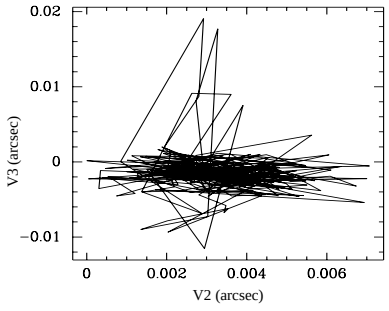

Pipeline Processing Summary

Exposure Summary

Target Name:	J1
RA (J2000):	10:45:04.38
Dec (J2000):	-59:40:52.5
X POSTARG:	
Y POSTARG:	
Detector:	AMBER
Grating:	H19
Aperture:	0.86 PAIR SQUARE
Exp Time (sec):	900.0
Rootname:	Y2XS0108T
Date:	5 Jul 96
Time:	15:14:17
Proposal:	06042
PI:	DUFOUR
Ground Mode:	SPECTROSCOPY
Position Angle:	26.33
First Channel:	0
# of Channels:	512
NXSTEPS:	4
Overscan:	5
YSTEPS:	2
Mean Dark Rate:	0.0131 cts/s/pix
Mean Dark Counts:	0.2105 cts/pix
Mean Scat. Light:	-0.02071 cts/pix

Figure 30.9: Calibration Summary Page

Logsheet Line# 42.300 **Observation: Y2ET0F0RT** **Proposal: 05539** *FOS*

Calibration Status

Flag	State	Reference File	Pedigree	Description
ERR_CORR	OMIT			Propogated Error Computation
CNT_CORR	COMPLETE	yref$d9h1244ay.r4h		Disabled Diode Correction
		yref$b2f1308hy.r5h		
		N/A		
OFF_CORR	OMIT	ytab$ba910502y.cy7		GIMP Correction
PPC_CORR	COMPLETE	mtab$a3d1145ly.cmg		Paired Pulse Correction
BAC_CORR	OMIT	N/A		Background Subtraction
		ytab$a3d1145gy.cy3		
		ytab$e3i09491y.cy9		
GMF_CORR	OMIT	ytab$ba31407ly.cy8		Scale Reference Background
SCT_CORR	OMIT	ytab$e3i09491y.cy9		Scattered Light Correction
FLT_CORR	OMIT	N/A		Flat-field Removal
		N/A		
SKY_CORR	OMIT	ytab$a3d1145dy.cy0		Sky Subtraction
		ytab$a3d1145fy.cy2		
		ytab$a3d1145gy.cy3		
		ytab$a3d1145jy.cy5		
WAV_CORR	OMIT	ytab$e5v11576y.cy6		Wavelength Scale Determination
FLX_CORR	OMIT	N/A		Flux Scale Generation
		N/A		
APR_CORR	OMIT	n/a		Aperture Throughput Correction
		n/a		
		n/a		
AIS_CORR	OMIT	N/A		AIS Flux Scale Generation
TIM_CORR	OMIT	n/a		Time Changes in Sensitivity
MOD_CORR	OMIT	N/A		Mode Dependent Corrections
		ytab$e5v13262y.cy4		

30.4 Evaluating Planned Observations

30.4.1 Planned Observations (Exposure Logsheet)

An examination of the RPS2 (RPSS for pre-COSTAR) input file or, more commonly, the concise proposal summary logsheet can be helpful in understanding the structure and content of an observation sequence. As will be emphasized in Chapter 32, the observational strategies employed, such as target acquisition or limitation of wavelength readout, can have a very profound effect on the quality of FOS data. An understanding of what was planned can be beneficial in comprehending what was actually obtained.

The exposure logsheets and RPS2 input files for post-COSTAR programs are available from the PRESTO web page:

`http://presto.stsci.edu/public/propinfo.html`

FOS program logsheets and RPS2 (RPSS) input files are available via the FOS WWW page **propfind** query:

`http://www.stsci.edu/ftp/instrument_news/FOS/propfind.html`

In Figure 30.11 we show one exposure logsheet as an example. This will be used occasionally in the following to outline a few checks you can run on your

data in order to assess whether what you see is what you expected. In our example the FOS observations started with a four-stage ACQ/PEAK target acquisition at the beginning of the visibility period, followed by science observations using the FOS/RD detector with the G270H grating and the circular 1.0" aperture. The investigators used the occultation time after the second visibility period to execute a side switch from FOS/RD to FOS/BL, which takes about 50 minutes. Then, in exposure 5, they re-acquired the target with a single-stage peak-up in order to insure good pointing accuracy and then continued their science observations, now using the G190H grating for a total of 100 minutes. By looking at the data files, but not the exposure logsheet or the RPS2, one can find out that this long integration was split into three separate exposures: the first filling the remainder of the re-acquisition orbit and then one each in the subsequent two orbits. Naturally, each such exposure will receive its own rootname and complete set of data files, and each will produce its own set of diagnostic paper product pages.

In summary, since FOS exposures are not interruptible, a single exposure logsheet line or RPS2 exposure line may produce several distinct FOS exposures and hence several sets of data files. Each set of data files will be identified by unique, usually consecutively ordered, rootnames.

Figure 30.10 shows in graphical form the time sequence of events and exposures during the execution of lines 1 through 6 of the sample exposure logsheet. For the example orbits shown the target visibility is 55 minutes and Earth occultation lasts 41 minutes. Note that the exposure for logsheet line 4 was shortened from 33 to 26 minutes in order to fit it into the available target visibility. The HST scheduling system routinely shortened or lengthened exposures by up to 20% in such cases

Figure 30.10: Timeline for FOS Activities in Sample Program

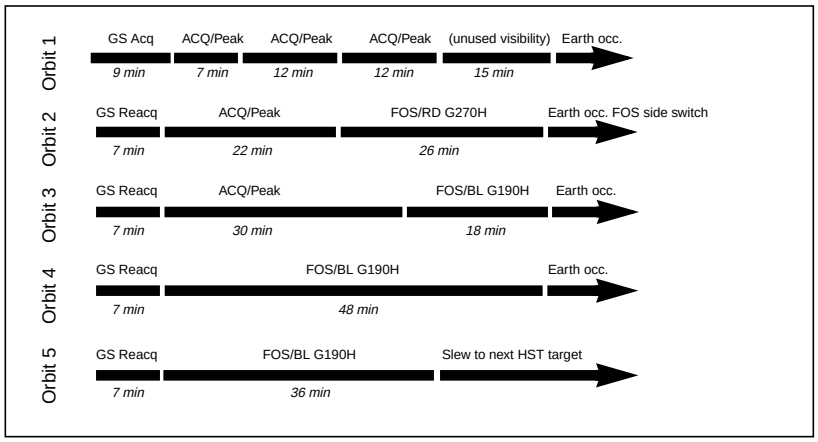

Figure 30.11: Sample FOS Exposure Logsheet

Exposure Number	Target Name	Instr Config	Oper. Mode	Aper or FOV	Spectral Element	Central Waveln.	Optional Parameters	Num Exp	Time	Special Requirements
1	ARP102B	FOS/RD	ACQ/PEAK	4.3	MIRROR		SCAN-STEP-Y=1.204 SEARCH-SIZE-X=1 SEARCH-SIZE-Y=3	1	1.4S	ONBOARD ACQ FOR 2 GROUP 1-7 WITHIN 3D GROUP 1-6 NO GAP
2	ARP102B	FOS/RD	ACQ/PEAK	1.0	MIRROR		SCAN-STEP-X=.602 SCAN-STEP-Y=.602 SEARCH-SIZE-X=6 SEARCH-SIZE-Y=2	1	2.0S	ONBOARD ACQ FOR 3
3	ARP102B	FOS/RD	ACQ/PEAK	0.5	MIRROR		SCAN-STEP-X=0.30 SCAN-STEP-Y=0.30 SEARCH-SIZE-X=3 SEARCH-SIZE-Y=3	1	10S	ONBOARD ACQ FOR 3.5
3.5	ARP102B	FOS/RD	ACQ/PEAK	0.3	MIRROR		SCAN-STEP-X=0.06 SCAN-STEP-Y=0.06 SEARCH-SIZE-X=5 SEARCH-SIZE-Y=5	1	10S	ONBOARD ACQ FOR 4
4	ARP102B	FOS/RD	ACCUM	1.0	G270H	2760		1	33M	
5	ARP102B	FOS/BL	ACQ/PEAK	0.3	MIRROR		SCAN-STEP-X=0.06 SCAN-STEP-Y=0.06 SEARCH-SIZE-X=5 SEARCH-SIZE-Y=5	1	30S	ONBOARD ACQ FOR 6
6	ARP102B	FOS/BL	ACCUM	1.0	G190H	1950		1	100M	

30.5 Assessing FOS Acquisitions

Nearly all FOS observations included an onboard target acquisition that used instrument observing modes to locate the science target in the desired aperture. Under normal circumstances, prior to any FOS acquisition or science observation sequence the FGS performed a guide star acquisition and commenced FINE lock guiding. A guide star re-acquisition was also performed at the start of all subsequent visibilities in the same visit. Occasionally, some aspect of the acquisition or re-acquisition failed. Appendix C provides for more information about guide star acquisition failure. Chapter 35 (for the GHRS) also contains useful discussions of a variety of guide star acquisition and guiding anomalies.

Before June 1993, the FOS aperture door was closed for the remainder of any exposure during which a guiding anomaly occurred. As a safety measure, commencing in June 1993 the FOS shutter door was always closed for the duration of the obset (typically remainder of the visit) if guide star lock was not

established at the start of any exposure. After October 1995, a significant number of FOS acquisitions failed in this manner due to anomalous losses-of-lock caused by FGS1.

This section describes each type of FOS acquisition by giving a detailed discussion of the acquisition method (in the "Understanding" subsection), a discussion of pointing accuracy limitations with the method, a description of and references to examples of the mode-specific paper products, tips for understanding and using the paper products to assess the observational data quality, a description of the structure and content of the output data products, analysis information, and, in some cases, very detailed background information for the most inquisitive users.

No FOS acquisition exposure (e.g., an ACQ/BINARY exposure or a single scan-pattern of an ACQ/PEAK) could be interrupted by Earth occultation.

Some additional practical information on target acquisition is given in Chapter 2 of the *FOS Instrument Handbook* version 6.

30.5.1 Binary Acquisition—ACQ/BIN

Binary search acquisition mode is indicated by a raw data header file (`.d0h`) OPMODE value of ACQ/BIN. This method was used for targets that are point sources with well known energy distributions. Although ACQ/BIN was designed to select the *n*th brightest object in a crowded field, this option was never correctly used except in calibration programs. The following discussion will describe how the brightest target was acquired.

Understanding ACQ/BINARY

The binary search algorithm used MIRROR and began by mapping the `4.3` aperture (only the 12 central diodes which cover the `4.3` aperture provide the data) with 3 *y*-scans which are stored in the raw data file as 3 groups. The first raster (i.e., group 1) was of the central region of the `4.3` aperture, the second (group 2) was of the lower region of the `4.3` aperture, and the third (group 3) was of the upper region of the `4.3` aperture. The binary search algorithm summed in each group the counts from all pixels that are bounded by the user-specified FAINT and BRIGHT limits. The program then compared the count levels in the three scans, and located the target in one of the three scans by finding the total number of peaks in the scan and the number of counts in each individual peak. The brightest peak, representing the target, was then selected. If more than five peaks per raster were found by the binary search algorithm, the target acquisition failed. If there were two peaks (within a diode width) in two adjacent scans, the algorithm summed up the number of counts in the two peaks to determine the brightness of the target. The search program then continued (up to eight more tries) to electronically deflect the image of the target in the *y*-direction (note the telescope was never moved in this search process) until the target image was on

the edge of the diode array, i.e., until the number of counts in the peak was half the maximum number of counts observed in the initial three scans. For each deflection the data were stored as a group.

The offset required to position the target on the edge of the diode array was stored in the .shh file. This quantity was then used to determine the slew that was necessary to place the object in the nominal center of the 4.3 aperture. Note that no further refinement of position was made in the binary search algorithm.

If ACQ/BINARY failed for any reason (*except* 8-steps-to-success described below), the telescope *did not slew* to place the target at the nominal center of the 4.3 aperture, and subsequent exposures in the visit were executed at the initial blind pointing position of the telescope.

Pointing Accuracy: ACQ/BINARY

If a binary search was successful, we can only determine the amount of telescope slew that occurred to place the target at the STScI-determined nominal aperture center on the diode array. We cannot locate the exact position of the target in the aperture unless a confirming image was acquired after the acquisition.

Since binary search determined the offset to place the target on the edge of the diode array and used that offset to calculate the offset slew required to place the target at the expected center of the 4.3 acquisition aperture, the accuracy of centering was dependent on both the accuracy of the half-power point algorithm and the 0.1" accuracy with which the location of the center of the 4.3 aperture was known (see *FOS ISR* 139).

The statistical 1-sigma uncertainty for ACQ/BIN is 0.08" for post-COSTAR FOS/BL and 0.12" for post-COSTAR FOS/RD. Pre-COSTAR uncertainties are estimated to be of similar order, but an additional worst-case uncertainty of up to 0.15" due to uncorrected GIM motion must be added in quadrature for all ACQ/BIN acquisitions prior to April 5, 1993.

If an ACQ/BIN spectrum has 11 groups, it may have been considered to have failed. Before June 1, 1993, all such acquisitions were returned to the blind pointing. Commanding was changed on that date to recognize the fact that any additional correction to be applied after the algorithm reached the eleventh step was typically of order 0.02" and of no significance. After this date, these so-called 8-steps-to-success “failures” resulted in the position implied by the last ACQ/BIN iteration being chosen as the pointing. Figure 30.12 illustrates some of the characteristics of ACQ/BINARY.

Figure 30.12: Binary Target Acquisition (pre-COSTAR sizes in parentheses)

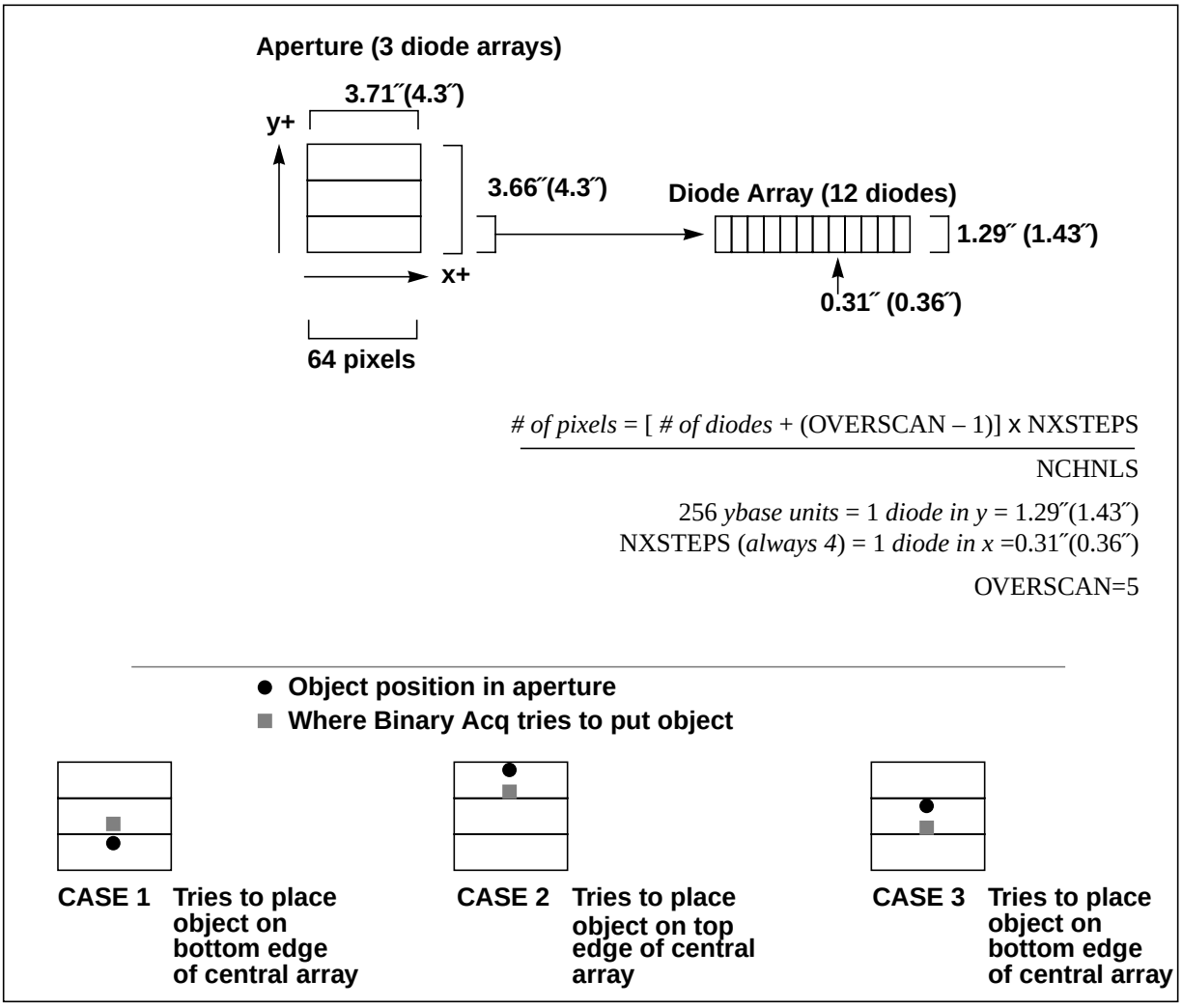

Paper Products: ACQ/BINARY

Figure 30.3 provides an illustration of the FOS paper products ACQ/BINARY diagnostic plots. The one-dimensional images (counts vs pixel) for each group are plotted as well as a separate map of Y-bases chosen for each deflection step. The final *x*- and *y*-offsets, and their equivalent V2 and V3 offsets required to center the target are given. A compass rose, oriented identically to the spatial coordinates of the individual plots, is also provided. Conversion of offsets to right ascension and declination is described in “Converting X,Y to RA, Dec” on page 33-9.

Output Data Products: ACQ/BINARY

The binary search target acquisition mode is identified by the OPMODE value of ACQ/BIN. The ACQ/BIN data (`.d0h` file) contains up to 11 groups (depending at which stage the algorithm stopped the search) and each group has images of 64 pixels (12 diodes scanned with NXSTEPS=4 and OVERSCAN=5). The central

pixel is defined to be number 32 of the numeric range 1–64. The **calfos** calibration only corrects the data for paired-pulse effects and converts the raw counts into a count rate. No further calibration procedures are applied.

Analysis: ACQ/BINARY

If there are fewer than four groups in the ACQ/BINARY data files, the binary search target acquisition has failed.

A binary search may have failed due to one of the following reasons:

- The FAINT limit provided by the observer was too low, i.e., the algorithm was confused due to the dominance of the wings of the PSF (particularly applicable to pre-COSTAR observations). This commonly yielded field-too-crowded failures.
- The algorithm was not completed in 11 steps because the target was extended or the GIM moved the target (for observations generally before April 5, 1993, when onboard GIM was not yet activated).
- The field was too crowded, i.e., the algorithm found more than five peaks in a scan.
- The source was much fainter than determined by the observer, i.e., there were very few counts in the observations.
- The FAINT limit provided by the observer was too high, i.e., the algorithm encountered fewer counts than the faint limit.
- The BRIGHT limit provided by the observer was too low, i.e., the algorithm encountered too many counts.

30.5.2 Peakup or Peakdown Acquisition (ACQ/PEAK)

This acquisition mode was used for bright targets, variable targets, targets whose energy distributions were not well known, and especially for those cases in which very accurate pointing was required. This acquisition mode was used extensively throughout the FOS operational lifetime. The highest pointing accuracies achieved with FOS used ACQ/PEAK and after July 1, 1992, all FOS flatfield, photometric calibration, and external wavelength calibration observations used high-precision multiple-stage ACQ/PEAK acquisitions.

Understanding ACQ/PEAK

An ACQ/PEAK stage consisted of a series of NXSTEPS=1, OVERSCAN=1 exposures made at each point in a user-specified scan pattern. All successful ACQ/PEAK stages ended with a telescope slew to the pointing corresponding to the brightest (for peakup) or faintest (for peakdown) exposure in the scan pattern. No attempts were made to interpolate positions between individual pointings in the scan pattern. Evaluation of the brightness of the signal at each dwell point was performed onboard by simple addition of the counts accumulated in all pixels with no correction for background, dead or noisy diodes, paired pulse, or even *edge-pixel exposure* effects.

As for ACQ/BIN, the first stage of a peak-up target acquisition was normally done in three integration steps with the 4.3" aperture and either the camera MIRROR or a disperser. As with all FOS acquisitions, the original target coordinates for the first stage were required to be accurate to about 1", so that the object fell within the 4.3" aperture. After this first stage the measured signals from the dwell points were stored in the raw data file as three groups. The dwell point with the maximum number of counts was determined and the telescope was positioned with the center of the aperture corresponding to this dwell point. The second stage, a 2 x 6 step pattern, using the 1.0" aperture, traced the location of the source within the 1.3" x 3.7" (1.4" x 4.3" pre-COSTAR) area where it was found in the first stage and these measures were recorded as groups in a separate data file. This narrowed the area in which the target was located to the surface area of the 1.0" aperture (to the one of the 12 integrations that had the most counts). The third stage of a peak-up sequence was normally a 3 x 3 point scan of the area of the 1.0" aperture, with the 0.5" aperture and a step size of about 0.3". This led to a pointing accuracy of about 0.2". If higher accuracy was needed, the surface area of the 0.5" aperture had to be scanned with the 0.3" aperture, possibly in two steps with decreasing step sizes. A variety of patterns and pattern-sequences were used by observers. Please refer to Table 32.3 for a listing of the FOS team-recommended patterns and nominal worst-case pointing accuracies.

No individual peakup or peakdown stage could be interrupted by Earth occultation. For much of the HST lifetime, telescope commanding imposed a maximum duration, including overheads, for any peakup/peakdown stage (or scan sequence) of 3000 seconds.

Pointing Accuracy: ACQ/PEAK

In the limit of perfect photon statistics, a positional accuracy upper limit for a particular coordinate in any ACQ/PEAK stage is one-half the step-size in that coordinate. This remains a good approximation for most commonly used apertures and scan patterns as the FOS team routinely recommended obtaining 10,000 counts in the peak dwell for so-called *critical peakups* (those that used the 0.3 or smaller aperture with step-sizes of 0.06" or smaller) and 50,000 counts in the most strongly exposed dwell of *critical peakdowns.* As Table 32.3 indicates, the most precise nominal worst-case pointing accuracy routinely recommended by the FOS team was 0.025" in each coordinate.

Paper Products: ACQ/PEAK

Figure 30.4 presents a typical FOS paper product ACQ/PEAK diagnostic plot for a 5 x 5 scan pattern. Apart from a period between July and November 1994 when anomalous scan parameter values were written in the ACQ/PEAK headers (see below), the pattern is plotted in the correct orientation and in the correct sense of telescope motion in detector coordinates. The offset to move the telescope to the brightest (or faintest in the case of peakdown) tile of the scan pattern is provided in both the detector (*x*,*y*) and telescope (V2,V3) frames. A compass rose is given. PA_APER is also given for easy conversion of (*x*,*y*) offsets to the (RA, Dec) frame, although we do not calculate the offset in (RA,Dec). See “Converting X,Y to RA, Dec” on page 33-9 for a description of how to convert to the (RA,Dec) frame. No contour plot is provided. No spectra or images from the individual tiles are plotted, but in some cases you may wish to inspect the individual groups that

contain these quantities. The standard jitter ball is provided which typically shows the scan pattern in (V2,V3) and indicates how closely the telescope moved to the desired dwell point.

Output Data Products: ACQ/PEAK

The *peakup* or *peakdown* mode is identified by the `.d0h` OPMODE value of ACQ/PEAK. Each stage of an ACQ/PEAK sequence produced its own set of output data files. An ACQ/PEAK scan-pattern with *x* rows and *y* columns produced output data files with (*x* x *y*) individual groups.

ACQ/PEAK measures with the MIRROR produced a one-line raster of 96 pixels (NXSTEPS=4, OVERSCAN=5 pattern with 20 diodes readout). Note that even the `4.3` aperture, the largest FOS aperture, illuminated only 12 diodes. ACQ/PEAK measures with a disperser produced 512 pixels (NXSTEPS=1, OVERSCAN=1 pattern with all 512 diodes read out by default). The number of diodes sampled in a dispersed light ACQ/PEAK could be altered by the specification of a limited wavelength range to be read out. These images and spectra are not calibrated by the pipeline, but may contain scientifically useful information. We recommend inspection of these data files (see below).

Analysis: ACQ/PEAK

You can determine the centering accuracy of most ACQ/PEAK stages by inspecting the distribution of counts in the tiles of the scan pattern. Notice that for many acquisitions, especially in the pre-COSTAR era, the centering accuracy is not the same in both FOS *x* and *y*. This led in some of these cases to compromised flat field and flux calibration.

The individual spectra in an ACQ/PEAK with either a disperser or MIRROR can yield valuable information about the distribution of light or excitation in extended sources, or provide additional spectroscopic information for point sources if the acquisition disperser was not used for any science observations. Care must be exercised, however, in analysis of these off-center observations as many such spectra will not be fully sampled by the diode array (see “Location of Image on Diode Array” on page 32-7).

In order to convert FOS *x*,*y* coordinates into sky coordinates, you need to know the position angle of the aperture, which is documented in the header keyword PA_APER (see “Converting X,Y to RA, Dec” on page 33-9) and which is routinely provided in the paper products.

The FOS paper products algorithm calculates observed counts per dwell tile from the `.c5` files, which have had several corrections applied that were not performed by the onboard ACQ/PEAK algorithm (most notably paired-pulse and edge-pixel exposure correction). In extremely rare cases involving very low count levels, the paper product algorithm may predict a different maximum tile than that actually chosen by the onboard processor. This discrepancy has been documented only in situations in which the FOS aperture door was closed due to guide star acquisition failure.

In mid-1994 the scan direction for some ACQ/PEAK exposures was changed at the same time that commanding overheads were made up to 20% more efficient. Between July and November 1994, ACQ/PEAK scan information was not written

to the header files. Analysis of ACQ/PEAK patterns in this period must be done manually with the information contained in the logsheet. The simplest approach to determine scan-pattern directions for your manual analysis is to run the FOS paper products for an equivalent ACQ/PEAK performed after November, 1994.

30.5.3 IMAGE Mode Target Acquisitions

Understanding FOS ACQ Imaging

FOS IMAGE mode observations mapped more than one position in the aperture with the diode array.

Spectral Element: MIRROR

FOS imaging mode with spectral element MIRROR was typically used for EARLY acquisition, INTeractive ACQuisition, or to obtain a verification image of the FOS large aperture to check the target position in the aperture.

Camera MIRROR images for interactive acquisition (logsheet entry INT ACQ) were designated by OPMODE=ACQ. Standard camera MIRROR images of the `4.3` aperture which did not require real-time interaction (logsheet entry ACQ) were designated, somewhat confusingly, by OPMODE=IMAGE. Both types of images have GRNDMODE=ACQUISITION and use the same set of pre-defined instrumental setups. The far less commonly used user-defined IMAGE command (logsheet entry IMAGE, spectral element MIRROR) allowed the user to specify image line and raster parameters for spectral element MIRROR and was designated by GRNDMODE=IMAGE, OPMODE=IMAGE. In the following we use the term FOS ACQ Imaging to refer to all of these imaging modes.

In a standard INT ACQ or confirming ACQ image the FOS Digicon was commanded through a pre-defined sequence of *x*-steps and *y*-steps which mapped the aperture. The 4.3˝ aperture was scanned with 64 strips, each of which was the height of the diode array, beginning at the bottom, *–y*, edge of the aperture. The post-COSTAR distance between the strips was 16 Y-base units or 0.0786˝for FOS/BL and 0.0812˝for FOS/RD The pre-COSTAR distance was 0.08958˝for both detectors. Each scan read out 20 diodes with the central 12 diodes spanning the 4.3˝ aperture. In the standard mode (NXSTEPS=4 and OVERSCAN=5) the number of pixels in each strip was 96. Thus the image has 96 x 64 pixels where each pixel were equally spaced on the sky (see Figure 30.13).

Figure 30.13: Digicon Faceplate Sampling Pattern in a Target Acquisition Image

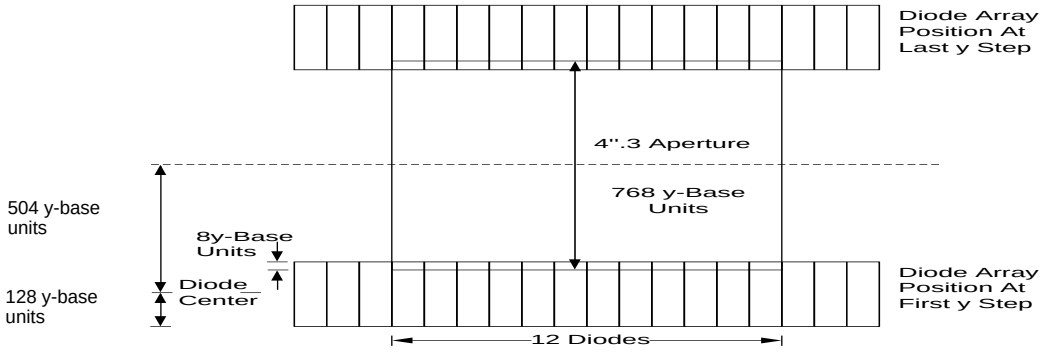

Spectral Element: Any Disperser

The rarely used user-defined dispersed-light IMAGE command (logsheet entry IMAGE with any disperser as spectral element) allowed the user to specify image raster parameters with a spectral element. Spectra with user-specified values for NXSTEPS and OVERSCAN at YSTEPS *y*-positions, symmetrically spaced about the default aperture center Y-base were obtained. So-called dispersed-light interactive target acquisitions were occasionally employed for solar system moving targets, usually comets, with a dispersed-light IMAGE mode observation at several *y*-positions in the `4.3` aperture. The maximum integrated count level in the entire spectrum determined the *y*-position offset of the initial blind pointing from nominal and the deviation of a well-known spectrum line from its anticipated *x*-position allowed determination of the blind pointing mis-centering in the *x*-direction.

Pointing Accuracy: FOS ACQ Imaging

Mirror Mode Images: Image centroiding accuracies varied, but for well-exposed images centering accuracies were about 0.1″ in both *x* and *y*.

Dispersed-Light Mode Images: Uncertainties of <0.5″ in both coordinates were achieved. This was typically sufficient for centering of comets in the `4.3` aperture.

Paper Products: FOS ACQ Imaging

Paper products for FOS images with spectral element MIRROR present grayscale renderings of the raw aperture image (see Figure 30.2). No image rectification or deconvolution is attempted. A compass rose provides orientation information and plate-scale fiducials are plotted. An exposure level key is also provided. See “Image Mode Spectra (IMAGE)” on page 30-47 for a discussion of dispersed-light image mode paper products.

Output Data Products: FOS ACQ Imaging

The calibrated INT ACQ and ACQ data files have 64 groups with each group having 96 pixels. The raw data file (`.d0h`) is an actual 96 x 64 image (1 group)

file. Output files for user-defined images contain header keyword YSTEPS groups of keyword (NCHNLS+(OVERSCAN-1))*NXSTEP pixels. Routine calibration processing produces `.c4` files which are no longer two-dimensional images, rather are multi-group files with one group for each raster of the image. The IRAF/STSDAS task **rapidlook** converts these processed files back to a two-dimensional representation suitable for examination with standard image processing tasks. A discussion of dispersed-light image mode data products is presented in “Image Mode Spectra (IMAGE)” on page 30-47.

Analysis: FOS ACQ Imaging

The substepping in both the *x* and *y* directions, and the elongated shape of the diodes, blurred and stretched the image (see Figure 30.14). A point source (which has the size of a PSF) on the photocathode was recorded by the same diode for four consecutive pixels in the *x* direction and 16 consecutive pixels in the *y* direction. The **tarestore** task in STSDAS can be used to deconvolve the image. In this task the image is trimmed and the flux resampled in the pixels. The **modeone** task also uses the **tarestore** task and displays the deconvolved image with the correct orientation on the sky (north and east are indicated).

Figure 30.14: Sample FOS Target Acquisition Image

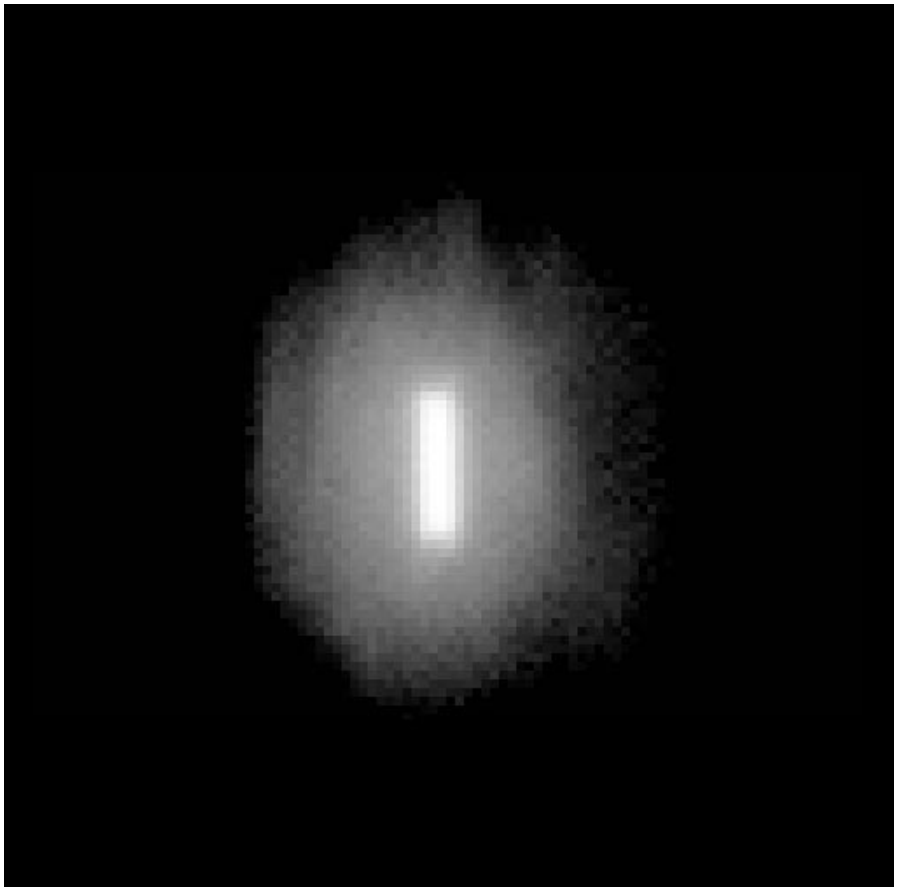

The position of the target in the image can be found by using the task **aperlocy** in STSDAS. This task computes the location of the image edges, the midpoint of each axis, the centroid of the image, and the total flux in the image. Note that **aperlocy** can not be used on restored images and that it will produce meaningful results only for images with a single source present. The output units of this task are diodes for the *x*-axis and Y-base units for the *y*-axis. This task also takes into account the elongated shape of the diodes in determining the target centroid in the aperture. The nominal center for the 4.3 aperture is at the pixel (48,32). To determine the nominal aperture center in diode and Y-base units, the following equations are used:

$$\text{aper\_center (X)} = \text{FCHNL} + \frac{(48-1)}{\text{NXSTEPS}}$$

$$\text{aper\_center (Y)} = \text{YBASE} + (32-1) \times 16$$

where:

- FCHNL is the first channel.
- NXSTEPS is the number of substeps.
- YBASE is the location of the diode array for the first group.

The centroid of the target can then be compared with the aperture center to determine the location of the target in the aperture. Note that the **aperlocy** task can also be used for images of the paired apertures. See the on-line help files in STSDAS for details.

30.5.4 Firmware Target Acquisition

Understanding ACQ/FIRMWARE

Firmware mode was occasionally used for pre-COSTAR planetary satellite observations, although this was an engineering mode. This procedure mapped the camera MIRROR image of the 4.3 aperture in *x* and *y* with small, selectable *y* raster increments. The microprocessor filtered this aperture map in real time and found *y*-positions of the peaks by fitting triangles through the data.

ACQ/FIRMWARE was less efficient than ACQ/BINARY and failed if more than one object were found. In practice this mode sometimes failed because the brightness limits were not set accurately by the observer. ACQ/FIRMWARE was used several times in the pre-COSTAR period and was included in an SMOV target acquisition testing program, but no ACQ/FIRMWARE acquisitions were performed in post-COSTAR science programs.

Pointing Accuracy: ACQ/FIRMWARE

Pre-COSTAR accuracies for ACQ/FIRMWARE were similar to those for ACQ/BINARY, approximately 0.15-0.20″ one sigma. No post-COSTAR evaluation of ACQ/FIRMWARE pointing accuracy was made.

Paper Products: ACQ/FIRMWARE

There are *no* ACQ/FIRMWARE-specific paper product displays. The standard spacecraft performance, jitter ball, and calibration status pages are produced.

Output Data Products: ACQ/FIRMWARE

The firmware target acquisition mode is identified by the OPMODE value of ACQ/FIRMWARE. The ACQ/FIRMWARE mode mapped the `4.3` aperture with a certain number (*m*) of Y-steps acquiring data from 20 diodes covering the aperture in the standard ACCUM mode. The target acquisition data therefore has *m* groups with 96 pixels (NXSTEPS=4 and OVERSCAN=5).

Analysis: ACQ/FIRMWARE

The microprocessor onboard the FOS searched for the peaks in the data array within a specific window and the target was centered at this location. The *m* groups could be plotted as a function of location and the position of the target in the aperture could be determined in a manner similar to the ACQ mode.

30.6 Assessing FOS Science Observations

After checking the target acquisition you may want to know whether the requested science integration time requirements were actually fulfilled. The exposure logsheet (see exposure number 4 in Figure 30.11) gives only a first estimate as requested exposure times were often modified by up to 20% to facilitate efficient orbit-packing. The actual on-source integration times are stored in the headers of the science data (e.g., the `.c1h` and `.c0h` files), in the header keyword EXPTIME. The Exposure Summary section of the FOS paper products Observation Summary page also provides this information. For example, logsheet exposure 4 in Figure 30.11 requested an exposure time of 33 minutes, but reference to Figure 30.10 shows that the actual integration time with the G270H grating was shortened to 26 minutes in order to fill the orbit up to occultation.

Alternatively, if an exposure should be much shorter than was planned, check whether the observation was interrupted by an earth occultation. In this case, the integration will have been resumed as a separate exposure with a new rootname after re-acquisition of the guide stars following the occultation. In the example of logsheet exposure 6 in Figure 30.11 a 100 minute exposure with grating G190H was requested. As shown in Figure 30.10 the initial G190H exposure could last only 17 minutes prior to occultation. A new G190H 48 minute exposure complete with separate rootname and data products entirely filled the next orbit and yet a third separate exposure of 35 minute duration in the orbit following rounded out the complete 100 minute exposure time requested. (If the proposer had used the appropriate RPS2 command, the last orbit could have been completely filled, but it was not in this case.) Since the three exposures were obtained in different orbits on different guide star re-acquisitions, it is important to check that no pointing or guiding anomalies have occurred and that all have produced comparable photometric results.

FOS exposures were not interruptible. Once data-taking stopped for occultation or SAA passage, the exposure was terminated. Upon target re-acquisition a new exposure began with a new observation rootname and resulted in a completely new set of science data products. Prior to co-adding such exposure segments they should be carefully compared to look for photometric or other differences that could be associated with pointing or guiding.

In the following sections we describe the details of each spectroscopic mode of FOS scientific data taking, namely ACCUM, RAPID, POLARIMETRY, PERIOD, and dispersed-light IMAGE. We describe the characteristics and structure of the mode-specific paper products and the electronic science data products. We will also provide guidelines concerning the analysis of the scientific data quality based upon evaluation of both the paper and electronic products.

The FOS paper products are useful for judging the quality of the spectra, including the quality of the calibration, the existence of artifacts, and the validity of specific features. Nonetheless, you may need additional detailed information on the single steps of the data calibration and on the characteristics of the instrument. Chapter 31 describes the pipeline calibration steps and how to recalibrate the data, which is always necessary. Chapter 32 delves into more detailed data analysis considerations, specifically error sources and attendant limiting accuracies for each of the major types of instrumental calibration.

The mode in which a given dataset was taken is identified in the data headers by the keywords OPMODE and GRNDMODE. The OPMODE (`.shh`) and GRNDMODE (`.d0h`, `.c1h`) keyword values are listed at the beginning of the output data products section in the following discussions of each of the individual science data-taking modes.

30.6.1 Spectrophotometry Mode (ACCUM)

Understanding ACCUM

ACCUM was the most commonly used FOS spectroscopic mode. ACCUM mode spectra with a total exposure time lasting more than a few minutes were read out at regular, *equally sized*, intervals to the ground or to the onboard tape recorders. The frequent readouts protected against catastrophic data loss. Since the data were read out at regular intervals, all observations longer than a few minutes (the time between readouts was usually about two minutes for FOS/RD and usually about four minutes for FOS/BL) were time resolved. The first readout was stored as group one, the next readout was added (accumulated) to the previous readout and the sum was stored as group two, and so on. The last group contains the spectrum from the full exposure time of the observation. The number of groups per observation depended on the length of the exposure and the detector used. Remember that for paired apertures and STEP-PATT not SINGLE, half of the specified exposure time was spent in each aperture with the data accumulated in alternating intervals of approximately 10 seconds.

Paper Products: ACCUM

ACCUM mode paper products produce three pages of mode-specific diagnostic plots. These are the flux vs. wavelength and log flux vs. wavelength page for the last group which contains the full exposure (see Figure 30.5), the corrected counts vs wavelength page for the last group (see Figure 30.6); and the group-by-group total counts plot (Figure 30.7). The last plot is particularly useful for assessing photometric repeatability and in revealing potential problems related to guiding, breathing, background, and intermittent noisy diodes. Please see additional notes in analysis section below concerning assessment of background count levels.

Output Data Products: ACCUM

Spectrophotometry mode is identified by an OPMODE keyword value of ACCUM and a GRNDMODE keyword value of SPECTROSCOPY. For the standard ACCUM mode, the default value of NXSTEPS was 4 and OVERSCAN was 5. ACCUM mode data files for SINGLE aperture exposures contain GCOUNT groups of 2064 pixels each. The `.d0*` and `.c4*` files of OBJ-OBJ or OBJ-SKY paired aperture observation data products may be longer as discussed in “Paired-Aperture File Structures” on page 30-6.

Analysis: ACCUM

In standard FOS ACCUM mode spectra the last group contains the accumulated total integration on the target. The paper products calibrated spectrum can be evaluated to check whether the flux level is roughly like that expected. (Alternatively, the IRAF/STSDAS task **fwplot** can also be used to perform this check.) If more than one detector readout occurred (i.e., the exposure was longer than two minutes for FOS/RD or four minutes for FOS/BL), use the paper products group counts plot to evaluate the overall photometric quality and repeatability of the measures. This plot can reveal the influence of poor guiding, breathing, re-centering events, and intermittent noisy diodes on individual groups that would normally not be expected from inspection of the last data group alone.

The background count rate is given in the Exposure Summary section and will be displayed in the paper product corrected count rate plot if it is on-scale. Although a model prediction of the background (and, for several dispersers, an approximation to the scattered light) has been removed from the quantities plotted in the paper products, it is useful to note that a 120 second total duration (30 seconds per pixel) standard FOS/RD ACCUM with 2064 pixels had a typical background component of 600-1200 dark counts per group. Similarly, a typical 240 second FOS/BL ACCUM exposure produced 900–1800 dark counts per group. It is often useful to compare this signal with the background-corrected quantity provided in the group counts plot. Extraction of individual group spectra can be accomplished with task **deaccum** (see “deaccum” on page 33-9).

If the spectrum was split up into two or more parts, for example because it was observed in more than one orbit due to occultations, you can obtain the sum of all integrations by adding up, with appropriate weighting, the last groups of all `.c1` spectra of your target taken with the same instrument configuration (combination of detector, aperture, and disperser).

For all but edge-pixels, the exposure time per pixel is *not* EXPTIME, but rather EXPTIME/NXSTEPS. Pipeline **calfos** processing correctly manages the exposure time for all pixels and populates the statistical error arrays according to actual detected count levels for all pixels.

30.6.2 Rapid Readout Mode (RAPID)

Understanding RAPID

For many astronomical targets where rapid variability in flux was suspected, but the precise period was unknown, or the expected variation was aperiodic, PERIOD mode of data acquisition was unsuitable because the bin folding period must be specified. In such cases the RAPID readout mode was used. RAPID mode was also used in cases where very strong signal would overflow the 16-bit FOS accumulators in the default ACCUM readout times (e.g., bright emission line sources). In this mode, the data were acquired using the normal substepping and overscanning techniques. The spectra were read out at intervals (chosen by the observer according to the scientific goals) that were much shorter than the normal four minute (FOS/BL) or two minute (FOS/RD) segments. Each readout was stored in the raw data file as a group. The number of groups in a RAPID mode observation `.d0h` file was equal to the number of individual readouts. For paired apertures and STEP-PATT not SINGLE, half of the specified exposure time was spent in each aperture with the data accumulated in alternating intervals of approximately 10 seconds or (readout time divided by 2), whichever was smaller.

Paper Products: RAPID

RAPID mode paper products produce three pages of mode-specific diagnostic plots. These are the flux vs. wavelength and log flux vs. wavelength page for the first group of the time-series (see Figure 30.5), the corrected counts vs wavelength page for the first group (see Figure 30.6); and the group-by-group total counts plot (Figure 30.7). As with ACCUM mode, the last plot is particularly useful for assessing photometric repeatability and in revealing potential problems related to guiding, breathing, background, and intermittent noisy diodes. Further, since the group counts plot is essentially a count rate light curve, it provides a quick look at a science objective of many RAPID readout programs. Please see additional notes in analysis section below concerning assessment of background count levels.

Output Data Products: RAPID

Rapid readout mode is identified by the keyword values OPMODE=RAPID and GRNDMODE=RAPID READOUT. There are GCOUNT groups of individual readouts. As with ACCUM mode, the default value of NXSTEPS is 4 and OVERSCAN is 5 and default spectrum length is 2064 pixels, however NXSTEPS was often modified by the user. The `.d0*` and `.c4*` files of OBJ-OBJ or OBJ-SKY paired aperture observation data products may be longer as discussed in “Paired-Aperture File Structures” on page 30-6 Additionally, the user could restrict the measured wavelength range, which produced a smaller number

of pixels to be read out, and which dould, in certain circumstances, preclude scattered light correction.

The .c3h (special mode processing output - see next chapter) file contains two data groups. The number of pixels in each group is equal to the number of readouts (groups) in the original data. Group 1 of the .c3h file contains the summed flux values where the value of each pixel is the sum of all pixels from an original readout (i.e., pixel 1 contains the sum of all pixel values from readout 1, pixel 2 is the sum of all pixels from readout 2, etc. This is similar to, effectively a flux-calibrated version of, the information plotted in the paper products group counts display). Group 2 contains the sum of the corresponding statistical error values (in quadrature). The .c3h files effectively provide the light curve of the target for the length of the observation. See “Details of the FOS Pipeline Process” on page 31-13 for more details on special mode processing.

Analysis: RAPID

The IRAF/STSDAS task to combine groups in a RAPID mode dataset is **rcombine** (see Chapter 3).

Often RAPID mode observations were taken with NSXTEPS values other than four. The standard calibration software routinely handles these cases without special user intervention.

A few programs used OVERSCAN=1 to facilitate extremely fast readout. OVERSCAN=1 data are not calibrated by routine operation of **calfos** as all FOS reference files are based upon OVERSCAN=5 calibration observations. As an approximation in these cases, the first 2048 pixels of STScI reference files can be resampled for the appropriate NXSTEPS and, after editing the OVERSCAN value in the header, used with **calfos**. Archive researchers should keep in mind that these OVERSCAN=1 observations were not designed with the intention of producing accurate absolute photometry.

Many FOS/BL programs included RAPID mode time-series with the G160L grating. In addition to the ultraviolet spectrum, the zeroth order signal was also recorded. Therefore, white-light curves were often recorded in concert with the ultraviolet observations. Careful assessment of the count levels in the zeroth order spike should be made before attempting quantitative analysis as this very strong signal often produced accumulator wraparound (overflow) even in the relatively short readout times common in RAPID mode programs.

The background count rate is given on the Exposure Summary page and will be displayed in the paper product corrected count rate plot if it is on-scale. Although a model prediction of the background (and, for several dispersers, an approximation to the scattered light) has been removed from the quantities plotted in the paper products, it is useful to note and compare these quantities with the detected count rates as shown in the corrected count vs wavelength plot. A similar comparison with the group count plot levels can be made in which the average background count level can be estimated as (5 x readout time)

The RAPID mode readout time interval (logsheet entry READ-TIME) was not always constant in actual practice due to the internal operation of the FOS. Determination of the precise start and stop times of the individual readouts in

many RAPID mode exposures requires special processing of engineering telemetry not normally available to the end user. If you need absolute or relative timing more precise than 0.125 sec, then you should contact `help@stsci.edu` for special support. Additional information on RAPID mode timing is found in “RAPID Mode Observation Timing Uncertainties” on page 33-5, as well as in the *FOS Instrument Handbook*, and in *FOS ISR* 154.

30.6.3 Spectropolarimetry Mode

Understanding SPECTROPOLARIMETRY

The polarimetry data consist of a number of exposures (POLSCAN=16, 8, or 4) with the waveplate set at different angles and taken consecutively (within one orbit). The Wollaston prism split the light beam into two spectra corresponding to the orthogonal directions of polarization. Hence, each exposure consists of the two orthogonal spectra obtained with a single waveplate angle. These spectra were deflected alternately onto the diode array, recorded as two pass directions, and stored as a single group in the raw data file. The first spectrum in the data group corresponds to the first pass direction (ordinary ray), the second to the second pass direction (extraordinary ray).

Paper Products: SPECTROPOLARIMETRY

There are *no* SPECTROPOLARIMETRY-specific paper product displays. The standard exposure summary, spacecraft performance, jitter ball, and calibration status pages are produced.

Output Data Products: SPECTROPOLARIMETRY

Spectropolarimetry mode[1] is identified by an OPMODE value of ACCUM and a GRNDMODE value of SPECTROPOLARIMETRY.

The number of groups in the raw data file is equal to NREAD x POLSCAN. Thus, normally (for NREAD=1) there will be as many groups in the raw data file as the number of waveplate positions used in the observation. The number of POLSCAN positions (and therefore the total number of groups in the raw data file) may be 4, 8, or 16 depending on the number of polscans requested.

The group contents of the raw (`.d0h`) data file are shown in Table 30.8. Note that the number of pixels in each group is twice the number of pixels in a single spectrum as there are two spectra appended together, one for each pass direction. The number of pixels in the spectrum depends on the values of NXSTEPS and OVERSCAN used.

1. Further details concerning polarimetry datasets and their calibration procedures can be obtained from within IRAF by typing “help spec_polar opt=sys”.

Table 30.8: Group Contents of Raw Polarimetry Science Data Files

Group #	Contents
1	Polscan 1: pass direction 1 and pass direction 2
2	Polscan 2: pass direction 1 and pass direction 2
3	Polscan 3: pass direction 1 and pass direction 2
...	....
15	Polscan 15: pass direction 1 and pass direction 2
16	Polscan 16: pass direction 1 and pass direction 2

The organization of calibrated polarimetry data files differs from the raw data files and calibrated data taken in other observing modes in that the two pass direction spectra from each readout are stored in separate data groups instead of being concatenated within one group. The calibrated fluxes, the corresponding statistical errors, and the data quality are stored in 2 x POLSCAN number of groups, similar to the wavelengths. *Note that for polarimetry data the statistical errors cannot be combined simply.* The errors in the Stokes parameters are calculated separately by the data reduction pipeline. The polarimetry-specific data are stored once again as groups in a separate file.[2]

The `.c0h` file is a dataset with 2 x POLSCAN groups with wavelengths for both pass directions through the Wollaston prism and each POLSCAN position. Note that the wavelengths for the different POLSCAN positions should be identical, but the wavelengths are offset between the two pass directions by a constant amount.

The `.c1h` file is a dataset with 2 x POLSCAN groups containing calibrated flux for both pass directions and each POLSCAN position. The calibrated fluxes are stored in exactly the same way as the wavelengths. Note that unlike calibrated flux data for non-polarimetric observations, the first group will not represent the absolute flux for the source, but only half, since the light was split into two spectra by the polarizer. Representative fluxes are formed by averaging the fluxes from the complete set of POLSCAN positions for each pass direction separately, and then summing the two. Since there is a wavelength shift between the spectra from the two pass directions, to combine the two mean spectra from both pass directions one spectrum must be shifted in wavelength to match the other. *Pass direction 2 is shifted onto pass direction 1. In the summed spectrum, any pixel that has contributions from only one pass direction is set to zero.* The total flux (Stokes I) is computed by the special mode processing phase of **calfos** and is stored in the `.c3h` dataset (see below) and so is more conveniently obtained from there.

The `.c2h` file is a dataset with 2 x POLSCAN groups with the statistical error of the calibrated flux for both pass directions and each POLSCAN position. The flux errors are stored in exactly the same way as the wavelengths and fluxes. As

2. See *FOS ISR* 078.

for the calibrated flux dataset, this dataset differs from the statistical errors for non-polarimetric data and the errors cannot be simply combined. We suggest that the error on the Stokes I parameter computed by the polarimetry processing be used as the total flux error.

The .cqh file is a dataset with 2 x POLSCAN groups with the data quality values for the calibrated fluxes. The organization is exactly the same as that of the calibrated fluxes dataset. The group organization of the .c0h, .c1h, .c2h, and .cqh files is shown in Table 30.9.

Table 30.9: Group Organization of the Calibrated .c0h, .c1h, .c2h, and .cqh Files

Group	Contents Depending on Calibration File
1	Polscan 1, Pass direction 1: wavelength, flux, error or data quality
2	Polscan 1, Pass direction 2: wavelength, flux, error or data quality
3	Polscan 2, Pass direction 1: wavelength, flux, error or data quality
4	Polscan 2, Pass direction 2: wavelength, flux, error or data quality
...	...
31	Polscan 16, Pass direction 1: wavelength, flux, error or data quality
32	Polscan 16, Pass direction 2: wavelength, flux, error or data quality

The .c3h file is a dataset with 56 groups containing the reduced polarimetry data. The dataset is organized into four sets of 14 groups, where groups 1 through 14 contain the Stokes parameter and polarimetry data for pass direction 1, groups 15 through 28 for pass direction 2, groups 29 through 42 contain the merged data from both pass directions 1 and 2, and groups 43 through 56 contain the merged data corrected for interference and instrument orientation. The organization of the .c3h file is shown in Table 30.10.

Note that the wavelengths corresponding to the first set of 14 groups are given by the wavelength array for the first pass direction (i.e., group 1 of the .c0h file), while for the second set of 14 groups (groups 15 through 28) the corresponding wavelengths are given by the wavelength array for the second pass direction (i.e., group 2 of the .c0h file). For the merged data in the third and fourth sets of 14 groups (groups 29 through 56), the corresponding wavelengths are given by the first pass direction.

Analysis: SPECTROPOLARIMETRY

All polarimetric observations should be recalibrated. The polarimetric calibration portions of **calfos** will soon include special corrections to remove the influence of the COSTAR optics on polarimetric measures.

Table 30.10: Group Organization of the Calibrated .c3h File

Group # Pass Direction 1	Group # Pass Direction 2	Group # Pass Direction 1&2	Group # Pass Direction 1&2 corrected	Contents
1	15	29	43	Stokes I
2	16	30	44	Stokes Q
3	17	31	45	Stokes U
4	18	32	46	Stokes V
5	19	33	47	Stokes I error
6	20	34	48	Stokes Q error
7	21	35	49	Stokes U error
8	22	36	50	Stokes V error
9	23	37	51	Linear polarization
10	24	38	52	Circular polarization
11	25	39	53	Polarization position angle
12	26	40	54	Linear polarization error
13	27	41	55	Circular polarization error
14	28	42	56	Polarization position angle error

30.6.4 Time-Resolved Spectrophotometry Mode (PERIOD)

Understanding PERIOD

This mode was designed for objects with known periodicity in the 50 msec to 100 sec range. To maintain the phase information of these observations, the known period (CYCLE-TIME) of the object was divided into *bins* or *slices*, where each bin had a duration time = period/BINS. The spectra acquired in this mode were stored in the different bins which correspond to a given phase of the period. The information obtained in each period was added to the pattern so that the phase information was maintained (so long as the period was known accurately).

Relativistic aberration is important for short periods and long observations. However, there is no correction for light travel time across the orbit.

Paper Products: PERIOD

There are *no* PERIOD-specific paper product displays. The standard exposure summary, spacecraft performance, jitter ball, and calibration status pages are produced.

Output Data Products: PERIOD

Time-resolved spectrophotometry mode is identified by the keyword values OPMODE=PERIOD and GRNDMODE=TIME RESOLVED.

The raw (.d0h) data file for time-resolved mode contains a single data group that is made up of all the individual spectral slices (or bins) stored sequentially. For example, if an observation used 374 detector channels, with NXSTEPS=1, OVERSCAN=5, and SLICES=32, the .d0h file would contain one data group having a total length of:

$$(374 + (5 - 1)) \times 1 \times 32 = 12096 \text{ pixels}$$

The calibrated flux, wavelength, error, and data quality files will have the data from the individual slices (bins) broken out into separate groups. For the example above, the .c0h, .c1h, .c2h, and .cqh files would have 32 groups of 378 pixels.

The .c3h file is organized as follows. Groups 1 and 2 contain the average flux and average errors, respectively, of all the individual calibrated spectra. Following these, there are pairs of groups where the first group in each pair contains the difference between an individual flux spectrum and the average, and the second group in each pair contains the sum of the errors for the individual spectrum and the average. See “Special Mode Processing (MOD_CORR)” on page 31-23 for details on how the average and difference spectra are generated. For example, if the observation consisted of 32 slices, the structure of the .c3h file would be that shown in Table 30.11.

Table 30.11: Group Structure of PERIOD Mode .c3h File with 32 Slices

Group #	Contents
1	Average of all 32 flux spectra from the .c1h file
2	Average of all 32 error spectra from the .c2h file
3	Spectrum 1 minus average
4	Combined spectrum 1 and average errors
5	Spectrum 2 minus average
6	Combined spectrum 2 and average errors
...	...
65	Spectrum 32 minus average
66	Combined spectrum 32 and average errors

Analysis: PERIOD

Only two scientific programs employed PERIOD mode. Due to implementation problems and errors, no PERIOD mode observations were completely successful. Successful tests were performed during Science Verification.

30.6.5 Image Mode Spectra (IMAGE)

Understanding IMAGE Spectra

FOS IMAGE mode observations imply mapping of more than one position in the aperture by the diode array. If a disperser was chosen as the spectral element, then spectra at YSTEPS *y*-positions, symmetrically spaced about the default aperture center Y-base were obtained. The specified exposure time was equally divided among the YSTEPS individual spectra, and was obtained in a continuing revolving series of approximately 10 second integrations at each individual Y-position until an exposure of EXPTIME was accumulated. Intermediate ACCUM-like readouts could occur. Although nearly all IMAGE mode FOS spectra were obtained for flux and flatfield calibration purposes, some measures of this type were used for the purpose of interactively acquiring moving targets with absorption lines at known wavelengths.

Paper Products: IMAGE Spectra

Figure 30.15 below shows an example of the one page of mode-specific FOS paper products for IMAGE mode spectra. Flux and wavelength calibrations are not routinely applied to IMAGE mode spectra as these calibrations are normally for the central *y*-levels of an aperture whereas an IMAGE mode spectrum, by definition, might be sampled from any *y*-position in the aperture. As a result, only a plot of the corrected count spectra for each *y*-position (YPOS) of observation is made versus *pixel number*. No group counts plot is made to assess photometric repeatability.

Note the dead diode at approximately pixel 1150 in all three groups of Figure 30.15.

Figure 30.15: FOS Paper Products Corrected Counts Plot for IMAGE Spectra

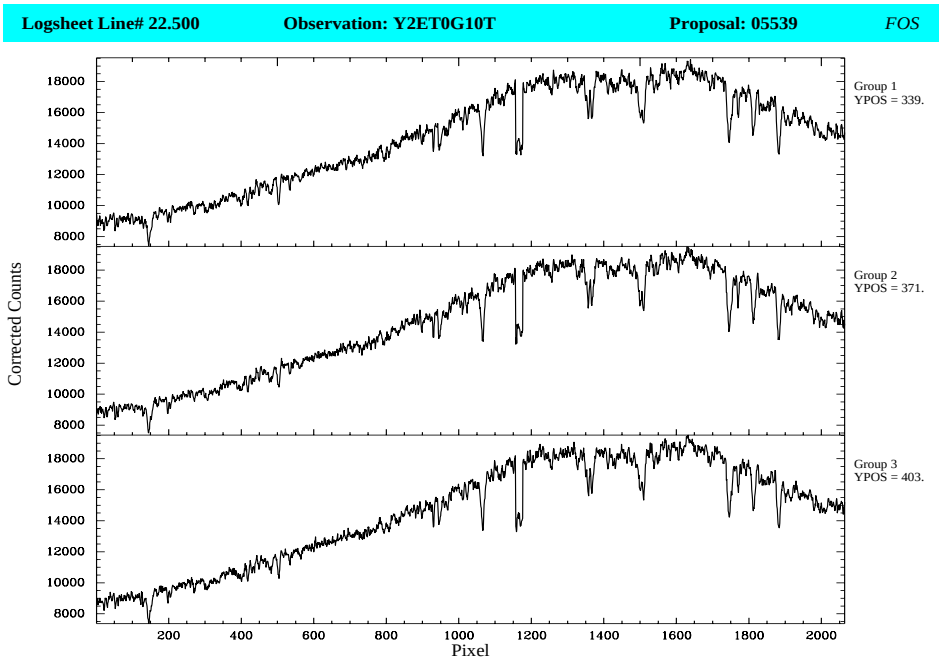

Output Data Products: IMAGE spectra

Image mode spectra are identified by an OPMODE value of IMAGE and a GRNDMODE value of IMAGE and a FGWA_ID of any spectral element except MIRROR. Normally, NXSTEPS=4 and OVERSCAN=5 were used to produce groups of 2064 pixels, but the full range of commandable values was allowed.

Usually one output group exists in the output data products for each raster spectrum line (YPOS) in the image. If more than one readout occurred (rare, but it could happen), then YSTEPS x NREAD groups exist in the data files. Each set of YSTEPS groups were accumulated in the same fashion as ACCUM mode measures, so that the last set of YSTEPS groups contains the accumulated spectra.

IMAGE mode spectra are not routinely flux calibrated by the pipeline because the *x*-position mapping to wavelengths is calibrated only for the aperture center Y-base. Therefore, the `.c1*` files are identical to the `.c5*` files (i.e. count rates corrected for everything but sensitivity).

Analysis: IMAGE spectra

The special FOS STSDAS routine **yfluxcal** can be used to flux calibrate IMAGE spectra on the assumption that the aperture-center wavelength calibration is applicable to the actual Y-base employed. This is a suitable assumption for virtually all calibration program IMAGE mode spectra.

.

Chapter 31

Calibrating and Recalibrating FOS Data

In This Chapter...

This chapter describes how data are processed in the standard pipeline calibration. The software used in the STScI calibration pipeline is the same as the **calfos** task used to re-calibrate data. Here we will emphasize the calibration procedures themselves and defer discussions of errors and uncertainties to the next chapter.

31.1 Pipeline Calibration Overview

The basic steps of the calibration pipeline, calfos, are summarized in Figure 31.1 and Table 31.1.

Figure 31.1: Pipeline Processing by **calfos**

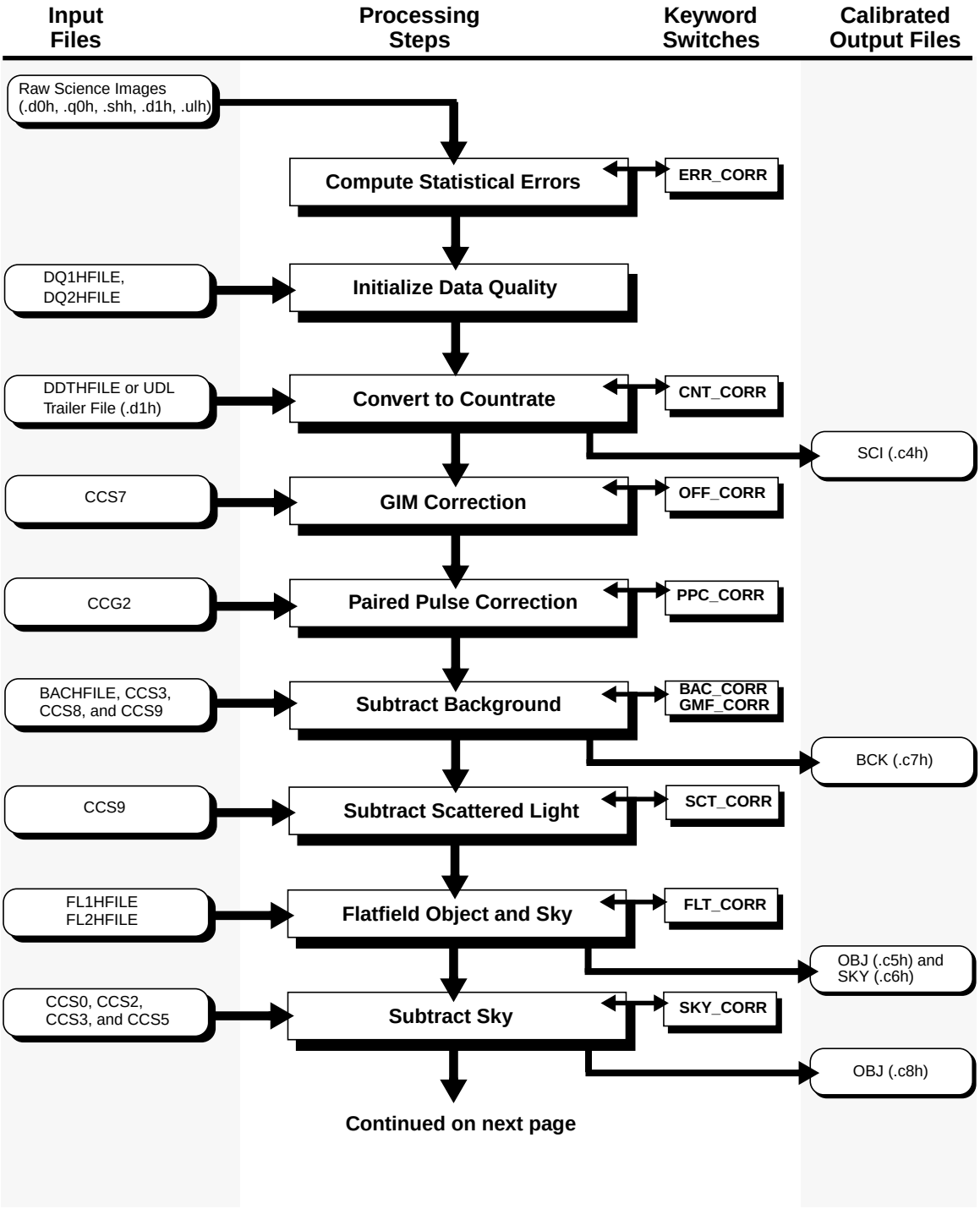

Figure 31.1: Pipeline Processing by calfos (Continued)

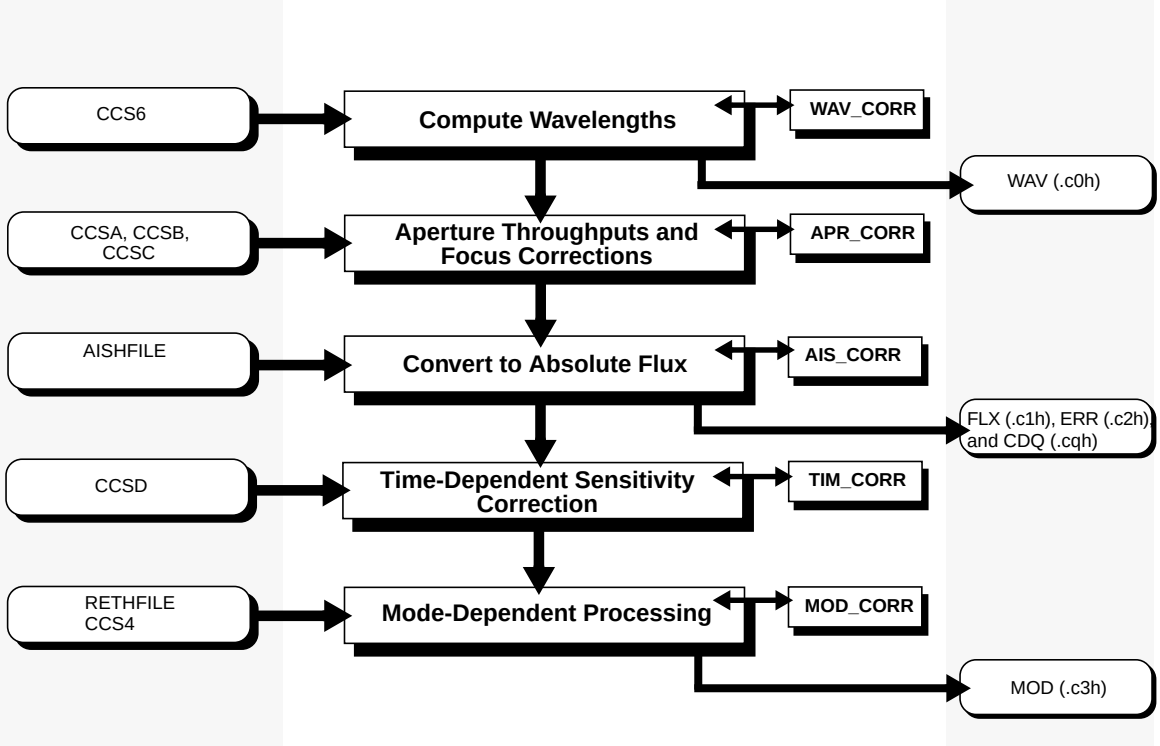

Table 31.1: Calibration Steps and Reference Files for FOS Pipeline Processing

Switch	Processing Step	Reference File or Table
ERR_CORR	Compute propagated error at each point in spectrum. Error file calibrated with science file and propagated statistical errors written to .c2h.	
CNT_CORR	Convert from raw counts to count rates by dividing each data point by exposure time and correcting for disabled diodes. Diode numbers are taken from ddthfile or from the unique data log.	`ddthfile`
OFF_CORR	Correct for image motion in the FOS X direction (dispersion) induced by magnetic field. Uses a model of the earth's magnetic field along with scale factors from table ccs7. This step should be applied for observations taken before April 5, 1993, after which the on-board GIM correction is used.	`ccs7`
PPC_CORR	Correct raw count rates for saturation in detector electronics using paired-pulse correction table (coccgr2).	`ccg2`
BAC_CORR	Correct for particle-induced background using default reference background (bachfile) if no background spectrum was obtained as part of the observation.	`bachfile`

Table 31.1: Calibration Steps and Reference Files for FOS Pipeline Processing (Continued)

Switch	Processing Step	Reference File or Table
GMF_CORR	If BAC_CORR is set to PERFORM, and the default background file (bachfile) is used, this file can be scaled to the expected mean count rate for the spacecraft geomagnetic position using the ccs8 reference table and subtracted from the count rate spectra by setting GMF_CORR to PERFORM. Scaled background is written to the .c7h file.	ccs8
SCT_CORR	Remove background scattered light. The scattered light is determined by calculating the mean value of diodes not illuminated by the selected grating. This mean is then subtracted from the observed spectrum. Un-illuminated diodes are found in the CCS9 reference table.	ccs9
FLT_CORR	Correct for diode to diode sensitivity variations by multiplying by the flatfield response file (fl1hfile). For paired aperture or spectropolarimetry observations, a second flatfield file is used.	fl1hfile, fl2hfile
SKY_CORR	If a sky spectrum was observed, the background is subtracted and the sky smoothed using a median and mean filter. Uses filter widths table (ccs3), aperture size table (ccs0), emission line positions (ccs2), and sky shift table (ccs5).	ccs0, ccs2, ccs3, ccs5
WAV_CORR	Compute vacuum wavelength scale for each object or sky spectrum using coefficients (ccs6).	ccs6
APR_CORR	Correct for relative aperture throughputs. Object data are normalized to the reference aperture used to derive the average inverse sensitivity used in AIS_CORR. This step is required if AIS_CORR is used. Additionally, object data are divided to correct for changes in aperture throughput due to changes in OTA focus.	ccsa, ccsb, ccsc
FLX_CORR	**POLARIMETRY ONLY**: Convert from count rate to absolute flux units by multiplying by inverse sensitivity curve. Uses inverse sensitivity file (iv1hfile) and, for paired aperture or spectropolarimetry, file (iv2hfile).	iv1hfile, iv2hfile
AIS_CORR	Convert from count rate to absolute flux units by multiplying by inverse sensitivity curves. This step replaces FLX_CORR and is different in that an average inverse sensitivity, determined from calibration of all epochs, is used. APR_CORR must be performed for this step to have meaning.	aishfile
TIM_CORR	Correct for changes in instrument sensitivity over time by dividing the object data by an appropriate correction factor.	ccsd
MOD_CORR	Perform ground software mode dependent corrections for time-resolved, rapid readout, or spectropolarimetry observations. For RAPID, write total flux and sum of statistical errors to groups 1 and 2 of .c3h file. For PERIOD mode, write pixel-by-pixel averages of all slices to groups 1 and 2 of .c3h file. For spectropolarimetry, data from individual waveplate positions is used to make Stokes parameters I, Q, U, and V and linear and circular polarization position angle spectra.	ccs4, rethfile

31.2 Input Files

calfos uses three different types of input files:

- Input data files: these are the observation data files, in Generic Edited Information Set (GEIS) format, i.e., a multi-group image.
- Reference files (GEIS format images).
- Reference tables (STSDAS tables).

31.2.1 Science Files Required by calfos

Table 31.2 lists the science files that are used as required input to **calfos**.

Table 31.2: Observation Input Files for calfos

File Extension	File Contents
.shh and .shd	Standard header packet
.ulh and .uld	Unique data log
.d0h and .d0d	Science data
.q0h and .q0d	Science data quality
.x0h and .x0d	Science header line
.xqh and .xqd	Science header line data quality
.d1h and .d1d	Science trailer line
.q1h and .q1d	Science trailer line data quality

31.2.2 Reference Files and Tables

Table 31.1 lists the types of calibration reference files that are used in the pipeline and the information these files contain. Although reference files can be generated for any combination of NXSTEPS, FCHNL (first channel), NCHNLS, and OVERSCAN, the routine calibration reference files have a length of 2064 pixels, corresponding to the standard keyword values:

- NXSTEPS = 4
- FCHNL = 0
- NCHNLS = 512
- OVERSCAN = 5

For other values of FCHNL, NCHNLS, and NXSTEPS **calfos** interpolates from or resamples the standard reference files. *Only* OVERSCAN = 5 *is supported by FOS calibration*. Highly accurate OVERSCAN=1 reference files

can not be simply extracted from the standard reference files as different values of OVERSCAN produced contributions from different numbers of physical diodes to the observed pixels. All FOS calibration observations were made with OVERSCAN=5.

Table 31.3: Reference Tables and Files Required by calfos

Header Keyword	Data Base Relation	Filename Extension	File Contents
CCS0	cyccs0r	.cy0	Aperture areas
CCS1	cyccs1r	.cy1	Aperture positions
CCS2	cyccs2r	.cy2	Sky emission line positions
CCS3	cyccs3r	.cy3	Sky and background filter widths
CCS4	cyccs4r	.cy4	Polarimetry parameters
CCS5	cyccs5r	.cy5	Sky shift parameters
CCS6	cyccs6r	.cy6	Wavelength dispersion coefficients
CCS7	cyccs7r	.cy7	GIM correction scale factors
CCS8	cyccs8r	.cy8	Predicted background (count rate)
CCS9	cyccs9r	.cy9	Un-illuminated diodes for scattered light correction
CCSA	cyccsar	.cya	OTA focus positions for aperture throughputs
CCSB	cyccsbr	.cyb	Aperture throughput coefficients
CCSC	cyccscr	.cyc	Throughput corrections versus focus
CCSD	cyccsdr	.cyd	Instrument sensitivity throughput correction factors
CCG2	coccg2r	.cmg	Paired-pulse coefficients
BACHFILE	cybacr	.r0h & .r0d	Default background file (count rate)
FL*n*HFILE	cyfltr	.r1h & .r1d	Flatfield file
IV*n*HFILE	cyivsr	.r2h & .r2d	Inverse sensitivity file (ergs cm^{-2} $Å^{-1}$ $count^{-1}$ $diode^{-1}$)[a]
RETHFILE	cyretr	.r3h & .r3d	Retardation file for polarimetry data
DDTHFILE	cyddtr	.r4h & .r4d	Disabled diode file
DQ*n*HFILE	cyqinr	.r5h & .r5d	Data quality initialization file
AISHFILE	cyaisr	.r8h & .r8d	Average inverse sensitivity file

a. Note that all references to inverse sensitivity, IVS, in the version 6 *FOS Instrument Handbook* contain the per diode component of this definition implicitly. The meaning of IVS is identical in both this document and in the *FOS Instrument Handbook*.

31.3 CDBS Reference Relations

The CDBS relations for the FOS reference files and reference tables are described below. Note that these are relations that point to the reference files and tables: they do not contain the data used. Multiple entries are allowed for each reference file or table type which are distinguished by effective (or USEAFTER) date.

- **cyccs0r:** This table is used to determine the aperture area for paired apertures. If STEP-PATT=OBJ-SKY (or STAR-SKY) is used, it is only for sky subtraction.
- **cyccs1r:** This table is used to determine which aperture (UPPER or LOWER) of a paired aperture was used for observing an object or sky spectrum.
- **cyccs2r:** Regions of the sky spectrum known to have emission lines. These regions are not smoothed before the sky is subtracted from the object spectrum.

The cyccs2r table values were never formally confirmed after science verification (SV). This had little or no practical impact as, only a few sky observations were taken, none of which were intended to aid the proposed science.

- **cyccs3r:** Filter widths used for smoothing the sky or background spectra.
- **cyccs4r:** Polarimetry information regarding waveplate pass direction angles, initial waveplate position angles, the pixel number at which the wavelength shift between the two pass directions is to be determined for computing the merged spectrum, and the phase and amplitude coefficients for correction of polarization angle ripple.
- **cyccs5r:** The shift in pixels to be applied to the sky spectrum before subtraction.
- **cyccs6r:** Dispersion coefficients to generate wavelength scales. There is one entry for each detector, disperser, aperture, and polarizer combination.
- **cyccs7r:** GIM correction scale factors used to scale the modeled shift of the spectrum due to the earth's magnetic field.
- **cyccs8r:** Predicted background count rates as a function of geomagnetic position used to scale the background reference file.
- **cyccs9r**: Un-illuminated diode ranges for each detector and grating combination. Used to determine the background scattered light.
- **cyccsar**: List of OTA focus positions versus time. Used to correct for aperture sensitivity dependent on focus position.

- **cyccsbr**: As a function of detector and disperser combination, coefficients to normalize aperture throughputs to the reference aperture used to determine the average inverse sensitivity calibration.
- **cyccscr**: Throughput corrections versus focus as a function of the combination of detector, disperser, and aperture.
- **cyccsdr**: As a function of detector and disperser combination, throughput correction factors to account for changes in instrument sensitivity over time.
- **coccg2r:** Paired pulse correction table used to correct for non-linear response of the diode electronics. Both detectors have the same correction constants, which are time independent. This table is shared with GHRS.
- **cybacr:** This relation is for the background reference files. For each detector there is one file that is used as a default background count rate in the event no background spectra were observed.
- **cyfltr:** This relation is for the flatfield reference files. These files are used to remove the small scale diode and photocathode non-uniformities. There are separate files for each detector, disperser, aperture, and polarizer combination.
- **cyivsr:** *(polarimetry only)* This relation is for inverse sensitivity reference files. These files are used to convert corrected count rates to absolute flux units. There are separate files for each detector, disperser, aperture and polarizer combination.

Figure 31.2: Pre-COSTAR Inverse Sensitivity Curves for Blue High Dispersion Gratings

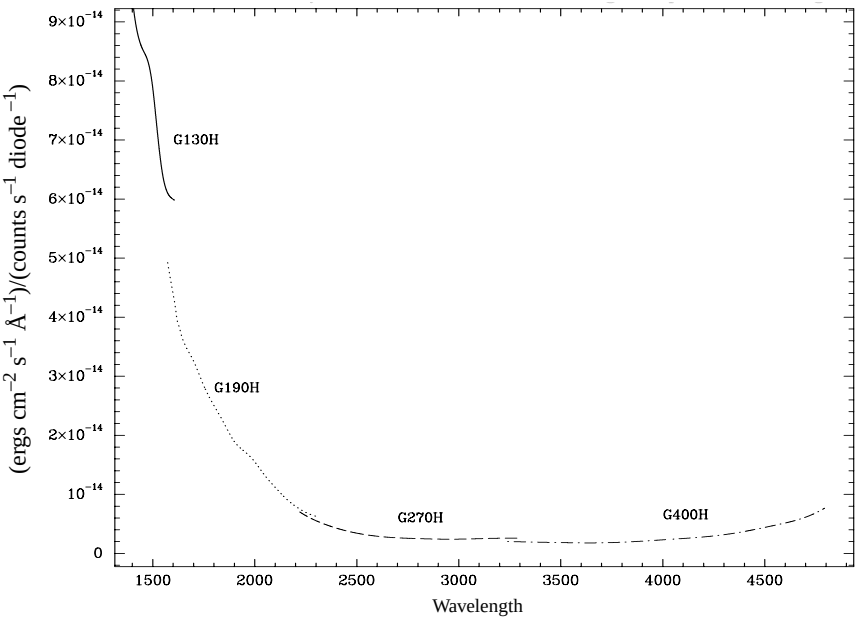

Figure 31.3: Pre-COSTAR Inverse Sensitivity Curves for Red High Dispersion Gratings

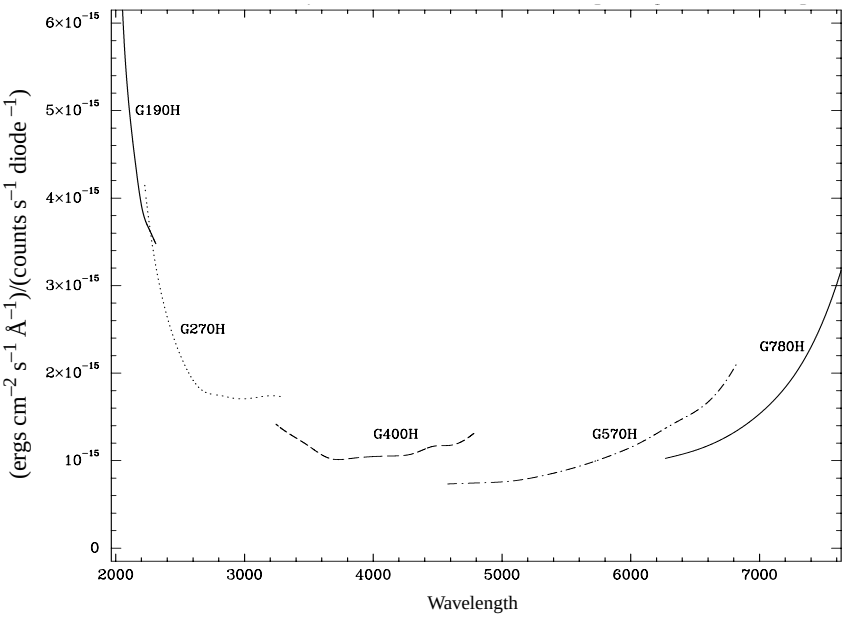

Figure 31.4: Post-COSTAR Sensitivity Curves for High Dispersion Gratings

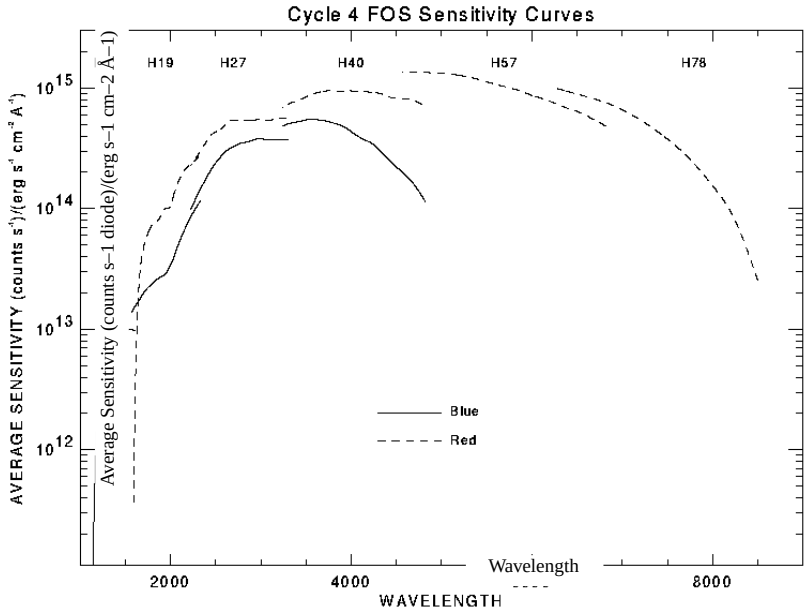

Figure 31.5: Post-COSTAR Sensitivity Curves for Low Dispersion Gratings

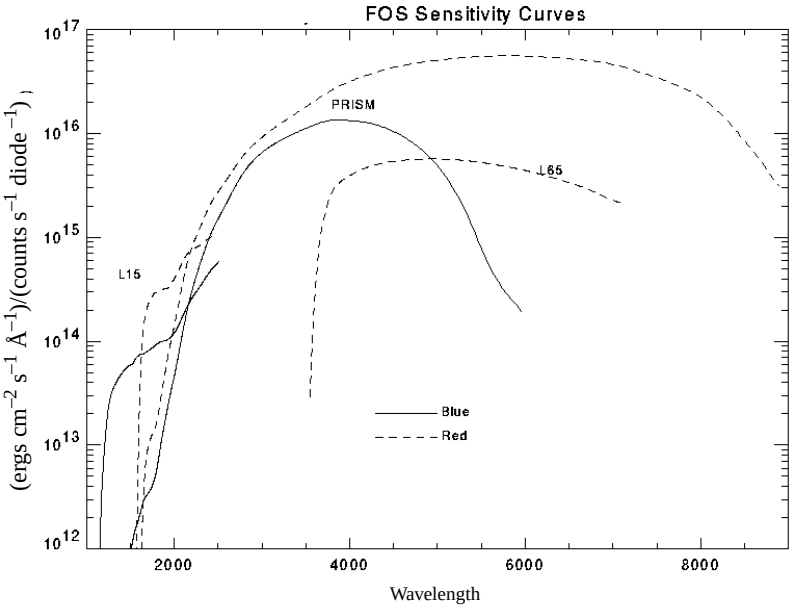

- **cyretr:** This relation is for retardation reference files used for spectropolarimetric data. The files are used to create the observation matrix *f*(*w*). There are separate files for each detector, disperser, and polarizer combination. The three available retardation files for the blue detector and waveplate B are plotted in Figure 31.6 with the appropriate disperser shown.

Figure 31.6: Retardation Reference Files

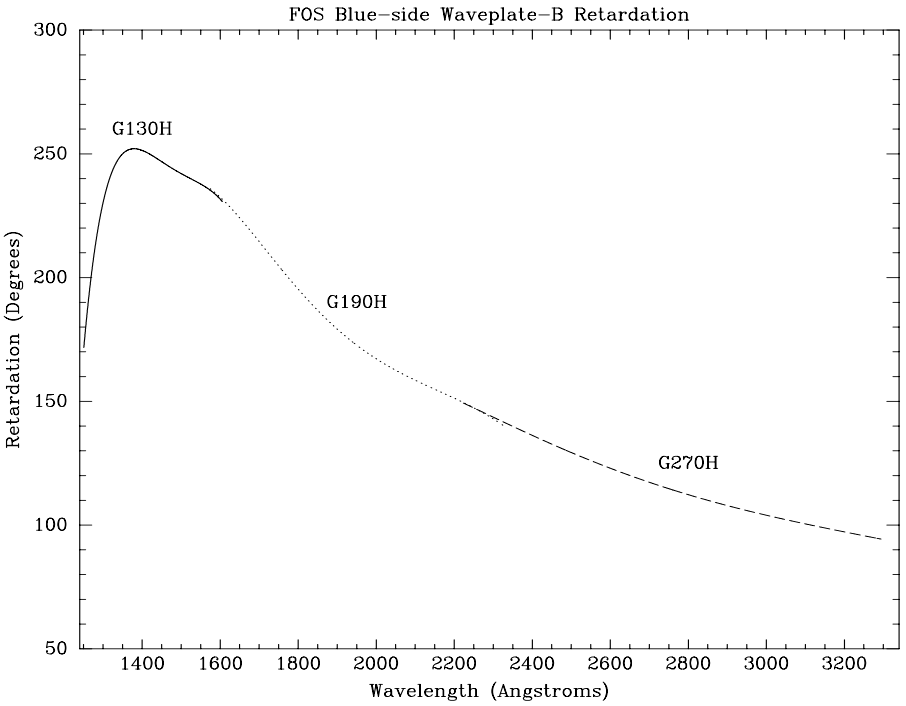

- **cyddtr:** This is the relation for the disabled diode files. The table is used only if the keyword DEFDDTBL = F in the .d0h file. The disabled diode information is also contained in the .ulh file. DEFDDTBL *must be set to* F *for proper re-calibration of any FOS data!* Over the operational lifetime of the FOS, 26 FOS/BL and 17 FOS/RD diodes were disabled. Note that the diodes listed in Tables 31.4 and 31.5 are numbered such that the first diode in the diode array is 0 and the last diode is 511. For use in IRAF and STSDAS, the diode number would be the diode number in the table + 1.

.

Table 31.4: Blue Detector Disabled Diodes

DISABLED Dead Channels	DISABLED Noisy Channels		DISABLED Cross-Wired Channels	ENABLED But Occasionally Reported Noisy
49	31	268	47	8
101	73	398	55	138
223	144	415		139
284	201	427		209/210
292	218	451		381
409	225	465		421
441	235	472		426
471	241	497		
8	16		2	7

Table 31.5: Red Detector Disabled Diodes

DISABLED Dead Channels	DISABLED Noisy Channels	ENABLED But Occasionally Reported Noisy	
2	110	97	258/259
6	189	114/115	261
29	285	116	268
197	380	142	285
153	381	163	410
212	405	174	
289	409	181	
308	412	225	
486		243	
9	8	14	

- **cyaisr**: This is the relation for the average inverse sensitivity reference files. These files are used to convert corrected count rates to absolute flux units. There is one file for each detector and disperser combination. Figures 31.2 and 31.3 show the pre-COSTAR inverse sensitivity for the most commonly used gratings for both detectors. The post-COSTAR sensitivity curves are plotted in Figures 31.4 and 31.5
- **cypsf:** This is the relation for the monochromatic pre-COSTAR point spread functions for the FOS, covering the wavelength range 1200–5400 Å for the blue side and 1600–8400 Å for the red side. These PSFs were modeled using the TIM software. In Figure 31.7, a sample blue side FOS PSF at 1400 Å is shown.

Figure 31.7: Example of a Pre-COSTAR Point Spread Function for the FOS

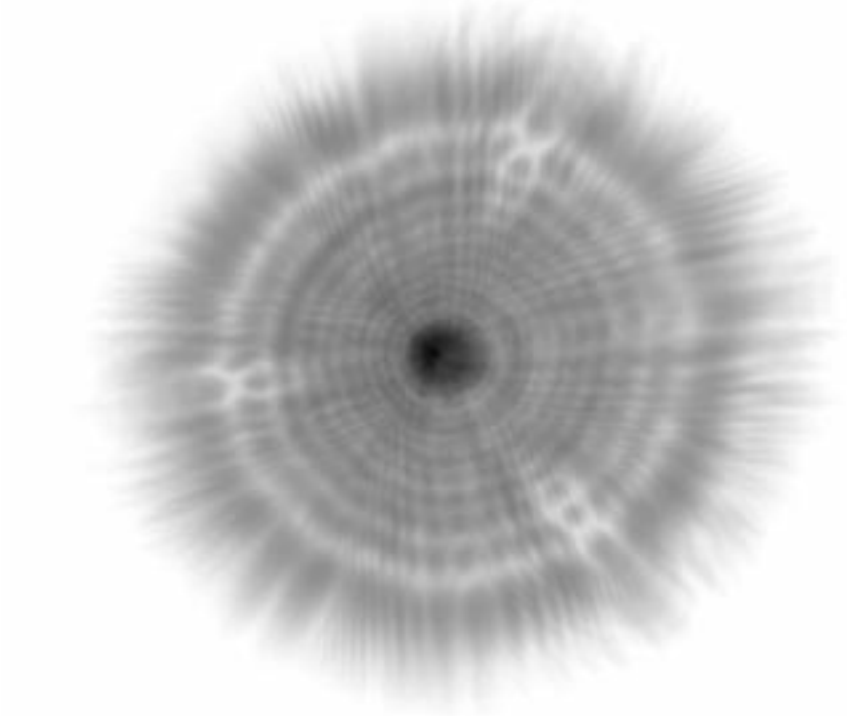

- **cylsf:** This is the relation for the monochromatic pre-COSTAR line spread functions for all of the non-occulting FOS apertures computed using the PSFs in cypsf. Figure 31.8 shows a sample monochromatic pre-COSTAR FOS LSF for the blue side `4.3` aperture. Pre-COSTAR LSFs are available at each PSF wavelength. Observation-derived LSFs are not stored in CDBS.

Figure 31.8: Example of a Pre-COSTAR Line Spread Function for the FOS

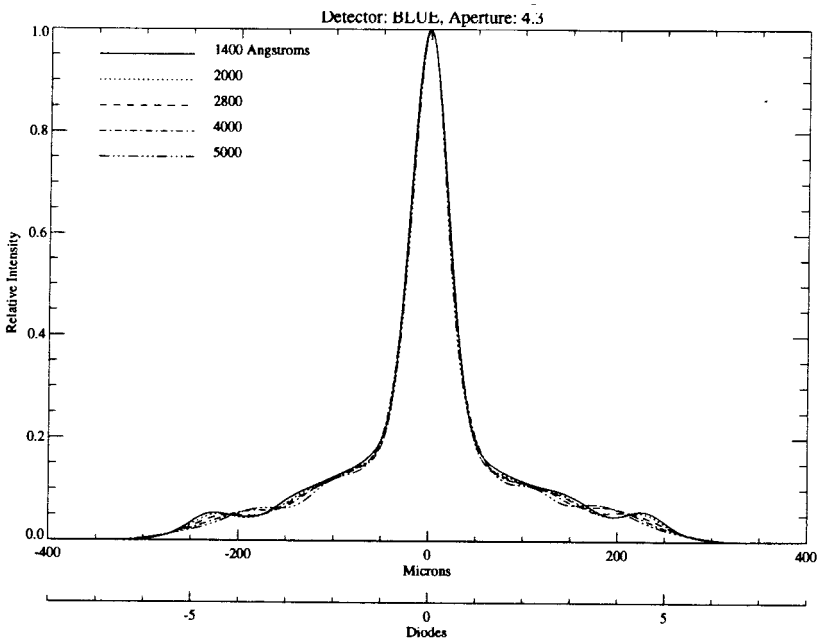

- **cyqinr:** This is the relation for the data quality initialization files. These files were intended to flag intermittent or noisy diodes, *but were never kept up to date* since dead diode quality flagging is handled in the **calfos** pipeline through the use of the DDTHFILE dead diode reference file.

31.4 Details of the FOS Pipeline Process

This section describes in detail the STScI pipeline calibration or re-calibration (**calfos**) procedures. Each step of the processing is selected by the values of keyword *switches* in the science data header file. All FOS observations undergo pipeline processing to some extent. Target acquisition and IMAGE mode data are processed only through step 6 (paired pulse correction) but are not GIM corrected. ACCUM data are processed through step 14 (absolute flux calibration) and RAPID, PERIOD, and POLARIMETRY data are processed through step 15 (special mode processing). The steps in the FOS calibration process are:

1. Read the raw data.
2. Calculate statistical errors (ERR_CORR).
3. Initialize data quality.
4. Convert to count rates including dead diode correction (CNT_CORR).
5. Perform GIM correction (OFF_CORR).
6. Do paired-pulse correction (PPC_CORR).

7. Subtract background (BAC_CORR).
8. Subtract scattered light (SCT_CORR).
9. Do flatfield correction (FLT_CORR).
10. Subtract sky (SKY_CORR).
11. Correct aperture throughput and focus effects (APR_CORR).
12. Compute wavelengths (WAV_CORR).
13. Correct time-dependent sensitivity variations (TIM_CORR).
14. Perform absolute calibration (FLX_CORR); superseded by AIS_CORR.
15. Do special mode processing (MOD_CORR) if RAPID, PERIOD, or spectropolarimetry.

These steps are described in detail in the following sections. A basic flowchart is provided in Figure 31.1.

Note: For *non*-polarimetry cases use *only* AIS_CORR; if both are set to PERFORM, AIS_CORR overrides FLX_CORR as a safeguard. For polarimetry use FLX_CORR; here it will override AIS_CORR should both be set to PERFORM.

31.4.1 Reading the Raw Data

The raw data, stored in the `.d0h` file, are the starting point of the pipeline data reduction and calibration process. The raw science data are read from the `.d0h` file and the initial data quality information is read from the `.q0h` file. If science trailer (`.d1h`) and trailer data quality (`.q1h`) files exist, these are also read at this time.

31.4.2 Calculating Statistical Errors (ERR_CORR)

The noise in the raw data is photon (Poisson) noise and errors are estimated by simply calculating the square root of the raw counts per pixel. An error value of zero is assigned to filled data, i.e., pixels that have a data quality value of 800.[1] For all observing modes except polarimetry, an error value of zero is assigned to pixels that have zero raw counts. Polarimetry data that have zero raw counts are assigned an error value of one.

From this point on, the error data are processed in lock-step with the spectral data. Errors caused by sky and background subtraction, as well as those from flatfields and inverse sensitivity files, are not included in the error estimate. At the end of the processing, the calibrated error data will be written to the `.c2h` file.

1. Data quality values are described in Table 30.2.

31.4.3 Data Quality Initialization

The initial values of the data quality information are the data quality entries from the spacecraft as recorded in the .q0h file. This step of the processing adds values from the data quality reference files to the initial values in the .q0h file. The routine uses the data quality initialization reference file DQ1HFILE listed in the .d0h file. A second file, DQ2HFILE, is necessary for paired-aperture and spectropolarimetry observations. These reference files contain flags for intermittent noisy and dead channels (data quality values 170 and 160, respectively). The data quality values are carried along throughout the remaining processing steps where subsequent routines add values corresponding to other problem conditions. *Only the highest (most severe) data quality value is retained for each pixel*. At the end of the processing the final data quality values are written to the .cqh file.

The noisy and dead channels in the data quality files were often out of date, but the dead diode table (DDTHFILE) contains the most accurate list of dead and disabled diodes. Noisy diodes are not flagged in routine processing. Normally, after three reports of noisy activity an offending diode was disabled. As a result, diodes that had fewer than three reports as noisy are not flagged in the data quality file.

31.4.4 Conversion to Count Rates (CNT_CORR)

At this step, the raw counts per pixel are converted to count rates by dividing by the exposure time of each pixel. Filled data (data quality = 800) are set to zero. *A correction for disabled diodes is also included at this point.* If the keyword DEFDDTBL in the .d0h file is set to TRUE, the list of disabled diodes is read from the unique data log (.ulh) file. Otherwise the list is read from the disabled diode reference file, DDTHFILE, named in the .d0h file. In pipeline calibration the DDTHFILE was more commonly used for the disabled diode information.

For re-calibration purposes, DEFDDTBL *should always be set to* FALSE *so that the FOS closeout calibration dead diode tables are used for the proper dead diode correction.*

The actual process by which the correction for dead diodes is accomplished is as follows. First, recall that because of the use of the OVERSCAN function, each pixel in the observed spectrum actually contains contributions from several neighboring diodes (see “Data Acquisition Fundamentals” on page 29-15). Therefore, if one or more particular diodes out of the group that *contributed to* a given output pixel is dead or disabled, there will still be some amount of signal due to the contribution of the remaining live diodes in the group. We can correct the observed signal in that pixel back to the level it would have had if all diodes were live; to do this, we divide by the relative fraction of live diodes. The

corrected pixel value is zero if all the diodes that contribute to that pixel are dead or disabled, otherwise, the value is given by the equation:

$$corr = obs\frac{total}{(total - dead)}$$

Where:

- *corr* – is the corrected pixel value.
- *obs* – is the observed pixel value.
- *total* – is the total number (live + dead) of diodes.
- *dead* – is the number of dead or disabled diodes.

This correction to the signal is applied at the same time the raw data are divided by exposure time. If the fraction of dead diodes for a given pixel exceeds 50%, then a data quality value of 50 is assigned. If all of the diodes for a given pixel are dead, both the data and error values are set to zero and a data quality value of 400 is assigned.

The count rate spectral data are written to the `.c4h` file at this point. Note that the S/N and the computed statistical errors in a given pixel are appropriate to the actually observed, not the corrected, count rate.

31.4.5 GIM Correction (OFF_CORR)

Data obtained prior to April 5, 1993, do not have an onboard geomagnetic-induced image motion (GIM) correction applied, and therefore require a correction for GIM in the pipeline calibration. Note that there are some observations obtained after April 5, 1993, that do *not* have onboard GIM correction, because the application of the onboard GIM correction depended on when the proposal was completely processed for scheduling on the spacecraft. Reference to keywords YFGIMPEN and YFGIMPER, respectively, indicate whether onboard GIM correction was enabled and whether any error occurred in its implementation. The GIM correction is determined by scaling a model of the strength of the geomagnetic field at the location of the spacecraft. The model scale factors are read from the CCS7 reference table. The correction is applied to the spectral data, the error data, and the data quality values.

A unique correction is determined for each data group based on the orbital position of the spacecraft at the mid-point of the observation time for each group. While the correction is calculated to sub-pixel accuracy, it is applied as an integer value and is therefore accurate only to the nearest integral pixel. This is done to avoid resampling the data in the calibration process. Furthermore, the pipeline correction (OFF_CORR) is applied only in the *x*-direction (i.e., the dispersion direction).

The correction is applied by simply shifting pixel values from one array location to another. As a typical example, if the amount of the correction for a particular data group is calculated to be +2.38 pixels, the data point originally at

pixel location 1 is shifted to pixel 3, pixel 2 shifted to pixel 4, pixel 3 to pixel 5, and so on. Pixel locations at the ends of the array that are left vacant by this process (e.g., pixels 1 and 2 in the example above) are set to a value of zero and are assigned a data quality value of 700.

Special handling is required for data obtained in ACCUM mode since each data frame contains the sum of all frames up to that point. In order to apply a unique correction to each frame, data taken in ACCUM mode are first *unraveled* into separate frames. Each frame is then corrected individually, and the corrected frames are recombined.

The *pipeline processing* GIM correction (OFF_CORR) is not applied to target acquisition data, image mode data, and polarimetry data. The correction can be applied to IMAGE mode *spectral* data by setting header keyword OFF_CORR to PERFORM prior to running **calfos**.

The *onboard* GIM correction is applied on a much finer grid than integral pixels and is made within the FOS so that data are recorded by the detector with the corrections already included. The onboard GIM correction is applied along both the direction of the diode array and in the perpendicular direction. In the *x*-direction the onboard GIM correction is applied in units of 1/32 of the width of the diodes and in the *y*-direction in units of 1/256 of the diode height.

The *onboard* GIM correction is calculated and applied every 30 seconds, and is applied to all observations except for ACQ/PEAK observations.

31.4.6 Paired Pulse Correction (PPC_CORR)

This step corrects the data for saturation in the detector electronics. The dead time constants q_0, q_1, and F are read from the reference table CCG2. The values of these dead time constants in the CCG2 table are $q_0 = 9.62\text{e-}6$ seconds, $q_1 = 1.826\text{e-}10$ sec^2/counts, and F = 52,000 counts per second. These quantities were determined in laboratory measurements prior to launch and were never modified (*FOS ISR*s 25 and 45). The following equation is used to estimate the true count rate:

$$x = \frac{y}{(1 - yt)}$$

Where:

- x – is the true count rate.

- *y* – is the observed count rate.
- *t* – is q_0 for y less than or equal to F.
- *t* – is $q_0 + q_1 * (y-F)$ for y greater than F.

The values of these different saturation limits in the CCG2 table are as follows:

- Observed count rates greater than the saturation limit of 57,000 counts per second (and recorded in the **calfos** processing log) are set to zero and assigned a data quality value of 300.
- All observed count rates that are between this severe saturation limit and 10 counts/second are corrected, but those lying between the predefined limits of large (55,000 counts/second) and severe saturation (57,000 counts/second) are assigned a data quality value of 190.
- Those that lie between the limits of moderate (52,000 counts/second) and large (55,000 counts/second) saturation are assigned a data quality value of 130, and the paired pulse correction is applied.
- Count rates between the threshold value (10 counts/second) and 52,000 counts/second have the paired pulse correction applied.
- Data with count rates below this threshold value (10 counts/second) do not have any paired-pulse correction.

31.4.7 Background Subtraction (BAC_CORR)

This step subtracts the background (i.e., the particle-induced dark count) from object and sky (if present) spectra. If no background spectrum was obtained with the observation (the situation for nearly all FOS exposures), a default background reference file, BACHFILE, which is scaled to a mean expected count rate based on the geomagnetic position of the spacecraft at the time of the observation, is used. The scaling parameters are stored in the reference table CCS8. The scaled background reference spectrum is written to the `.c7h` file for later examination.

If an observed background was used (rarely the case), it is first repaired; bad points (i.e., points at which the data are flagged as lost or garbled in the telemetry process) are filled by linearly interpolating between *good neighbors*. Next, the background is smoothed with a median filter, followed by a mean filter. The median and mean filter widths are stored in reference table CCS3. No smoothing is done to the background reference file, if used, since the file is already a smoothed approximation to the background. Spectral data at pixel locations corresponding to repaired background data are assigned a data quality value of 120. Finally, the repaired background data are subtracted.

Although this is called background subtraction, it is really a *dark count* subtraction.

31.4.8 Scattered Light Correction (SCT_CORR)

Scattered light observed in FOS data is produced by the diffraction patterns of the FOS gratings, the entrance apertures, and the micro-roughness of the gratings.

The routine pipeline scattered light correction is applied only for those gratings that produce spectra in which the detector had regions of zero sensitivity to dispersed light or that did not fully illuminate all the science diodes (Table 31.6). The values listed in the table apply to spectra with FCHNL=0, NCHNLS=512, NXSTEPS=4, and OVERSCAN=5, i.e., the default FOS observing mode. For the listed combinations, these *dark* diodes can be used to estimate the scattered light illuminating all of the diodes. For the valid combinations, the average count rate for these diodes is determined and subtracted from the whole data array, including the *dark* pixels. If the dark pixels were excluded from readout by the use of a restructured wavelength range, no scattered light correction is made.

The correction applied in this way is only a wavelength-independent first-order approximation. The **calfos** task reports (via the standard output) whether it performs this step, along with the subtracted value. Group parameter SCT_VAL gives the value subtracted from each group. This information is also provided in the paper products and, if you have a dataset from the pipeline, is in the trailer file.

For details of the correction please see *FOS ISR* 103. Note that the scattered light correction is in addition to the background subtraction. Effectively, *the scattered light correction serves to remove residual background, as well*.

Table 31.6: Regions Used for Scattered Light Subtraction

Detector	Grating	Minimum Pixel Number	Maximum Pixel Number	Total Pixels
Blue	G130H	31	130	100
Blue	G160L	901	1200	300
Blue	Prism	1861	2060	200
Red	G190H	2041	2060	20
Red	G780H	11	150	140
Red	G160L	601	900	300
Red	G650L	1101	1200	100
Red	Prism	1	900	900

Since the scattered light characteristics of the FOS are now well understood, a scattered light model is available at STScI. It is available for use as a post-observation parametric analysis tool (**bspec**) in STSDAS to estimate the amount of scattered light affecting a given observation (see *FOS ISR* 127). The amount of scattered light depends on the spectral energy distribution across the whole detector wavelength range of the object being observed and on the sensitivity of the detector. For cool objects the number of scattered light photons can dominate the dispersed spectrum in the UV. Thus, in order to model the

scattered light in the FOS appropriately, the red part of the source spectrum has to be *very well* known. For an atlas of predicted scattered light as a function of object type and FOS disperser and additional guidelines for modeling FOS grating scatter with **bspec**, see *FOS ISR* 151.

31.4.9 Flatfield Correction (FLT_CORR)

This step removes the diode-to-diode sensitivity variations and fine structure (typically on size scales of ten diodes or less) from the object, error, and sky spectra by multiplying each by the inverse flatfield response as stored in the FL1HFILE reference file. A second flatfield file, FL2HFILE, is required for paired aperture or spectropolarimetry observations. No new data quality values are assigned in this step.

Different locations on the FOS photocathodes displayed quite different flatfield characteristics so that FOS flats were aperture-dependent. Additionally, FOS flatfields for some dispersers were quite time-variable. Care must be taken to use the correct flatfield reference file for the date and aperture of observation.

31.4.10 Sky Subtraction (SKY_CORR)

If the sky was observed, the flatfielded sky spectrum is repaired in the same fashion as described above for an observed background spectrum. The spectrum is then smoothed once with a median filter and twice with a mean filter, except in regions of known emission lines, which are masked out. The CCS2 reference table contains the pairs of starting and ending pixel positions for masking the sky emission lines. The sky spectrum is then scaled by the ratio of the object and sky aperture areas, and then shifted in pixel space (to the nearest integer pixel) so that the wavelength scales of the object and sky spectra match. The sky spectrum is then subtracted from the object spectra and the resulting sky-subtracted object spectrum is written to the `.c8h` file. Pixel locations in the sky-subtracted object spectrum that correspond to repaired locations in the sky spectrum are assigned a data quality value of 120.

This routine requires table CCS3 containing the filter widths, the aperture size table CCS0, the emission line position table CCS2, and the sky shift table CCS5.

For OBJ-SKY (or STAR-SKY) observations, half the integration time is spent on the sky. The only science observations made of the sky were taken by mistake and were not required for proposal science. Additionally, the CCS2 table values were never confirmed.

Note that—especially for extended objects—paired aperture observations could be obtained in the so-called “OBJ-OBJ” mode, in which no sky subtractions were performed (see “Paired Aperture Calibration Anomaly” on page 31-25).

31.4.11 Computing the Wavelength Scale (WAV_CORR)

A *vacuum* wavelength scale at *all* wavelengths is computed for each object or sky spectrum. Wavelengths are computed using dispersion coefficients corresponding to each grating and aperture combination stored in reference table CCS6. *Corrections for telescope motion or motion of the Earth are not made in the standard pipeline calibration.* The computed wavelength array is written to the `.c0h` file.

For the gratings the wavelengths are computed as follows:

$$\lambda(\text{Å}) = \sum_{p=0}^{3} l(p) \times x^p$$

For the prism, wavelengths are computed as:

$$\lambda(\text{Å}) = \sum_{p=0}^{4} \frac{l(p)}{(x - x_0)^p}$$

Where:

- *l(p)* – are the dispersion coefficients in table CCS6.
- *x* – is the position (in diode units) in the object spectrum, where the first diode is indexed as 0.
- x_0 – is a scalar parameter also found in table CCS6.

Note that the above equations determine the wavelength at each diode. This must be converted to pixels using NXSTEPS. For example, if NXSTEPS=4, the values for *x* are given as 0, 0.25, 0.5, 0.75, 1, etc., for pixels 1, 2, 3, 4, 5, etc.

For multigroup data, as in either rapid-readout or spectropolarimetry mode, there are separate wavelength calculations for each group. These wavelengths may be identical or slightly offset, depending on the observation mode.

31.4.12 Aperture Throughput Correction (APR_CORR)

This calibration step consists of two parts: normalizing throughputs to a reference aperture and correcting throughputs for focus changes. Both steps are relevant only if the average inverse sensitivity files are used, see AIS_CORR in the next sub-section.

Each aperture affected the throughput of light onto the photocathode. To prepare the object data for absolute flux calibration, the object data must be normalized to the throughput as would be seen through a pre-determined reference aperture (the 4.3 aperture is always used). The normalization is calibrated as a second-order polynomial and is a function of wavelength. The polynomial is evaluated over the object wavelength range and divided into the object data. The coefficients are found in the CCSB reference table.

Once the object data has been normalized, the throughput is compensated for variations in sensitivity due to focus changes. The CCSA table contains a list of dates and focus values. The sensitivity variation is modeled as a function of wavelength and focus, the coefficients of which are found in the CCSC table. This model is evaluated and divided into the object data. (Although post-COSTAR focus-dependent corrections are unity, this step still must be performed for proper calibration).

31.4.13 Absolute Flux Calibration (AIS_CORR and FLX_CORR)

This step multiplies object (and error) spectra by the appropriate inverse sensitivity vector to convert from count rates per pixel to absolute flux units (erg s^{-1} cm^{-2} $Å^{-1}$). Two different methods of performing this calibration were used. The pipeline used the so-called FLX_CORR method from the time of HST launch to March 19, 1996. The pipeline processing method, for *non-polarimetric* observations, was changed to the AIS_CORR method on March 19, 1996. AIS_CORR calibration files are available for all FOS observing epochs and AIS_CORR is *the only recommended* method for the flux calibration (or re-calibration) of non-polarimetric FOS observations. On the other hand, spectropolarimetric measures will continue to be processed via the FLX_CORR method.

AIS_CORR: This step is functionally no different than FLX_CORR except for the way in which absolute flux is calibrated. The absolute flux calibration is based on data from all calibration observation epochs. An average sensitivity function for the entire pre- or post-COSTAR period for the 4.3 reference aperture is contained in the AISHFILE reference file for each combination of detector and disperser. As necessary, TIM_CORR factors (see following sub-section) correct the sensitivity to the date of observation and APR_CORR factors (see preceding sub-section) correct for the throughput of the aperture employed. The calibrated spectral data are written to the .c1h file, and the calibrated error data are written to the .c2h file. The final data quality values are written to the .cqh file.

FLX_CORR: Now used for spectropolarimetry flux calibration only. The inverse sensitivity data are read from the IV1HFILE reference file. A second inverse sensitivity file, IV2HFILE, is required for paired-aperture or spectropolarimetry observations. Individual reference files are required for every combination of detector, disperser, and aperture. Time-dependencies are, in principle, tracked via multiple reference files with different USEAFTER dates.

For both flux calibration methods, points where the inverse sensitivity is zero (i.e., not defined) are flagged with a data quality value of 200. The calibrated spectral data are written to the .c1h file, and the calibrated error data are written to the .c2h file. The final data quality values are written to the .cqh file.

31.4.14 Time Correction (TIM_CORR)

This step corrects the absolute flux for variations in sensitivity of the instrument over time and is an important component of the AIS_CORR flux calibration. The correction factor is a function of time and wavelength. The factor is calculated by linear interpolation for the observation time and wavelength coverage. The factor is divided into the object absolute flux. The coefficients are found in table CCSD. TIM_CORR is used only with AIS_CORR calibration.

This is the final step of processing for ACCUM mode observations.

31.4.15 Special Mode Processing (MOD_CORR)

Data acquired in the rapid-readout, time-resolved, or spectropolarimetry modes receive specialized processing in this step. All data resulting from this additional processing are stored in the .c3h file. See the discussions of output data products for each of these modes on pages 30-40, 30-42, and 30-46.

RAPID Mode: For RAPID mode, the total flux, integrated over all pixels, for each readout is computed. The sum of the statistical errors in quadrature for each frame is also propagated. The following equations are used in the computation.

$$sum(F) = \left(\sum_{x=1}^{NDAT} f(x,F) \right) \left(\frac{NDAT}{good} \right)$$

$$errsum(F) = \sqrt{\left(\sum_{x=1}^{NDAT} ef^2(x,F) \right) \times \left(\frac{NDAT}{good} \right)}$$

Where:

- *f(x,F)* – is the flux in pixel *x* and readout *F.*
- *ef(x,F)* – is the associated error in the flux for pixel *x* and readout *F.*
- *sum(F)* – is the total flux for readout *F.*
- *errsum(F)* – is the associated error in the total flux for the readout *F.*
- *NDAT* – is the total number of pixels in the readout *F.*
- *good* – is total number of good pixels, i.e., pixels with data quality less than 200.

The output .c3h file contains two data groups, where the number of pixels in each group is equal to the number of original data frames. Group 1 contains the

total flux for each frame, where pixel 1 is the sum for frame 1, pixel 2 the sum for frame 2, etc. Group 2 of the .c3h file contains the corresponding propagated errors.

POLARIMETRY Mode: For the POLARIMETRY mode, the data from individual waveplate positions are combined to calculate the Stokes I, Q, U, and V parameters, as well as the linear and circular polarizations and polarization position angle spectra (for details of calculating the Stokes parameters see *FOS ISR* 078). Four sets of Stokes parameter and polarization spectra are computed. The first two sets are for each of the separate pass directions, the third for the combined pass direction data, and the fourth for the combined data corrected for interference and instrumental orientation.

PERIOD Mode: For PERIOD mode, the pixel-by-pixel average of all slices (NSLICES separate memory locations) and the differences from the average for each slice of the last frame are computed. The following equations are used in the computation:

$$average(x) = \left(\frac{\sum_{L=1}^{NSLICES} f(x, L)}{good(x)} \right)$$

$$errave(x) = \frac{\sqrt{\left(\sum_{L=0}^{NSLICES-1} (ef(x, l))^2 \right)}}{good(x)}$$

$$diff(x, L) = f(x, L) - average(x)$$

$$errdiff(x, L) = \sqrt{(ef(x, L)^2 + errave(x)^2)}$$

Where

- NSLICES – is the number of slices.
- *f(x,L)* – is the flux in slice *L* at pixel *x.*
- *ef(x,L)* – is the error associated with the flux in slice *L* at pixel *x.*
- *average(x)* – is the average flux of all slices at the pixel *x.*
- *errave(x)* – is the error associated with the average flux at pixel *x.*
- *good(x)* – is the total number of good values, i.e., data quality <200, accumulated at pixel *x.*
- *diff(x,L)* – is the flux difference at pixel *x* between slice *L* and the average.
- *errdiff(x,L)* – is the error associated with the flux difference.

The first two data groups of the output .c3h file contain the average flux and the associated errors, respectively. Each subsequent pair of data groups contains the difference from the average and the corresponding total error for each slice.

31.5 Paired Aperture Calibration Anomaly

Any HST data taken with a paired aperture prior to January 1, 1995 may need manual editing of certain .d0 header fields prior to recalibration with **calfos**.

Several programs used both the upper and lower portions of a paired aperture with Exposure Logsheet (or RPS2) entries of STEP-PATT=STAR-SKY, OBJ-OBJ, or OBJ-SKY in order to sample different portions of extended objects in alternating 10-second dwells throughout an exposure. The diagnosis of this problem is slightly complicated, but in the following, please realize that whenever "chopping" between apertures was invoked, the data recorded through each aperture segment were always recorded separately so that correct calibration of the data from each aperture segment is possible after the manual header update.

Prior to January 1, 1995 important keywords in the headers of all FOS paired aperture exposures for STEP-PATT not equal to SINGLE were constructed on the assumption that SKY was sampled in one aperture segment. This occurred even if STEP-PATT=OBJ-OBJ had been specified in the logsheet. Additionally, prior to February 1, 1994 the only way to obtain spectra with both segments of the paired apertures in this alternating fashion was to specify the potentially misleading STEP-PATT=STAR-SKY. Naturally, **calfos** calibrates these exposures as if sky subtraction is intended and the final .c1 file contains the difference between nominal default star and sky apertures.

The simplest approach to correcting this problem is to change the YSTEPn keywords (i.e., YSTEP1, YSTEP2, etc) from "SKY" to "OBJ." Values of "NUL" or "BCK" should not be changed. Modern versions of **calfos** (revised after January 1, 1995) will process these updated data correctly and produce separate calibrated spectra for the two aperture segments.

As a general rule, no sky subtraction observations were *intended* by any observer in the FOS science program after SV ended (January 1, 1992). On a very few occasions OBJ-SKY observations were obtained through implementation error when only OBJ (i.e., STEP-PATT=SINGLE) was intended. Particularly for extended targets, you should broadly assume that any SKY observation, whether explicitly requested in the logsheet STEP-PATT or not, may contain additional spectra from nearby regions of an extended source and should be recalibrated only after header update.

31.6 Recalibrating FOS Data: A Checklist

You will use the IRAF/STSDAS task **calfos**. to recalibrate your FOS spectra. This task sequentially performs each step described in the preceding section.

Here is a checklist of things that you should routinely do to re-calibrate any FOS exposure:

1. ***Add new or updated keywords****:* The first thing to do is make sure that your data have all the required keywords in their headers. The STSDAS task **addnewkeys** will update the headers of your `.d0h` files accordingly. This task insures that the AIS flux calibration method keywords are in the header and also adds the scattered light correction keyword to older pre-COSTAR files. Note that a default set of reference filenames is used for the new calibration switch keywords - you must update these as part of the next point on this checklist.
2. ***Get correct reference file names****:* Next you must determine which are the correct reference files to use. You can determine the correct reference files and tables to use for re-calibration of any exposure by using the StarView FOS calibration reference file screen (see section 1.3 for a complete description of this procedure). Alternatively, the FOS WWW Reference File Guides provide a listing of recommended FOS reference files as a function of observing epoch for each type of reference file or table.
3. ***Update header files***: In order to recalibrate FOS data using updated calibration files, you need to edit the header of the original science data, `.d0h`, with the task **chcalpar** and replace the names of the original calibration files with those of the new ones. If required, you should also update the values of YSTEPn for paired aperture exposures as described in section 31.5
4. ***Set DEFDDTBL to "F" (false)***: As noted earlier, some header files may have had the Default Dead Diode Table keyword set to TRUE in order to use the `.udl` file to specify the list of dead diodes for original pipeline processing. Since a complete history of dead diode occurrence dates is now available, only the DDTHFILE should now be used to identify dead diodes. Under no circumstances should DEFDDTBL be set to "T". Naturally, it is also a good idea to make sure that all other calibration switches are set properly at this point.
5. ***Run the calfos calibration routine***: **calfos** will create new calibrated output files with the same suffixes as the originally delivered data, namely `.cnh` and `.cnd` (n=0...8).

If you are concerned about any aspect of the appearance of your calibrated data, you should compare the final data with flatfield (and other) reference files used in the data reduction process to make sure that spurious features were not introduced through improper data handling in the pipeline or in your recalibration.

31.7 Post-Calibration Output Files

The several types of calibrated output files produced by **calfos** are listed in Table 31.7. More detailed descriptions of each type of file are provided in Chapter 30.

Table 31.7: Output Calibrated FOS Data Files

Filename Extension	File Contents
.c0h and .c0d	Calibrated wavelengths
.c1h and .c1d	Calibrated fluxes
.c2h and .c2d	Calibrated statistical error
.c3h and .c3d	Special mode data
.cqh and .cqd	Calibrated data quality
.c4h and .c4d	Count rate object and sky spectra
.c5h and .c5d	Flatfielded object count rate spectrum
.c6h and .c6d	Flatfielded sky count rate spectrum
.c7h and .c7d	Background count rate spectrum
.c8h and .c8d	Flatfielded and sky subtracted object count rate spectrum

If the reference files and reference tables used in the pipeline processing do not reflect the actual instrument performance, calibration errors can occur, which can lead to artificial features in the calibrated science data. In the next chapter, we address a variety of sources of error in FOS calibration and assess limiting accuracies in the STScI instrument calibration.

Figure 31.9: Partial Sample Post-COSTAR FOS .c1h Header

```
GCOUNT  =                   77 /
        / FOS DATA DESCRIPTOR KEYWORDS
INSTRUME= 'FOS               ' / instrument in use
ROOTNAME= 'Y3JK0709T         ' / rootname of the observation set
FILETYPE= 'FLX     '           / file type
BUNIT   = 'ERGS/CM**2/S/A'     / brightness units

        / CALIBRATION FLAGS AND INDICATORS
GRNDMODE= 'RAPID-READOUT     ' / ground software mode
DETECTOR= 'BLUE              ' / detector in use: amber, blue
APER_ID = 'B-2               ' / aperture id
POLAR_ID= 'C                 ' / polarizer id
POLANG  =                 0.0 / initial angular position of polarizer
FGWA_ID = 'H13                 / FGWA id
FCHNL   =                   0 / first channel
NCHNLS  =                 512 / number of channels
OVERSCAN=                   5 / overscan number
NXSTEPS =                   4 / number of x steps
YFGIMPEN=                   T / onboard GIMP correction enabled (T/F)
YFGIMPER= 'NO                ' / error in onboard GIMP correction (YES/NO)

        / CALIBRATION REFERENCE FILES AND TABLES
DEFDDTBL=                   F / UDL disabled diode table used
BACHFILE= 'yref$b3m1128my.r0h' / background reference header file
FL1HFILE= 'yref$e7813577y.r1h' / first flat-field header file
FL2HFILE= 'N/A               ' / second flat-field header file
IV1HFILE= 'yref$e3h14503y.r2h' / first inverse sensitivity header file
IV2HFILE= 'N/A               ' / second inverse sensitivity header file
AISHFILE= 'yref$fac08361y.r8h' / average inverse sensitivity header file
RETHFILE= 'N/A               ' / waveplate retardation header file
DDTHFILE= 'yref$d9h1244ay.r4h' / disabled diode table header file
DQ1HFILE= 'yref$b2f1306ry.r5h' / first data quality initialization header file
DQ2HFILE= 'N/A               ' / second data quality initialization header file
CCG2    = 'mtab$a3d1145ly.cmg' / paired pulse correction parameters table
CCS0    = 'ytab$a3d1145dy.cy0' / aperture parameters
CCS1    = 'ytab$aaj0732ay.cy1' / aperture position parameters
CCS2    = 'ytab$a3d1145fy.cy2' / sky emission line regions
CCS3    = 'ytab$a3d1145gy.cy3' / bkg and sky filter widths
CCS4    = 'ytab$e5v13262y.cy4' / polarimetry parameters
CCS5    = 'ytab$a3d1145jy.cy5' / sky shifts
CCS6    = 'ytab$e5v11576y.cy6' / wavelength coefficients
CCS7    = 'ytab$ba910502y.cy7' / GIMP correction scale factors
CCS8    = 'ytab$ba31407ly.cy8' / predicted background count rates
CCS9    = 'ytab$e3i09491y.cy9' / scattered light parameters
CCSA    = 'ytab$fad1554cy.cya' / OTA focus history
CCSB    = 'ytab$g1512585y.cyb' / relative aperture throughput coeff
CCSC    = 'ytab$fad1554hy.cyc' / aperture throughput vs OTA focus
CCSD    = 'ytab$fad1554ky.cyd' / time changes in sensitivity

        / CALIBRATION SWITCHES
CNT_CORR= 'COMPLETE'           / count to count rate conversion
OFF_CORR= 'OMIT              ' / GIMP correction
PPC_CORR= 'COMPLETE'           / paired pulse correction
BAC_CORR= 'COMPLETE'           / background subtraction
GMF_CORR= 'COMPLETE'           / scale reference background
SCT_CORR= 'COMPLETE'           / scattered light correction
FLT_CORR= 'COMPLETE'           / flat fielding
SKY_CORR= 'SKIPPED '           / sky subtraction
WAV_CORR= 'COMPLETE'           / wavelength scale generation
FLX_CORR= 'OMIT              ' / flux scale generation
APR_CORR= 'COMPLETE'           / aperture throughput corrections
AIS_CORR= 'COMPLETE'           / AIS flux scale generation
TIM_CORR= 'COMPLETE'           / time changes in sensitivity correction
ERR_CORR= 'COMPLETE'           / propagated error computation
MOD_CORR= 'PERFORM           ' / ground software mode dependent reductions

HISTORY   FL1HFILE=yref$e7813577y.r1h       FLT_CORR=COMPLETE
HISTORY   INFLIGHT  01/03/1994
HISTORY   Based on SMOV Superflats: proposal 4776
HISTORY   AISHFILE=yref$fac08361y.r8h       AIS_CORR=COMPLETE
HISTORY   INFLIGHT 01/02/1994 - 15/07/1995
HISTORY   1st delivery: post-costar ais time+aperture dependent flux cal
END
```

31.8 User Calibrations

Some users may wish to create their own calibration reference files or tables for certain parts of the pipeline calibration. IRAF/STSDAS tools exist to generate certain types of user reference files. In nearly all cases, however, some manual editing of reference file headers may be necessary after producing the new calibration data.

- ***Wavelengths:*** IRAF/STADAS tasks **hst_calib.fos.y_calib.linefind** and **.hst_calib.fos.y_calib.dispfity** are required. **linefind** is used to find the positions in a WAVE spectrum of candidate comparison lines from a template list of lines. (The FOS comparison line template lists may be found in the Calibration Tools section of the FOS WWW page.) The identified lines are then fit in **dispfity** with an appropriate polynomial (order 3 for all FOS grating spectra). See the STSDAS help files for detailed information on these tasks. The results of the fit must be entered into an STSDAS table to be used with pipeline calibration. Be careful to insure that sufficient lines are used to characterize the fits throughout the spectrum. Remember that due to the design of the spectrograph an internal to external wavelength system offset exists between internal calibration arc spectra and external astronomical source spectra and that this offset must be included in any new wavelength calibration (see Chapter 32 for further discussion of internal to external offsets, filter-grating wheel offsets, and other instrumental characteristics affecting wavelength accuracies). Also, please refer to *FOS ISRs* 149 and 156 and references therein.
- ***Flatfields:*** IRAF/STADAS task **stadas.hst_calib.fos.y_calib.flatfield** can be used to generate new FOS flatfields. In general, a spectrum of an object with few lines is used. Continuum levels are marked interactively throughout the spectrum and a spline is fit through these points. The original data is then divided by the spline to produce a unity-normalized flatfield, which can be inverted for use as a **calfos** inverse flatfield. The output of **flatfield** can be highly subjective in some cases. FOS IDT-developed software exists for more objective generation of FOS flatfields, but its description is beyond the scope of this manual (see *FOS ISRs* 135 and 157 for recent comprehensive discussions of FOS team flatfield generation techniques.
- ***Sensitivity Functions:*** Tasks **stsdas.hst_calib.fos.y_calib.absseny** and **absfity** are used to generate FOS inverse sensitivity functions (IVS files for use with FLX_CORR only). Unfortunately, all AIS reference files and tables were generated using IDL software written by the FOS team. No STSDAS tasks exist to generate these reference materials. The methods involved are discussed in FOS ISRs 144 and 158.
- ***Background:*** Refer to *FOS ISR* 146 and the references contained therein for a discussion of FOS background modeling techniques. The task **y_calib.parthity** is required for this calibration.

Chapter 32
FOS Error Sources

In This Chapter...

Overall FOS calibration accuracy and the quality of your observations are governed by a variety of factors both internal and external to the instrument, which include:

- The location of the target within the science aperture as determined by the target acquisition strategy that was employed and by the quality of the FGS acquisitions and guiding.
- The location of the target on the photocathode, which, in addition to having been influenced by acquisition-related consequences, is affected by FOS mechanism positional repeatability.
- The location of the mapping of the photocathode output image (the spectrum) onto the detector diode array.
- Orbital position-related phenomena such as GIM, background levels, and telescope breathing.

- Intrinsic properties of the FOS such as grating-scattered light and LSF and PSF characteristics imposed by the FOS optics, time-dependent photocathode changes, and sporadically dead or noisy diodes.
- Telescope focus (pre-COSTAR).
- The photon statistics of the detected signal.

Table 32.1 summarizes the accuracies you can expect from your data when you have recalibrated it with the latest **calfos** software and the best reference files (as recommended by StarView—see Chapter 1 in Volume 1), assuming your target acquisition was successful and appropriate for your science aperture, and, for photometry, assuming the 1.0 or 4.3 aperture was used. Note that a typical science observation may have systemic errors as much as two or three times those listed in Table 32.1, if the acquisition miscentered the target or the observations were taken during a period when the Y-bases were in error. In some cases improvements can be made further by using the calibration information and post observation refinement tasks described in this Data Handbook.

Below we first address important factors affecting various calibration accuracies and the data quality (e.g., target centering, mechanism repeatabilities, and image location). Then we discuss the limitations associated with each type of FOS calibration and their associated impact on FOS data quality, providing information to help you estimate the accuracy in your particular science observations.

32.1 Target Location in Aperture

This section discusses factors that affect the degree to which a target is centered in the aperture. Table 32.2 summarizes the nominal initial accuracies for different kinds of acquisitions. Target miscentering affected:

- The amount of light transmitted by the aperture hence the photometric accuracy of the observation.
- The degree to which the calibrated photocathode granularity was sampled, hence the limiting S/N after flatfield calibration.
- The centering of the collimated beam on the disperser parallel to dispersion, hence the wavelength calibration accuracy.
- For apertures larger than `1.0`, the positioning of the image on the photocathode with respect to those portions of the photocathode output that were sampled by the readout electronics (the diode array).

Table 32.1: FOS Calibration Accuracies (1 σ)

Attribute	Limiting Accuracy	Comments
Absolute photometry	3–4%	Requires accurate centering and Y-bases; Substantial color effects if pointing (or equivalent Y-base) worse than 0.1". Extended source correction required.
Relative photometry within a given spectrum	+/– 2%	Full range of uncertainty may be seen as a systematic effect on scale-lengths of 200–300 Å. Requires accurate centering and Y-bases. Substantial color effects if pointing (or equivalent Y-base) worse than 0.1".
Relative photometry over large wavelength range	+/– 2%	Full range of absolute flux system color uncertainty over wavelength range 1200–5500 Å. Effect is roughly proportional to wavelength baseline.
Flatfield correction	Pre-COSTAR:2% rms achievable Post-COSTAR:1% rms achievable 3-5% temporal limits in some regions	Requires accurate centering.
Relative image photometry	Limited by photon statistics	"White light" images only.
Absolute wavelength	Without WAVECAL: +/– 1.0 diode With WAVECAL: +/– 0.11 diode (28 km/sec at high dispersion)	Systematic offsets currently set limit without WAVECAL
Relative wavelengths	+/– 0.1 diode (25 km/sec at high dispersion)	FOS/RD G570H shows systematic 0.2 diode offsets from Hβ to Hα.
Timing	From headers: absolute: ~0.25 sec; Relative: ~0.125 seconds	From engineering telemetry: absolute: ~0.125 sec; relative: ~0.02 sec.
Polarization	Pre-COSTAR: ~0.5%; post-COSTAR: ~0.1%	Typically photon statistics limited.

Table 32.2: FOS Target Acquisition Calibration Accuracies

Attribute	Limiting Accuracy
BINARY	Pre-COSTAR: 0.12" 1σ + 0.15" GIM Post-COSTAR: 0.08" FOS/BL; FOS/RD: 0.12" 1σ
PEAKUP	0.025" each coordinate
ACQ	0.1" each coordinate
Blind Pointing	Pre-COSTAR: varies by FGS: ~65% within 1"; Post-COSTAR: varies by FGS: up to ~80% within 1" in cycle 6

32.1.1 Target Acquisition Limitations

We can not stress too strongly the utility of assessing the accuracy of your target acquisition.

The target acquisition strategy, or lack of one, was of paramount importance in centering the target in the science aperture. Target acquisition methods, their limiting accuracies, and methods of assessing their quality are thoroughly discussed in “Assessing FOS Acquisitions” on page 30-26. In summary, the pointing accuracy limitations of FOS target acquisition methods are:

- ACQ/BINARY:
  - Pre-COSTAR, for both detectors, algorithm-related uncertainty of 0.12" (1 σ) to which an additional uncertainty of 0.15" due to possible uncorrected GIM motion must be added in quadrature. The GIM-related component was effectively removed by the onboard GIM correction (keyword YFGIMPEN=T) implemented April 5, 1993.
  - Post-COSTAR FOS/BL one σ algorithm-related pointing uncertainty of 0.08". Post-COSTAR FOS/RD one σ algorithm-related pointing uncertainty of 0.12".
- ACQ/PEAK:
  - Pointing accuracy was limited, on the assumption of perfect photon statistics, to one-half the step-size in each coordinate of the last pattern in the scan sequence. The worst-case upper limit of the most precise pattern routinely recommended was 0.025" in each coordinate. This was the value achieved by all FOS externally pointed calibration observations obtained after July 1, 1992 and was the ultimate limiting positional accuracy of FOS photocathode granularity and sensitivity calibration.

The accuracies and characteristics of ACQ/BINARY and the most commonly used ACQ/PEAK target acquisition strategies are listed in Table 32.5.

- ACQ/IMAGE (INT ACQ):
  - Pointing accuracy was limited by the centroiding accuracy that could be obtained with interactive measurement software and, in the pre-onboard GIM correction period, by the GIM motion. One σ limiting measurement accuracy was typically 0.1" in each detector coordinate. GIM uncertainty of up to 0.15" should be added in quadrature for observations made prior to April 5, 1993.

Target acquisition was the main cause of target miscenterings in the FOS apertures and miscentering was one of the most important photometric error sources. It usually produced gray light losses, but for larger miscenterings with apertures larger than `0.5`, which were relatively common in the pre-COSTAR period, substantial color effects were possible, especially in grating overlap regions or other regions of high “s-curvature.” See “Target Miscentering” on page 32-21.

32.1.2 Guiding and Guide Star Acquisition Limitations

“Assessing FOS Acquisitions” on page 30-26 summarizes the accuracies of HST guiding and provides references to additional information for the detailed assessment of the guiding and the guide star acquisition (and re-acquisition) characteristics associated with FOS observations. For the typical situation, reference to the FOS paper products jitter ball plot for the exposure provides sufficient information to reveal anomalous guiding during the observation.

In summary, normal FINE LOCK guiding provided one σ guiding accuracies of 0.007" or less. Nominal guide star re-acquisitions allowed the continuation of this pointing accuracy from one orbit to another. All FOS calibration observations were obtained in FINE LOCK with guide stars in two FGSs.

32.1.3 Jitter

Jitter was mostly due to the thermal instability of the solar panels. The greatest excursions occurred when the spacecraft crossed the terminator and lasted for a few minutes. The jitter caused the telescope to mispoint, moving the target in the aperture. This problem was minimized, but not completely eliminated with the introduction of compensating spacecraft commanding in April 1992. Prior to April 12, 1992, rms jitter was 17 mas (orbital day) and 12 mas (night). Starting on April 12, 1992, rms jitter dropped to 7 mas (day and 6 mas (night). For observations obtained after February 5, 1995 jitter excursions can be evaluated by examination of the jitter files or the jitter ball in the FOS paper products. This problem had the largest effect on the small apertures (0.3" and smaller), because the target could move out of the aperture for a short period and even for the larger apertures the associated photometric errors cannot be accurately determined because the exact Y-base of the spectra was unknown. The photometric error introduced by jitter was rarely more than 1%, and always less than 3%.

32.2 Mechanism Stability

This section discusses non-repeatable motions of moving parts in the FOS optics—these motions would position the image of the aperture at different physical locations on the photocathode. These positional uncertainties affected the following:

- Wavelength calibration as the *x*-position of the spectrum may not duplicate that obtained for the STScI wavelength calibration spectra.
- Flatfield calibration as the position of the spectrum may not sample the same photocathode granularity as the STScI calibration.

32.2.1 Filter-Grating Wheel Non-Repeatability

Although the positions of the filter-grating wheel (FGW) in the beam were stabilized by so-called *detents* or *notches*, there was still some mechanical variability of the wheel position, even at the same detent, from observation to observation. The *x*-component of any FGW residual positioning uncertainty caused an offset in the observed wavelengths from the calibrated dispersion curve. Additionally, any offset in either *x* or *y* added a small uncertainty to the flatfield calibration.

The amplitude of the FGW mechanism positioning uncertainty is discussed thoroughly in *FOS ISRs* 145 and 142. The 1 σ FGW non-repeatability determined in those ISRs was 0.12 diodes or approximately 0.47 quarter-stepped pixels. Recent analysis of a larger set of FGW motions indicates a peak-to-peak maximum displacement of 0.5 diode width (+/– 125 km/sec at high dispersion) with no changes over the lifetime of the FOS.

Summary of FGW Motion

- ***x-motion:***
  - pre-COSTAR: 1σ motion = 0.12 diode = 0.5 pixel ~ 0.035" = 30 km/sec
  - post-COSTAR: 1σ motion = 0.12 diode = 0.5 pixel ~ 0.03" = 30 km/sec

- ***y-motion:***
  - pre-COSTAR: 1σ motion = 8-9 Y-bases = 0.050"
  - post-COSTAR: 1σ motion = 8-9 Y-bases = 0.045"

32.2.2 Aperture Wheel Non-Repeatability

There was no reason to believe that aperture wheel non-repeatability contributed significantly to errors in FOS spectra. Pre-launch measurements indicate the variability was very small. Attempts to measure these on orbit are discussed in *FOS ISR* 131 and were limited by residual GIM motion (0.02 diodes

1σ). Pre-launch measurements indicated a non-repeatability an order of magnitude smaller than on-orbit GIM motion residuals.

32.3 Location of Image on Diode Array

This section discusses factors that affect the degree to which the photocathode image is accurately directed onto the diode array for readout. Factors which produce displacement of the photoelectrons between photocathode and diode are the commanded magnetic deflection (Y-bases) and GIM motion. Incorrect location of the image on the diode array could affect:

- At each position, the absolute photometric accuracy and the shape of the spectrum in the `1.0` and larger apertures.
- Target acquisition accuracies in the ACQ/BINARY and, in rare circumstances, ACQ/PEAK modes.

32.3.1 Y-bases

The amount of magnetic deflection required to direct photoelectrons from a designated portion of the photocathode onto the diode array for readout was characterized in *Y-base* units. Depending upon the ambient magnetic characteristics of the Digicon at the time of observation differing Y-base deflections could have been necessary to image the same portion of the photocathode onto the diode array. Pre-COSTAR calibration data to determine these optimum deflections initially showed that there was a trend with time in Y-base for all gratings with FOS/BL. These trends were not as clearly seen with FOS/RD.[1] Post-COSTAR analyses showed that the change of Y-base deflection with time for all FOS/BL gratings continued, while the Y-bases for all gratings observed with FOS/RD remained randomly scattered.[2] See Figures 32.1 and 32.2 which show the measured Y-base as a function of time for FOS/BL and FOS/RD dispersers, respectively. The dashed lines represent one σ departures from the solid line best linear fits to the data. The light, or dotted lines, represent typical peak-to-peak displacements due to FGW uncertainty. The horizontal “error bar” style lines in these figures indicate the actual Y-base values used.

The amount of scatter in the mean Y-base location increased after on-board GIM correction started in April, 1993 as frequent DEPERM commanding (clearing of the ambient magnetic field in the detector) was turned off for all but ACQ/PEAK exposures. The uncertainties in the Y-bases affected both ACQ/BINARY pointing accuracy and FOS photometric accuracy. The size of these uncertainties required that, lest positional and photometric accuracy be compromised, all ACQ/BINARY acquisitions be followed with an ACQ/PEAK stage for those cases in which science was performed in an aperture smaller than

1. *FOS ISRs* 096 and 110.

2. *FOS ISRs* 133 and 152.

1.0. The photometric quality of the data, especially for FOS/RD and the 1.0 and 4.3 apertures, could be compromised due to the fluctuations in the location of the spectrum (see the discussion in “Image Centering (Image Location) Factors” on page 32-22).

Furthermore, the shapes of the spectra on the photocathode were not linear, but had a curvature of +/– 20 Y-base units (the so-called “s-curve” of the disperser). Figures 32.3 and 32.4 show the scale of the s-curvature with formal one σ measurement uncertainties for each FOS/BL and FOS/RD grating, respectively. Therefore, the photometric effect of Y-base uncertainty was not a simple matter of losing light in a uniform fashion, rather due to the s-curvature of the spectra, the effect was also wavelength (and disperser) dependent.

No systematic temperature-related Y-base changes were expected in the relatively small (10 degree C.) FOS on-orbit operating range and none were ever observed.

Commencing in mid-1993, FOS Y-bases were updated approximately every six months. The updates were made so as to include the anticipated linearly extrapolated trending over the ensuing six month period from the date of update. With a few notable exceptions (the June 1992 to December 1993 period for all FOS/BL dispersers and the January 1994 to January 1995 period for FOS/BL G130H as seen in Figures 32.1 and 32.2) Y-base updates resulted in worst-case 10 Y-base unit deviations from the final linear trend determined from all of the Y-base measurements. Absolute photometric accuracy and, especially, spectrum shape, could be affected for large aperture observations made with these dispersers in the time periods mentioned above. The dates of all FOS Y-base updates are included in Table 32.3.

Table 32.3: FOS Y-base PDB Update Dates

Pre-COSTAR	Post-COSTAR
October 01, 1990	January 13, 1994
October 10, 1990	November 04, 1994
November 11, 1991	October 16, 1995
September 21, 1992	January 02, 1996 (FOS/BL G190H, G270H, G400H only)
August 11, 1993	June 15, 1996
December 17, 1993	December 18, 1996
	February 11, 1997

Summary of Y-base Uncertainties and Impacts

Repeated independent determinations of the same Y-base yield an external +/-25 Y-base unit (pre-COSTAR: ~0.14"; post-COSTAR: ~0.12") full-amplitude scatter for observations taken on the same day. This scatter is attributable to the effects of residual GIM (minimally) and, primarily, FGW non-repeatability

uncertainties. The internal measurement error in any individual Y-base value is +/- 5 Y-base units (one σ).

The photometric impact of an erroneous Y-base depends on the size of the error, the aperture involved, and the detector-disperser combination employed. On average, for post-COSTAR point sources, if we assume that a Y-base were known with an accuracy of only 20 Y-base units (approximately 1/13 diode height), for the large apertures (≥1.0") 3-5% of the light in general could be lost and up to 10% at certain wavelengths where the s-curvature is substantial. The light loss is larger, but harder to quantify, for extended objects and pre-COSTAR point sources (see *FOS ISR* 096).

There is essentially no photometric impact due to Y-base uncertainties for FOS apertures smaller than `1.0` as the displacements required to place the images of these apertures off the diode array are simply much larger than the observed uncertainties.

Y-base errors had no impact on measured positions in IMAGE mode observations made with the MIRROR. The brightness of objects within the field of view could be mis-represented, however.

For large aperture (`1.0` and larger) observations, Y-base uncertainty is a prime contributor to photometric, especially spectral shape (color), uncertainties. Refer to Figures 32.3 and 32.4 to determine the spectral regions in which loss of signal is most likely to occur in your spectra. There is little or no photometric impact on apertures smaller than `1.0`.

Remember, 256 Y-base units = 1.43" (pre-COSTAR) and 1.29" (post-COSTAR)

Figure 32.1: FOS/BL Y-bases as a Function of Time

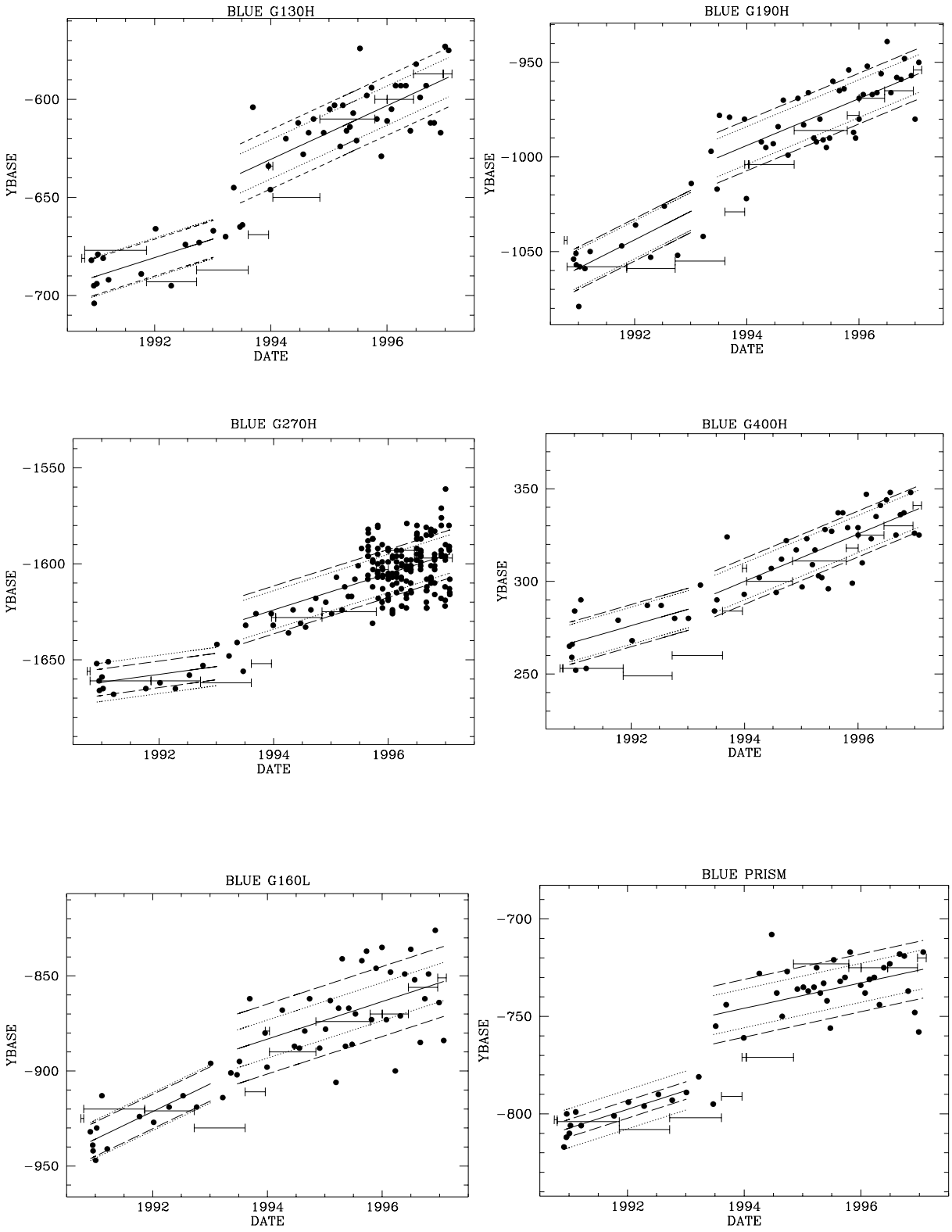

Figure 32.2: FOS/RD Y-bases as a Function of Time

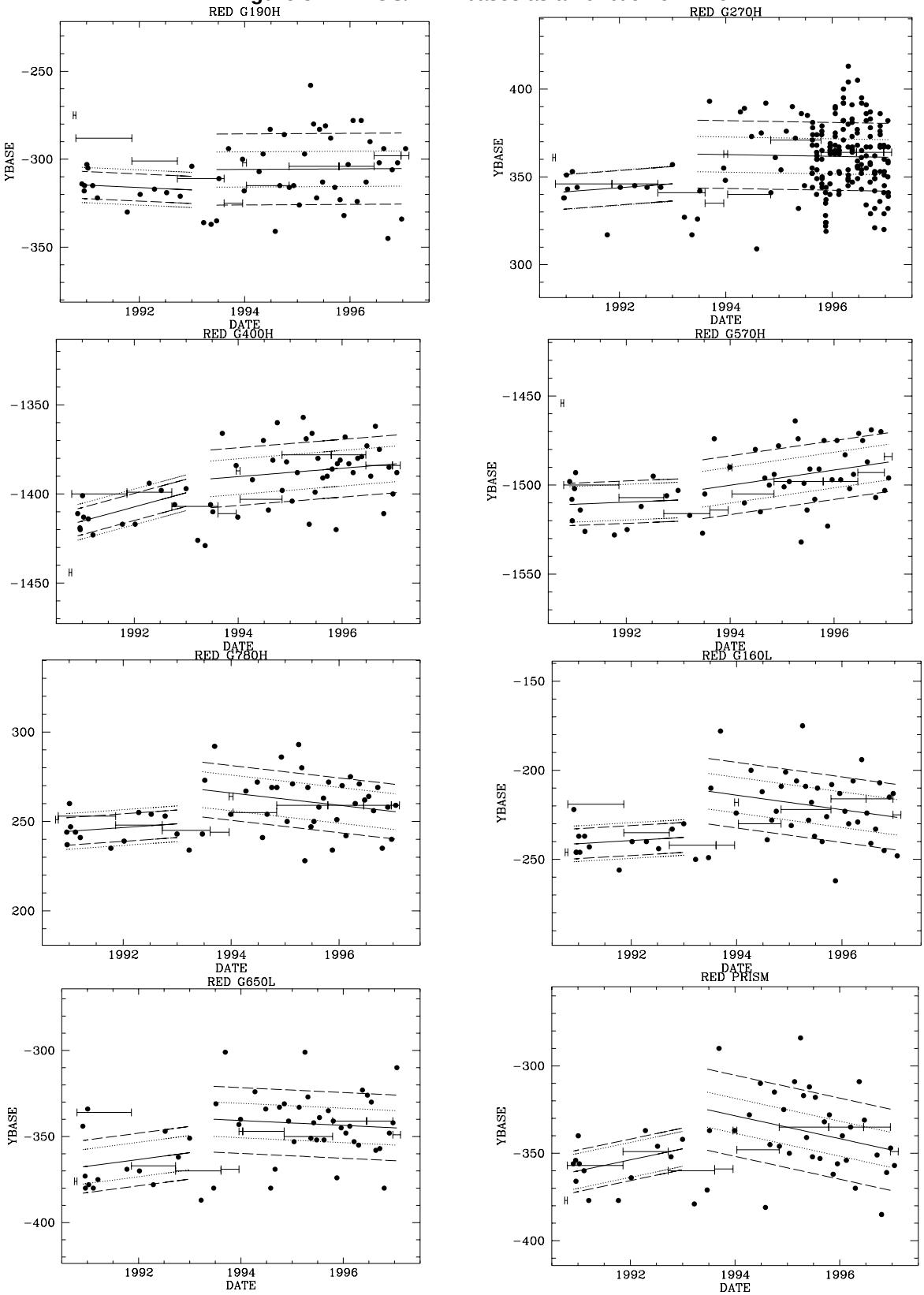

Figure 32.3: Normalized Spectrum Shape on Photocathode (“s-curve”) : FOS/BL

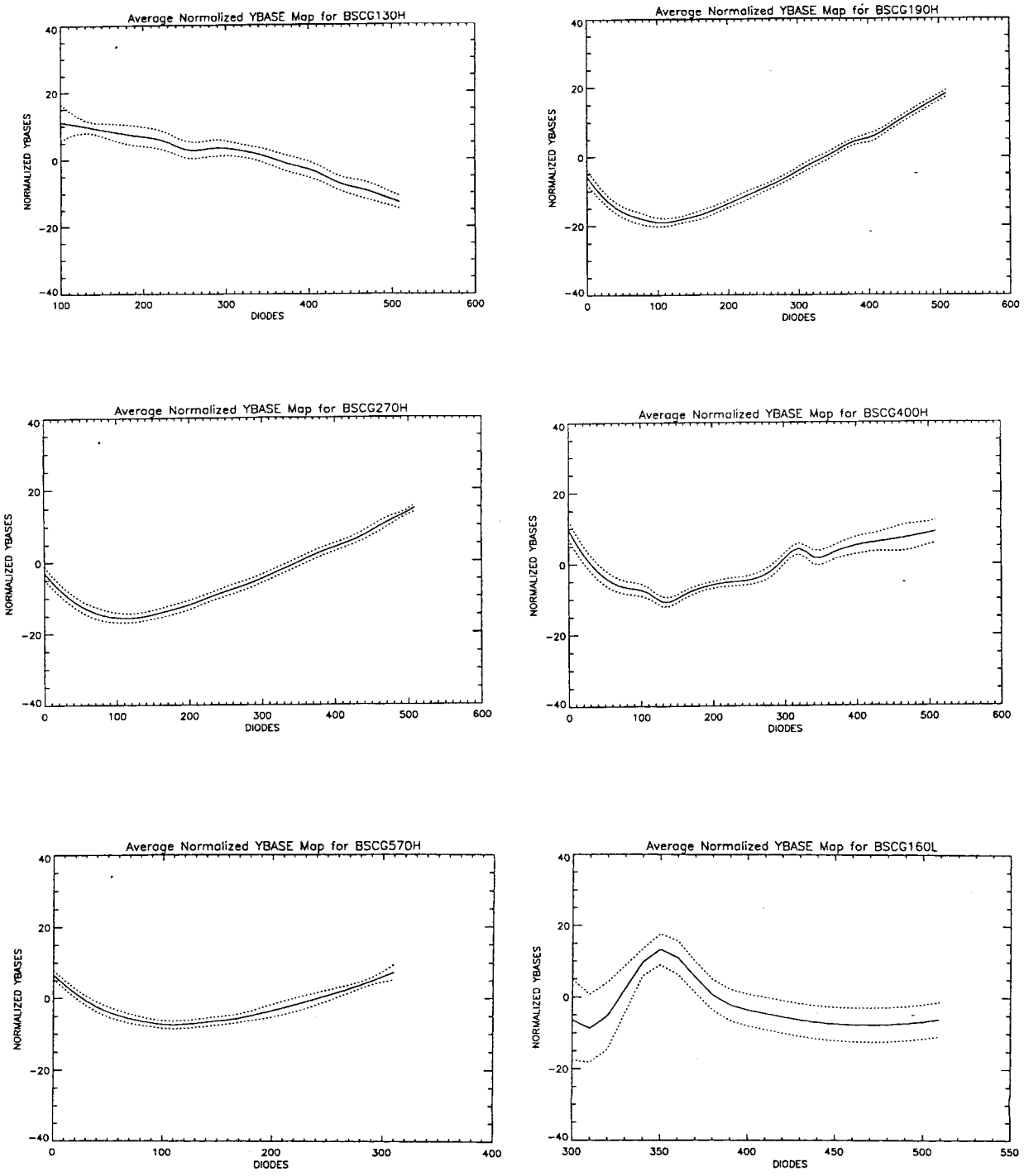

Figure 32.4: Normalized Spectrum Shape on Photocathode (“s-curve”) : FOS/RD

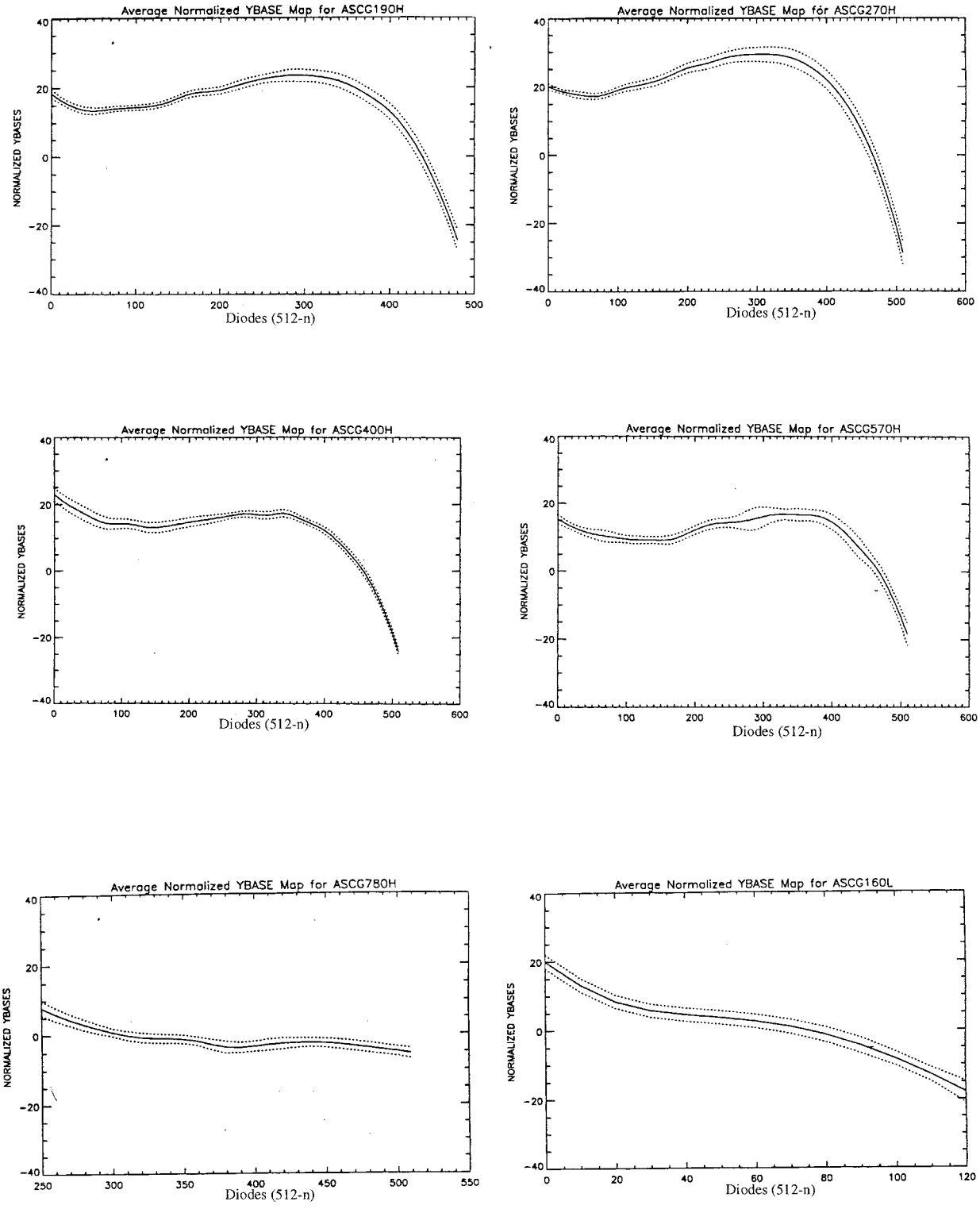

32.3.2 Geomagnetically Induced Image Motion (GIM)

Off-line geomagnetically-induced image motion (GIM) correction was needed only for data taken before April 5, 1993. For spectra taken later, the GIM correction was applied onboard the spacecraft.

As noted in the previous section, photoelectrons from the transmissive FOS photocathode were magnetically deflected onto the diode array. Due to insufficient magnetic shielding of the Digicon detectors, particularly for FOS/RD, the geomagnetic field affected where the photoelectrons landed on the diode array. The effective magnetic field experienced by the electrons depended on the location of the spacecraft in the geomagnetic field. A positional shift of the recorded spectrum due to the changes in the effective magnetic field occurred both parallel to the dispersion direction (*x*) and perpendicular to the dispersion direction (*y*). As of April 5, 1993, this geomagnetically-induced image motion (GIM) problem was corrected in real-time onboard the spacecraft through the application of a spacecraft position-dependent correction to the magnetic deflection that compensated (in both *x* and *y*) for the effects of the geomagnetic field. However, before April 5, 1993, there were no real-time onboard corrections for GIM.

The effect of the x-shift in the photoelectron impact point was to effectively shift the spectrum in the dispersion direction as a function of time. This displacement can be seen in data taken before April 5, 1993 by plotting the individual groups of raw data on a single plot (use the STSDAS **grspec** task) and noting the shift (in *x*) of the centroids of individual emission or absorption lines. In routine post-observation calibration **calfos** applies a correction for the GIM x-shift (as long as the OFF_CORR switch is set to “PERFORM”) in the creation of the calibrated spectral data (`.c0h` and `.c1h` files).[3]

Pre-onboard GIM Correction

The post-observation GIM correction for a given readout segment in an observation is determined from the orbital position of the spacecraft at the mid-point of the observation time for the segment. To avoid resampling the data, and hence losing error information, the correction is applied as an integral pixel shift, although the accuracy of this correction is therefore +/– 0.5 pixel where each pixel is 1/NXSTEPS diodes (1/4 diode in the standard spectrophotometry modes).

In post-observation processing there is no way to correct for the photometric effects of the shift in *y* introduced by GIM. The y-shift caused the s-curve of dispersed light to move along the long dimension of the diodes, and as with

3. Before May 1991, **calfos** did not correct for GIM. All data in the HST Archive were reprocessed and given new header keywords after the GIM correction was added to **calfos**. Therefore, if your FOS data were processed before May 1991, you should retrieve the updated raw data from the HST Archive instead of recalibrating the data on your tape.

Y-base error, could produce a wavelength-dependent loss of light off the edge of the array. The resultant time-dependent error in the overall flux level and in the shape of the spectrum was most severe for poorly-centered observations and for the large apertures. The typical size of uncorrected GIM motion was 0.15" or about 25 Y-bases. For well-centered observations with no Y-base error and the `4.3` aperture the error was <5%. You can use the models of light loss as a function of Y-base offset, wavelength, disperser, and detector given in *FOS ISR* 096 to estimate the effect of GIM motion on your observations.

Depending upon when the program was prepared for scheduling, some data taken after April 5, 1993 may not have had the onboard GIM correction applied. The header keyword YFGIMPEN will tell you if the onboard correction was enabled; if the value is “TRUE” then the onboard correction was applied.

Onboard GIM Correction

The onboard GIM correction is applied on a finer grid than is provided by the pipeline GIM correction on both the x and y axes, so that both wavelength and photometric effects of GIM are minimized. In the x-direction the onboard GIM correction is applied in units of 1/32 of the width of the diodes, while in the y direction the unit is 1/256 of the diode height (or Y-bases). The onboard GIM correction is calculated and updated every 30 seconds (please see *FOS ISR* 098 for complete technical details of the onboard GIM algorithm).

GIM Summary

- ***Post-COSTAR:*** +/-0.02" residual motion (peak-to-peak)
  - *x*-motion (peak-to-peak): 0.06 diode = 0.25 quarter-stepped pixel = 0.02" = ~15 km/sec.
  - *y*-motion (peak-to-peak): 4-5 Y-bases.
- ***Pre-COSTAR:*** +/-0.15" (peak-to-peak) before correction commenced April 5, 1993
  - *x*-motion: corrected to nearest pixel (hence, 0.125 diode = 0.5 quarter-stepped pixel = 0.044" = ~30 km/sec.
  - *y*-motion: up to 25 Y-bases not corrected.

32.4 OTA Effects

32.4.1 Thermal Breathing

The change in temperature as the spacecraft crossed the terminator caused the secondary mirror support structure to expand and contract which moved the secondary mirror and changed telescope focus. This effect was termed *thermal*

breathing and occurred on timescales equal to the orbital period of the spacecraft. The pre-COSTAR photometric error associated with thermal breathing could up to 4–7% and affected the flux in a random and uncorrectable way. The post-COSTAR effect was reduced due to the much narrower PSF and, for well-centered point source observations typically affected only the `0.3` and smaller apertures, where 2-3% variation occasionally was seen even for well-centered targets. Larger aperture point source data with misaligned Y-bases or extended source data could be affected, as well. Only in very long (> 2000 seconds) RAPID mode observations is the effect discernible (and possibly correctable)**.**

32.4.2 Telescope Focus Changes

Systematic variations of pre-COSTAR FOS sensitivity occurred because OTA focus adjustments did not occur with sufficient frequency to keep up with the shrinkage of the graphite epoxy structure caused by outgassing (desorption) on orbit.[4] A change in focus by 15 microns led to photometric changes of up to 8% in the `4.3` aperture. The photometric variations also depended on aperture and very slightly on wavelength. The current **calfos** flux calibration procedure (APR_CORR, AIS_CORR, and TIM_CORR) corrects for all these variations.

Following the installation of COSTAR, OTA focus was monitored very closely and the COSTAR Deployable Optical Bench (DOB) was moved immediately to compensate for each secondary mirror move that was made. No significant focus-related FOS sensitivity variations occurred in the post-COSTAR period.

32.5 Calibration Accuracies

Now we turn to a discussion of the important output quantities (e.g., fluxes, wavelengths, polarimetry, and others), their limiting accuracies, factors affecting the accuracy of each, and some suggestions for assessing their quality in your data. Table 32.1 on page 32-3 provides a high-level summary of the accuracies discussed in these sections.

4. *FOS ISR* 102.

32.6 Photometric Accuracies

There are 10 principal sources of photometric errors which will affect the calibration accuracy achieved in any given FOS dataset. These are:

- Time-dependent variations in FOS sensitivity.
- Target miscentering.
- FGW mechanism non-repeatability.
- Thermal breathing.
- Jitter and Guiding.
- Change in telescope focus.
- Thermal breathing.
- Location of spectra.
- GIM.
- Extended source calibration error.
- Calibration system offsets.

After recalibration of your FOS data with AIS_CORR using the best reference files from the calibration close-out, these error sources will typically still affect the accuracy of your data. Table 32.4 summarizes the approximate levels of photometric inaccuracy introduced by these error sources, for both the pre- and post-COSTAR cases. In the subsections below we describe these error sources in great detail.

Table 32.4: FOS Photometric Errors not Removed by AIS_CORR Calibration

	Level of Error		
Source of Error	**Pre-COSTAR**	**Post-COSTAR**	**Comment**
Miscentering target in aperture	~5% variable	~3% variable	Depends on target acquisition technique and aperture used. Error can be estimated.
Y-base of spectra	3-10%	1-10%	Introduces spectrum shape (color) anomalies. Strongly affects extended objects
FGW non-repeatability	3-10%	1-10%	Similar scale and effect to that of Y-base offset
Thermal breathing	~4-7%	~1-3%	Aperture dependent
Jitter	<3%	<1%	Aperture dependent
GIM[a]	<5%	<1%	Introduces spectrum shape (color) anomalies. Strongly affects extended objects

a. Pre-COSTAR GIM estimate refers to period before April 5, 1993.

To summarize the principal impacts for different types of observations are:

- ***Y-base uncertainty***—absolute and relative (color) effects.
- ***Target centering*** (target acquisition predominant contributor)—absolute and, for centering errors larger than 0.2", relative effects).
- ***Extended object***—must be re-calibrated, if it partially fills the aperture there can be color effects.

If your observations used a small aperture (`0.5` and smaller), the primary source of flux calibration errors are:

- ***Target centering*** (target acquisition predominant contributor)—leads to absolute photometric errors; color OK.
- ***Jitter, guiding, and breathing***—absolute photometry errors; color OK.
- ***Extended object***—must be re-calibrated, color OK.

32.6.1 Flux Calibration (Photometry) Overview

Non-polarimetry FOS observations should always be re-processed with the close-out AIS_CORR reference files and tables.

All recalibrated FOS fluxes are referred to the HST white dwarf model-based flux system (Bohlin et al., 1995, *AJ*, 110, 1316 and Bohlin, 1996, *AJ*, 111, 1743). Many pipeline-calibrated datasets in the Archive are referred to the older HST/IUE flux scale (Bohlin et al., 1990, *Ap.J.Supp.*, 73, 413). Additional important FOS flux calibration references are *FOS ISRs* 125 (pre-COSTAR flux calibration), 144 (post-COSTAR flux calibration), and 136 (post-COSTAR aperture throughputs).

The FOS flux calibration was obtained from carefully centered (<=0.025" pointing accuracy in each coordinate) and flatfielded observations of spectrophotometric standard stars. Five standard stars, G191B2B, BD+28D4211, BD+33D2642, BD+74D325, and HZ44, were used for the pre-COSTAR calibration observations. For the post-COSTAR calibrations, this set and three additional white dwarf standards, GD71, GD153, and HZ43 were used. All pre-COSTAR observations were made with the `4.3` aperture and post-COSTAR observations were made with either the `4.3` or the `1.0` aperture. Typical formal S/N of binned spectral regions for these observations were 100 or often substantially greater.

Two methods of flux calibration have been used: FLX_CORR and AIS_CORR.

- ***FLX_CORR:*** Only spectropolarimetry data are reduced with the FLX_CORR method. One average set of sensitivity corrections was applied to all pre-COSTAR data regardless of when the data were taken or how far

the telescope may have been from nominal focus. Similarly, only one epoch was used to set the post-COSTAR polarimetry flux calibration, but no time-dependent variables, such as focus or sensitivity changes existed for the post-COSTAR timeframe. FLX_CORR method photometry was substantially inferior to fluxes derived from the AIS_CORR method as several important sources of photometric error could not be removed in FLX_CORR processing.

For example, pre-COSTAR FLX_CORR pipeline-calibrated fluxes may contain errors of up to 5% (FOS/RD) or up to 8% (FOS/BL) due to the pre-COSTAR sensitivity decline, of 5% due to telescope focus changes, and 3-15% (depending on spectral region) due to the offset between the IUE-based absolute flux system and the newer white dwarf model system (see See “Absolute Photometric Calibration System Offsets” on page 32-36.).

- ***AIS_CORR:*** All other flux-calibrated modes use this method of flux calibration, which includes corrections for time-dependent sensitivity variations, as needed, and for the actual focus history of the telescope. In the post-COSTAR era the effect of OTA focus changes is non-existent and that of time-dependent sensitivity variation is much less severe than for the pre-COSTAR period. All AIS_CORR corrections and aperture throughputs, with the exception of those for the `0.1-PAIR` and the two barred apertures are based on actual observations. The barred aperture sensitivity has been defined as identical to that of the `4.3` aperture, and `0.1-PAIR` throughputs defined as 20% of the `4.3` for pre-COSTAR and 40% post-COSTAR.

Time-Dependent Variations in FOS Sensitivity

As noted above, FOS sensitivities occasionally displayed time-dependent variations. All sensitivity variations which could clearly be attributed to systematic time variations were incorporated into the latest calibration reference files and can be removed by re-calibrating the data with the AIS_CORR flux calibration method and the most recent reference files and tables.

From early 1991 through mid-1992 the FOS experienced a systematic decline in sensitivity for all gratings and detector combinations. The systematic FOS/BL degradation in sensitivity by early 1992 amounted to approximately 10% for all gratings, and approximately 5% per year for FOS/RD (except for the G190H grating). The degradation in the FOS/RD G190H and G270H regions occurred at a rate of ~10% per year and was quite wavelength dependent.[5] All pre-COSTAR degradation leveled off between mid-1992 and the end of 1993. In Figure 32.5 we show the time dependence of the pre-COSTAR sensitivity for FOS/BL G130H which was typical for that detector. Pre-COSTAR sensitivity changes for FOS/RD G400H, which were typical of most spectral regions for that detector, are shown in Figure 32.6 and for the FOS/RD G190H in Figure 32.9.

Post-COSTAR sensitivity shows a dip relative to the pre-COSTAR values between approximately 1500 and 2500 Å. Except for FOS/RD G190H and G160L post-COSTAR sensitivity has shown no believable systematic temporal variation

5. *FOS ISR* 077.

(see Figures 32.7 through 32.11). From February, 1994 through July, 1994 FOS/RD G190H sensitivity dropped by approximately 2% and then increased from 3 to 15% between July, 1994 and September, 1996. These changes are contemporaneous with substantial flatfield changes in portions of this grating. FOS/RD G160L showed similar changes shortward of 2200 Å. Figures 32.8 and 32.10 show the time dependence of post-COSTAR FOS sensitivity for the FOS/RD G190H grating.

The thick lines in Figure 32.8 indicate the average time-dependent sensitivity correction applied by the TIM-CORR calibration step (as contained in the `.cyc` reference file).

Overall Flux Calibration Accuracy Summary

The overall accuracy of the FOS photometric calibration for well-centered sources in the larger apertures, following recalibration with the appropriate updated reference files, is currently estimated to be 3% (1 σ) for all grating modes except for FOS/RD G160L, FOS/RD PRISM and G780H longward of 7500 Å; for those specific settings the accuracy is 4% (1 σ). In addition, there may have been systematic changes in the sensitivities at the 2% level which were not accurately tracked in the calibrations over some periods of times (see Figures 32.7, 32.8, and 32.11).

The relative photometry within a given standard spectrum is estimated to show roughly ± 2% curvature about the mean over correlation lengths of approximately 250 Å (see for example the relative spectra in Figure 32.14 and Figure 32.15, which show limiting examples of this effect that occurred occasionally in standard star spectra). Excursions to ± 4% are seen in some extreme cases.

The principal factors which contribute to this overal calibration accuracy include the following.

- The white dwarf models empirically reproduce the G191B2B and other standard star stellar flux distributions to roughly 1% in the visible region (using Landolt visible region normalizing photometry) and 2% in the ultra-violet. The reference system slope uncertainty over the 1200–5500 Å range is +/– 2%.
- The FOS exhibits ~2% or better repeatability for observations taken near in time in a given mode for all modes except FOS/RD PRISM and G160L and the long-wavelength region of G780H (at λ > 7500 Å), where repeatability is good to ~3%. See *FOS ISR* 144 for plots of accuracies for each mode as a function of wavelength.

The sensitivity calibration files are computed as the mean of independent standard star observations over some time period, with any variations from observation to observation within that time period attributed to non-reproducibility in the FOS, and not to variations in the sensitivity (except for FOS/RD G190H and G160L). For any time periods and wavelength regions where true time variations have not been removed, there can be systematic effects in the absolute calibration scale at the 2-4% level (see Figure 32.7 for example—and consult *FOS ISR* 144 and the final closeout sensitivity ISR (158, in preparation) if you are concerned about effects at this level.)

Actual FOS observations could have more uncertainty than this global 3% limiting accuracy, especially if the pointing uncertainty exceeded 0.1–0.2" as it often did, particularly in the pre-COSTAR era.

Indeed, for any individual observation, the overall calibration accuracy is limited by a series of factors that, for the most part, can not be removed in calibration processing. These are described in the remainder of this section.

32.6.2 Aperture Centering (Target Location) Factors

Target Miscentering

Inaccurate centering of a target in the aperture led to photometric errors because of the loss of signal out of the aperture. The flux from the source was underestimated systematically. The largest errors occurred for observations with the smallest (`0.3` or smaller) apertures. *Miscentering is likely to be the dominant error affecting flux calibration for small aperture observations.* One can estimate the photometric error due to miscentering of the target in the aperture from the information supplied in Figures 32.12 and 32.13 and Table 32.5. Figures 32.12 and 32.13 show, for several important apertures, the post-COSTAR diminution of the transmitted flux from a point source versus the pointing error (miscentering). The fall-off in the signal is gradual except when the target is within about 0.1" of the edge of the aperture. The light loss is ~50% when the target lies on the aperture edge. Table 32.5 gives the maximum pointing errors for different types of target acquisitions; actual values should be determined by examination of the FOS paper products.

For example, with the `0.3` (B-2) aperture a target miscentering of 0.12" (the centering accuracy routinely achieved with ACQ/BINARY acquisition mode) led to a flux loss of about 60% with respect to perfect centering. The expected flux loss for a pointing accuracy of 0.03" (typically reached with a high precision multi-stage peak-up sequence) led to flux losses of less than 4% in the `0.3` aperture. Observing with the `1.0` aperture, the same pointing accuracy of 0.03" led to no measurable flux losses. For this aperture, the pointing accuracy of the binary target acquisition technique was sufficient. It resulted in flux losses of less than 3%

Determine your pointing accuracy from the FOS paper products for ACQ/PEAK acquisitions or assume one σ values from Table 32.5 for ACQ/BINARY. Use Figures 32.12 and 32.13 to estimate light loss for this degree of miscentering.

Here are a few points to remember:

- For the `4.3` aperture, large *y* miscenterings have observable results that mimic the effect of poor Y-bases. Color anomalies and, especially, grating overlap region flux mismatches are a common consequence of poor large aperture centering. Many pre-COSTAR observations used only very approximate target acquisition strategies for `4.3` aperture observation,

often under the mistaken impression that because of the large PSF one did not have to center accurately. Typically, any large aperture miscentering of more than 0.2" (40 Y-bases) in *y* will yield clearly discernible spectrum shape anomalies. Small aperture observation spectrum shapes are not affected by miscentering, although photometric accuracy is, of course.

- Highest precision *absolute* spectrophotometry required precise centering of <0.06", preferably 0.025" in each coordinate.
- Highest precision *relative* spectrophotometry with apertures larger than `0.5` required precise centering of <0.06", preferably 0.025" in *y*.

Jitter and Guiding

The effect of jitter and guiding errors is aperture dependent. The duration of jitter events is typically short and the size of guiding errors is typically small (1 σ=0.007") so that large aperture observations are not affected unless the target was poorly centered by the target acquisition. Smaller aperture observations can be affected. Typical random jitter produced <3% light loss for `0.3` pre-COSTAR and <1% post-COSTAR.

Examine the paper products jitter ball plot for anomalous tracking. Examine the paper products group counts plot to assess photometric repeatability between readouts.

32.6.3 Photocathode Centering (FGW Repeatability)

Random FGW repeatability could introduce an offset relative to the expected y-position of the spectrum on the photocathode, hence had the effect of introducing Y-base error. The scale of typical FGW non-repeatability was such that by itself it would have had a very modest effect on large aperture fluxes and no effect on small aperture fluxes. However, the combination of FGW displacement with random Y-base variation or poor target centering could lead to both absolute and relative (color) photometric losses.

The primary *photometric* effect of any x-component of FGW non-repeatability was to introduce some uncertainty as to the exact correspondence between the portion of the photocathode granularity sampled by an arbitrary observation and that sampled by STScI calibration observations. The net effect, for most gratings, was to introduce a small amount of random additional noise, typically on the order of <1%, into the flatfielded spectrum (See “Flatfield Calibration” on page 32-38.).

32.6.4 Image Centering (Image Location) Factors

Y-base and GIM effects

Absolute and relative (spectrum shape or color) accuracies are limited by Y-base uncertainties for the `1.0` and larger apertures. The size of the spectrum

and the positioning of the spectrum s-curve on the diode array were the limiting factors. Smaller apertures were typically not affected as the scale of Y-base error (<25 Y-bases in most cases as seen in Figures 32.1 and 32.2) was much smaller than the distance between the edge of the aperture image on the photocathode and the height of the area on the photocathode that was readout. Y-base photometric effects could be substantial for the large apertures, especially for extended objects. The exact amount of light lost depended on the size of the error, but commonly 3-10% effects were seen pre-COSTAR and 1-10% effects post-COSTAR. Note the apparent effect of poor Y-bases in Figure 32.14 which shows the ratio of flux-calibrated standard star spectra to the reference energy distribution. Of particular interest is the 1200–1600 Å. region in the BD+28D4211 observations near 1994.4. The installed Y-bases for FOS/BL G130H deviated at that time by nearly 40 Y-base units from the nominal trend (see Figure 32.1). Clear 4–5% effects are seen in these precisely centered observations made with both 1.0 and 4.3 apertures (see Figure 32.17).

Look for broad features similar to the residuals seen in Figures 32.14 and 32.15. The shape of the features can be anticipated by considering the effect of shifting the s-curves in Figures 32.3 and 32.4 toward the top and bottom of the diode array. Reference to Figures 32.1 and 32.2 provides an idea of how close the installed Y-bases were to the continuing trend. Remember that the typical scale of Y-base uncertainty was up to 25 Y-bases, which could be exacerbated by similar amounts of FGW positioning offsets.

32.6.5 Telescope Factors

OTA Focus

As noted in “Telescope Focus Changes” on page 32-16 the focus of the telescope had a pronounced effect on FOS throughput in the pre-COSTAR period. The AIS_CORR flux calibration completely corrects the wavelength-dependent throughput of each aperture for this effect.

Breathing

Thermal breathing introduced an aperture-dependent variation in throughput as a function of orbital position. Naturally, the effect was worse for the smaller apertures. For the pre-COSTAR period a 4–7% light loss occurred; in the post-COSTAR period the effect was more typically 1–3%.

Examine the paper products group plot for any series of readouts lasting more than 1000 seconds. Figure 32.16 shows an example of an approximate 3% thermal breathing effect for a precisely centered, low jitter (peak-to-peak excursions = 0.01") photometric target observed through the `0.3` aperture in a RAPID mode time-series of nearly eighty 30-second integrations all in one visibility.

Figure 32.5: Pre-COSTAR Typical Sensitivity Time Dependence: FOS/BL

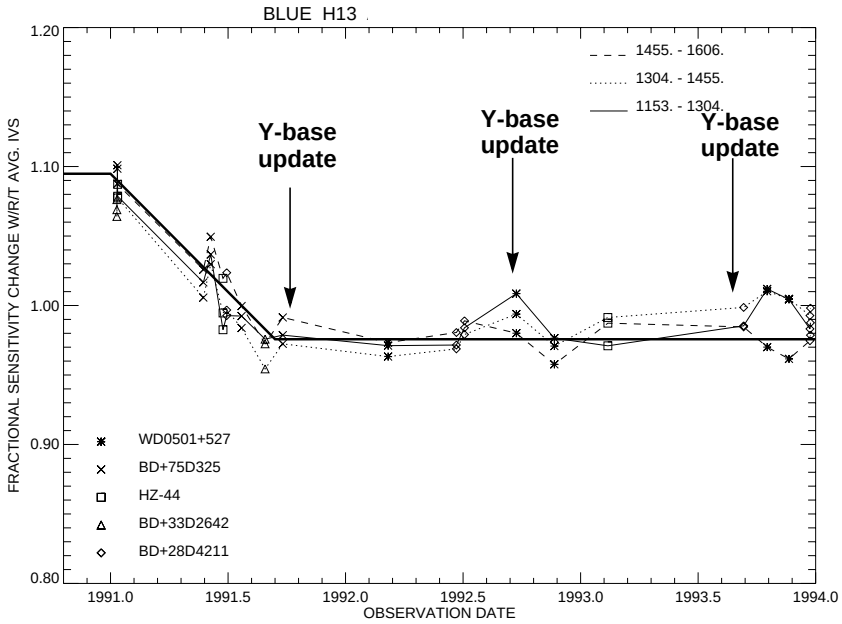

Figure 32.6: Pre-COSTAR Typical Sensitivity Time Dependence: FOS/RD

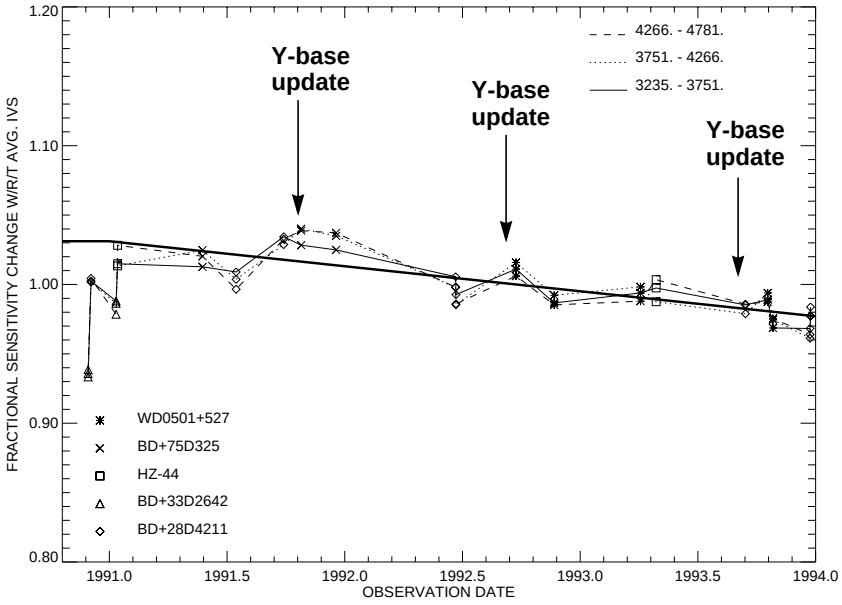

Figure 32.7: Post-COSTAR Sensitivity Time Dependence: FOS/BL

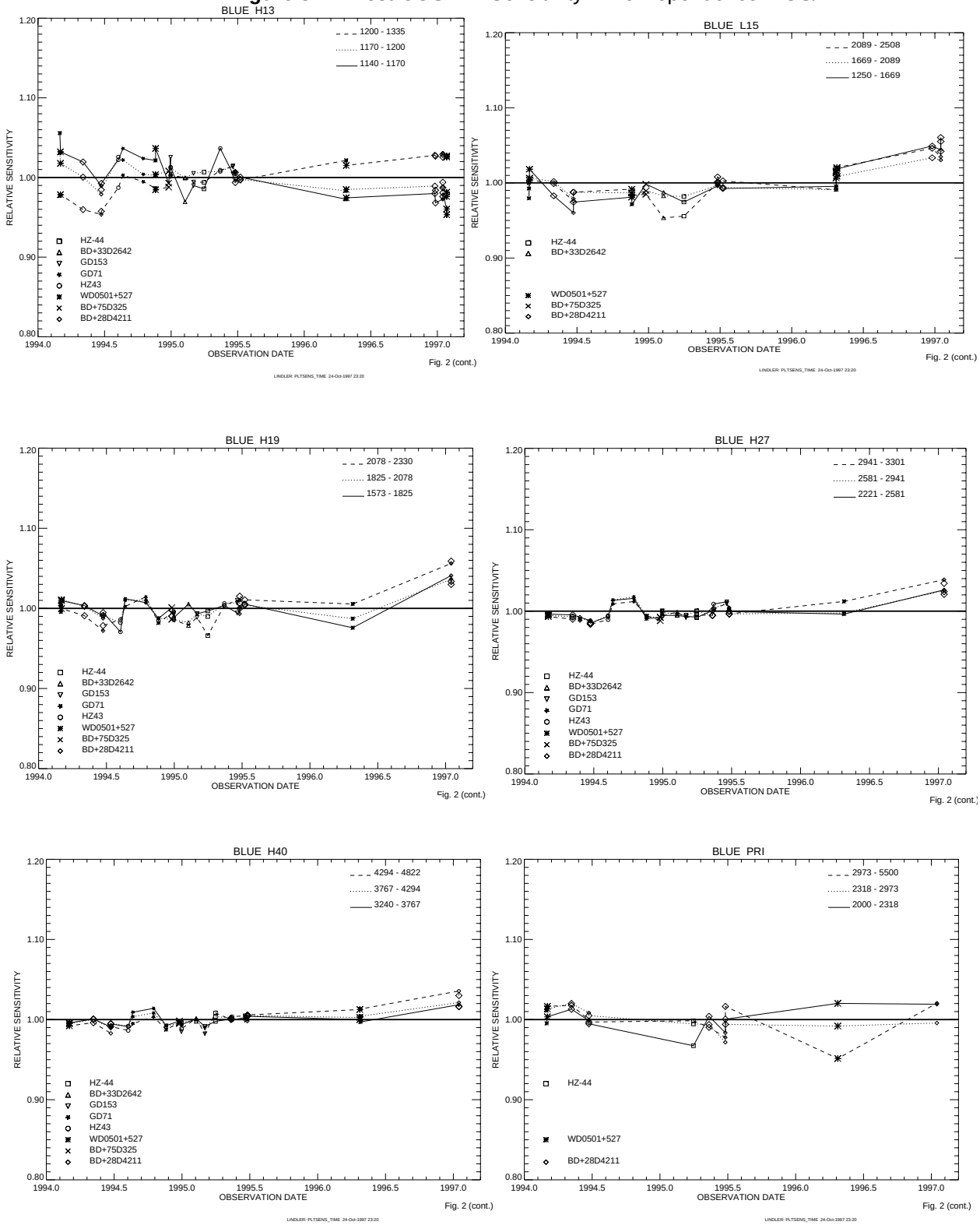

Fig. 2 (cont.)

Figure 32.8: Post-COSTAR Sensitivity Time Dependence: FOS/RD G190H

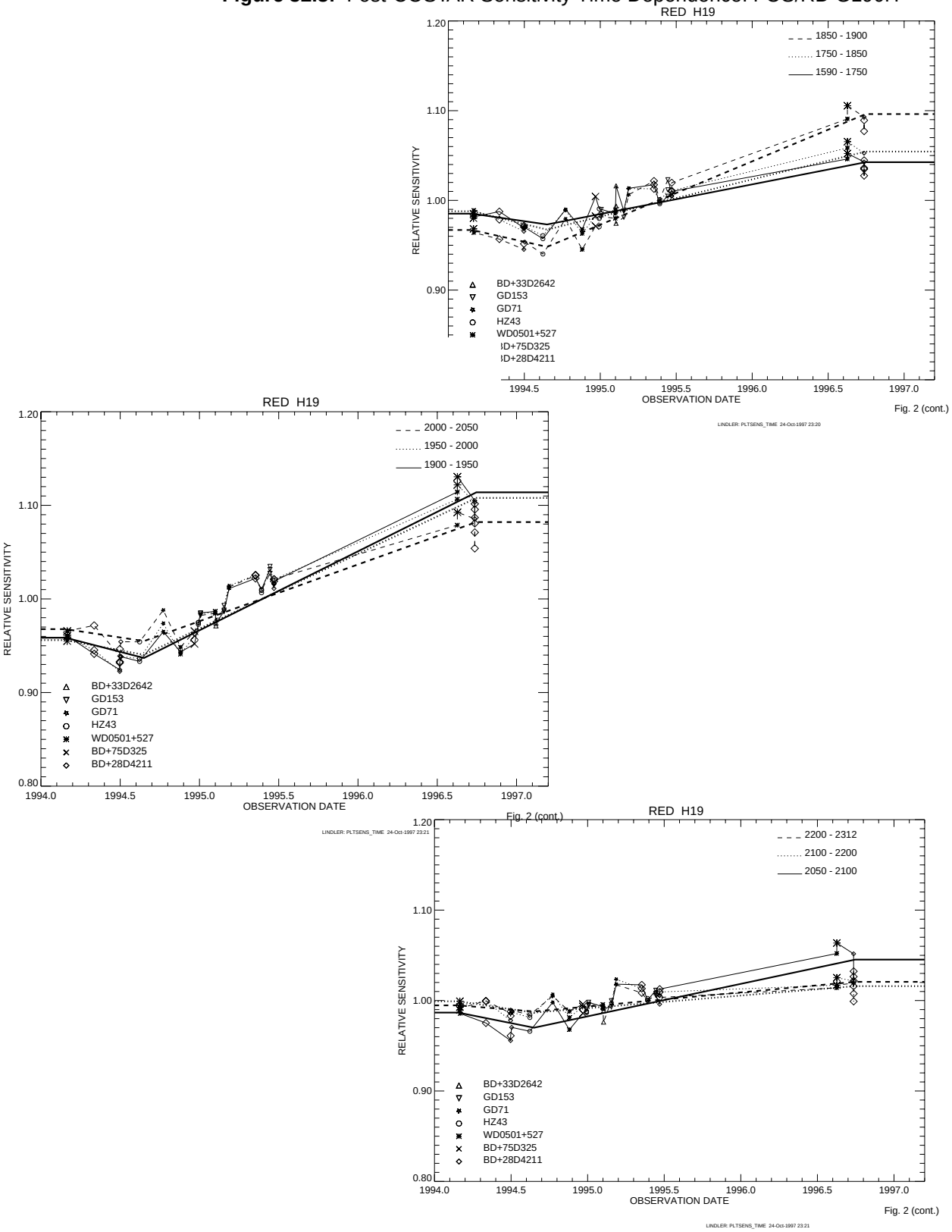

Figure 32.9: Pre-COSTAR Time Dependence in FOS/RD G190H Grating

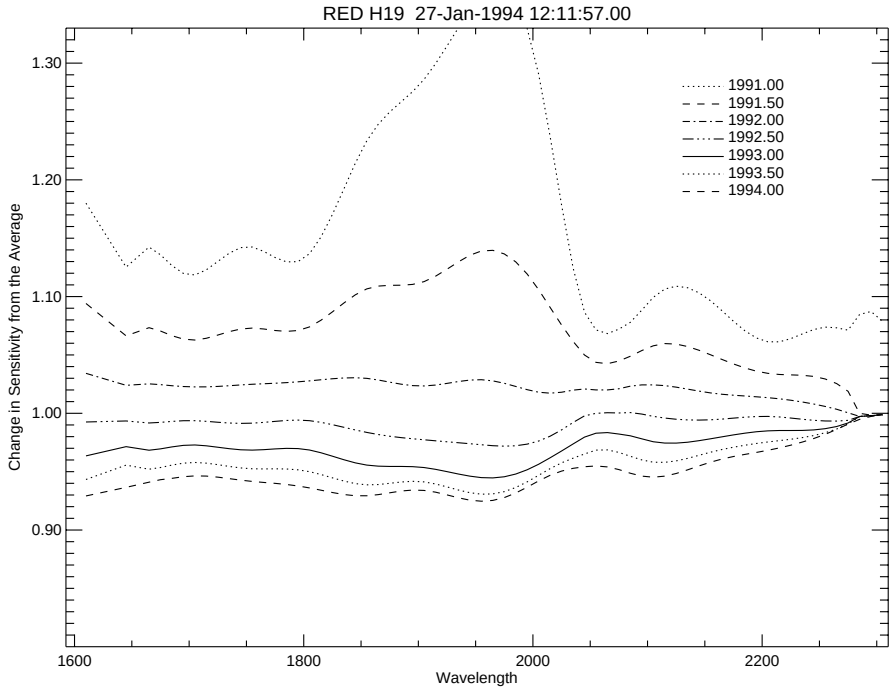

Figure 32.10: Corrections as a Function of Wavelength for FOS/RD G190H

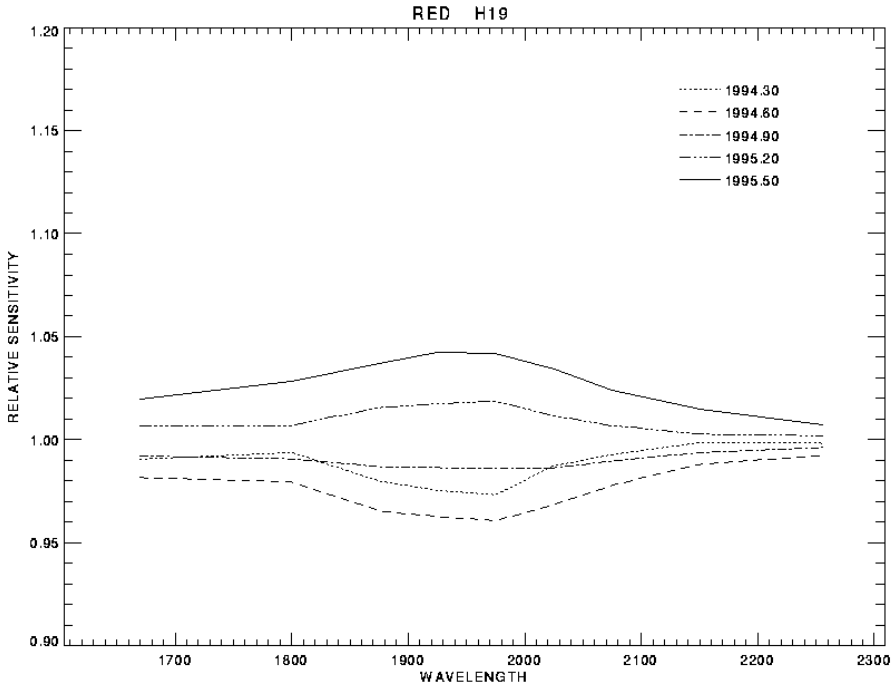

Figure 32.11: Post-COSTAR Sensitivity Time Dependence: FOS/RD

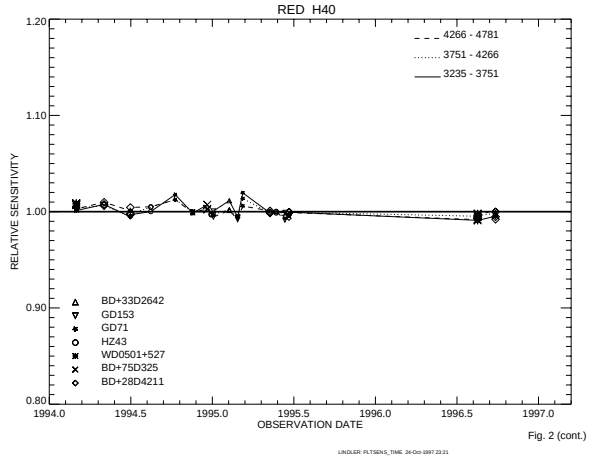

Fig. 2 (cont.)

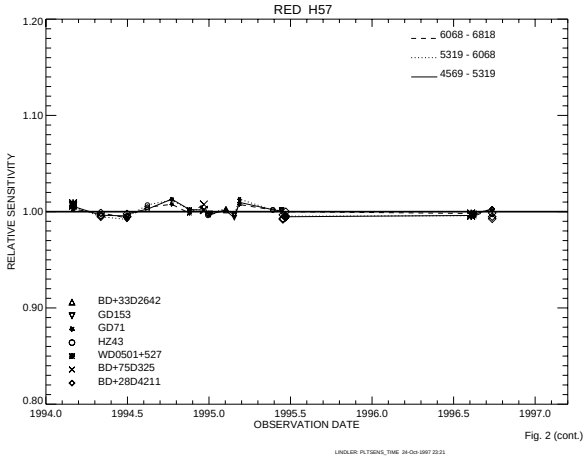

Fig. 2 (cont.)

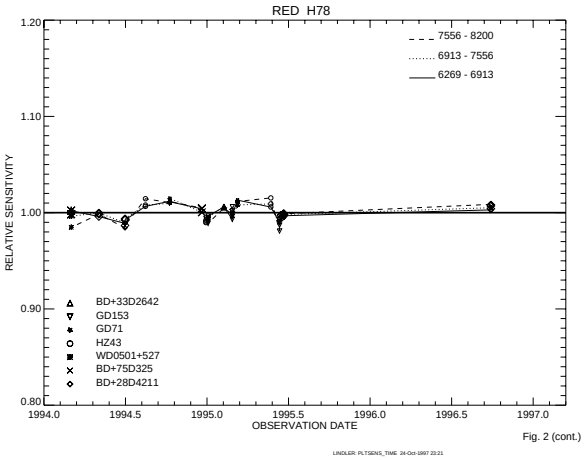

Fig. 2 (cont.)

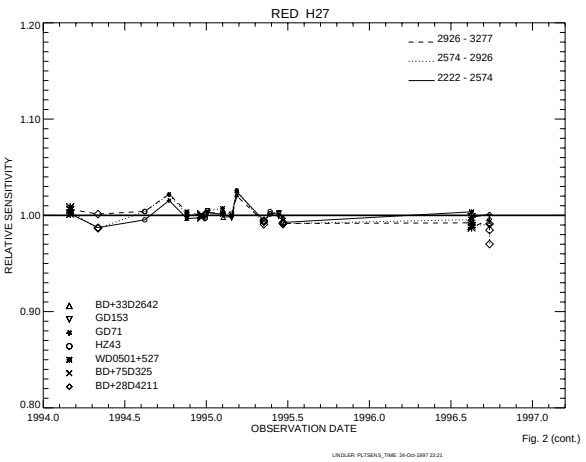

Fig. 2 (cont.)

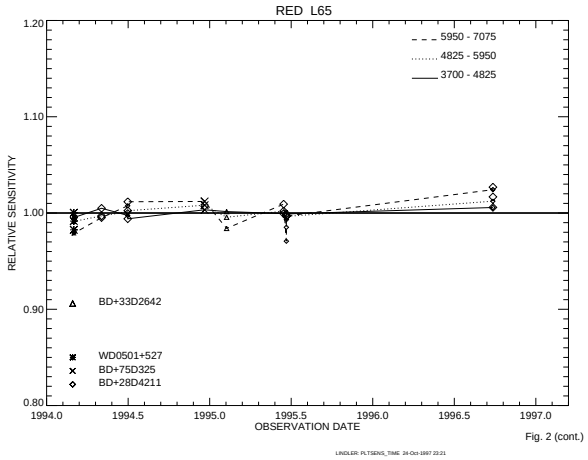

Fig. 2 (cont.)

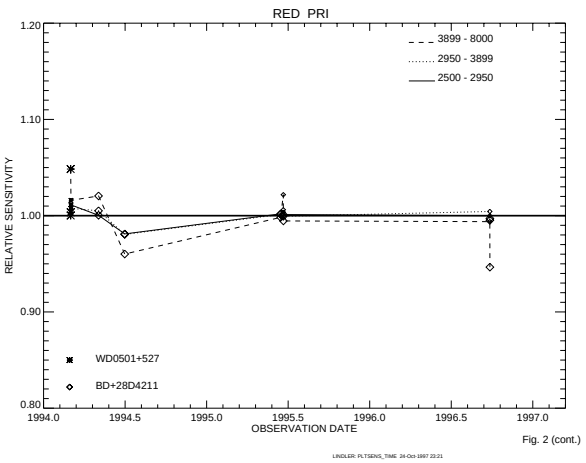

Fig. 2 (cont.)

Figure 32.12: Post-COSTAR Transmitted Flux Versus Pointing Error: FOS/RD

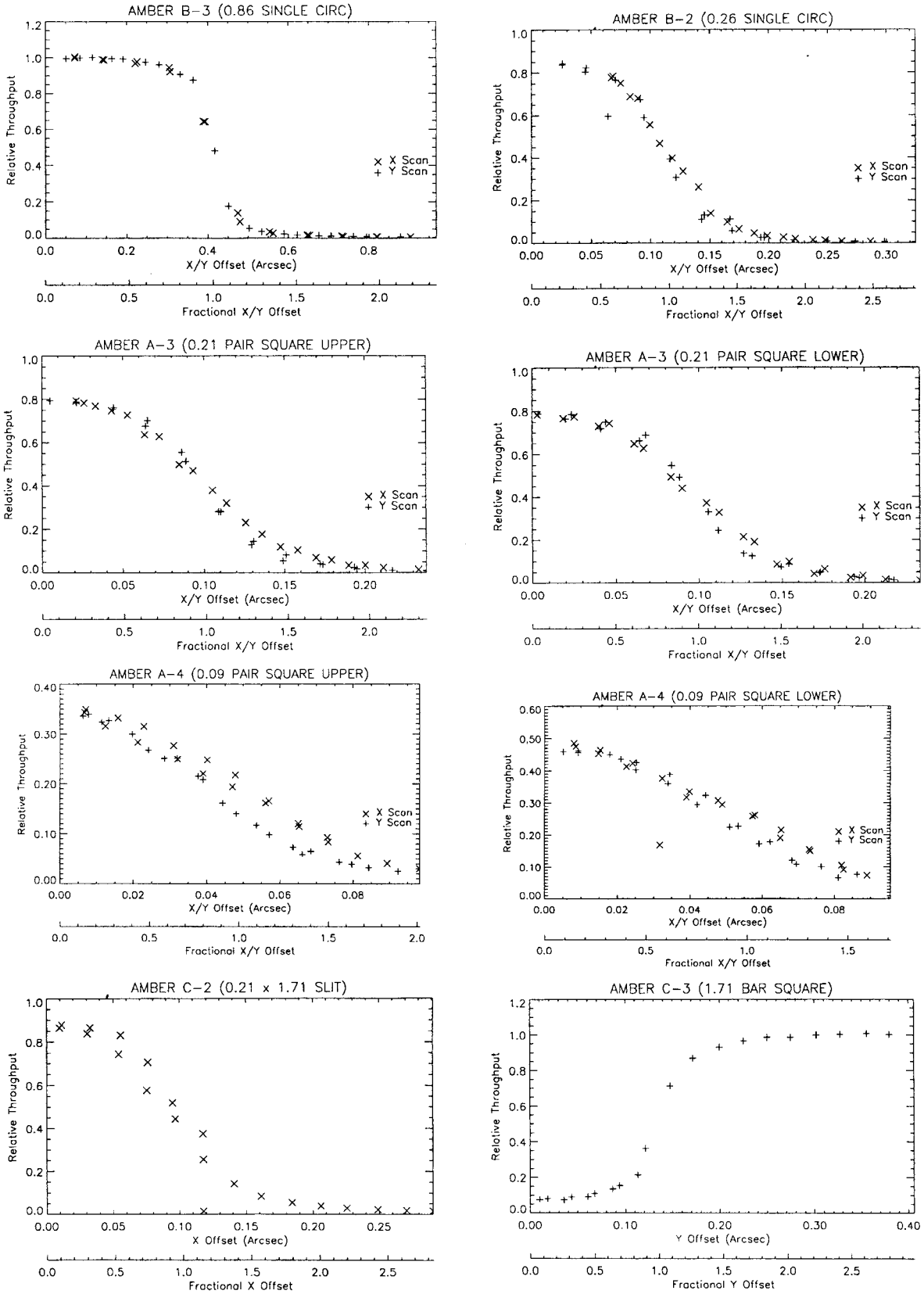

Figure 32.13: Post-COSTAR Transmitted Flux Versus Pointing Error: FOS/BL

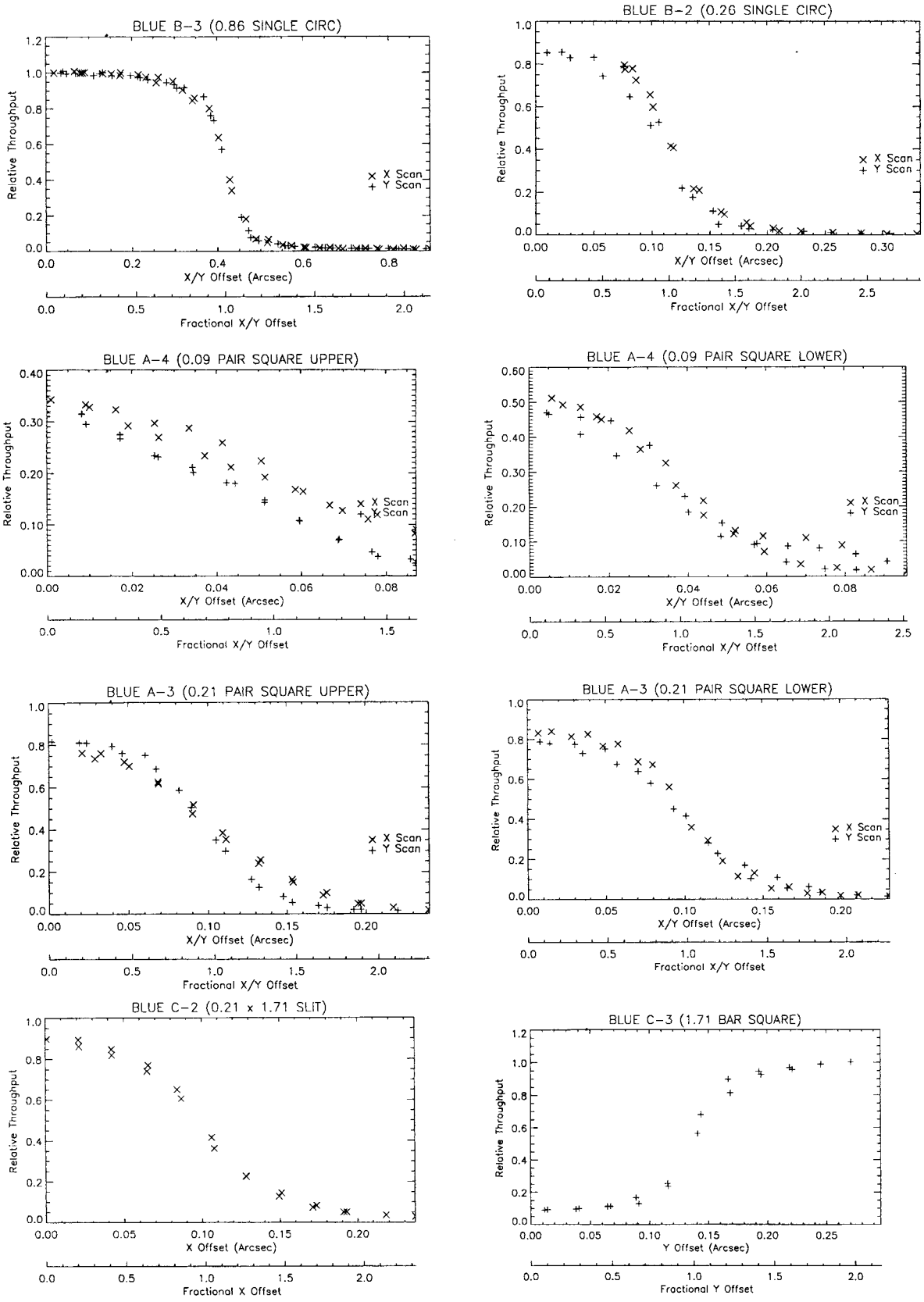

Figure 32.14: FOS Standard Stars Compared with Models: FOS/BL

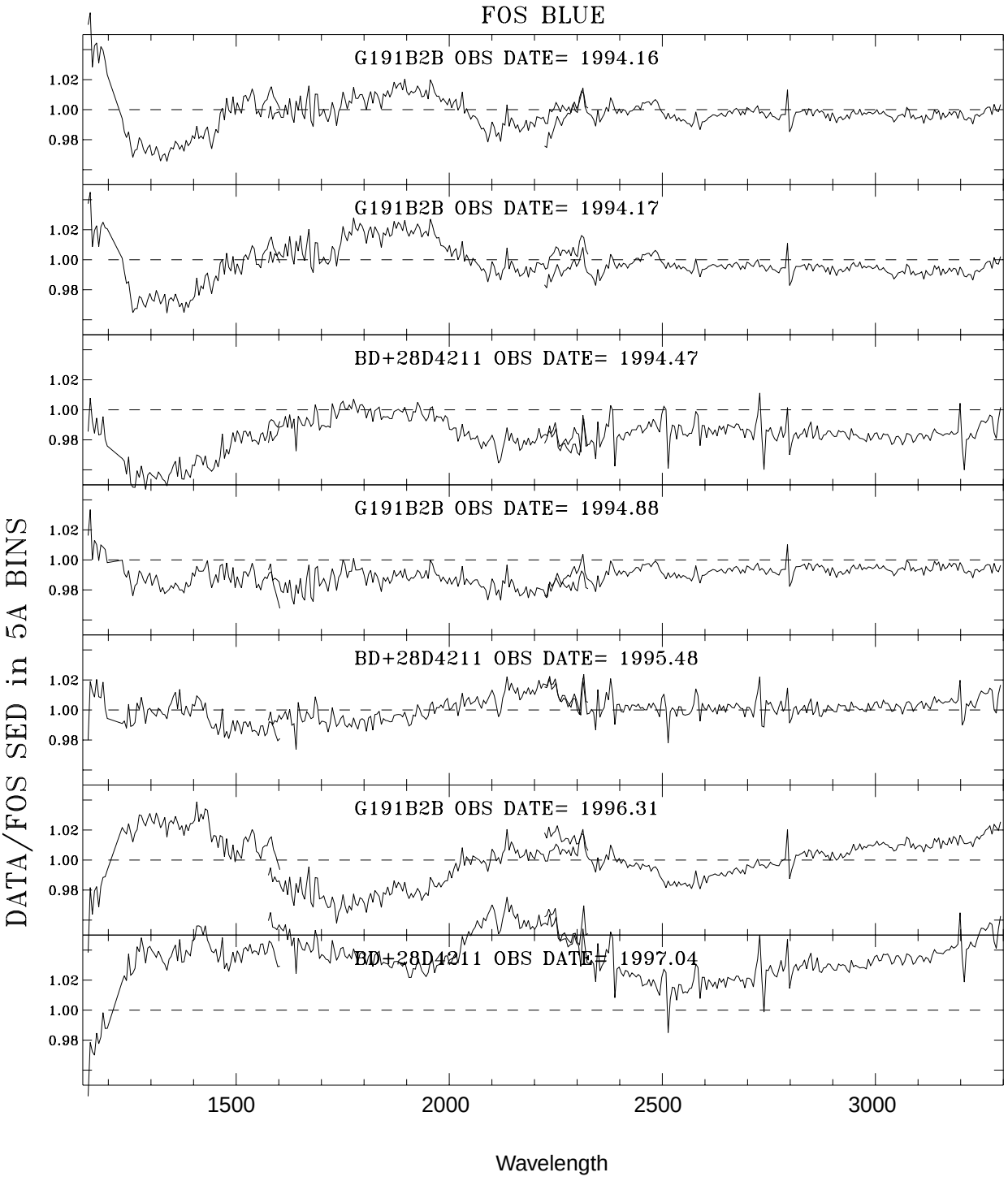

Figure 32.15: FOS Standard Stars Compared with Models: FOS/RD

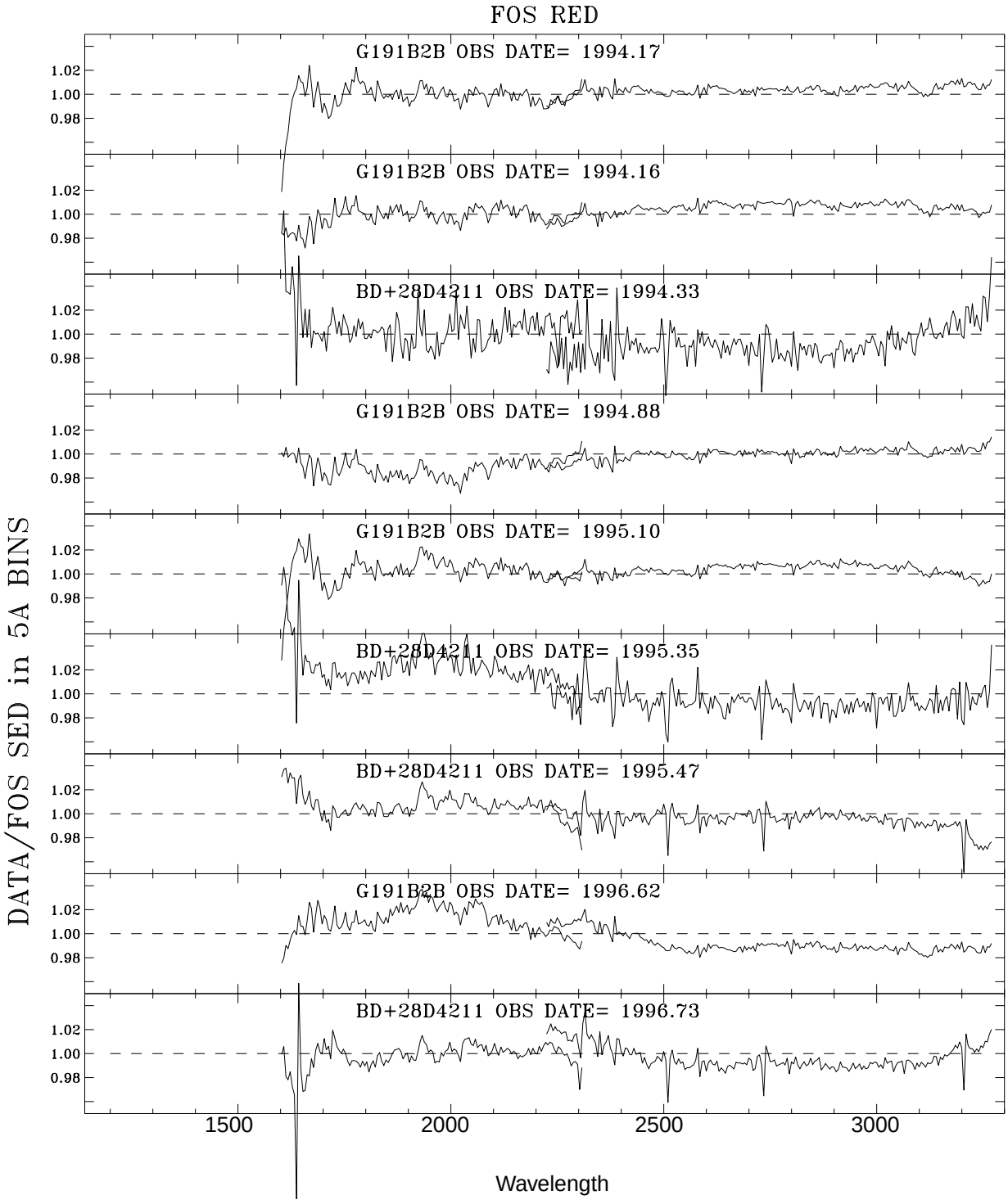

Figure 32.16: Example of Breathing Effect on Well-Centered 0.3 Observation

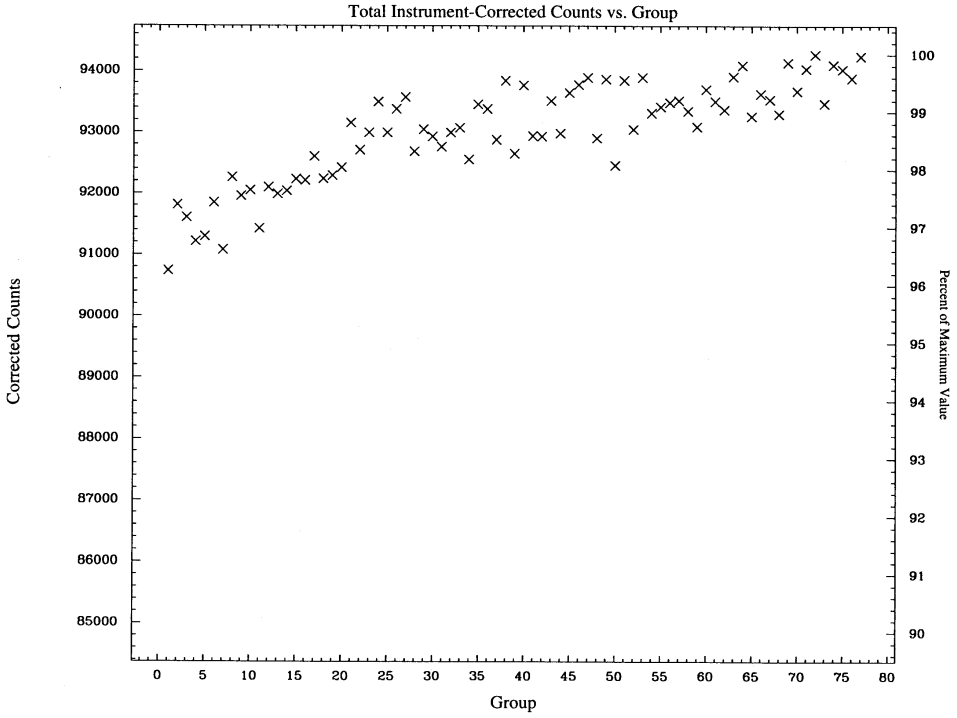

Figure 32.17: Relative Light Loss Due to Mis-centering or Y-base Error (FOS/BL G130H)

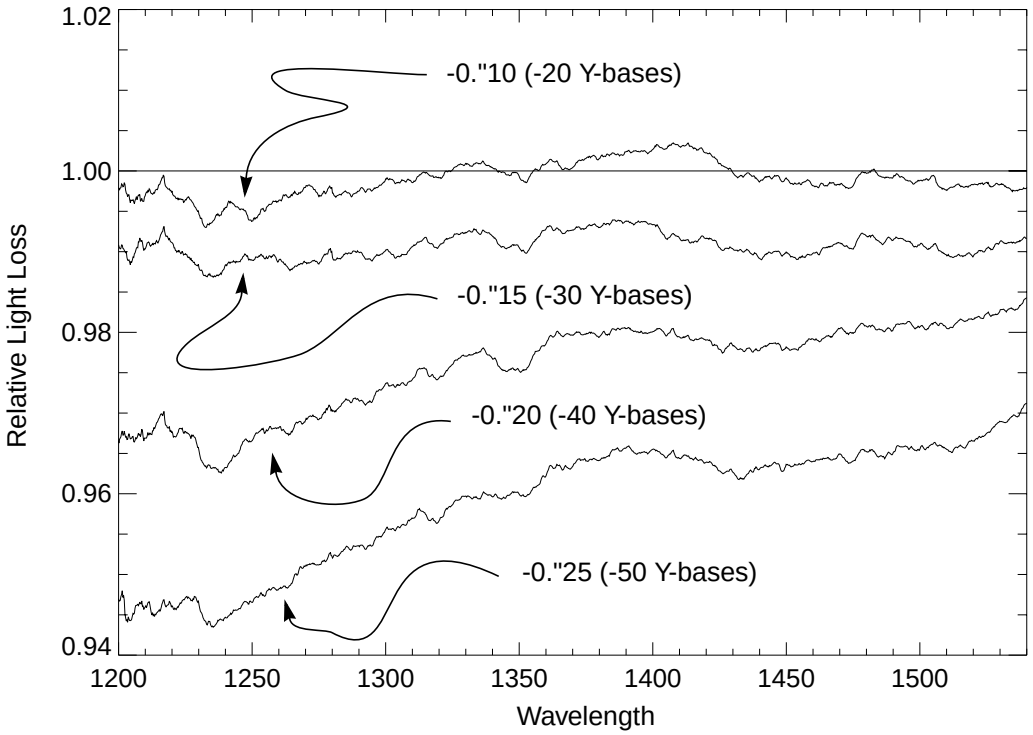

Table 32.5: Target Acquisition Pattern Pointing Accuracies

Aperture	Pattern Name	Search-size-X	Search-size-Y	Step-size-X (arcsec)	Step-size-Y (arcsec)	Pointing Accuracy (arcsec)
4.3	A	1	3	-	1.23	-
1.0	B1	6	2	0.61	0.61	0.43
0.5	C1	3	3	0.29	0.29	0.21
0.3	D1	5	5	0.17	0.17	0.12
	D2	5	5	0.11	0.11	0.08
	D3	5	5	0.052	0.052	0.04
	E1	4	4	0.17	0.17	0.12
	E2	4	4	0.11	0.11	0.08
	E3	4	4	0.052	0.052	0.04
	F1	3	3	0.17	0.17	0.12
	F2	3	3	0.11	0.11	0.08
1.0-PAIR	B2	6	2	0.61	0.61	0.43
0.5-PAIR	C2	3	3	0.29	0.29	0.21
0.25-PAIR	P1	5	5	0.17	0.17	0.12
	P2	5	5	0.11	0.11	0.08
	P3	5	5	0.052	0.052	0.04
	P4	4	4	0.11	0.11	0.08
2.0-BAR	BD1	1	11	-	0.052	0.03
0.7-BAR	BD2	1	11	-	0.052	0.03
SLIT	S	9	1	0.057	-	0.03
ACQ/BINARY FOS/RD	Z	-	-	-	-	0.12 (1-σ)
ACQ/BINARY FOS/BL	Z	-	-	-	-	0.08 (1-σ)

32.6.6 Extended Source Aperture Dilution Correction

The **calfos** flux calibration of *all extended sources is always incorrect!* You should always apply the aperture dilution corrections found in this section.

Flux calibrations are determined from observations of standard stars and compensate automatically only for any light in the PSF that falls outside the aperture. For observations of *extended* sources, a correction needs to be applied to the final flux calibrated spectrum to correct for the non-pointlike illumination pattern. The correction is given by:

$$I = \frac{F \times A(ap) \times T_{4.3}}{\Omega}$$

where:

- I = Specific surface intensity of a diffuse source in ergs s^{-1} cm^{-2} $Å^{-1}$ $arcsec^{-2}$.
- F = Flux in the calibrated spectrum.
- $A(ap)$ = Relative point source transmission through the aperture area when A(`4.3`) = 1. These are given in Tables 32.6 and 32.7.
- Ω = Solid angle of the aperture or object, whichever is smaller, in square arcseconds, e.g., 4.3" x 1.43" (pre-COSTAR) and 3.66" x 1.29" (post-COSTAR) for the `4.3` aperture.
- $T_{4.3}$ = Absolute transmission for a point source at zero focus of the `4.3` aperture. This number is estimated to be ~0.73+/-0.03 (pre-COSTAR) and 0.95+/-0.02 (post-COSTAR).[6]

Pre-COSTAR aperture throughputs are given in Table 32.6 below. Substantial wavelength-dependent differences do not exist for the pre-COSTAR instrument, but detector differences are seen for equivalently sized apertures.

The deployment of COSTAR produced a narrower PSF, which led to considerably higher aperture throughputs. For the large apertures (`1.0` and larger) post-COSTAR there is no measurable difference in aperture throughput between FOS/RD and FOS/BL. Therefore, we list both detectors separately only for the `0.3` aperture and the slit in Table 32.7. Throughputs do change as a function of wavelength (or grating). Therefore, we list ratios for the different dispersers separately. The numbers are from *FOS ISR* 136.

Bar aperture throughputs are assumed to equal unity for all cases.

6. See *FOS ISRs* 106 and 107.

Table 32.6: Recommended Pre-COSTAR Aperture Corrections and Uncertainties at Nominal OTA Focus (4.3 aperture = 1.0)

Grating	BLUE	RED	UNC[a]	BLUE	RED	UNC	BLUE	RED	UNC	BLUE	RED	UNC
Mode	B-3 (1")			B-1 (0.5")			B-2 (0.3")			C2-SLIT		
HIGH	0.58	0.60	.02	0.41	0.44	.02	0.27	0.31	.03	0.39	0.41	.02
LOW	0.65	0.67	.06	0.46	0.50	.04	0.31	0.35	.03	0.43	0.45	.03
PRISM	0.53	0.54	.06	0.37	0.39	.04	0.26	0.30	.03	0.37	0.39	.03

a. The uncertainties (UNC) do not include the possible contributions of pointing errors, OTA breathing, jitter, or Y-base errors in an arbitrary science observation.

Table 32.7: Post-COSTAR Average Aperture Throughput Ratios Relative to 4.3

Grating	BLUE and RED		BLUE	RED	BLUE	RED
	B3 (1")	B1 (0.5")	B2 (0.3")		C2-SLIT	
G130H	0.875	0.730	0.640	---	0.615	---
G190H	0.900	0.810	0.720	0.720	0.715	0.715
G270H	0.920	0.870	0.780	0.790	0.745	0.770
G400H	0.950	0.890	0.800	0.830	0.780	0.800
G570H	0.960	0.890	---	0.840	---	0.810
G780H	0.960	0.895	---	0.780	---	0.820
G160L	0.895	0.790	0.700	0.720	0.675	0.720
G650L	0.955	0.900	---	0.840	---	0.795
PRISM	0.910	0.835	0.730	0.770	0.720	0.760

32.6.7 Absolute Photometric Calibration System Offsets

Many FOS observations in the HST Archive and in the literature have been flux-calibrated on the now obsolete absolute photometric system of Bohlin et al. (1990). All re-calibrated FOS observations have been calibrated with the AIS_CORR system which produces fluxes on the white dwarf flux scale, based upon eight standard stars[7]. The older system differs from the AIS_CORR scale by <15% for wavelengths < 2000 Å, ~5% for the wavelength range 2000–3500 Å and <3% for wavelengths > 3500 Å (see Table 32.8). An illustrative comparison of the previous flux scale and the white dwarf flux system is shown in Figure 32.18.

7. *FOS ISR* 144.

Table 32.8: FLX_CORR and AIS_CORR Calibration System Differences

Wavelength	% Uncertainty
Far UV	~10%
Near UV	~5%
Visible	~3%

Figure 32.18: FLX_CORR to AIS White Dwarf Flux System Ratio

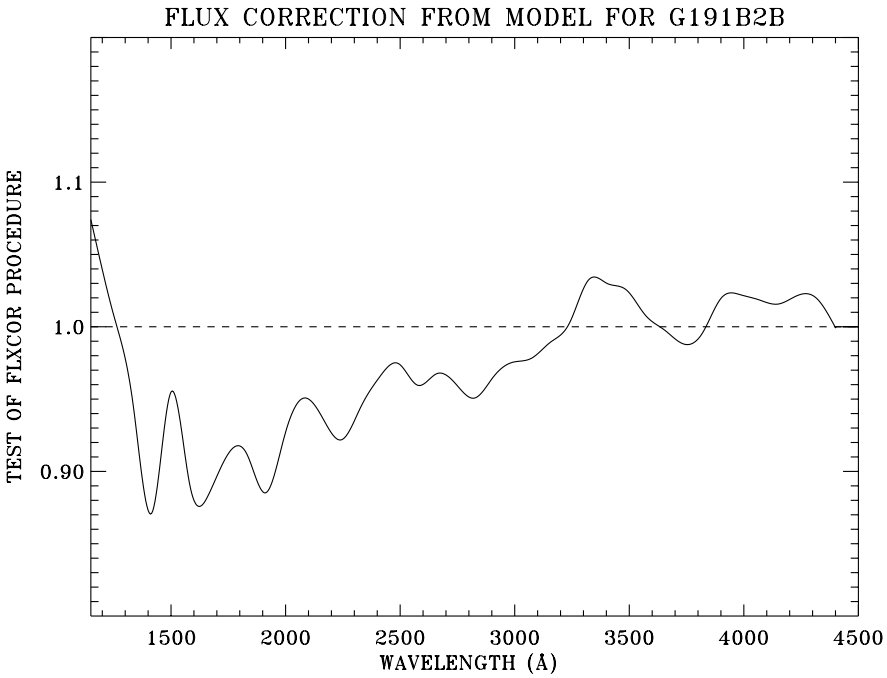

32.6.8 Overlap Region of Adjoining Gratings

Often fluxes do not agree well in the wavelength overlap regions of two FOS dispersers. Koratkar and Evans (1998, Ap.J. submitted) surveyed a total of 151 FOS pre-COSTAR observations of AGN, which are typically much fainter objects acquired with substantially less accuracy than FOS calibration sources. They found 5% agreement as typical in the overlaps between G130H, G190H, and G270H. FOS spectrophotometric standard stars typically show much better agreement in these regions, but inspection of Figures 32.14 and 32.15 shows that 2-5% variations were occasionally seen for these objects, as well. The effect of the spectrum s-curvature in the overlap regions combined with the influences of relatively poor centering (common for the AGN) and/or Y-base and FGW uncertainties to reduce the amount of light recorded by the diode array at the edges of these regions. Note that a 5% error in the 100 or so pixels at the edges of the spectrum does not imply a similar level of error at the center of the observed spectral region.

There can be some wavelength calibration uncertainty in certain overlap regions, but this does not exceed more than 0.5 diodes. This uncertainty is due to the lack of arc comparison lines in the overlap region of the gratings, so the wavelength solution must be an extrapolation. For the affected FOS overlap regions, this error in the wavelength calibration introduces a negligible (<<1%) error in the flux calibrations.

32.7 Flatfield Calibration

The structure in the FOS flatfields is dominanted by photocathode granularity. Target location on the photocathode and time changes in the photocathode itself are the dominant source of uncertainty in the FOS flatfields. The flatfields limit the signal-to-noise achievable (in the limit of infinite counting statistics) and the reliability with which line features can be identified. The major factors affecting the accuracy with which the FOS flat field reference files will correct the flatfield granularity in your observations are:

- Target acquisition accuracy.
- Filter-grating wheel non-repeatability.
- Temporal changes in the FOS photocathode granularity.

Y-base uncertainties are generally not a major contributor to FOS Flat Field uncertainty.

In the subsections below we provide a complete overview and discussion of the FOS flat fields, how they were produced, which observations they are applicable to, and how improvements can be made. Concerned readers will want to read these sections in detail.

32.7.1 Flatfield Summary

Since photocathode granularity is the dominant component of FOS flatfield structure, factors which affect the illumination of the photocathode dominate the degree to which a calibration flatfield is appropriate for your data. Given the small spatial scale of photocathode variation, the best flatfield correction is obtained only for those targets that were acquired with accuracies comparable to those used in STScI calibration programs. Secondly, given the temporal variation present in some spectral regions, the accuracy of flatfield correction is also affected by the ability of flatfield calibration observations to track the variation.

The overall flatfield correction generally has an accuracy of better than 3%. Features in certain specific dispersers, apertures, spectral regions, and times of observation can be somewhat poorer as changes may not have been adequately tracked by calibration observations. Limiting accuracy of order 1% is possible for observations taken close to flatfield calibration observations and for which nearly exact alignment of photocathode granularity is accomplished (see Figure 32.23 as an example of some of the best flatfield correction possible with the FOS).

High-precision (S/N > 30) spectroscopic measurements with the FOS required that the observations sample the same portion of the photocathode as did the flatfield calibration observations. This sampling repeatability was limited by the target acquisition accuracy (for calibration and high S/N observations, typically 0.04" which corresponds to 0.025" in each coordinate) and filter-grating wheel positional repeatability (approximate 1σ deviation of 0.04"). The photocathode granularity could vary by 5 to 10% over distances as small as 0.2". Small *x*-offsets, typically 1 pixel or less, could occur in the granularity pattern from one observing epoch to another. Paired aperture granularity was substantially different from that for the single apertures.

Post-COSTAR extended source flatfielding can be improved by using the last epoch of *pre-COSTAR* flatfields for the detector-disperser combination, due to the more extended nature of the pre-COSTAR PSF.

For a limited subset of gratings, mapping of the post-COSTAR granularity in the direction perpendicular to dispersion is available at one epoch which you can examine by reference to the special set of drift-scan FOS calibration observations made in calibration program 6916 (December 1996 and January 1997).

Working with Flatfields

You should be particularly wary of unusual features in your data. In order to assess the impact of the flatfield used in the data reduction process for any particular FOS observation, and as a careful check:

- Compare the flatfield reference file data with your raw science data.
- Compare the flatfield reference file data with any raw count rate data for any standard stars taken as nearly contemporaneously as possible with your science data in order to assess suspicious features in your science data. Inspection of similar science observations can be helpful, as well.
- Compare the flatfield reference file data with the raw count rate data used to produce the flat.
- Compare the flatfield used in the calibration of the target spectrum with other available flats for the instrumental configuration.[8]
- Remember the presence of variations in several gratings, notably FOS/RD G190H throughout the FOS lifetime, FOS/RD G400H from early 1995 through February 1997, and the FOS/BL G160L bad blemish that compromised all SINGLE and LOWER aperture data ever taken with this grating.
- Try shifting your spectrum by +/- 2 pixels to account for x-pixel shifts and hence better align your spectrum with the granularity.
- If your object is extended, try using a pre-COSTAR flatfield from the last epoch of *pre-COSTAR* flatfields for the detector-disperser combination or examining the drift-scan observations of calibration program 6916.

---

8. Detailed information about flatfields is provided in *FOS ISRs* 075, 078, 088, 134, 143, and 157.

32.7.2 Flatfield Details

FOS flatfields are prepared from precisely pointed (≤0.025" pointing accuracy in each coordinate), high S/N observations (S/N ≥ 200 per pixel, typically) of two relatively featureless spectrophotometric standard stars, BD+28D4211 and G191B2B (also known as WD0501+527). All FOS flatfield reference files are actually unity-normalized inverse flatfields, that are applied as multiplicative operators in **calfos** data reduction to correct for small-scale (less than 10 diode width) differences in the sensitivity. These pixel-to-pixel sensitivity variations resulted mainly from small-scale inhomogeneities in the photocathode (the so-called *granularity*). A much less important contributing factor was diode-to-diode variation in sensitivity, as this effect was greatly diminished by the OVERSCAN data-taking process which caused each output pixel to contain contributions from five different diodes.

If the appropriate observational strategies were employed, the overall flatfield correction generally has an accuracy of better than 2-3%. However, flatfielding for certain specific dispersers, apertures, spectral regions, and epochs of observation can be somewhat poorer. For example, substantial (5 to 10%) flatfield variation did occur on spatial size-scales as small as 0.2" for several detector and disperser combinations, so that precise flatfield correction is only possible for science targets acquired with the same high pointing accuracy used for calibration observations. The standard recommendation of the FOS team was that any program requiring S/N >30 should use the same target acquisition accuracy used in the STScI calibration observations.

So-called *superflats* and *superflat-derived flats* produced by comparison of raw data with *superspectra* (highly accurate countrate distributions from the FOS gratings obtained via a cross-correlation technique)[9] provide the best quality flatfields. Some SV epoch flats and all polarimetry flats were produced with a more subjective, much less accurate technique that involved normalizing a standard star spectrum with a continuum spline fit (see *FOS ISR* 075). These *subjective flats* often did not completely remove larger features and features with high local rates-of-change due to the uncertainty in the continuum normalization process required for their preparation.

Time Dependence

The FOS/RD G190H, G160L, and, to a lesser extent, G270H flatfields displayed marked time dependence throughout both the pre- and post-COSTAR periods. Several other gratings (e.g., FOS/RD G400H, G570H, and FOS/BL G130H, G160L displayed varying degrees of generally more modest temporal change. Figure 32.19 illustrates the striking changes in the FOS/RD G190H flatfield that took place within the first two years of operation. The strong feature at approximately 1950 Å. continued until mid-1995 when it began to disappear. By the end of the FOS lifetime, the granularity at that wavelength had returned to near launch levels.

---

9. The superflat observational and analysis procedures are explained in detail in *FOS ISRs* 088, 134, and 157.

Figure 32.19: FOS/RD G190H Flatfield Changes

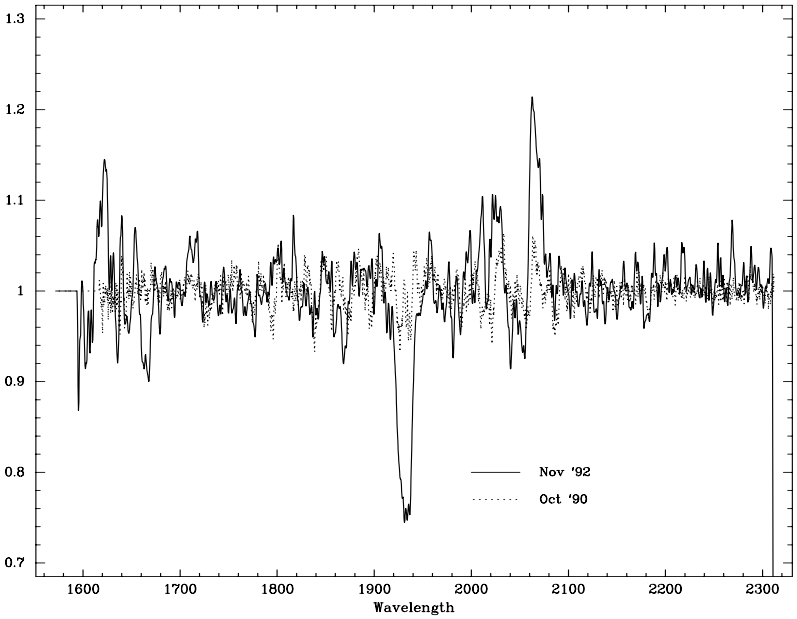

Aperture Dependence

All pre-COSTAR flatfields are somewhat aperture dependent as the PSF filled many of the apertures. However, individual aperture-specific flatfield observations were not made for many apertures in the pre-COSTAR period. Little post-COSTAR aperture dependence existed between the single apertures or between the paired apertures for a particular disperser, but substantial differences did exist between single and paired apertures for any disperser because substantially different portions of the photocathode were sampled by the centers of the different aperture sets. Due to these substantial photocathode granularity spatial variations, flatfield reference files derived from single aperture observations should never be used to correct paired aperture observations and vice versa.

Figures 32.20 and 32.21 provide a characterization of the overall photocathode granularity corrections by showing, at low-scale, representative SINGLE aperture flatfields for high dispersion gratings for both FOS detectors.

Figure 32.20: Typical SINGLE Aperture Flatfield Granularity: FOS/BL

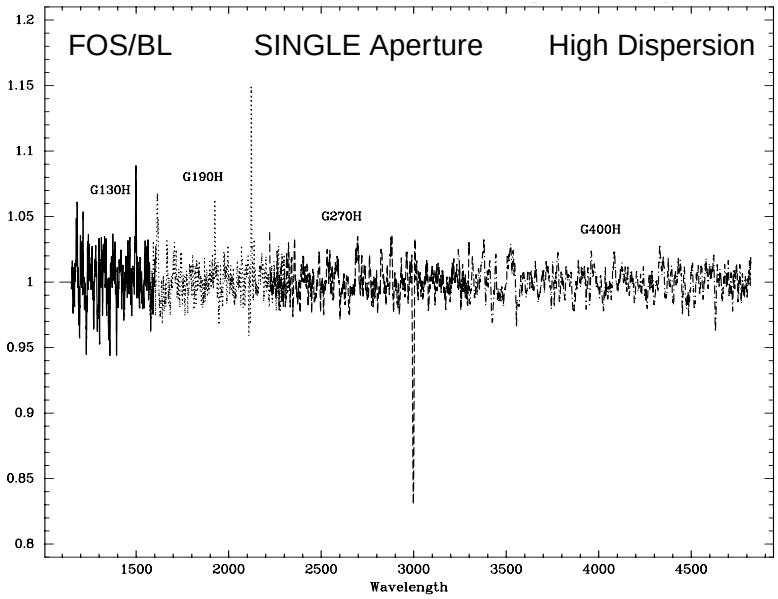

Figure 32.21: Typical SINGLE Aperture Flatfield Granularity: FOS/RD

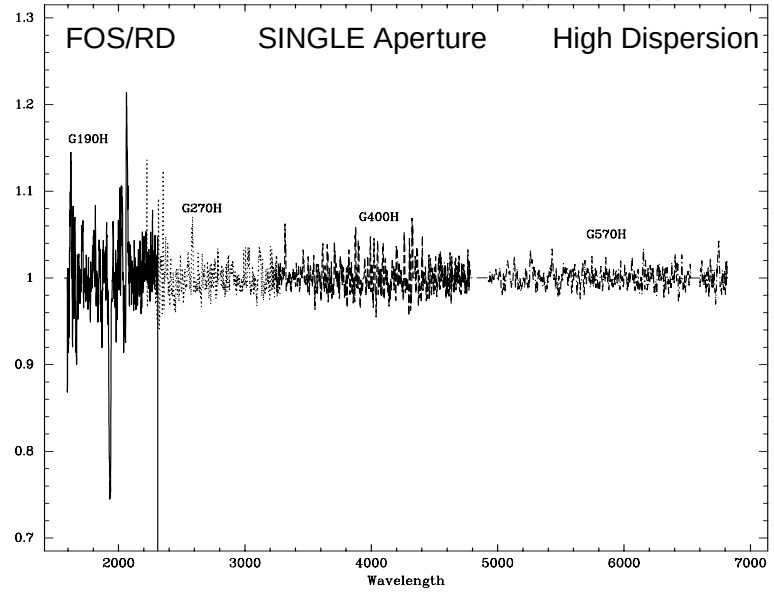

Granularity Shifts Along Dispersion

Small x-shifts of the observed granularity did occur relative to the positions at the standard star epochs due to slight changes from time-to-time in the internal magnetic environment of the detectors. This observed effect was typically +/– 1 pixel or less, with one documented 2 pixel shift. As a result, shifting your observed spectrum relative to the flatfield prior to re-calibration can occasionally

improve the granularity correction. Tests performed with standard star data have indicated, however, that small-scale, even sub-pixel, offsets between identical observations can introduce pattern noise at the 1% level. As a result, 1% rms is deemed the practical limit with post-COSTAR superflat-based flatfields, good aperture centering, and precise x-coordinate alignment.

FOS flats are not interpolated between standard star observation epochs. They are each prepared from an individual high S/N observation of a standard star and typically applied over a time-range that is inclusive of the date of standard star observation. As a result, you might be able to improve the flatfielding at a particular epoch by interpolating between two flatfield reference files, but the x-shift pattern noise considerations mentioned above may limit the benefit of this procedure.

Granularity Perpendicular to Dispersion

For a limited subset of gratings, mapping of the post-COSTAR granularity in the direction perpendicular to dispersion is available at one epoch which you can examine by reference to the special set of drift-scan FOS calibration observations made in calibration program 6916 (December 1996 and January 1997). These observations, taken in RAPID mode, sampled the entire height of either the 4.3 or `1.0` aperture at approximate 0.1” intervals (see proposal for details) for several commonly-used gratings. Comparison of the individual readouts allows characterization of the flatfield rate-of-change perpendicular to dispersion. Additionally, the influence of target miscentering (and Y-base misalignment) on wavelength-dependent aperture throughput can be evaluated from these data.

Application of Inappropriate Flatfield

If an incorrect, or inappropriate, flatfield reference file is used to flatfield the data, small *emission-like* or *absorption-like* features will appear in the spectrum corresponding to sensitivity variations that were introduced or left uncorrected by the flatfielding. Depending upon the scale of the shift or mismatch, these artifacts can be range from as little as 1–2% up to >20% in size.

Figure 32.22 shows an example of a spectrum that was flatfielded incorrectly. Panel (a) shows the count rate data in the `.c5h` file that results from using both correct (solid line) and incorrect (dotted line) flatfield files. Panel (b) shows a blowup of the region from pixels 300 to 1300 of the same data.

Figure 32.22: Incorrectly Flat-Fielded Spectrum of the Red G190H Grating

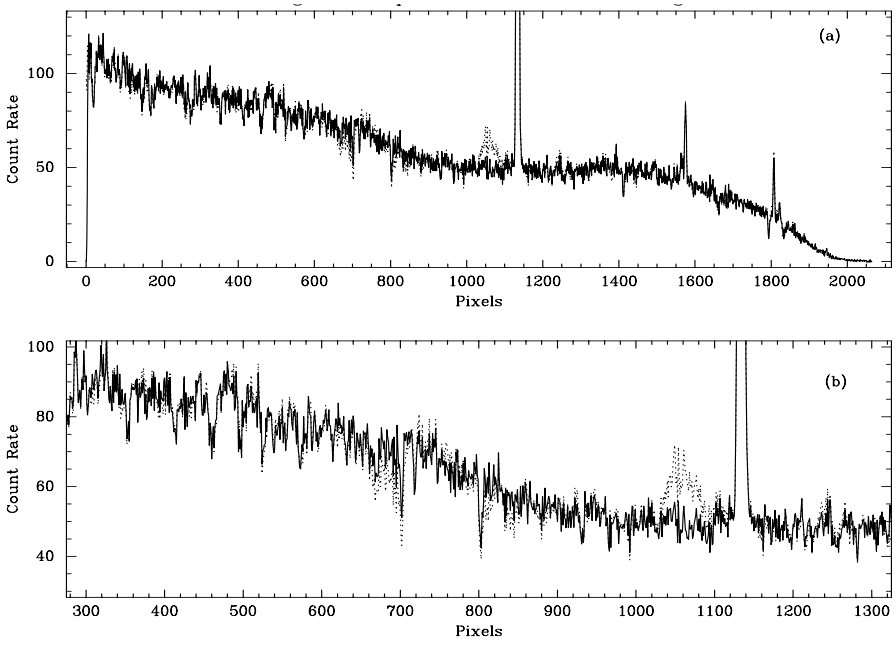

Flatfield Generation Rules

The following general recommendations summarize the guidelines that have been used for the applicability of FOS flatfield reference files and in generating the FOS flatfield reference file set from the various calibration observation datasets. They are provided as a guide for those interested in comparing their observations with other flats and with standard star observations other than those used for the generation of the flats.

Pre-COSTAR

FOS/BL:

- For all FOS observations *before* January 1, 1992 made with SINGLE apertures use the science verification (SV) `1.0` aperture flats.
- For observations *after* January 1 1992 use `4.3` aperture superflats.
- FOS/BL data taken in a paired aperture during 1991 should be corrected with `4.3` aperture flats computed for the UPPER and LOWER aperture positions of the superflat measures in program 2821 or should be left uncorrected. The pipeline leaves them uncorrected.
- In no circumstances should the SV `1.0` SINGLE aperture flats be used to correct data taken in a paired aperture.

FOS/RD:

- For the G190H, G270H, and G160L dispersers, the Cycle 3 superflats of Lindler et al.[10] should be used for all observations obtained after August 7, 1993.
- For G400H, G570H, G650L, and the PRISM, the Cycle 3 superflats of Lindler et al. should be used for all observations obtained after June 18, 1992.
- For all other FOS/RD observations with the above dispersers, the FOS/RD flatfield obtained closest to the observation date should be used.
- No SINGLE aperture flats should be used to correct data obtained with a paired aperture.
- For G780H, no pre-COSTAR flatfields exist—unity correction is applied in the pipeline. Alternative is to smooth post-COSTAR flats.
- For all barred apertures, no pre-COSTAR flatfields exist —unity correction is applied in the pipeline.

Post-COSTAR:

- Due to the offset in aperture location between `4.3` and other SINGLE apertures and `1.0-PAIR` and other paired apertures, `4.3` aperture flats are always used only for `4.3` aperture observations and `1.0-PAIR` aperture flats are always used only for `1.0-PAIR` aperture observations.
- UPPER paired aperture flats are always used for UPPER paired aperture observations and LOWER paired aperture flats are always used for LOWER paired aperture observations. Only one speoch of LOWER aperture flats exists in most cases.
- `0.3` aperture flats are used for `0.5`, `0.3`, and SLIT aperture observations.
- `0.25-PAIR` aperture flats are used for `0.5-PAIR`, `0.25-PAIR`, and `0.1-PAIR`, aperture observations, except for FOS/RD G570H `0.1-PAIR` for which `0.1-PAIR`-derived flats are used.
- Following the above rules, Each observation of BD+28D4211 or G191B2B with a particular aperture defined a new flatfield reference file to be used until the next observation epoch of one of those targets.
- For all barred apertures, no post-COSTAR flatfields exist — unity correction is applied in the pipeline. Drift-scan observations could be used as a guide.
- As for pre-COSTAR data, no SINGLE aperture flats should ever be used to correct data obtained with a paired aperture.

10. *FOS ISR* 134.

Characterization of Flatfields for Individual Gratings

Pre-COSTAR flatfields were generally smoothed with a 3-point boxcar smoothing function. Post-COSTAR flats were not smoothed. As a general rule, features in post-COSTAR flatfields were narrower than their pre-COSTAR counterparts by an amount greater than the influence of the smoothing function.

The descriptions of various flatfields that follow are generally restricted to the SINGLE apertures unless otherwise indicated:

FOS/BL:

- **G130H:** Generally 5% features were seen throughout this region. No large-scale temporal variations were noted. The vicinity of Lyman α is always slightly suspect due to poor specification of the continuum level in this vicinity in the standard star spectra and difficulty in matching the standard star feature to the template superspectrum. As a result, correction at the wavelength of Lyman α is often masked to unity in the reference files. A very strong (> 20%) feature is present at 1400 Å in LOWER paired aperture flats.
- **G190H:** A strong (~20% correction) feature was present at approximately 2100 Å. Nearly all other features in this region were at the 5% level. Little time-variation was seen.
- **G270H:** A strong (~20% correction) feature is also seen in this region at approximately 3000 Å. Nearly all other corrections in the region are at the 3–4% level. No significant temporal changes were recorded.
- **G400H:** A slightly broad feature was present at 3550 Å. Temporal variations at the 10% level were seen at 4650 Å. Most other corrections in this region were at the 3% level.
- **G160L:** One particularly illustrative feature is the strong photocathode blemish that showed up in FOS/BL G160L spectra in the 1500–1560 Å region for all SINGLE apertures. This feature displayed a strong spatial dependence such that errors of greater than 20% or more were common, even after flatfielding. As Figure 32.23 illustrates clearly, this strong blemish is seen in the `4.3` and `1.0` SINGLE aperture spectra and, though slightly weaker, with the `0.3` aperture (which always sampled a photocathode location concentric with the `1.0` SINGLE), and is very prominent in the `1.0-PAIR-LOWER` location (approximately 1.3" below the SINGLE aperture location). However, the feature is nearly absent in the `1.0-PAIR-UPPER` spectrum! Due to this striking behavior, the FOS group recommended in May 1995 that any subsequent science observations requiring quantitative analysis of features in the 1500–1560 Å region (notably C IV) be performed only with the UPPER paired apertures. Please check your data for this problem.
- **PRISM:** Due to the rapidly changing wavelength scale and the difficulty of aligning standard star spectra with template superspectra, the quality of PRISM flatfields is limited. Careful alignment of the flatfield with target spectrum is required.

FOS/RD:

- **G190H:** These flats showed significant wavelength structure (Figure 32.19) and they displayed strong (>10%) wavelength-dependent temporal variations during the first year of HST operation when flatfields were not routinely monitored. The most obvious features were at approximately 1950 and 2050 Å. Between January 1992 and June 1992, the G190H, G160L, and G270H FOS/RD flatfields were monitored monthly. During this intensive monitoring period none of these flats varied by more than 2%. For the duration of the pre-COSTAR period, and indeed post-servicing, these flats were monitored regularly though less frequently. Several substantial (≥5%) new features appeared in the G190H region between June and November 1992. For the remainder of the pre-COSTAR era (ending December 1993) changes were less than 2%. Post-COSTAR time-variation of FOS/RD G190H flatfields was also observed. Between November 1994 and February 1995, 2 to 4% changes occurred in the same spectral regions that were active in the pre-COSTAR era. By June 1995 the strong feature at 1950 Å. diminished by a factor of two, although it was still present at the 10% level. By September 1996 this feature had essentially vanished.
- **G270H:** This region showed flatfield changes in the pre-COSTAR period as did FOS/RD G190H, but the variations and sizes of the features were much smaller. This region was monitored at the same rate as G190H and displayed little additional variation in the pre-COSTAR period. A variety of features continued to exist at the 5–15% level in the post-COSTAR period and only a few 2–3% variations occurred.
- **G400H:** Generally well-behaved in the pre-COSTAR era, this spectral region began to display substantial changes between standard star observations made in July 1994 and June 1995. Of particular note is a variable SINGLE aperture feature in the vicinity of 4475 Å that affects the He I λ4471 line seen in many hot objects. Throughout this region there are a number of 10% features, several of which fall in the vicinity of the hydrogen lines.
- **G570:** Several strong and, in the post-COSTAR case, sharp features were present in this region. No strong variability has been noted for the granularity in this region.
- **G780:** Only post-COSTAR flats exist. The S/N of the standard stars was somewhat poorer in this spectral region, so the quality of these flats longward of 7500 Å. is quite poor.
- **G160L:** This region showed flatfield changes in the pre-COSTAR period as did FOS/RD G190H, though the variations and sizes of the features were not as large. This region was monitored at the same rate as G190H and displayed little additional variation in the pre-COSTAR period. A variety of features continued to exist at the 5–15% level in the post-COSTAR period and only a few 2–3% variations occurred.
- **G650L:** Typically 5–10% features are seen. Little variation was detected.

- **PRISM:** Due to the rapidly changing wavelength scale and the difficulty of aligning standard star spectra with template superspectra, the quality of PRISM flatfields is limited. Careful alignment of the flatfield with target spectrum is required.

Figure 32.23: Raw and Flatfield-Corrected FOS/RD G270H

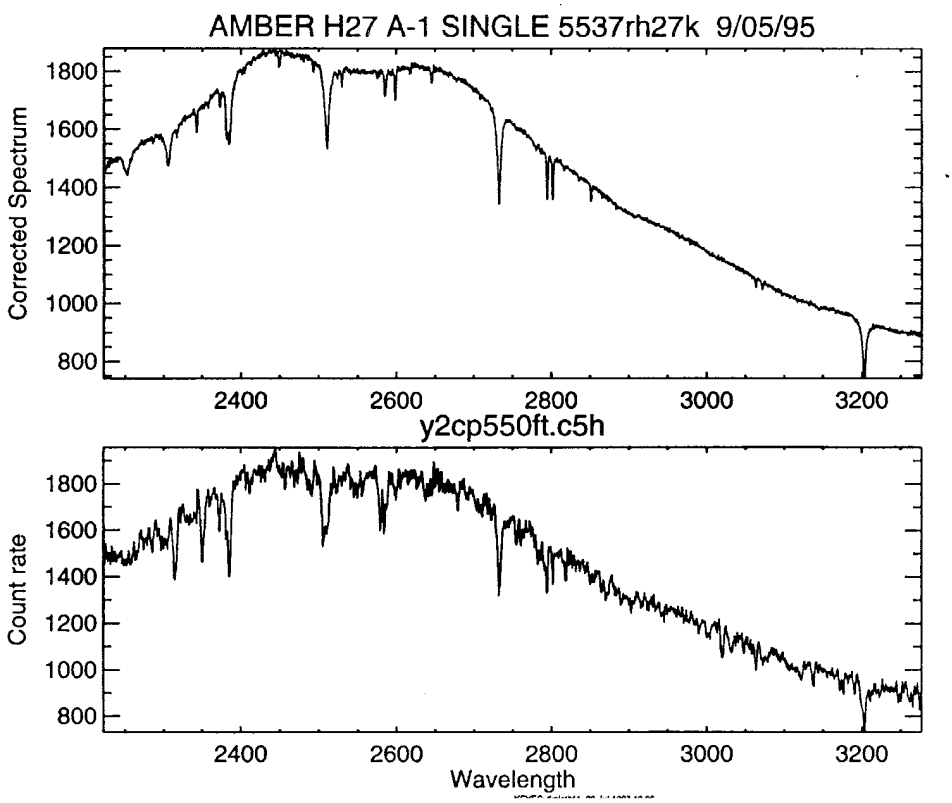

Figure 32.24: Photocathode Blemish at 1500–1560 Å

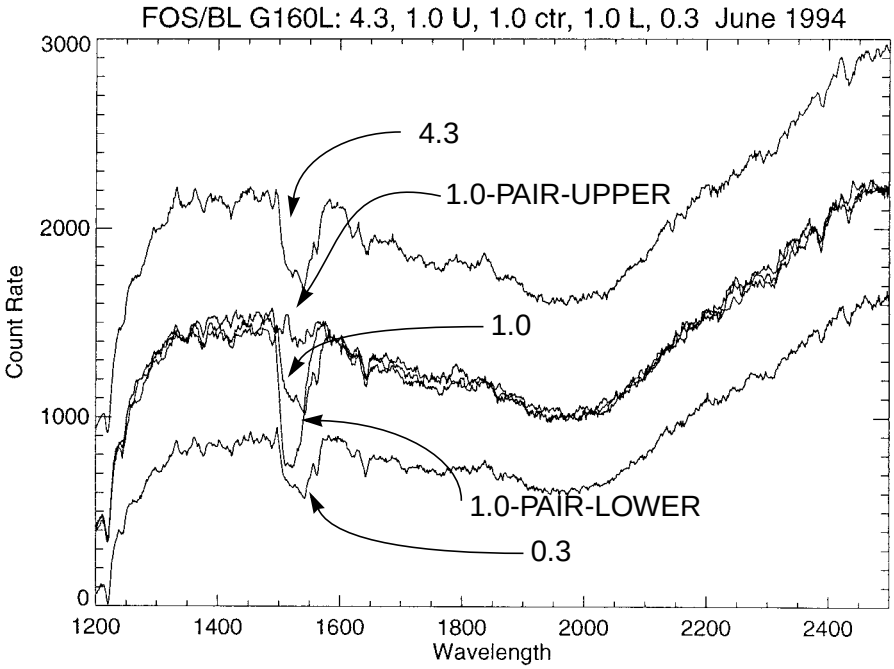

32.8 Wavelength Calibration

The principal sources of uncertainty in FOS wavelength calibration are:

- Filter-grating wheel (FGW) non-repeatability (includes systematics).
- Residual image displacement after GIM correction.
- Target miscentering (target acquisition).
- Accuracy and applicability of the dispersion solutions.
- Internal and external wavelength system offsets.
- Spacecraft motions.

All FOS wavelengths are *vacuum wavelengths!* This is different from IUE and, of course, ground-based observations.

The FOS dispersion relations are polynomial fits, typically cubics, that relate the measured x-position, in diodes, of the centroids of well-known internal Pt-Ne lamp emission lines, the *template spectra*, to their vacuum wavelengths. The arc spectra were secured by observations entirely internal to the FOS, called WAVECALS, which were not impacted by the spherical aberration of the primary mirror or the introduction of COSTAR. Although dozens of epochs of internal

WAVECAL exposures were obtained over the lifetime of the instrument, the FOS default (pipeline) wavelength calibration is a set of dispersion relations based upon a single epoch of observation made in June, 1991.

Systematic differences of up to 1 diode (~250 km/sec at high dispersion; ~1250 km/sec at low dispersion) between the default wavelength calibration and the wavelength scale appropriate to a random observation were possible. The bulk of these differences were attributable to FGW non-repeatability. In order to remove the influence of FGW position differences and achieve the full capability of FOS wavelength accuracy, a WAVECAL exposure had to be taken consecutively with the science exposure without any motion of the FGW in between.

For any individual disperser, the applicability of the default dispersion relation to your observation, that is the uncertainty in the routine standard FOS wavelength calibration, depended on the factors discussed below:

Filter-grating wheel (FGW) non-repeatability: The FGW non-repeatability introduces a 1σ uncertainty of ~0.12 diodes. This corresponds to ~30 km s^{-1} for the high dispersion gratings. The largest (peak-to-peak) variations observed were of the order of 1 diode. The full range of variation was as likely to occur over a few days as over a few years. On average no large time-related changes have been observed for the wavelength calibration for any disperser and detector combination.

Recall that the standard wavelength solution is not a mean of many dispersion curves, rather it is based on a single epoch. As a result, we must consider the possibility that the reference epoch could have been obtained near an extremum of the FGW positional distribution. There is evidence to suggest this may be the case for several gratings. Therefore, a possible systematic shift of up to one full diode (250 km/sec at high dispersion) may exist between the standard wavelength calibration and the calibration appropriate to your data.

The only way to avoid the large uncertainties introduced by FGW non-repeatability was to have included a WAVECAL exposure before or after the science exposure without any intervening motion of the FGW. If you have an FOS/BL G130H or G160L observation, you can estimate the FGW offset by determining the observed wavelength of Lyman alpha.

Target mis-centering (target acquisition accuracy): The second largest (and most common) component of FOS wavelength uncertainty is that produced by the target not being at the center of the science aperture. For the most precise FOS acquisitions, the worst-case centering accuracy was 0.025" or 0.08 diodes (20 km/sec at high dispersion).

Even if the target was well centered in the aperture, the highest possible accuracy could be achieved only if wavelength calibration spectra were taken together with the science data *without moving the FGW in between*.

Target centering accuracy can be assessed with the FOS paper products.

GIM effects: Residual inaccuracies in the magnetic deflection after GIM correction can result in peak-to-peak spectral displacements of 0.06 diodes (~15 km/sec at high dispersion).

You can examine the individual readouts of a RAPID sequence or use task **deaccum** (see Chapter 33) for an ACCUM spectrum to see if the centroids of your features are displaced from one group to another.

Accuracy and applicability of the dispersion solution: The rms errors in the various pipeline dispersion relations range between 0.01 and 0.08 diodes[11] with 0.035 diodes being a typical value for FOS dispersion fits in general. However, some spectral regions in the arc spectra have fewer lines than do others (see *FOS ISR* 067).

Line measurement: The typical 1σ centroiding accuracy for FOS arc lines at high dispersion is 0.02 diodes. You should also consider the measurement uncertainty for lines in your spectrum and may have poorer accuracies.

Spacecraft motion: No correction is made for spacecraft orbital motion around the Earth or for Earth orbital motion around the Sun (see section 33.3 for determining heliocentric corrections for Earth orbital motion only). HST orbital motion can produce an uncertainty of up to 0.034 diodes. Uncorrected Earth orbital motion can produce an uncertainty of up to 0.12 diodes.

Internal-to-external wavelength system offsets: Since the beam from the internal lamps, unlike that for an external source, does not completely fill the collimator, there can be a slight difference in illumination of the dispersers by the two types of sources that leads to a small shift between the measured positions of the same wavelength in internal and external source spectra. A correction for this offset has to be taken into account in the absolute wavelength calibration. Consecutive observations of a radial velocity standard source and an internal WAVECAL were used to determine this internal-to-external offset of the wavelength scale. Internal-to-external offsets appear to be grating dependent and there is weak evidence of some wavelength dependence for at least one grating.

For example, the FOS/RD G570H appears to record velocities in the 4800-5000 Å region that are approximately 50 km/sec more positive than those in the 5800-6500 Å region. Whether this effect is due to a paucity of lines for an adequate definition of the dispersion relation shortward of 5000 Å. or is a wavelength-dependent internal-to-external offset inherent to the grating is currently under investigation. Regardless of the resolution of this matter, the effect

11. *FOS ISRs* 067, 149, and 156.

is real and should be included in any comparison of velocities measured in these two wavelength regions.

The mean internal-to-external offsets of the FOS wavelength calibration are 0.102 +/– 0.1 diodes for FOS/BL and 0.176 +/– 0.105 diodes for FOS/RD.

Summary: Addition of all the random uncertainties listed above in quadrature allows us to characterize the wavelength uncertainty in the measurement of a well-defined line in the spectrum of an object that has been precisely centered in the science aperture with the most accurate FOS target acquisition strategy.

- If, as was usually the case, no contemporaneous WAVECAL was taken, the overall 1σ random uncertainty is 0.16 diodes for the accuracy with which the wavelength scale is known in an individual FOS spectrum. The absolute wavelength accuracy is compromised by the single epoch nature of the default dispersion fits, and the possibility of a residual FGW displacement between your observation and that of the observations that defined the dispersion relation. At this time, therefore, the worst-case disagreement between your observations and the standard wavelength scale must be assumed for any given grating setting unless you have independent confirmation of the wavelength scale. This is 1 diode.
- If a contemporaneous WAVECAL allows the removal of FGW uncertainty, the overall 1σ uncertainty is 0.11 diodes.

If the full measure of wavelength accuracy is important for your purposes, you should check the exposure logsheet or Phase II RPS2 (pre-COSTAR RPSS) specification file as described in section 30.4 in order to determine whether a WAVECAL exposure was made consecutively with the science exposures without motion of the FGW.

32.9 Other Data Problems

In this section we describe how to recognize and correct other problems that might affect re-calibrated FOS data. The problems addressed here are:

- Effect of a dead diode.
- Effect of a noisy diode.
- Background light.
- Influence of grating-scattered light.

32.9.1 Dead Diodes

During calibration processing, **calfos** uses the dead diode reference file (the list of all disabled diodes) to determine how many diodes contributed towards the counts for each pixel. This information is needed to calculate the exposure time per pixel and convert counts to count rates. If an incorrect or incomplete dead diode reference file is used, **calfos** does not have an accurate reporting of the diodes that were used for the onboard integration. This can lead to serious errors in the count rates and fluxes for affected pixels. The effect of an incomplete dead diode correction (see Figure 32.5) has a very distinct signature, which looks like an *absorption or emission feature* with sharp edges, extending over a fixed number (NXSTEPS x OVERSCAN) of pixels (usually 20). Further, the dead diode absorption feature typically does not extend to zero counts because more than one diode contributed to the counts in any given pixel. The depth of the absorption feature for a pixel affected by a single missed disabled diode is 1 – [(OVERSCAN – 1) / (OVERSCAN)], or usually 20%. In Figure 32.5, panel (a) shows the raw counts and the dead diodes labeled 1-20. Panel (b) shows the count rate data from the pipeline processing from the .c4h file. Some of the dead diodes were correctly removed in this pipeline calibration while others were not. If there is a dead diode in your data that is not included in your dead diode reference file, you will see absorption features similar to those in this panel. In this particular case, a dead diode reference file for the wrong epoch was used in the processing of the data. Note also the 20% "emission" feature where a correction was applied to a region in which no dead diode existed. Panel (c) shows the .c4h file *after* the correct dead diode reference file was used in the calibration.

If you notice a feature in your data similar to the absorption feature described above, you should suspect a spurious dead diode in your observations. Tables 31.4 and 31.5 list all diodes that were disabled during the FOS lifetime. Normally, a diode was disabled and a new dead diode reference file created after the third report of anomalous behavior by that diode. Although the USEAFTER of the new reference file was set to the date of the first reported anomaly, your data may contain an earlier, unreported occurrence. If your suspected diode has been subsequently disabled (see Tables 31.4 and 31.5) you may use a later dead diode reference file to correct your data as long as the alternate reference file does not also correct diodes that are fully functional in your data. You may also contact the STScI Help Desk (help@stsci.edu) for further assistance in producing a special dead diode correction table for re-calibrating your observation.

32.9.2 Noisy Diodes

The effect of a noisy (or *hot*) diode was typically to produce an *emission feature* extending over a fixed number (NXSTEPS x OVERSCAN) of pixels (typically 20). Figure 32.25 shows an observation where pixels 400 to 420 are affected by a noisy diode. Unlike a dead diode, the profile of the feature need not be particularly flat since the degree of spurious signal generation by the diode may

Figure 32.25: Effect of Incorrect Dead Diode Correction

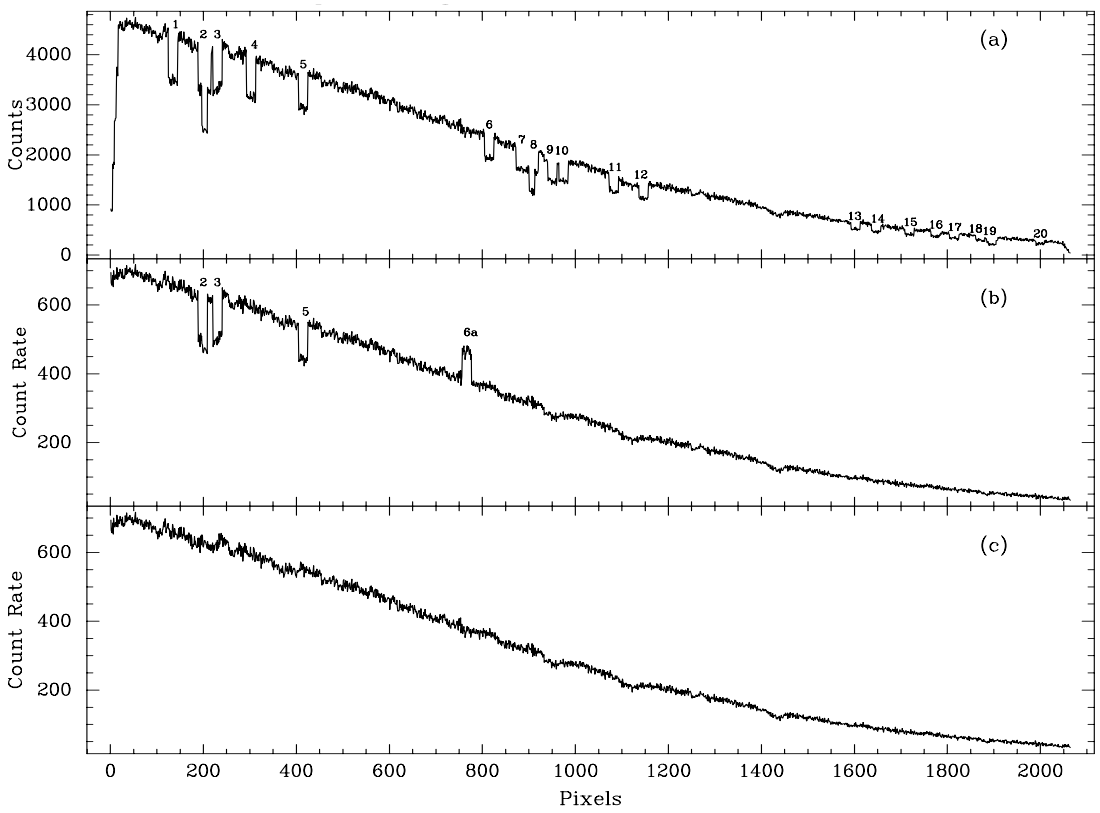

have varied from one 300 millisecond internal readout cycle to another. *The effect of a noisy diode cannot be removed by recalibrating the data*.

Noisy diodes sometimes appear for only very short intervals within an exposure. Look at individual groups of your data in the group counts paper products plot as an initial diagnostic of the possible presence of a noisy diode in your data. You might see that one or a few groups have substantially greater signal than the rest. Similarly, for ACCUM mode you can use task **deaccum** (see section 33.4) to plot the whole spectrum accumulated in each individual readout interval to isolate a noisy event to only a few groups.

Cycle 6 Observations: A particularly strong noisy diode appeared around diode 250 (pixel 1000 for quarter-stepped data) in FOS/RD spectra on several occasions after July 1, 1996.

If you notice a feature in your data similar to the emission features described above, you can manually edit the data to cosmetically smooth over or blank out the affected pixels. IRAF or STSDAS tasks to do this include **fixpix** or **splot** in its *etch-a-sketch* mode.

Figure 32.26: Effect of Noisy Diodes

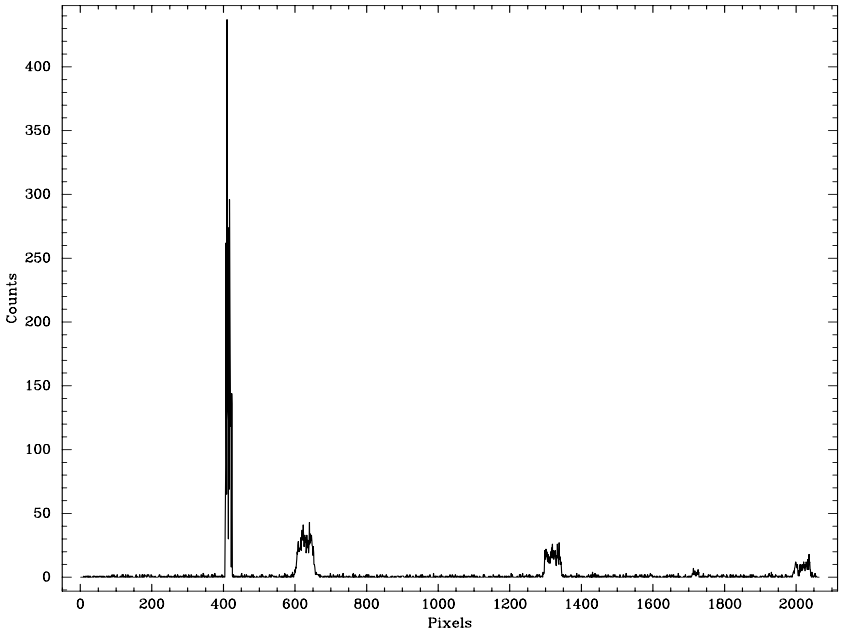

32.9.3 Detector Background (Dark)

The FOS was subject to two types of background effects caused by high energy particles:

- Light generated by Cerenkov radiation as particles hit the faceplate.
- Counts generated by the direct interaction of the particles themselves with the detector.

The default reference background files used in **calfos** contain model predictions of the mean particle-induced background. level for each detector. The background reference file data are shown in Figure 32.27 for both the FOS/RD (upper curve) and the FOS/BL (lower curve) detectors. This model was obtained from observations made during Science Verification (see *FOS ISRs* 071, 076, 079, and 080). For typical observations obtained with no simultaneous dark data, the background reference file is appropriately scaled on an observation group-by-group basis to account for the location of the spacecraft in the geomagnetic field. The scaled background file, which is *essentially an estimate of the mean dark rate per pixel for each group processed*, is written to the `.c7h` file (in units of counts-second^{-1}), and subtracted in the pipeline calibration.

The dark contribution in short exposures was dominated by individual events that typically affected individual diodes. Many FOS exposures, and all individual readouts, were not lengthy enough to allow a uniform dark distribution to build up in all pixels at sufficiently high S/N for the pipeline mean correction to have high accuracy. For example, a one-orbit (2000 second) FOS/RD ACCUM exposure (500 seconds effective exposure in each pixel) at low latitude produced a mean

dark level of about 5 counts-pixel^{-1}. Random excursions of at least a factor of two about this mean level were to be expected and were often seen.

Figure 32.27: Background Reference Files: Dotted Line: FOS/RD, Solid Line: FOS/BL

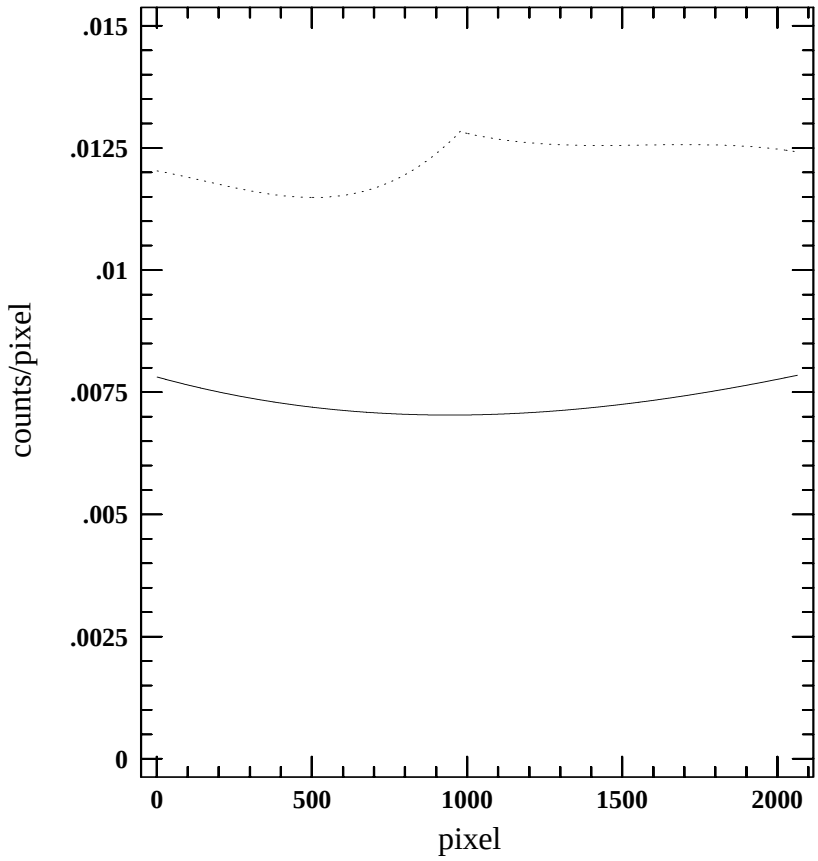

Further, there were some indications that the geomagnetic model used to scale the reference background file in the **calfos** pipeline[12] may have underestimated the background counts in science data by approximately 10% at low geomagnetic latitudes (< 20 degrees) and by about 20-30% at high geomagnetic latitudes. At present no refinement of these uncertainties is possible without a detailed study of the dark as a function of the ambient geomagnetic field measured by the onboard magnetometer. These uncertainties are not significant for strong sources (you can verify this by comparing the counts in the `.c5h` and `.c7h` files), but could cause substantial errors in the derived flux and spectral shape of weaker sources. For example, a V~19 magnitude star with an effective temperature of 10000 K, produced the same count rate at 2700 A. as the low latitude mean background of the FOS/RD detector.

12. *FOS ISRs* 099 and 114.

On the other hand, *FOS ISR* 146 examined all dark measures made through July 1, 1996 and essentially confirmed the SV mean levels as a function of geomagnetic latitude, λ_{gm}. No correlation of the dark rate with geomagnetic longitude (apart from the vicinity of the SAA), solar angle, or solar cycle was found. The mean background from this analysis is:

FOS/RD:

$$Rate_{Red} = 8.8 \times 10^{-3} - 8.0 \times 10^{-6}\lambda_{gm} + 5.2 \times 10^{-6}\lambda_{gm}^{2}$$

FOS/BL:

$$Rate_{Blue} = 4.3 \times 10^{-3} + 3.0 \times 10^{-5}\lambda_{gm} + 3.0 \times 10^{-6}\lambda_{gm}^{2}$$

Very few FOS observations obtained simultaneous background data due to the commanding requirement that forced the allocation of half the observing time to this measurement. In these rare cases signal from an unilluminated portion of the photocathode was used for background subtraction. The error in this background subtraction was simply related to the statistical error in the background data.

The FOS grating-scatter correction (See “Scattered Light” on page 32-58.) is effectively a scattered light *plus* residual mean background correction. After the standard mean dark correction has been applied, the scattered light algorithm calculates the mean count level in a range of unilluminated pixels (if one exists - see Table 31.6 for a listing of unilluminated pixel ranges) and this mean correction is subtracted from all pixels in the spectral region. This procedure does serve to correct underestimates of the model dark background, but for the same statistical reasons mentioned earlier, the corrected fluxes of faint sources can often vary around or drop below zero. Nonetheless, examination of any unilluminated region in the `.c4h` data can help in understanding the degree to which the background of your spectrum is dominated by individual particle events.

Accuracies

Mean rates may contain 10-30% uncertainties depending upon geomagnetic latitude. In nearly all cases, these uncertainties in the dark model are dominated by the statistical uncertainties in the estimated mean dark signal. That is, individual particle events dominate the dark count distribution for shorter exposures. The distribution of dark count per pixel begins to even out and resemble the scaled model mean values for exposures >2000 seconds

You can refer to the .c7h file and the FOS paper products for information about the background subtraction made for your data. The mean dark level is reported in the exposure summary section of the FOS paper products. When it is a significant contributor to the total signal, the mean dark count per group is visible in the group counts plot, as well. Additionally, as described above, you can examine any unilluminated pixels in the `.c4h` file as an indicator of the statistical nature of the actual dark signal in your observation.

32.9.4 Scattered Light

As a single pass spectrometer with blazed, ruled gratings and detectors that were sensitive over large spectral ranges, the FOS was subject to *scattered light* which originated primarily in the diffraction patterns of the gratings and the entrance apertures, as well as in the micro-roughness of the grating rulings due to their ruled surfaces.

Pre-flight laboratory data showed that the scattered component increased with increasing wavelength. The G130H, G190H, G270H, G160L, and PRISM spectra (below 2500 Å) were substantially affected by scattered light. A comparison between spectra taken with the solar blind (scatter-free) GHRS and with the FOS (see Figure 32.28) illustrates the conclusions of *FOS ISRs* 101 and 114 that FOS grating-scatter contamination dominated ultraviolet observations of late type stars. The scattered light appeared to be independent of wavelength in the regions observed and depended only on the magnitude and color of the target.

FOS ISR 103 described the **calfos** grating-scatter correction procedure, first implemented in March, 1994. The correction algorithm determines the mean detected signal for those diodes that are insensitive (or not illuminated) in a given dispersed spectrum and uses this mean as a measure of the wavelength-independent scattered light for the entire spectral range of the grating. This mean scattered signal is subtracted as a constant from all pixels in the spectrum. Only those gratings that have insensitive or unilluminated pixels (see Table 31.6) can be corrected in this fashion. If the wavelength range readout was restricted (e.g., in RAPID mode) it was possible that no data were recorded by the insensitive pixels. No scattered light correction was made in these cases. The algorithm was altered in February, 1996 to use the median, rather than the mean, with the additional proviso that all deviations from the median greater than 4σ are eliminated in order to remove the impact of strong signals due to particle hits from the determination.

The **calfos** scattered light correction is effectively a residual mean background correction. For those gratings for which only a small number of pixels are used to form the mean scattered light correction (e.g., FOS/RD G190H), poor results may occur. Often at low count rates the quality of scattered light correction is obviated by poor photon statistics in the target spectrum. The corrected fluxes often vary about zero or are negative for faint sources.

The scattered light modeling task, **bspec**, which uses optical principles to describe the contribution of scattered light to the observed spectrum, is available for use as a post-observation parametric analysis tool to estimate the amount of scattered light affecting a given observation (see *FOS ISR* 127). The amount of scattered light depends on the spectral energy distribution of the object across the whole wavelength range to which the detector is sensitive and on the detector sensitivity as a function of wavelength over that range. As we noted, for red objects the number of scattered light photons can dominate the dispersed spectrum in the UV. For an atlas of predicted scattered light as a function of object type and FOS disperser and additional guidelines for modeling FOS grating scatter with **bspec**, see *FOS ISR* 151.

Data contaminated by grating scatter with a ratio of scattered counts to intrinsic counts of up to 5 can likely be corrected with **bspec** modeling provided the intrinsic target spectrum is accurately known for longer wavelengths (that is, over the entire range of detector sensitivity), and provided the exposure times were such that sufficient S/N exists from the weak signal counts component in the total of (signal+scattered) counts. It is also advisable to have available a spectrum of the target at longer wavelengths, at least within the adjacent FOS spectral range.

You can refer to the SCT_VAL group parameter of the `.c1h` file for information about the scattered light correction made to your data. The mean correction level is also reported in the exposure summary section of the FOS paper products. Comparison of this value with the signal level in the `.c4h` file gives an indication of the severity of the scattered light contamination in the spectrum. If you have an accurate spectral energy distribution of your object at longer wavelengths, you can model the grating scatter with **bspec**.

Figure 32.28: Scattered Light Comparison of GHRS and FOS

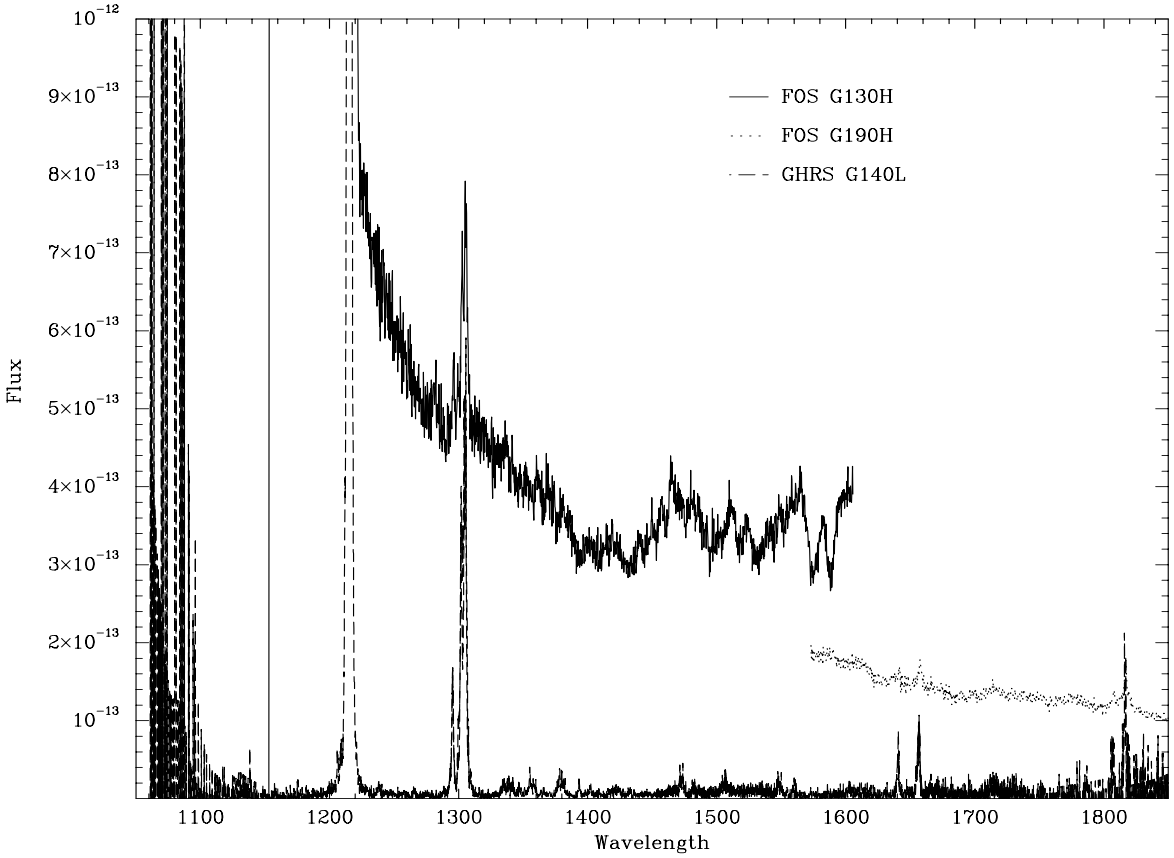

32.10 PSF/LSF

32.10.1 Point Spread Functions

Pre-COSTAR:

FOS ISR 104 presents a comprehensive series of TIM modeled monochromatic FOS point spread functions. Default values for dust and mirror micro-roughness were included in the PSF models as was pointing jitter with an rms of 7 milliarcsec. FOS/BL PSFs were calculated every 200 Å. throughout the range 1200-5400 Å. FOS/RD PSFs were calculated every 200 Å. throughout the range 1600-8400 Å.

Observational white light PSFs for the `4.3` aperture are described in *FOS ISR* 148. These PSFs were formed by superposition of numerous ACQ images of the same point source located at different positions in the `4.3` aperture.

The model PSFs were used to produce theoretical aperture throughputs and aperture throughput ratios relative to the `4.3` aperture (see *FOS ISR* 105).

Theoretical aperture throughputs for miscentered targets were also derived from the model PSFs (see *FOS ISR* 107).

Post-COSTAR:

Post-COSTAR observational white light PSFs for the `4.3` aperture are described in *FOS ISR* 148. These PSFs were formed by superposition of numerous ACQ images of the same point source located at different positions in the `4.3` aperture.

The pre-COSTAR PSFs are available from the STScI anonymous FTP site, `ftp.stsci.edu`. See the FOS WWW Calibration Products and Tools page for further information.

32.10.2 Line Spread Functions

Pre-COSTAR:

Both FOS/BL and FOS/RD monochromatic LSFs for each non-occulting FOS aperture were derived from the pre-COSTAR model PSFs (see *FOS ISR* 104). The LSFs were computed for a point source perfectly centered in each aperture. FOS/BL LSFs were calculated every 200 Å. throughout the range 1200–5400 Å. FOS/RD LSFs were calculated every 200 Å. throughout the range 1600–8400 Å.

Observational white light LSFs for the `4.3` aperture are described in *FOS ISR* 148. These LSFs were formed by integration of the pre-COSTAR white light PSFs described above.

Post-COSTAR:

Observational white light LSFs for the `4.3` aperture are described in *FOS ISR* 148. These LSFs were formed by integration of the post-COSTAR white light PSFs described above.

Observational line profiles of unresolved spectrum lines (observational dispersed light LSFs) are available in ASCII format from the FOS WWW page for FOS/BL G130H, G190H, and G270H, and FOS/RD G190H, G270H, and G400H and the `4.3`, `1.0`, and `0.3` apertures.

These LSFs, which are the subject of forthcoming *FOS ISR* 155, clearly display typical Voigt profiles with both a Gaussian core and Lorentzian wings. For S/N < 10 only the Gaussian core is evident. At higher S/N through the two larger apertures, the Lorentzian wings develop at approximately 20% of peak intensity. The width of the LSF is determined by the width of the response of the FOS detector element, a nominal 1 diode FWHM Gaussian profile (*FOS ISR* 061).

The FOS/RD G270H has the narrowest core (FWHM~1 diode), whereas the FOS/BL G270H has the widest core (FWHM~1.25 diodes). All FOS/BL profiles have broader wings than those in the FOS/RD spectra. The different profiles are attributable to different magnetic and optical focus quality for the two detector

assemblies as well as possible grating alignment differences in the optical paths inside the FOS.

The FOS/RD G270H profile most nearly matches the FOS/RD white light profile, while the FOS/RD G130H comes closest to the FOS/BL white light profile.

You can download the post-COSTAR ASCII LSF listings from the FOS WWW Calibration Products and Tools page. The pre-COSTAR LSFs are available from the STScI anonymous FTP site, `ftp.stsci.edu`. See the FOS WWW Calibration Products and Tools page for further information.

32.11 Astrometry and Aperture Location

Pre-COSTAR:

No precise aperture location measures were made in the pre-COSTAR period. The absolute location of the `4.3` aperture was determined to approximately 1" accuracy. Each single aperture was assumed concentric with the `4.3`. Post-COSTAR calibrations, which are applicable for the purpose of assessing aperture concentricity, suggest that the circular apertures are indeed concentric but are all displaced by approximately 0.1" from the center of the `4.3` (see FOS ISR 137 for precise aperture offsets).

Post-COSTAR:

The absolute locations of the `1.0` apertures were chosen as the fiducial and the relative positions of all the other FOS apertures were measured with respect to them. ACQ/PEAK scan steps with precise pointing telemetry were used to determine the positions of the apertures. The absolute locations of the `1.0` apertures were determined with 1 σ accuracies of 0.24" and 0.30" for FOS/BL and FOS/RD respectively. All relative aperture locations except for the 4.3, were determined with 0.02" 1 σ accuracy (see *FOS ISR* 138). The uncertainty in the relative position of the 4.3 aperture was 0.1" (see *FOS ISRs* 137 and 139).

The FOS plate scale (see Table 29.2) is accurate to 2% in each coordinate.

32.12 Timing Accuracies

The fundamental internal FOS time interval is an *FOS clock tick* of 7.8125 μsec duration, which is equal to 8 ticks of the HST 1.024 MHz clock. FOS event timings as *reported in engineering telemetry*, which was not routinely available to observers and which did not provide *directly* the quantities of interest to astronomical researchers, were recorded with the full precision and accuracy of

the FOS clock. All FOS timings reported in the science data products, including those of interest, were recorded with a truncated timing *precision* of approximately one-eighth of a second and an accuracy that could be even poorer—see below.

The finer details of FOS exposure timing extend far beyond the scope of this document (refer to Appendix A of *FOS ISR* 154 as the best available low-level description of FOS data acquisition procedures and timings). In summary, at the end of an observing segment (i.e., what will become an output group) the transfer of detected counts from FOS memory to storage on the spacecraft proceeded only after some communication between the FOS microprocessor and the HST Science Data Formatter (SDF). The normal data-taking commanding of the FOS did not require FOS exposures to start at *precise* pre-selected start times, and there was no direct record in any telemetry of when an exposure actually started. The engineering telemetry did record the so-called LINESTART time; that is, the precise time when the SDF told the FOS to commence sending data from the FOS memory to the SDF. A truncated version of LINESTART time was recorded in the FOS headers as FPKTTIME (the so-called *first-packet-time*). It was also possible to calculate exactly the length of time that the FOS had spent actually recording signal by using fundamental FOS data-taking quantities which were recorded accurately in the headers.

Then, in principle, one can start with the LINESTART (or less accurately, FPKTTIME) and subtract both the time required for post data-taking electronic "handshaking" between the FOS and the SDF and the time actually spent taking data to determine the start time of an observation (see Section 33.1).

Unfortunately, the length of time required for the handshake between the FOS and the SDF could vary from 0.001 to 0.255 seconds depending upon the load on the SDF. As a result, FOS observation start times calculated even with the highly precise LINESTART from the engineering telemetry give results 0.001 to 0.255 seconds later than the actual start time. It is not possible to determine the *absolute* start times more precisely than with this level of uncertainty. Due to the fact that FPKTTIME is a truncation, not a rounding, of LINESTART, an observation start time calculated from FPKTTIME may range from as much as 0.25 seconds earlier to 0.125 seconds later than the actual value.

Further, under *normal* loading of the SDF and for most FOS exposure time regimes the duration of the handshake interaction could vary by up to approximately 0.02 sec between readouts of the FOS memory. The dominant component of this variation was internal to the SDF. Under normal circumstances the actual interval between start times of individual groups (e.g, in a RAPID exposure) should be nearly the same. Relative group timings can be accurately determined from relative LINESTART timings with the understanding that variations of order 0.02 sec or less commonly will be seen in the length of these intervals due to the influence of SDF loading. Since the interval between successive FOS group starts was fixed by FOS commanding to be an integral number of FOS data-taking cycles, called INTS, it may be possible to improve the accuracy of relative group timings further with post-observation analysis which can only be facilitated with the engineering telemetry and STScI site-specific software. Unfortunately, the very low-level details of FOS commanding cause

essentially random variations in the group-to-group intervals of certain RAPID mode observations when the readout time of the FOS memory is comparable to the internal FOS data-taking cycle time (the INT). A description of this phenomenon is beyond the scope of this document. If your LINESTART intervals seem to vary randomly or have substantial excursions outside of the typical 0.02 sec range, you should contact `help@stsci.edu`. Similarly, if accuracies of better than 0.02 sec in relative timing and/or 0.255 sec in absolute timing are required, please contact STScI.

In any event, always use timings derived from FPKTTIME or the engineering telemetry; do NOT attempt to form times based upon start time of observation and anticipated or requested group integration times.

Timing Summary

- FOS exposure times used in the calibration of absolute fluxes are correct to the full accuracy of the internal FOS clock (7.8125 μsec).
- The actual length of RAPID mode exposures will always differ to some extent from that specified in the proposal.
- FOS science header timings are truncated at the one-eighth second level.
- FOS engineering telemetry, available only at STScI, provides all timing information at accuracy of FOS clock (7.8125 μsec).
- Absolute timings from engineering telemetry are late by 0.001-0.255 sec. Absolute timings from FPKTTIME in science header may be anywhere in a range from 0.25 sec early to 0.125 sec late.
- Relative timings contain an inherent variable uncertainty normally on the order of 0.02 sec. This uncertainty can be evaluated with detailed examination of the engineering telemetry with perspective incorporating a fuller understanding of the FOS data-taking commanding that is beyond the scope of this document (see *FOS ISR* 154).

32.13 Polarimetry

In FOS polarimetry mode the incoming beam was split into orthogonal polarization components by a Wollaston prism behind the entrance aperture. Although SINGLE apertures were always used, the two dispersed beams ultimately illuminated different portions of the photocathode located above and below the position illuminated by the standard unpolarized SINGLE aperture beam. The two photocathode positions accordingly required separate flatfields, wavelength calibrations, and Y-base deflections. The two spectra were alternately deflected onto the diode array and recorded in 10-second intervals throughout an exposure. Polarimetry exposure sequences (POLSCANs) consisted of 4, 8, or 16

individual exposures at unique polarizer rotations. These sequences had to fit within one orbital visibility. In the limit of minimal jitter or GIM motion, the same portions of the photocathode were *nominally* illuminated and recorded in each exposure.

As with non-polarimetric observations, no concurrent WAVECAL exposure was routinely taken with polarimetry data, so the limiting accuracies of the default pipeline polarimetry wavelength calibration are the same as for the non-polarimetry case described earlier (See “Wavelength Calibration” on page 32-49.). Different dispersion relations are applied to the two pass directions. When the beams are combined, the lower pass direction is simply shifted onto the wavelength grid of the upper pass direction with no interpolation or resampling. The error in this arbitrary shift can be determined by simply comparing the output wavelengths for the two pass directions on a pixel-by-pixel basis.

All FOS polarimetry calibration observations were taken with POLSCAN=16.

Polarimetry flatfields were always produced via the often subjective, non-superflat, continuum-fitting technique. The same comments made earlier in the flatfield section (See “Flatfield Calibration” on page 32-38.) about this method of flatfielding apply here, as well, but are of much less importance as polarimetry data are often binned heavily in analysis.

Polarimetry flux calibration is performed with the FLX_CORR method and the WD absolute flux system. This has little effect on the derived values of Q and U as the influence of the sensitivity function divides out in the calculation of those quantities. Recall that no correction is made in the FLX_CORR calibration for the influence of telescope focus or time-dependent photocathode sensitivity variation. These factors can cause an additional variable flux calibration error of 0–15% for pre-COSTAR observations, but should not impact post-COSTAR calibration.

Pre-COSTAR:

Since the pre-COSTAR PSF overfilled all apertures, spacecraft jitter could impact some exposures in a POLSCAN sequence more than others, thereby introducing photometric effects that limited polarization measurement accuracy. For similar reasons, prior to the implementation of the onboard GIM correction, FOS polarimetry was not feasible.

Following implementation of the onboard GIM correction, pre-COSTAR polarimetry accuracies were limited by the effects of residual GIM motion, FGW positioning, and jitter on the fraction of the s-curve of the large PSF that was recorded by the diode array. Visual inspection of pre-COSTAR calibrated polarimetry observations indicates that variations in these quantities produced scatter in total polarization of the order of 0.5% and occasionally was somewhat worse. The uncertainty in the retardation calibration also contributed a systematic instrumental polarization equal to 2% of the linear polarization (see *FOS ISR* 078). The impact of photon statistical uncertainties always must be considered, but it can be minimized by appropriate binning of the data.

Post-COSTAR:

The COSTAR mirrors added two low angle-of-incidence (7 degrees) reflections ahead of the FOS optics. These additional reflections acted to convert

some of the linearly polarized component into the circular component and vice versa. A correction algorithm for the linear polarization has been devised and will be implemented in **calfos** in early 1998. Until that time no post-COSTAR polarimetry data are fully calibrated by STScI algorithms available for general release. In the meantime, if you have a need for recalibration of post-COSTAR polarimetry, please contact `help@stsci.edu`.

The wavelength-dependent post-COSTAR instrumental polarization in Q varies from 0–3% over the FOS/BL 1600–3300Å spectral range and COSTAR-induced U varies from 0-0.5% over the same range. Panel a) of Figure 32.29 shows the magnitude of the COSTAR-induced instrumental polarization in high S/N observations of unpolarized spectrophotometric standard BD+28D4211 that have been combined into 64 bins. The discontinuity in U around 2300 Å. is due to the break between the G190H and G270H gratings. Panel b) of Figure 32.29 shows a residual of ~0.08% in Q for the same binned spectrum after correction for the instrumental polarization with the algorithm to be included in **calfos**. Note that in the 1800–2100Å region where the waveplate retardation goes through a 180 degree rotation, the limiting residual is ~0.2%. For bright objects, the polarization angles are known to within about +/-5 degrees. Koratkar et al. (1998, *Ap.J.* submitted) find that the post-COSTAR combined effects of residual GIM and spacecraft jitter do not produce polarization greater than 1%. Additional sources of error in polarization are due to the photon statistics of the observation and the error in the retardation calibration (2% of the linear polarization—see *FOS ISR* 078). Post-COSTAR polarimetry observations made with only four polarizer rotations (POLSCAN=4) contain an additional 0.4% uncertainty in Q. Note that polarimetry data for even very bright calibration sources must be binned in post-calibration data reduction in order to reach the levels of precision stated here.

Typically, photon statistics will be the dominant source of uncertainty in your observations.

The forthcoming *FOS ISR* 150 will be the definitive discussion of the technical and calibration details of FOS polarimetry. This document, which will be announced on the FOS WWW page is planned for release in spring, 1998.

Figure 32.29: Unpolarized Standard Star BD+28D4211: a) Prior to Correction and b) After Correction for Post-COSTAR Instrumental Polarization

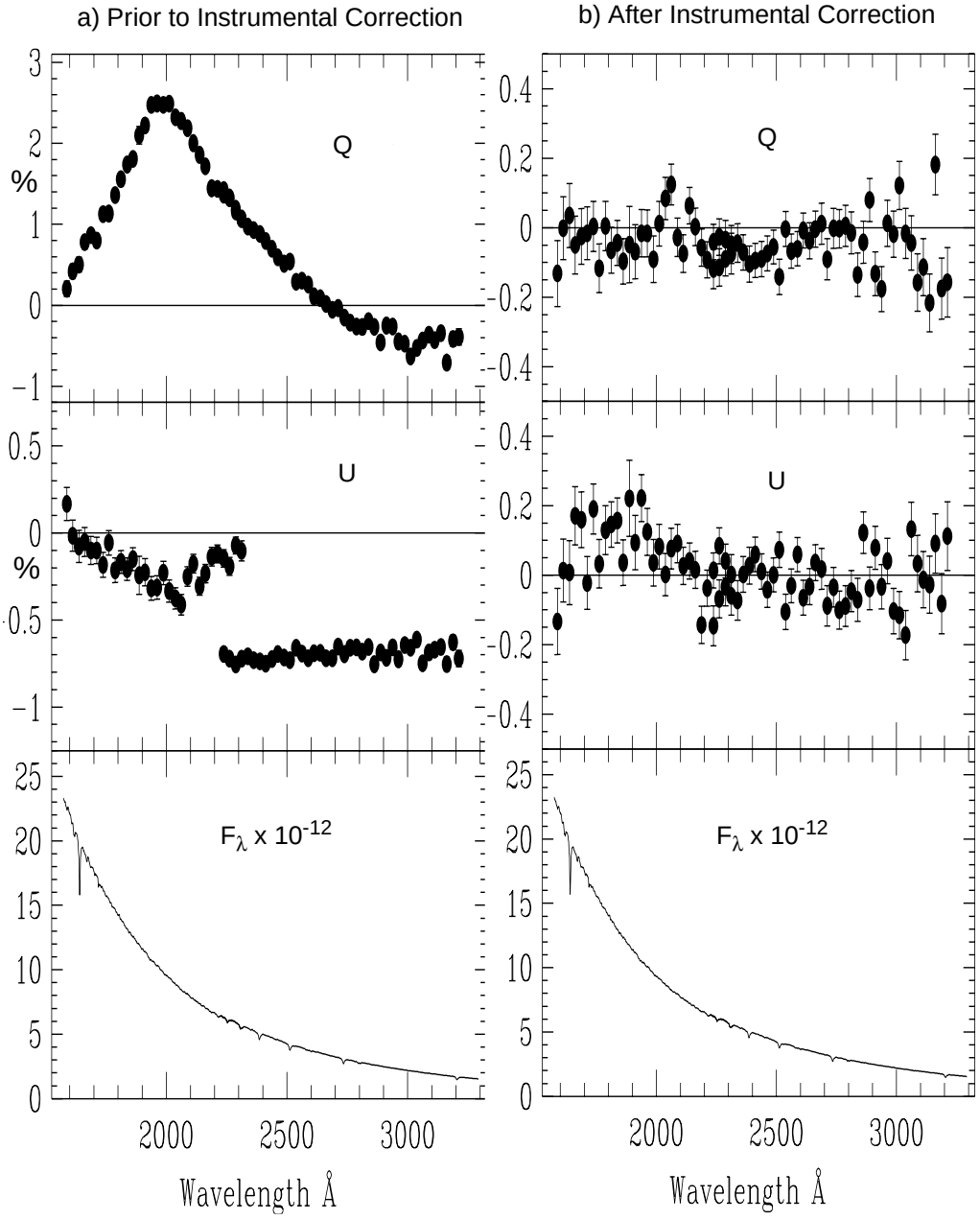

figure courtesy A. Koratkar, 1998, Astrophys. J. submitted.

Chapter 33
FOS Data Analysis

In This Chapter...

Procedures for assessing the quality of data obtained with each FOS operating mode are discussed in the target acquisition assessment and science observation assessment sections of Chapter 30. Procedures for analyzing FOS calibration data quality and accuracy limitations, as they apply to a given dataset, are given in Chapter 32.

Several IRAF/STSDAS routines exist for displaying and analyzing spectroscopic data (see Table 3.5). General purpose spectroscopic tasks, such as **splot**, **mkmultispec**, and others, are also described in Chapter 3.

This chapter presents a series of generally unrelated discussions of individual data analysis topics several of which were inspired by frequently asked questions received by the STScI FOS team from General Observers. Also included are descriptions of additional useful IRAF/STSDAS tasks for evaluating, improving, and analyzing FOS data.

33.1 Calculating Exposure Times

The basic times most observers will be interested in are:

- Start and end times (of the observation, or of the integration for a given group).

- Exposure time per pixel (i.e., the integration time which contributes to the counts in each pixel), for the whole observation, or a given group.

The following section presents detailed information on the determination of these quantities from header information *only*. The determination of FOS start and stop times from header information is limited to an accuracy of +0.125 to –0.255 seconds (see Chapter 32). If you need more accurate start times, contact the Help Desk, `help@stsci.edu`. In Table 33.1, we summarize how to obtain these basic quantities from header keywords and group parameters.

Table 33.1: Timing Information for FOS

Type of Information	Source	Units
Observation start time	EXPSTART[a]	Modified Julian date
Group start time	FPKTTIME[b] – group_elapsed_time	Modified Julian date
Group_elapsed_time	FPKTTIME (group 1) – EXPSTART	Seconds
Group exposure time *per pixel*	EXPOSURE[b]	Seconds
Group end time	FPKTTIME[b]	Modified Julian date
Observation end time	FPKTTIME[b] (last group)	Modified Julian date

a. Header keyword
b. Group parameter

33.1.1 Exposure Time Details

The different times in the FOS headers are:

- ***LIVETIME:*** The fundamental unit of integration time. This is the time between opening and closing the 512 accumulators. The shortest time is 3 ms. The header keyword is LIVETIME.
- ***DEADTIME:*** Time required for housekeeping chores. It is normally 10ms. The header keyword is DEADTIME.
- ***Exposure time per pixel:*** This is the integration time per pixel that contributes to the counts observed in that pixel. This differs from the exposure time per spectrum because of substepping. The header keyword EXPOSURE gives the total exposure time for a non-edge pixel in seconds.
- ***Exposure time per group:*** This is the integration time for a given group, which is equivalent to the integration time per diode and is exclusive of instrument overheads. The exposure time of the group (exp_{group}) (units of seconds) using the header keywords is determined as follows:

$$exp_{group} = \text{EXPOSURE} \times \text{NXSTEPS}$$

This simple equation in terms of the basic FOS time and data acquisition terms is given to the full accuracy of the FOS clock by:

$$exp_{group} = \text{LIVETIME x 7.8125E-6 xINTS x NXSTEPS x OVERSCAN x YSTEPS x NPAT}$$

In this calculation we have not accounted for the deadtime because we are interested in calculating only the time over which the photons were collected.

- ***Elapsed time per group:*** This is the total time associated with an entire group. It is longer than the exposure time of a group because of the added deadtime. The following equation can be used to determine the elapsed time of a group for nearly all observations.

$$elapsed\ time_{group} = \text{(LIVETIME + DEADTIME) x 7.8125E-6 x INTS x NXSTEPS x OVERSCAN x YSTEPS x SLICES x NPAT}$$

This elapsed time can be used to determine theapproximate start and stop time of each group in the data. The procedure is as follows:

The FPKTTIME in the group parameters of the .d0h file is the time at which the FOS memory for that group was read out and *is inclusive of all deadtime for the group*. Unfortunately, it may also include an indeterminate additional interval of up to 0.13 second caused by HST SDF overheads. In the headers this time is given (to the accuracy of about 0.125 second) in units of modified Julian date, which is the Julian date minus 2400000.5. This time can be converted from modified Julian date to the standard notation using the **epoch** task. For many FOS datasets in the HST Archive obtained prior to January 1, 1995, the exposure start time is incorrectly populated. The time at which the integration was started is given by:

$$start\ time = \text{FPKTTIME}_{group} - elapsed\ time_{group}$$

Please note that the start time for each individual group should be calculated from the FPKTTIME of the relevant group and not simply by a recursive addition of group elapsed time to the start time of a previous group.

The group parameters can be determined by running the task **grlist** to determine all the groups in the d0h file and then finding the value of the necessary keyword using **hedit**. Note that the FPKTTIME is accurate only to approximately 1/8 second.

- ***Exposure time for the observation***: This is the total time during which the FOS accumulated data for the observation and is given in the header keyword EXPTIME. This should be the exposure time given in Phase II instructions. This is given by the equation:

$$exptotal = \text{EXPOSURE x NXSTEPS x NREADS x NMCLEARS}$$

In the basic FOS data acquisition units, this is:

$$exp_{total} = \text{LIVETIME x 7.8125E-6 x INTS x NXSTEPS x OVERSCAN x YSTEPS x NPAT x SLICES x NREAD x NMCLEARS}$$

- ***Elapsed time for the observation:*** This is the total time spent by the FOS for a given observation, which includes the deadtime during which photons were not accumulated. Corresponding to the exposure time for the observation is the elapsed time for the observation. This is given by:

$$elapsed\ time_{observation} = \text{(LIVETIME + DEADTIME) x 7.8125E-6 x INTS x NXSTEPS x O VERSCAN x YSTEPS x NPAT x SLICES x NREAD x NMCLEARS}$$

33.1.2 Timing

Observation start and stop times are determined from the header information with a precision of +0.125 to –0.255 second, while exposure times are determined with a precision of 7.8125 microseconds. This has particular impact on certain RAPID mode timings as described in “RAPID Mode Observation Timing Uncertainties” on page 33-5.

Start and End Times

The *start* time of the observation (i.e., the time at which the integration was begun for the first group of data) is given in modified Julian date in the header keyword EXPSTART. The modified Julian date is the Julian date minus 2400000.5. Prior to January 1, 1995 EXPSTART was incorrectly populated with FPKTTIME. You should insure that your EXPSTART is approximately equal to the difference between FPKTTIME for the first group and group elapsed time.

The *end* time of the integration for each group of data is given in modified Julian days in the group parameter FPKTTIME. The end time of an observation is the FPKTTIME of the last group of the observation. Again, in many FOS datasets obtained before January 1, 1995, the EXPEND keyword is incorrectly populated with LPKTTIME rather than FPKTTIME of the last observation group. You should insure that the FPKTTIME of the last group has been used for EXPEND.

To calculate the approximate group start time, subtract the *group elapsed time* from FPKTTIME. The group elapsed time (which will be nearly the same for all groups in a given observation) can be calculated in two ways: 1) for datasets obtained after January 1, 1995: as FPKTTIME for the first group of data minus EXPSTART, or 2) for any dataset: from the formula given in the previous section. The start time of each subsequent group is then given as FPKTTIME for that group minus the group elapsed time (see Table 33.1).

As noted earlier, an additional uncertainty of approximately 0.13 seconds exists since the HST Science Data Formatter can be delayed in issuing the command to read out the FOS memory, which is recorded as FPKTTIME.

Exposure Times

The *elapsed time* for an observation differs from the *exposure time* (the actual integration time during which counts are accumulated) because the elapsed time includes the deadtime during which the FOS is doing housekeeping (e.g., reading out the diodes) and therefore not integrating. The total *exposure time* for the entire observation (all groups) is given by the keyword EXPTIME in the data header.

The *exposure time per pixel*, the integration time which contributed to the flux observed in a given pixel, differs from the exposure time for the spectrum whenever substepping is employed. The exposure time is divided among the NXSTEPS individual substepped spectra which together produce the single spectrum. The (typical) exposure time per pixel is therefore given by the exposure time divided by NXSTEPS. This quantity is contained in the group parameter EXPOSURE.[1]

33.2 RAPID Mode Observation Timing Uncertainties

Under certain circumstances, the start times of individual exposures in an FOS RAPID mode time series must be calculated by a special algorithm, which requires information available only from the engineering telemetry stream. The reason for this requirement is that the interval between individual groups in a RAPID (or rarely, ACCUM) mode sequence is not always constant

If *absolute* or *relative* start times of RAPID mode exposure sequences must be known to accuracies more precise than 0.125 seconds, then we recommend that RAPID mode observers contact the Help Desk (E-mail: `help@stsci.edu`) for help in determining the precise start times of the exposures.

FOS ISR 154 provides a detailed description of the causes of uncertainties in the start times of FOS exposures and provides many low-level details of FOS data taking

1. Note, however, that the actual exposure time for a given pixel may be different from EXPOSURE, either because the pixel did not receive input from OVERSCAN diodes (because it was an edge pixel or because it was fed by input from one or more disabled diodes), or because a particular readout was rejected by the onboard burst noise rejection algorithm. Thus EXPOSURE actually reports the maximum possible exposure time per pixel. The **calfos** task correctly calculates the *count rate* of each pixel, taking into account the number of diode readouts which contributed to the counts observed in each pixel, using the information in the disabled diode reference table to compensate for disabled diodes and the noise rejections tallied in the reject array (the `.d1h` file) to compensate for times when the counts from a particular diode were not accumulated into memory due to noise rejection.

33.3 Heliocentric Radial Velocity Calculation

FOS output wavelengths (`.c0` files) are placed on the wavelength system of the dispersion coefficients in the CCS6 reference table. As described in Chapter 31 those coefficients contain an “internal/external” correction to account for the different illumination patterns produced on the dispersers by internal and external beams. However, no corrections for spacecraft motions of any kind are applied to **calfos**-calibrated wavelengths.

The procedure described here calculates the heliocentric motion of the Earth at the time of observation. This procedure does *not* correct for the small effect (at FOS dispersions) of HST orbital motion.

The IRAF task **rvcorrect** is used to compute radial velocity corrections. **rvcorrect** is in the IRAF **astutil** package and it calls on task **observatory**, which is also found in **astutil.** The following steps are an example of its use for an HST dataset where the HST velocity around the Earth is ignored (maximum residual: +/- ~7.8 km/s):

1. Set parameters to their default values.

   ```
   cl> unlearn rvcorrect
   ```

   Use the default **observatory** task parameters except the following, which must be set to prevent **rvcorrect** from calculating an unwanted diurnal velocity correction based on the observatory position with respect to the Earth's center.

Figure 33.1: Observatory pset Values

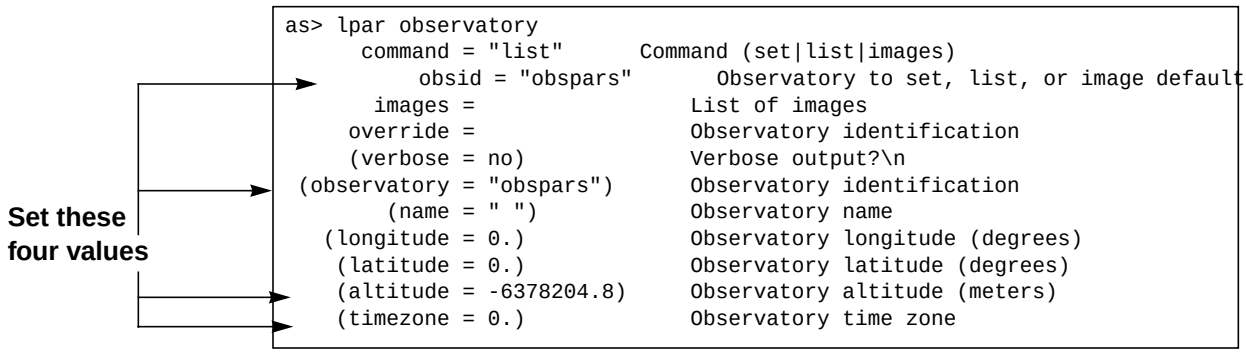

2. Create an ASCII file (named `rvcor.in` in the following example) with a row entry for each spectrum. Each row will contain: UT, RA, DEC, EPOCH, and Observed Velocity (more examples are provided in the help file for the task). Here is an example of file `rvcor.in`:

```
93 01 21 18:50:07 0.2974443291667E+03 0.4896100000000E+02  2000 0
93 01 21 20:05:09 0.2974443291667E+03 0.4896100000000E+02  2000 0
```

3. Run the **rvcorrect** task:

   ```
   cl>rvcorrect f=rvcor.in > outputfile
   ```

The above example produced the following output file. VHELIO contains the (very small, in this case) correction for the heliocentric velocity of the telescope with respect to the target.

```
       HJD       VOBS   VHELIO  VLSR  VDIURNAL   VLUNAR   VANNUAL  VSOLAR
2449009.81098     0.00    2.38   2.72   0.000      0.001    2.381    0.342
2449009.88335     0.00    2.35   2.69   0.000      0.001    2.349    0.342
```

Read the **rvcorrect** task help carefully, particularly to insure that you keep the signs of the velocities in the appropriate frame.

33.4 FOS/BL G160L Zero-Order Photometric Calibration

A rough calibration of the FOS/BL G160L zero-order sensitivity for photometry is provided here. No zero-order calibrations for other dispersers are available.

The FOS/BL G160L zero-order was normally read out by the diode array. The spectral passband for the zero-order of this detector and disperser combination ranged from 1150 to approximately 5500 Å. For a flat continuum source, the effective wavelength of the passband was approximately 2400 Å. The signal strength in the zero-order depended on the integral of the target spectral energy distribution and the detector sensitivity over the entire bandpass.

A very approximate calibration of the FOS/BL zero-order sensitivity was originally provided in *FOS ISR* 091 and improved in Eracleous and Horne, *ApJ*, 433, 313, 1994. These original calibrations are updated here for some errors and are superseded by the sensitivity values, *S*, given below.

Flux (FOS/BL G160 zero-order) [in mJ] = C / (T x S)

where C is the detected counts per second in the entire profile of the zero-order spectral feature, T is aperture throughput relative to the `4.3` aperture as unity (see Table 32.5 and Table 32.6), and S = 520 (pre-COSTAR) or 620 (post-COSTAR) counts per second per mJ.

Note that since C is defined as the total signal in the zero-order feature, *but is somewhat peculiarly expressed in counts/sec*, you must be careful about the distinction between total exposure time and exposure per pixel in the output `.c5h` data products. Therefore, you should calculate C by adding up the zero-order signal in your `.c5h` file and dividing by NXSTEPS.

This calibration is based upon pre-COSTAR observations of AE Aqr and A0620-00, both of which are close binary systems with quite red spectra that are dominated at wavelengths longer than 3000 Å by their K-type components. This approximate calibration is estimated to be accurate to about 50%.

33.5 Converting FOS X,Y to Spacecraft V2,V3

Although the conversion of telescope offsets from the FOS (*x*,*y*) reference frame to the telescope (V2,V3) reference frame is provided in the FOS paper products for all acquisition slews, you may occasionally need to calculate this rotation for other purposes. As noted in Chapter 29, the FOS (*x*.*y*) coordinate system is defined so that the *x*-axis is parallel to the diode array and the *y*-axis is perpendicular to the diode array. Further, the (*x*.*y*) coordinate frame is rotated with respect to the telescope (V2,V3) coordinate frame. Figures 33.2 and 33.3 show the coordinate axes for both detectors before COSTAR was installed. The (V2,V3) axes were rotated 180˚ by the introduction of COSTAR.

Figure 33.2: Pre-COSTAR Orientation of FOS/BL, (Here PA_APER=110˚)

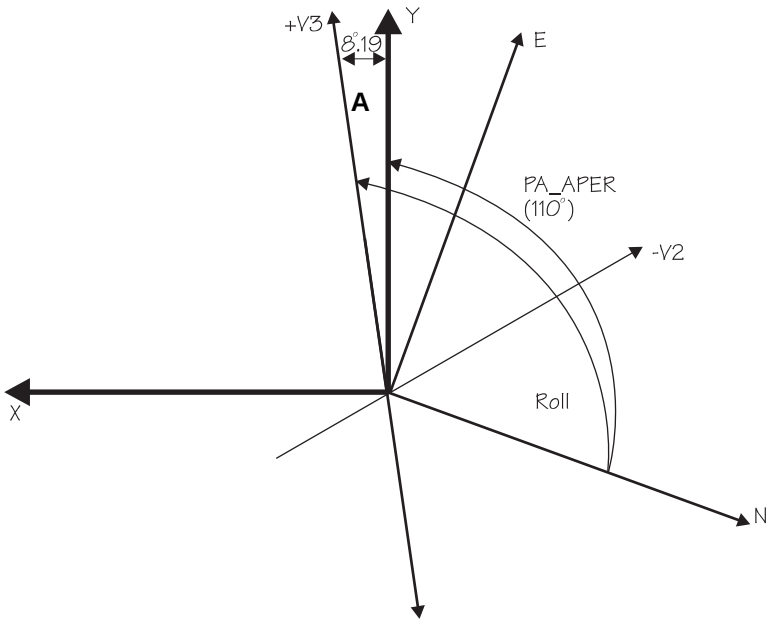

Figure 33.3: Pre-COSTAR Orientation of FOS/RD (PA_APER=40˚)

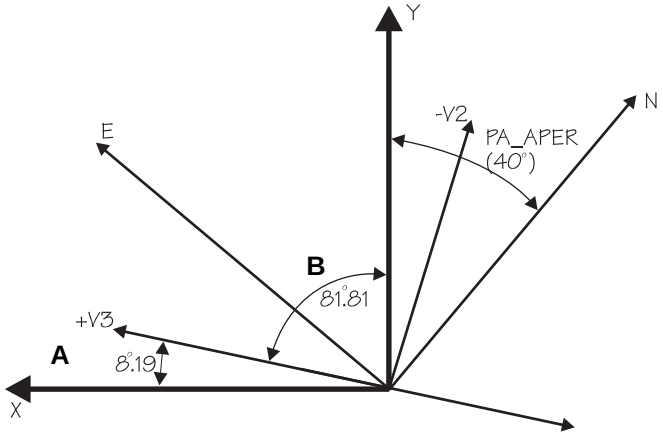

From the figures above we see that the coordinate transformation for FOS/BL is given by:

$$V2 = X \sin(A) - Y \cos(A)$$
$$V3 = X \cos(A) + Y \sin(A)$$

While the pre-COSTAR transformation for FOS/RD is given by:

$$V2 = X \sin(B) - Y \cos(B))$$
$$V3 = X \cos(B) + Y \sin(B)$$

where:

- pre-COSTAR: A= 8.19˚ and B = 81.81˚
- post-COSTAR: A= 188.19˚ and B = 261.81˚

33.5.1 Converting X,Y to RA, Dec

The conversion of an (*x*,*y*) offset to an (RA,Dec) offset is, of course, an additional simple rotation added to the expressions in section “Converting FOS X,Y to Spacecraft V2,V3” on page 33-8. The position angle of the aperture (PA_APER) is the angular orientation of the +*y*-axis of the aperture measured in degrees east of North. PA_APER is given in the FOS paper products and in science data headers.

33.6 Other Useful FOS Tasks in STSDAS

Chapter 3 provides details on several IRAF/STSDAS tasks useful for displaying and analyzing spectroscopic data; these tasks include **splot**, **mkmultispec**, **fwplot**, and **sgraph**. Following are brief descriptions of several more tasks that are useful for investigating or improving FOS data quality. In all cases, the on-line IRAF/STSDAS help file contains additional practical information.

33.6.1 deaccum

This task unbundles individual groups of an ACCUM multigroup spectrum. In ACCUM operation the data are readout at regular intervals and the output after each readout is stored as a separate group containing the accumulated sum of all readouts. The product of the **deaccum** task is a multigroup spectrum in which each individual group contains only the signal accumulated during each individual readout interval. This data format is very useful when the groups are plotted together for inspecting the effects of noisy diodes or poor guiding during the exposure. This check is always a good idea to do as it allows inspection of the entire spectrum as opposed to the more limited paper product group count diagnostic.

We recommend running **deaccum** with all of your ACCUM mode .c1h files. It will also work with statistical error (.c2h) files and correctly unbundles these data in quadrature. This task will *not* work for data files that contain wavelengths (.c0h) or data quality values (.q0h or .cqh files). The group parameter EXPOSURE is updated in the output image headers to reflect the change in exposure time associated with each data group. For example, to unstack the calibrated flux data in the image y3ci0203t.c1h, and write the results to the new image y3ci0203u.c1h, use the command:

```
fo> deaccum y3ci0203t.c1h y3ci0203u.c1h
```


33.6.2 gimpcor

The size of geomagnetically-induced motion can often be important when analyzing photometric losses due to image drift off the diode array and when assessing the widths or wavelengths of spectral features.

Since the **calfos** (pre-onboard) GIM correction is applied on an integral pixel basis in the *x*-direction only, uncorrected motions of up to +/- 0.5 pixels can occur in X. This effect is much smaller for observations corrected by the onboard GIM correction. For observations obtained prior to the implementation of the onboard GIM correction (the presence of header keyword YFGIMPEN set to “T” tells you if the onboard correction has been performed), the actual decimal magnitude of GIM motion can be evaluated with STSDAS task **gimpcor**. This information can be useful for evaluation of the GIM-related uncertainties in observing modes to which the correction is not applied, as well, such as pre-onboard GIM-correction spectropolarimetry and IMAGE mode.

This task calculates the *x*-direction GIM correction in fractional diodes predicted by the FOS GIM model. Rounding of the output to the nearest integer gives the actual correction that would have been applied by **calfos** in normal pipeline processing if the OFF_CORR switch were enabled.

The size of the *y*-motion, which is important for the evaluation of photometric losses, is also calculated. Recall that no GIM correction is made in the *y*-direction prior to the implementation of the onboard GIM correction.

gimpcor is essentially a small version of **calfos**, but **gimpcor** does not actually perform any corrections. All inputs required for running **calfos** are also required for running **gimpcor**. The image motion corrections are output in diodes, not pixels, for *x* and Y-base units for *y*. For example, the following command can be used to show the magnitude of the GIM correction for the observation y0nt0303t (an observation made in RAPID mode, with each line corresponding to each readout of the science diodes). Note that components of the geomagnetic field are also given along the V1, V2, and V3 axes.

```
          fo> gimpcor y0nt0303t
Y0NT0303T       XOFF       YOFF        B(V1)      B(V2)      B(V3)
Y0NT0303T      0.7937   -18.9236    -0.144756  -0.252337  -0.187240
Y0NT0303T      0.7774   -22.6758    -0.158107  -0.241623  -0.200176
Y0NT0303T      0.7540   -26.3918    -0.171826  -0.228918  -0.211748
Y0NT0303T      0.7235   -29.9800    -0.185674  -0.214425  -0.221575
       ....
Y0NT0303T     -0.1363    30.6008    -0.142325  -0.105515   0.195814
Y0NT0303T     -0.0940    31.9168    -0.134098  -0.119314   0.193947
```


33.6.3 unwrap

The FOS accumulators will overflow if more than 65,535 counts are recorded in any individual readout interval. In many cases an overflow can be corrected by the **unwrap** task. All pixels greater than a threshold value will be examined for wraparound. This algorithm is not foolproof, especially if more than one wraparound has occurred. Some experimentation with the threshold value usually results in a good correction for reasonably smooth continua or emission lines. An alternate IDL algorithm that is somewhat more robust than **unwrap** is available on the FOS WWW page in the Calibration Tools section.

This example will unwrap the image `y20vk10gr.d0h` using a threshold value of 20000 and creating an unwrapped image called `uw10g.d0h`.

```
fo> unwrap y20vk10gr.d0h uw10g.d0h thresh=20000.
```

33.6.4 waveoffset

Determination of wavelength offsets between two spectra can be made with the STSDAS routine **waveoffset**.

This routine computes the offset of one spectrum from a reference spectrum, as a function of wavelength and diode position in the frame of the reference spectrum. The input spectra may be divided into a number of equally sized bins. Each bin in the target spectrum is cross-correlated with the corresponding bin in the reference spectrum and an offset is determined. The offsets for all bins are placed in an output table as both diode and wavelength offsets.

The following example will compute the offset between upper and lower apertures for the spectra in file `h57red`. The upper aperture is in the first group of the file and the lower aperture in the second group. The wavelengths for the first group are stored in `wh57red` (group 1). Results are written to a table called `offsets.tab`.

```
fo> waveoffset h57red[1] wh57red[1] h57red[2] tab=offsets
```